

**Architectural integration of photovoltaic and solar thermal
technologies in multi-family residential buildings in the
Mediterranean area
Case study of Amman, Jordan**

Dissertation zur Erlangung des akademischen Grades Doktor der
Ingenieurwissenschaften (Dr. -Ing.)
an der Fakultät Gestaltung
der Universität der Künste Berlin

vorgelegt von
Master of Engineering
Jenan Abu Qadourah

September 2019

This publication is licensed under [CC BY-NC-SA 4.0 international](https://creativecommons.org/licenses/by-nc-sa/4.0/).

1. Gutachter: Prof. Dr. Nytsch-Geusen
2. Gutachter: Prof. Dr. Christoph Gengnagel

Tag der Disputation: 30. June. 2020

Universität der Künste Berlin, September 2019
Fakultät Gestaltung, Institut für Architektur und Städtebau
Fachgebiet Versorgungsplanung und Versorgungstechnik (VPT)

Declaration

I hereby declare on oath that I have made the present work without unauthorized or foreign assistance and have used no sources and aids other than those I have indicated. Parts taken literally or in the content are marked as such.

Signature:

A handwritten signature in black ink, appearing to be 'J. Claus', written over a horizontal line.

Date: 17. 09. 2019

Acknowledgments

First of all, I would like to acknowledge my supervisor, Prof. Dr.-Ing. Christoph Nytsch-Geusen, for his valuable and supportive guidance, motivation, and immense knowledge throughout my Ph.D. experience, which has contributed to the enrichment of this dissertation, and its successful completion.

I would like also to thank my second supervises, Prof. Dr.-Ing. Christoph Gengnagel for his time, interest, and helpful comments.

My deepest appreciations to my Ph.D. colleagues, with whom I have shared a unique experience in Berlin and supported me during the study.

My appreciation also goes to Mutah university, Jordan, for financing a three-year scholarship towards my doctorate at Berlin university of the arts (Udk).

Dedication

This thesis is dedicated to people without whom, none of my success would have happened:

To my Parents,

*Whose love, encouragement, support, and prayers make me able to get
such success*

To my husband, Alaa

For his patient, care, and encouragement to achieve my dream

Together we achieved our first milestone

To my daughters, Joury and Hala

*For supporting me and my husband during our Ph.D. journey, and bringing
moments of laughter and happiness to each day*

To my brothers and sisters,

For their continuous support

Abstract

Nowadays, society is becoming increasingly conscious of the adverse effect of energy use on the environment, contributing to the depletion of fossil fuels and increasing global warming. Because of the substantial contribution of building energy to these concerns, the intention should be not only to improve building energy efficiency but also to promote the use of renewable technologies, especially solar energy. Today building-integrated photovoltaic (BIPV) and building-integrated solar thermal (BIST) technologies are recognized by building designers as innovative technology for clean energy and greenhouse gas reduction, especially in cities, where multi-story buildings are dominant with limited roof area.

For the Mediterranean area, the high level of solar radiation and plentiful sunny hours make it appropriate for solar system installation, however, the development of solar energy is still limited. Moreover, due to the high population growth rate, lack of local resources, high energy price, and urbanization, one of the priorities in the Mediterranean area is to promote the energy efficiency of the building both on the supply side and demand side.

Therefore, this research aims to investigate the potential of installation of the photovoltaic (PV) and solar thermal (ST) technologies in the new multi-family residential building envelope in the Mediterranean area, taking Amman, Jordan, as a case study. The focus of this research is on the typical multi-family residential buildings in Amman, as it is the city where about 50% of the new construction in Jordan is taking place, and the residential buildings are the major consumers of energy and electricity in Jordan. The multi-family buildings also form about 75% of the total housing stock in Jordan. The typical multi-family building studied here is composed of five main floors, contains ten residential apartments; the area of each apartment is 150 m². It is assumed that the building is located in a common residential urbanized zone in Jordan, with 6 m sides offset and 8 m back offset, assuming that one side is facing the main street, and all the buildings have a maximum allowable height of 15 m. All the architectural parameters related to the multi-family buildings have been defined through analyzing the residential building stock in Jordan.

In order to achieve the research aim, the possibility of reducing the energy demand of the typical multi-family building in Amman, Jordan, through passive and architectural design strategies was firstly investigated. After that, different performance criteria were evaluated, mainly quantitative criteria including energy consumption, energy production, and life cycle assessment (energy, carbon, cost). In addition to the qualitative criteria, including visibility and functionality, the purpose here is to emphasize the substantial function of BIPV systems. Each performance criterion was assessed alone. Then, all the performance criteria results were presented in a decision support matrix, which can be used as a comparison to evaluate and identify the solar system's application of choice, based on the criteria of the user. Moreover, a new energy index was formulated to evaluate the overall annual energy performance of BIPV design in terms of multifunctional effects on building energy.

Different methods were adopted in this research; the qualitative criteria were evaluated based on the literature review analysis, while the quantitative criteria were evaluated by using different simulation software, previous literature review, and spreadsheet calculations.

Literature review analyses were conducted in order to identify the relevant possibilities and the aesthetical solution the market offers, and the multiple benefits for PV and ST integration. The knowledge acquired from this part played a significant role in choosing and designing the proposals of PV and ST installation into the multi-story building envelope. Regarding the simulation studies, different building and energy simulation software was used to simulate and optimize the energy performance of the typical multi-family building in Amman, Jordan, through passive and architectural design strategies, as well as to find out the optimum design of the energy system in terms of energy performance (energy demand of the system, and solar energy fraction), and to investigate the energy-saving potential of PV and ST systems with various designs (tilt angles, azimuth, installed area, etc.). For the building energy simulation, each zone in the building was modeled as a space of its own. The energy demand was calculated on an hourly basis for a period of a whole year. The results from the simulation analysis, related literature and guidelines were adopted to conduct a life cycle assessment through spreadsheet calculation, to determine the long-term performance in terms of energy and carbon emissions, as well as cost considerations, taking into account the current market practice. The cradle-to-grave approach was adapted for the environmental life cycle assessments.

The general conclusion of this research is that installing the PV modules into the multi-family buildings envelope in Amman, Jordan, makes a positive contribution in terms of energy performance, as PV systems can cover up to 97% of the new building electricity demand when they are installed on both the roof and south façade, and up to 43% is covered by installing the PV modules into the south facade. Regarding the environmental life cycle assessment, the results proved the carbon saving potential of all the proposed PV systems, as the energy payback time (EPBT) is between 1.5- 3.5 years and the carbon payback time (CPBT) is between 3.4- 7.8 years. However, for the life cycle cost assessment the result showed that due to high capital cost and low cost of electricity, neither system is currently feasible for investment, as the payback time (PBT) is between 9.0- 16 years. However, with future advances in each system and more efficient designs, the payback periods would become tangible and therefore yield better performances. Lastly, the results were used to derive a decision support matrix aimed at providing a friendly approach to facilitate the implementation of solar building applications.

Kurzfassung

In letzter Zeit wird sich die Gesellschaft zunehmend der negativen Auswirkungen auf die Umwelt durch hohe Energieverbräuche bewusst, die wesentlich zur Erschöpfung fossiler Brennstoffe und zur globalen Erwärmung beitragen. Aufgrund des wesentlichen Beitrages des Gebäudeenergiesektors sollte hier nicht nur die Gebäudeeffizienz gesteigert werden, sondern auch die Verwendung von regenerativen Energien mit Fokus auf solarer Energienutzung. Heutzutage sind in die Gebäudehülle integrierte Photovoltaik (PV) und Solarthermie (ST) von Gebäudeplanern anerkannte Technologien um saubere Energie zu generieren und Treibhausgase zu reduzieren. Diese integrierten Technologien können vor allem in Städten, in denen hauptsächlich mehrgeschossige Gebäude vorkommen und Dachflächen limitiert sind zum Einsatz kommen.

Für die im Mittelmeerraum herrschenden Bedingungen mit hoher solarer Einstrahlung und einer großen Anzahl an Sonnenstunden sind solare Systeme zwar äußerst geeignet, werden jedoch noch nicht in entsprechendem Maße eingesetzt. Darüber hinaus ist es aufgrund von der hohen Bevölkerungswachstumsrate, dem Mangel an lokalen Ressourcen, hohen Energiepreisen und der Urbanisierung eine der Prioritäten im Mittelmeerraum, die Energieeffizienz von Gebäuden sowohl auf Angebots- als auch auf Nachfrageseite zu fördern. Daher ist das Ziel dieses Forschungsbeitrages, die Potentiale von PV- und ST-Installation in der Gebäudehülle von neu errichteten Mehrfamilienhäusern (MFH) im Mittelmeerraum zu untersuchen, wobei Amman in Jordanien als Fallstudie herangezogen wird. Der Großteil des Wärme- und Stromverbrauches wird in Jordanien von Wohngebäuden verursacht und ca. 75 % des Wohngebäudebestandes besteht aus Mehrfamilienhäusern, weshalb der Fokus der Forschung auf diesem Gebäudetyp liegt. Da in Amman etwa 50 % der Neubauten in Jordanien errichtet werden, wurde dieser Standort als Untersuchungsgebiet gewählt. Das untersuchte typische MFH hat 5 Hauptgeschosse und besteht aus 10 Wohnungseinheiten mit einer Fläche von jeweils 150 m². Es wurde angenommen, dass sich das Gebäude einem stark urbanisierten Wohnungsgebiet befindet und zu den Seiten hin 6 m und an der Rückseite 8 m Freifläche angrenzt. Bei einer zulässigen Höhe von 15 m soll eine Seite des Gebäudes an eine Hauptstraße angrenzen. Alle architektonischen Parameter im Zusammenhang mit dem MFH in Jordanien wurden durch eine Analyse des Wohnungsbestandes von Jordanien definiert.

Um das Forschungsziel zu erreichen, wurde zunächst die Möglichkeit untersucht, den Energiebedarf des typischen MFH in Amman, Jordanien, durch passive und architektonische Gestaltungsstrategien zu reduzieren. Danach wurden verschiedene Bewertungsgrößen eingeführt, hauptsächlich quantitative Kriterien wie Energieverbrauch, Energieerzeugung und Ökobilanz (Energie, CO₂ und Kosten). Neben den qualitativen Kriterien wie Sichtbarkeit und Funktionalität werden bei den integrierten PV-Systemen auch die wesentlichen Funktionen hervorgehoben. Jedes Leistungskriterium wurde für sich im Einzelnen bewertet. Die Ergebnisse dieser Bewertung wurden in einer Matrix zusammengefasst, welche den Nutzer bei der Auswahl des gewünschten Solarsystems entsprechend den am wichtigsten erachteten Bewertungsgrößen unterstützen soll. Zusätzlich dazu wurde ein Energieindex formuliert, mittels welchem die jährliche Gesamtenergieeffizienz des integrierten PV-Konzeptes im Hinblick auf multifunktionale Auswirkungen auf die Gebäudeenergie bewertet werden kann.

In der durchgeführten Forschungsarbeit wurden folgende Methoden angewandt: die qualitativen Kriterien wurden auf Grundlage von Literaturrecherche evaluiert und die quantitativen Kriterien durch die Anwendung von verschiedener Simulationssoftware, vorangegangener Literaturrecherche und Tabellenkalkulation ermittelt. Es wurden Literaturrecherchen durchgeführt, um die relevanten Möglichkeiten und die ästhetischen Lösungen, die der Markt bietet, sowie die vielfältigen Vorteile für die Integration von PV und ST zu identifizieren. Die in diesem Zusammenhang gewonnenen Erkenntnisse spielten eine wichtige Rolle bei der Auswahl und Gestaltung der Vorschläge für die PV- und ST-Installation in der untersuchten mehrgeschossigen Gebäudehülle.

Im Rahmen der Simulationsstudien wurden zwei sich ergänzende Gebäude- und Energiesimulationssoftware eingesetzt, um die Energieeffizienz des typischen Mehrfamilienhauses in Amman, Jordanien, durch passive und architektonische Planungsstrategien zu simulieren und zu optimieren. Dieser Ansatz wurde auch genutzt, um die optimale Auslegung des Energiesystems in Bezug auf die Energieeffizienz (Energiebedarf des Systems und Solarenergieanteil) zu ermitteln und das Energieeinsparpotential von PV- und ST-Systemen mit verschiedenen Bauformen (Neigungswinkel, Azimut, installierte Fläche etc.) zu untersuchen. Für die Gebäudesimulationen wurde jede Zone im Gebäude als eigener Raum modelliert. Der Energiebedarf wurde auf Stundenbasis für den Zeitraum eines ganzen Jahres berechnet.

Die Ergebnisse der Simulationsanalyse und der vorangegangenen Literatur- und Richtlinienrecherche wurden verwendet, um unter Anwendung einer Tabellenkalkulation eine Ökobilanz aufzustellen. Auf dieser Basis wurde die langfristige Performance in Bezug auf Energie- und CO₂-Emissionen sowie Kostenüberlegungen unter Berücksichtigung der aktuellen Marktpraxis ermittelt. Für die durchgeführte Ökobilanzierung wurde der Cradle-to-Grave-Ansatz in angepasster Form verwendet.

Das allgemeine Fazit dieser Forschungsarbeit ist, dass die Installation von PV-Module in der Gebäudehülle von MFH in Amman, Jordanien, einen positiven Beitrag zur Energieeffizienz leisten kann. PV-Systeme können bis zu 97 % des Gebäudestrombedarfs von neu errichteten MFH decken, wenn sie gemeinsam an der Dach- und Südfassade installiert werden und bis zu 43 % durch ausschließliche Installation in der Südfassade. Die Durchführung der Ökobilanz zeigte, dass die Energierückgewinnungszeit für die untersuchten PV-Systeme –zwischen 1,5 und 3,5 Jahren und die CO₂-Rückgewinnungszeit zwischen 3,4 und 7,8 Jahren liegt. Für die Lebenszykluskostenbetrachtung zeigte das Ergebnis jedoch, dass aufgrund der hohen Investitionskosten und der niedrigen noch subventionierten Stromkosten in Jordanien derzeit kein System für Investitionen geeignet ist, da die Amortisationszeit zwischen 9 und 16 Jahren liegt. Mit weiterentwickelten Systemen und effizienteren Designs würden diese Amortisationszeiten jedoch vermindert und somit bessere Leistungen erzielt werden können. Schließlich wurden die Ergebnisse genutzt, um eine Matrix abzuleiten, die bei der Entscheidung für Umsetzungsmaßnahmen von solaren Gebäudeanwendungen auf benutzerfreundliche Weise unterstützen soll.

Contents

1 Introduction	2
1.1 Motivation	2
1.2 Research aims	7
1.3 Research questions	7
1.4 Research structure and approach overview	8
2 Research context	10
2.1 Overview	10
2.2 Potential of solar energy in Jordan	12
2.3 Climate analysis of Amman	13
2.4 Energy in Jordan	17
2.5 Jordan renewable energy strategies and regulations	20
2.6 Photovoltaics and solar thermal technology market in Jordan	23
2.7 Photovoltaics and solar thermal technology cost in Jordan	25
2.8 Solar energy application in Jordan	25
2.9 Solar renewable energy barriers and recommendations	27
2.10 Residential stock in Amman, Jordan	30
3 Literature review	36
3.1 Introduction	36
3.2 Building-integrated photovoltaic (BIPV)	36
3.2.1 BIPV definition	36
3.2.2 BIPV markets	37
3.2.3 BIPV systems classifications	38
3.2.4 Life cycle cost assessment	45
3.2.5 Carbon and energy life cycle assessment	46
3.2.6 Energy performances of BIPV systems	48
3.3 Building-integrated solar thermal (BIST)	50
3.3.1 BIST definition and advantages	50
3.3.2 BIST market	50
3.3.3 BIST classifications	52
3.3.4 Life cycle cost assessment	58
3.3.5 Carbon and energy life cycle assessment	60

3.3.6 Energy performance of BIST	61
3.4 Summary and identification of knowledge gap.....	63
4 Methodology	64
4.1 Research approach.....	64
4.2 Software selections.....	65
4.3 Building energy improvement.....	67
4.4 Energy supply system improvement	68
4.5 ST and PV applications performance evaluation	68
4.5.1 Overall energy performance (net primary energy demand)	70
4.5.2 Environmental life cycle assessment.....	70
4.5.3 Life cycle economic assessment.....	71
4.5.4 Qualitative criteria	72
4.6 Decision support matrix	74
5 Improving energy performance of the typical multi-family building	76
5.1 Introduction	76
5.2 Base case model setup.....	76
5.3 Energy performance of the base case model	85
5.4 Energy demand optimization strategies.....	90
5.5 Results and discussion.....	93
5.6 Summary	103
6 Energy performance of solar energy systems	104
6.1 Introduction	104
6.2 System configurations	104
6.3 Simulation input and systems design	107
6.4 Results and discussion.....	119
6.5 Potential of battery installation.....	127
6.6 Summary	132
7 ST and PV roof and façade applications	134
7.1 Introduction	134
7.2 Assessment of the PV and ST potential area.....	134
7.3 Roof application	142
7.4 Façade BIPV application.....	148
7.4.1 Defining façade photovoltaic systems.....	149

7.4.2 Selection of BIPV modules and Polysun input	155
7.4.3 Impacts of BIPV on building energy performance.....	159
7.5 Summary	167
8 Life cycle assessment of photovoltaic applications	168
8.1 Introduction	168
8.2 Energy life cycle performance	168
8.3 Environmental life cycle performance	170
8.3.1 Manufacturing of PV module	172
8.3.2 Transport to site	178
8.3.3 On-site installation.....	179
8.3.4 Operation and maintenance	179
8.3.5 Decommissioning, disposal, and recycling of waste	180
8.3.6 Total life cycle environmental performance.....	180
8.4 Economic life cycle performance.....	185
8.4.1 Assumptions and values	185
8.4.2 Results of economic performance	187
8.5 Summary	193
9 Multi-assessment support matrix	194
9.1 Criteria for support matrix.....	194
9.2 Development of decision support matrix	195
9.3 Summary	199
10 Research conclusions	200
10.1 Summary and outlook	200
10.2 Research limitations and future work.....	208
References	210
List of Acronyms.....	226
List of Figures	228
Appendixes.....	234

1 Introduction

1.1 Motivation

According to the International Energy Agency, it is estimated that about 40% of the worldwide primary energy is consumed by the building sector, more than half of this energy is used for space heating, cooling, and hot water preparation. This energy is mostly generated by burning fossil fuels (IEA, 2017a), contributes to CO₂ emissions and has an impact on climate change (Koo et al., 2017). It is also expected that the world's energy demand will increase in the future due to many factors, such as population growth, improving quality of life and increasing demand for building services. This leads to increasing energy prices and levels of energy poverty (IEA, 2017a; Prieto *et al.*, 2017). Moreover, implementing energy-saving measures will not be sufficient to cope with increasing building energy consumption (Prieto et al., 2017). Therefore, it is necessary for further prosperity to ensure a secure, equitable, affordable and sustainable supply of energy using renewable energy sources.

Among the different resources, solar energy is relatively the most potential resource, especially in the Mediterranean area (GTZ, 2009), due to its high level of solar radiation and longtime of sunny hours. Particularly along the southern and eastern shore with more than 2,000 hours/year, the Global Horizontal Irradiance (GHI) ranges in the area between 1,600 kWh/m²/year to 2,600 kWh/m²/year. While in the northern Mediterranean area the potential is lower but remains very interesting with a GHI ranging from about 1,000 kWh/m²/year to 1,600 kWh/m²/year (see Figure 1-1).

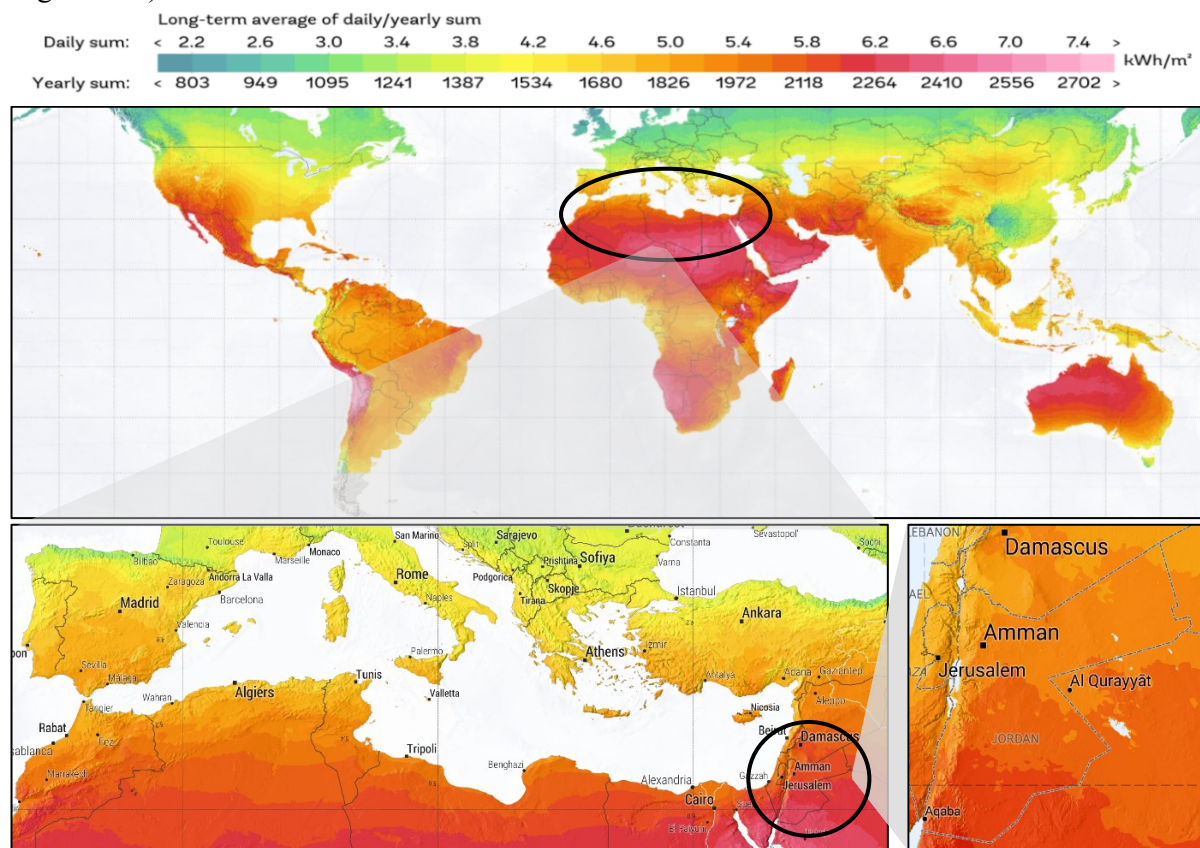


Figure 1-1: Global horizontal Irradiance (GHI), world, Mediterranean area, and Jordan Maps. Source of pictures: (World bank group, 2019).

Such favorable condition makes the development of solar technologies, particularly suitable in the Mediterranean area. However, their contribution to the total primary energy supply is still fairly limited, especially in the northern and eastern Mediterranean area (see Figure 1-2), as the fossil fuels (oil, gas, and coal) make up 80% of the energy supply: 94% in the southern and eastern countries, 75% of the northern countries of the Mediterranean area (OME, 2012; Pittaluga, 2013; Salem and Kinab, 2015). Moreover, the average primary energy demand is expected to rise by 4.2%/year in the southern and eastern countries against 1.1% of the northern countries of the Mediterranean area, and the electricity consumption rises by 6% in southern and eastern countries vs. 1.7% of the northern countries of the Mediterranean area (Hafner *et al.*, 2012; OME, 2012). Accordingly, the energy growth factors in the south and the east Mediterranean area are significantly stronger, particularly due to demography, population growth, increasing living standards and business needs (Hafner *et al.*, 2012). Also, due to the political situation, especially in the eastern Mediterranean countries, more specifically, Jordan is facing a real challenge, as it located in the center of the conflict zone with its political stability situation has been an attraction for the surrounding refugees. It has affected the population growth, which leads to an increase in housing and energy demand (Alnsour, 2016b). Moreover, it is lacking indigenous energy resources and relies on imported gas and oil from foreign countries. According to the ministry of energy and mineral resources, Jordan imports around 97% of its energy needs in 2015 (see Figure 1-2), which causes a financial burden on the national economy in Jordan (MEMR, 2017).

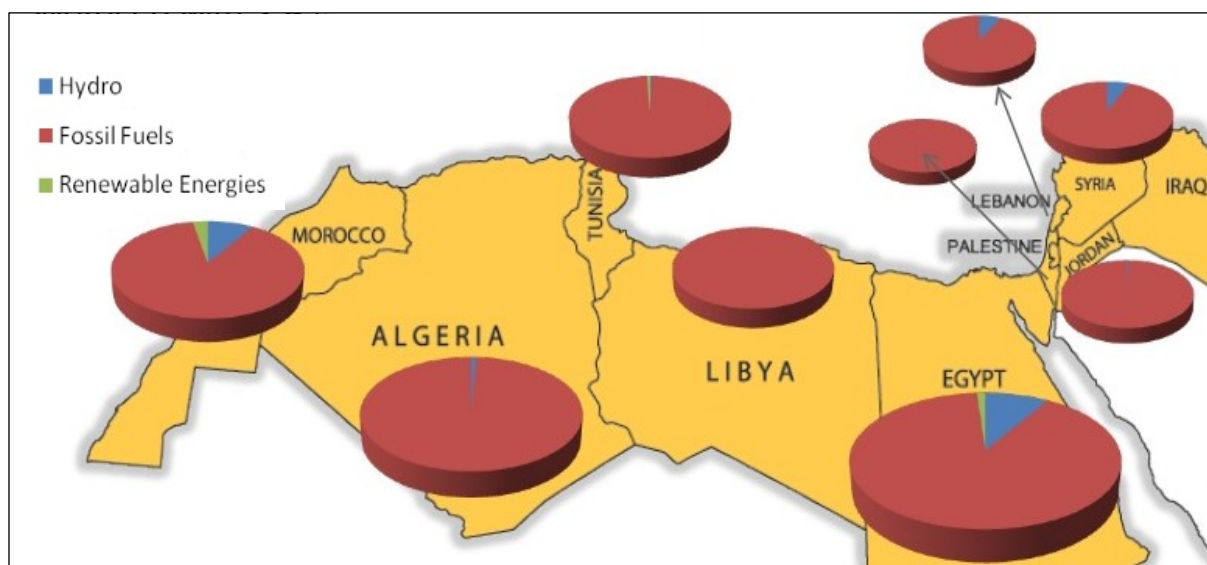


Figure 1-2: Primary energy consumption mix for the southern and eastern Mediterranean countries in 2011. Source: (Mahmoud, 2013).

Residential buildings, in particular, are major consumers of energy in Jordan with up to 24% of the total energy consumed and about 42% of the total consumed electricity (MEMR, 2018).

Moreover, during the last two decades, the building and construction sector in Jordan has accelerated at a high rate, and 75% of the growth results from the residential sector (RSS, 2007). Amman, the capital of Jordan, is the city where about 45% of the new constructions in Jordan are taking place. The multi-family apartment buildings in the country form 73% of the total housing stock and more than 80% of all buildings in Jordan (Younis, 2017).

Despite the high solar potential of Jordan, it has approximately 300 sunny days annually with an average annual irradiation of 2,050 kWh/m²/year. Solar energy technologies are not extensively used except for solar water heaters (SWH), which are used for domestic water heating, it is an economically feasible technology to use, compared to all other conventional water heating systems (Kiki *et al.*, 2008; AlShamaileh, 2010; Etier, Al and Ababne, 2010; Sakhrieh and Al-Ghandoor, 2013; Abdelhai, 2014). Regarding the photovoltaics application in Jordan, it is still a new technology and it is not spread (Aberg *et al.*, 2014; Knaack *et al.*, 2014). Moreover, there are a few studies that have been made in the field of solar renewable energy and most of them focused on the technical and economic aspects neglecting the architecture integration aspects (Al-adwan, 2013; Tous, 2013).

In view of the situation explained in the above discussion (high population growth rate, lack of local resources, high energy price, and urbanization), one of the priorities in the Mediterranean countries, and more specifically in Jordan, is to promote the energy efficiency of the building both on supply-side and demand-side. And this is can be done through design and construct the new buildings to consume as less energy as possible by considering the passive and architectural design strategies and cover the increasing demand for energy, as much as possible, from solar energy, in particular, photovoltaic (PV) and solar thermal (ST) technologies.

PV and ST technologies are commonly mounted onto buildings' roofs as pure technical elements. Roofs are usually out of sight, especially in multi-story buildings, and by placing the PV and ST, the designers tried to hide them to avoid negative impacts on the building's aesthetic. However, recently, due to growing urbanization, multi-story buildings are dominant with limited roof area (Abdelhai, 2014; Aberg *et al.*, 2014). Therefore, additional solar-accessible areas (such as external façade) are needed to provide the necessary energy for building applications.

When the PV and ST technologies are integrated into the building facade, they acts as a multi-functional integral elements (Grete, Prof, and Mnal, 2001; Buker and Riffat, 2015); they do not only fulfill a technical energy purpose (i.e. heating, cooling, and power) but also contribute to the building fabric from an architectural and materials perspective (Hestnes, 1999; Munari Probst and Roecker, 2007). Also, they could affect the amount of heat transfer through the building envelope, and accordingly the energy demand in the building, since they change the thermal resistance of the building envelope (Lai and Hokoi, 2015). In addition, it can also eliminates the need for new land and an additional support structure, which provides a further advantage of cost-saving (Basnet, 2012). Moreover, integration of PV and ST technologies represents a real challenge to the architects to achieve multifunctional roles, as various factors must be considered, such as the photovoltaic module temperature, installation angle, and orientation, shading, effect of PV and ST integration on building thermal performance, aesthetic, installation and maintenance cost, etc. (Kaan and Reijenga, 2004).

Despite the various benefits and potential of BIPV and BIST systems, their wider take-up has been faced with several issues, such as the lack of research exists on the performance of multifunctional PV and ST facade in the Mediterranean countries and more specifically in Jordan (Mandalaki, Tsoutsos and Papamanolis, 2014). In addition to the lack of simple tools for the early design stage, reduce the confidence of architects in adopting BIPV and BIST systems (IEA, 2012; Jelle, 2016), and lack of knowledge of technological possibilities and product options (IEA, 2012; Bonomo, Frontini and Chatzipanagi, 2015).

Furthermore, the lack of lifetime performance information of BIPV and BIST systems in environmental and economic terms also serve as barriers, especially since BIPV and BIST systems are known for their high costs of implementation (Chrysovalantou Lamnatou *et al.*, 2015; Li, Qu and Peng, 2017). Therefore, there is a need for knowledge of energy performance that can assist the selection and application of BIPV and BIST in the early stages of building design, to promote the use of BIPV and BIST to further enhance the energy-efficient capabilities of buildings. Targeting to professionals such as architects and building owners, they can include information on long-term economic and environmental impacts, especially since the cost is often a deciding factor.

Based on the above discussion, this research investigates the potential and performance of BIPV and BIST technologies installation into a multi-family residential building in the Mediterranean area, taking the capital of Jordan, Amman, as a case study. A multi assessment approach is applied in this research, considering different performance criteria, including the building energy performance (heating, cooling and lighting energy demand and energy production) and the aesthetic sides of buildings, the lifetime energy, environmental and economic performance, as well as the qualitative (visibility and functionality) criteria. In addition to the installation of PV and ST systems to the building, the potential in reducing the energy demand of the typical new multi-family building in Jordan through passive and architectural design is also investigated.

The research focused on the integration of PV & ST technology into the new building envelope, since ST and PV facilities can be particularly well-integrated if they are planned along with the building as a whole from very early in the design process (Martín-Chivelet *et al.*, 2018). As the study focused on the new building (design stage), simulation software has been used to investigate the energy performance of the active solar systems and the building for different integration possibilities, in order to evaluate the existing building's performance and estimate energy savings and production through different proposed design options. This will help to evaluate the feasibility of PV and ST systems integration into buildings and to estimate the contribution of this renewable energy solution. Moreover, it will provide building designers with additional first-hand information on the energy efficiency of BIPV and/or BIST to increase and enhance widespread adoption. Multiple benefits can also be used as a comparison to evaluate and identify the BIPV and/or BIST technology of choice, depending on the criteria of the user.

It is important to mention that although this research focused on the Mediterranean area, the outcomes can be adapted to the cities that have almost the same climate condition in terms of average, max, and minimum temperatures, and annual global horizontal radiation (see Figure 1-3). Moreover, other considerations have to be taken into account when it adopted for other countries such as electricity infrastructure, and governmental policies.

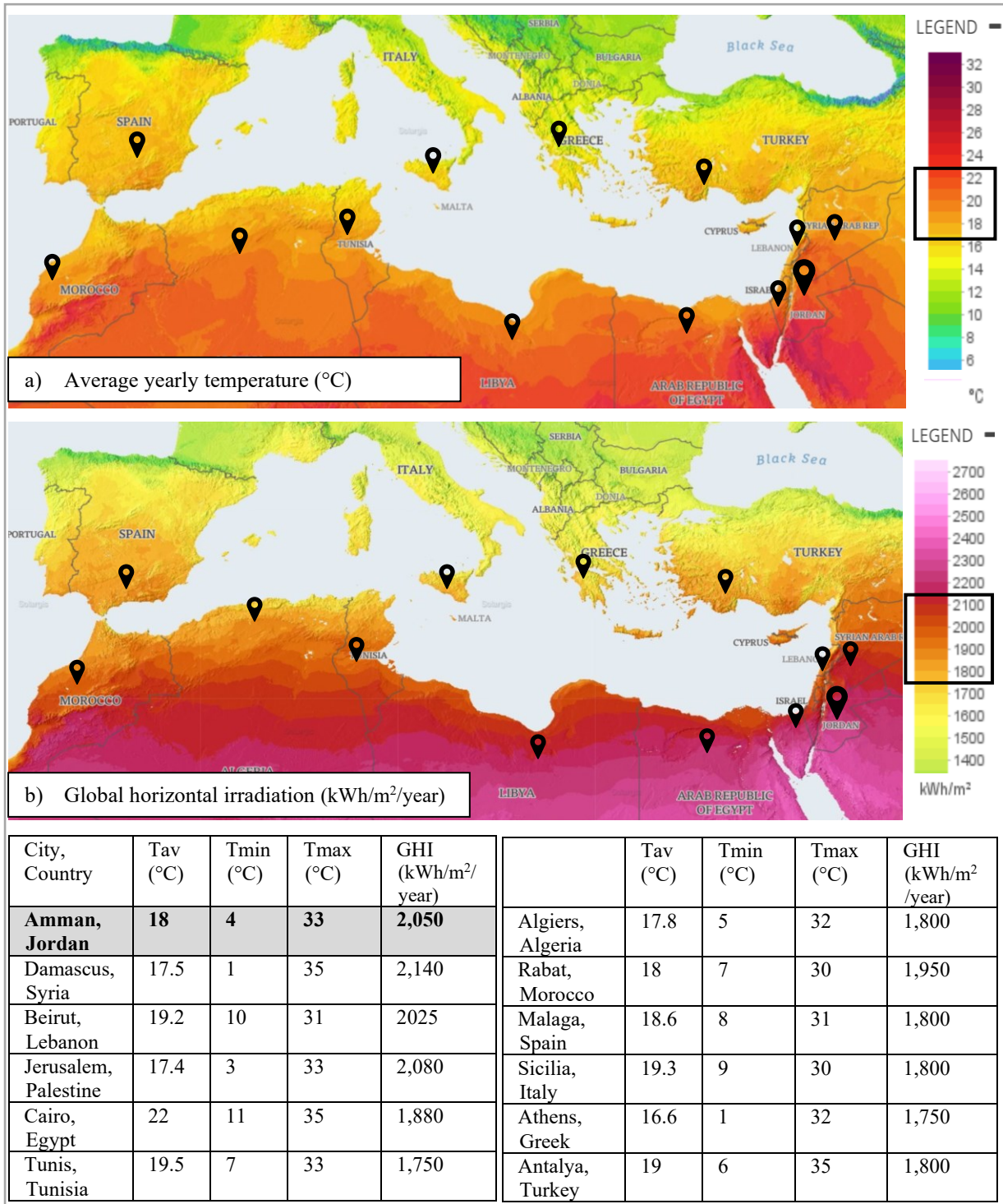


Figure 1-3: Climate overview for the Mediterranean cities around the Red sea including: a) Annual average temperature b) Global horizontal irradiation. Source of pictures: (World bank group, 2019), Souse of date: (Meteonorm 7, 2018).

1.2 Research aims

Based on the above discussion, the main aim of this research is:

- To assess the overall potential benefits of adopting different possibilities and solutions of the architectural integration of PV and ST technologies into a multi-family building in Amman, Jordan. Considering different aspects; enhancing the overall architectural expression of the building in addition to the energy generation and improving building energy performance. Also, a life cycle assessment is performed to identify the long-term benefits, in terms of energy, environmental and economic performance. The knowledge created in this area serves to provide information for architects to assist them in adopting photovoltaic technology in a multi-family building in Amman, Jordan.

The research also includes other minor aims:

- To explore the reasons for the limited adoption of PV and ST systems in building envelopes.
- To examine the recommendations on the architectural integration quality of PV and ST technologies.
- To improve the multi-family energy performance by improving the building envelope, applying passive strategies and the installation of energy-efficient systems.
- Develop an energy index (net primary energy demand) that considers the overall energy performance of the building (energy production, energy saving).
- Develop a graphical representation of the building-integrated solar systems that consider lifetime energy, carbon, cost and aesthetic.

1.3 Research questions

In order to accomplish the research aims, the research explores the following key question:

- What is the potential of integrated PV and ST technologies into the new multi-family buildings in Amman, Jordan, in terms of energy, environmental, cost and qualitative (visibility and functionality) performance?

And the sub-questions:

- What are the reasons for the low take-up of photovoltaic and solar thermal collector systems in a multi-family residential building in the Mediterranean area?
- How can the energy performance of the multi-family building in Amman, Jordan be enhanced by improving the building envelope, passive measures, and energy-efficient systems?
- Where in the building envelope should the active technologies be installed, and how should they be designed?
- How much energy can the solar active systems cover for the new multi-family building?
- What is the energy, environmental and economic performance of a solar system installed in a multi-family building in Amman, Jordan over its lifetime?

1.4 Research structure and approach overview

The research thesis is organized into ten chapters. The overall structure of the thesis is summarized in Figure 1-4 with each chapter paired with a sentence about its key content where each working process can be followed.

The current chapter (**Chapter 0**) serves as an introductory chapter that discusses the research motivation, the research aims, and questions. Also, the main content of the thesis is outlined. **Chapter 2** presents the research context, climate, and energy analysis. In **Chapter 3**, a review of BIPV and BIST and their technical features, prices, technologies and the most common solutions on the building roofs and facades are presented. In addition, previous studies and researches related to the energy performance of the BIPV and BIST are reviewed. As buildings are usually designed to last for many years, the importance of life cycle assessment is also emphasized. **Chapter 4** presents the main research methodology for this research. The possibility of reducing the energy demand of the typical multi-family building in Amman, Jordan by means of passive design strategies using simulation software is presented in **Chapter 5**. After that in **Chapter 6**, different solar supply energy systems are proposed and compared with each other, and with a reference system (a conventional Jordanian energy supply system without solar technologies). The potential of battery installation in the photovoltaic system for the improved multi-family building in Amman Jordan is also investigated using simulation software. In **Chapter 7**, the potential of implementing the PV and ST on the roof and facades of the new multi-story building in Amman, Jordan is investigated, and several arrangements of the solar thermal collectors and photovoltaic modules application on the roof and façade are proposed and investigated through varied cases. The resulting impact is analyzed through the estimation of the electricity yield, and the impact of the facade PV cases on the energy demand for heating, cooling and lighting in the space with simulation software. After that, an environmental and economic life cycle assessment is performed in **Chapter 8**. **Chapter 9** a decision-support matrix is developed to aid architects, building designers, clients, etc., in making decisions pertaining to the choice of the solar energy system. The decision matrix consists of several criteria which are based on the results generated in the previous chapters. The thesis concludes with **Chapter 10**, which includes key findings and recommendations. The major contributions and significance of the study are highlighted, as well as, the research limitations and recommendations for future research.

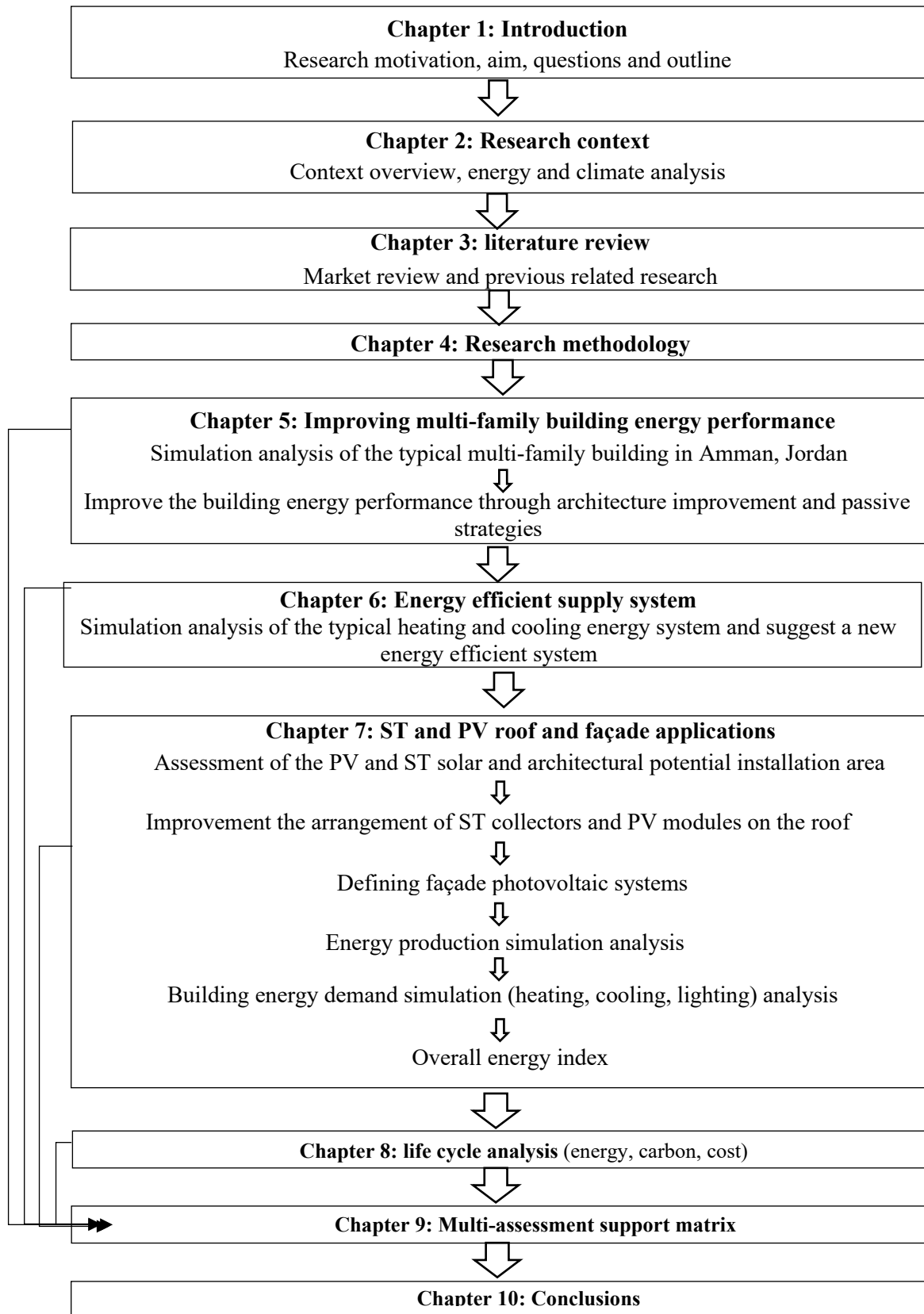


Figure 1-4: Research thesis structure.

2 Research context

2.1 Overview

Jordan is located between 29°11' North and 33°22' North, and between 34°19' East and 39°18' East, it is total area: 92,3 km²; 91.9 km² land, and 329 km² water. Jordan is a small country situated in southwestern Asia in the east of the Mediterranean sea, bounded by Syria on the north, by Saudi Arabia on the south, by Iraq on the east, and Palestine on the west. Jordan has access to the Red Sea through the port city of Aqaba. The capital city is Amman, there are also other important cities such as Irbid, Ma'an and Al Karak (Figure 2-1) (Jordan Meteorological Department, 2003).

The principal geographical feature of Jordan is an arid plateau that thrusts abruptly upward from the eastern shores of the River Jordan and the Dead Sea, reaching a height of about 610 to 915 m (2,000 to 3,000 ft), then sloping gently down towards the Syrian desert in the extreme east of the country (Jordan Meteorological Department, 2003).

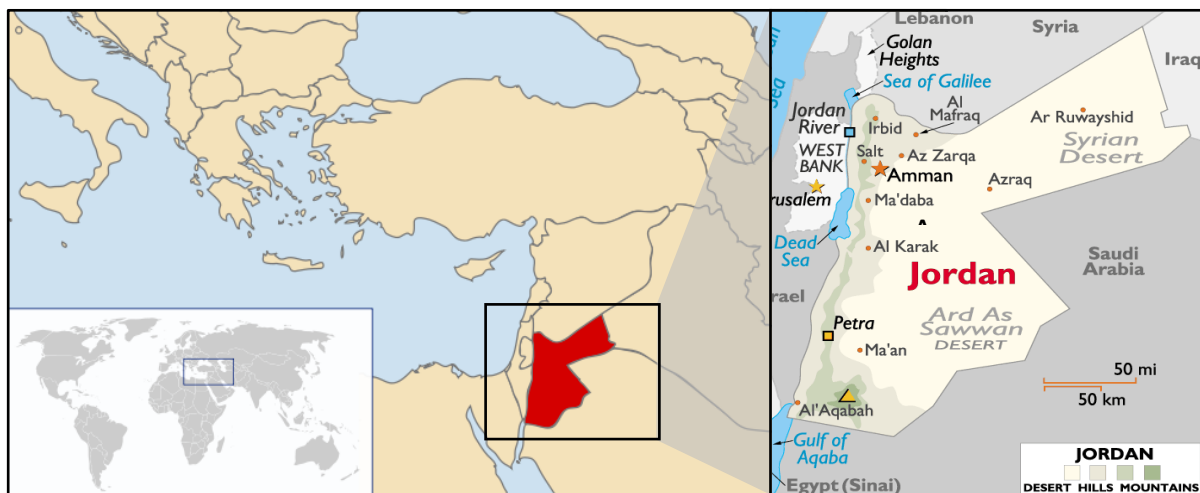


Figure 2-1: Jordan location, map. Source of pictures: (Abdalla, 2013; Maps Jordan, 2019).

In the past 50 years, Jordan has been a platform for accommodating multiple surrounding countries. Being in the center of the conflict zone, its political stability situation has been an attraction for the surrounding refugees. It has affected the population growth (Figure 2-2), which leads to an increase in housing demand and energy demand (Alnsour, 2016b).

According to the results of the general population and housing census in 2015, the total number of Jordan's population reached 9.5 million. About 6.6 million of the population are Jordanians (i.e., 70%), and the population growth is 2.3%/year of its own citizens, around 40% of the total population lives in Amman (Jordanian Department of Statistics, 2015; Alnsour, 2016a).

The housing sector has observed a massive increase in housing units from about 376,800 units in 1979, to 835,600 units in 1994, and about 1.2 million units in 2010, around 32,000 housing units are required annually in Jordan, Amman is the city where 45% of the new construction in Jordan taking place (Jordanian Department of Statistics, 2015).

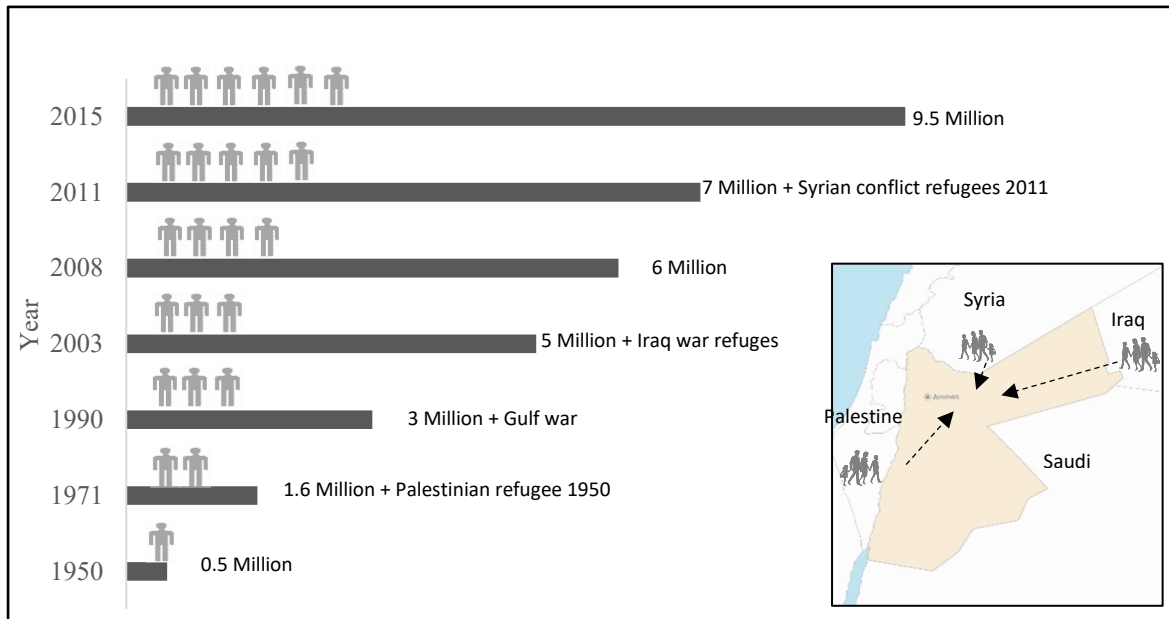


Figure 2-2: Jordan population growth from 1950-2015. Source of data: (Jordanian Department of Statistics, 2015).

Climate and topography overview

Jordan has a range of geographic features, from Jordan Rift Valley in the west to the desert plateau of the east, with a range of small hills running in between. Although most of the Jordan area is classified as a hot-arid climate, it can be divided into three climatic regions (Al-Asir *et al.*, 2009a), see Figure 2-3. According to the geographic and topographic characteristic, each with a distinct climate as follows:



Figure 2-3: Climate regions in Jordan. Source: (Al-Asir *et al.*, 2009a).

1) The Jordan Rift Valley (The Ghor) Region: Ghor area is very similar to the subtropical climate region. This region runs along the whole length of Jordan. The Rift Valley is below sea level of over 400 meters at the Dead Sea, turning into the most minimal spot on earth, and extends a maximum width of 15 km. The Rift Valley ends in the south at Aqaba. The weather is very hot in the summer and warm in winter. During summer the mean daily maximum temperature is around 39 °C. During winter the mean minimum temperature is about 9 °C, rainfall amount around 80-390 mm (Al-Asir *et al.*, 2009).

2) The highlands (mountain) region: Moderate climate region, warm dry summer and cold wet winter characterize the climate in these regions with a good amount of rainfall. The main meteorological station in this zone is at the University of Jordan. It comprises mountainous and hilly regions that run through Jordan from north to south. It reaches the highest rainfall in Jordan, particularly in the northern part of this region such as Ras Munif and Irbid. The altitude of the highland's region varies from 500-1,000 m reaching 1,500 m in the south. Generally, this region is characterized by its pleasant climate, and most of the population of Jordan lives in this region, including the capital city Amman, and other major cities such as Irbid, Zarqa, Karak. It is characterized by cold wet winter and cool dry summer varies from one area to another. In January the average temperature in Amman is 8 °C with an average minimum of 3 °C, while in August the average temperature is 30 °C and the average maximum is 32.5 °C. The temperature during the hottest spells reached 43 °C, the average daily range between day and night is about 14 °C in Amman. The annual rainfall in Amman is about 340 mm (Al-Asir *et al.*, 2009).

3) The Desert Region (Badia): Hot-arid region, very hot dry summer and very cold winter characterize the climate in these regions with very little precipitation and clear sky during most of the year. This region occupies about two-thirds of the total area in Jordan. It extends in the east Jordan between the western heights and the eastern border of both Iraq and Saudi Arabia. There is an extreme variation in the climate of the desert between day and night, and between summer and winter. Summer temperatures can exceed 40 °C. While in winter, it can be bitterly cold, dry and windy during nights and early mornings. The temperature is low with an average daily of 8.6 °C with a minimum of 3 °C, and sometimes the temperature decreases to below freezing point. The desert area has very little rainfall; the average annual rainfall in this region is less than 50 mm (Al-Asir *et al.*, 2009).

2.2 Potential of solar energy in Jordan

Jordan is honored with an abundant supply of solar energy since it lies in the “global Sunbelt”, the daily average solar irradiance (average radiation intensity on a horizontal surface) ranges between 4-8 kWh/m².day.

This corresponds to a total annual global horizontal radiation of 1,400-2,300 kWh/m²/year (see Figure 2-4). The average sunshine length is more than 300 days/year.

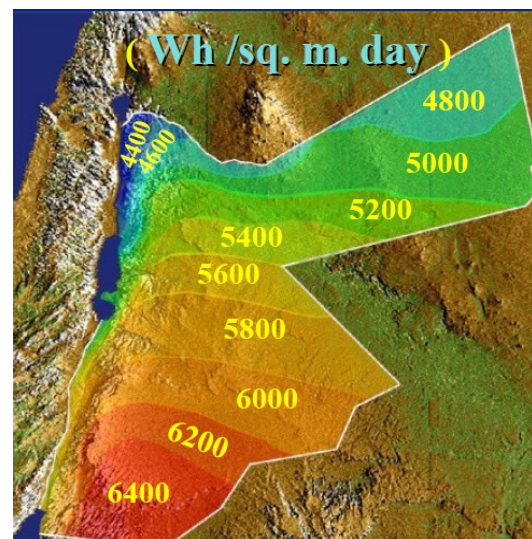


Figure 2-4: Annual global horizontal irradiance in Wh/m².day in Jordan. Source: (Abdalla, 2013).

2.3 Climate analysis of Amman

This study is focused on the capital of Jordan, Amman which is located in highlands region, because Amman is the most densely populated region in Jordan (Al-Asir *et al.*, 2009), and due to the high rate of investments in building industry over the last few decades (Potter *et al.*, 2009; Goussous, Siam and Alzoubi, 2014). Therefore, in this section, climatic characteristics of Amman is analyzed using different tools, such as Excel charts, Ecotect weather tool, climate consultant. This climate data provided by the Meteonorm 7 software which will be used later in this research as input in different simulation software mainly IDA ICE and Polysun, more details about the used simulation tools are described in Chapter 4.

- **Air temperature**

The coldest month is January with an average temperature of 8 °C and minimum mean temperature 2 °C; while the warmest month is July with an average temperature of 27 °C and the maximum average temperature is 35 °C (Figure 2-5). There is a high range of mean diurnal temperatures of about 12.5 °C throughout the year (Meteonorm 7, 2018).

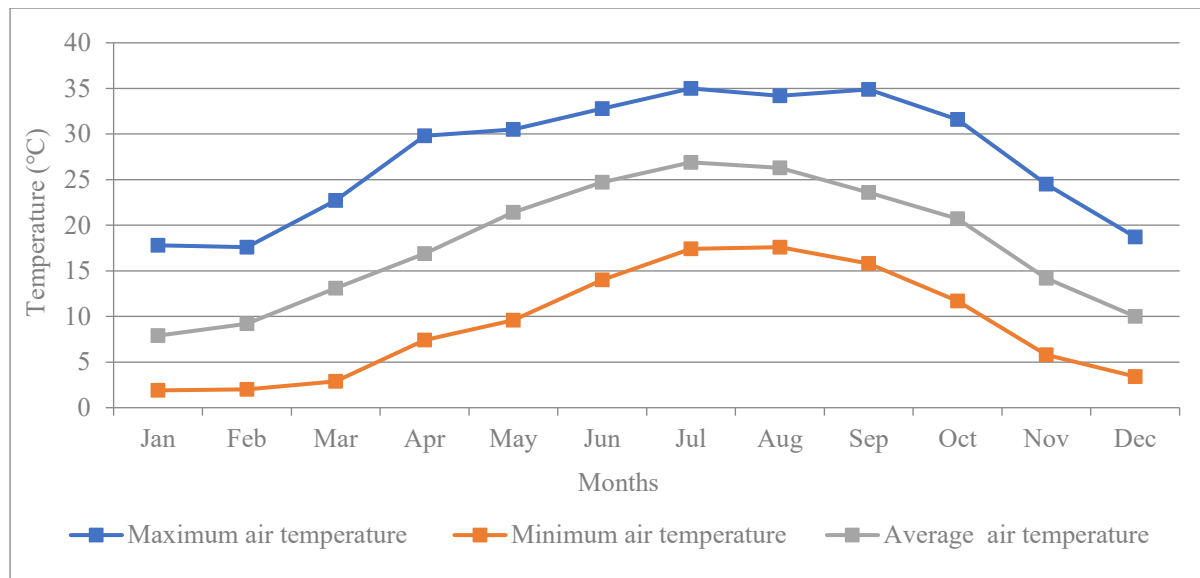


Figure 2-5: Mean minimum, maximum and average temperatures in Amman. Source of weather data: “AMMAN JO” weather file from Meteonorm 7.

- **Relative humidity and precipitation**

As illustrated in Figure 2-6, the mean relative humidity in Amman ranges from about 25% in May to about 60% in January and the rainy season is between October and May, with about 70% of the annual rainfall occurring through December to March, while the driest months are June, July, August, and September with an average of 0 mm of rainfall (Meteonorm 7, 2018).

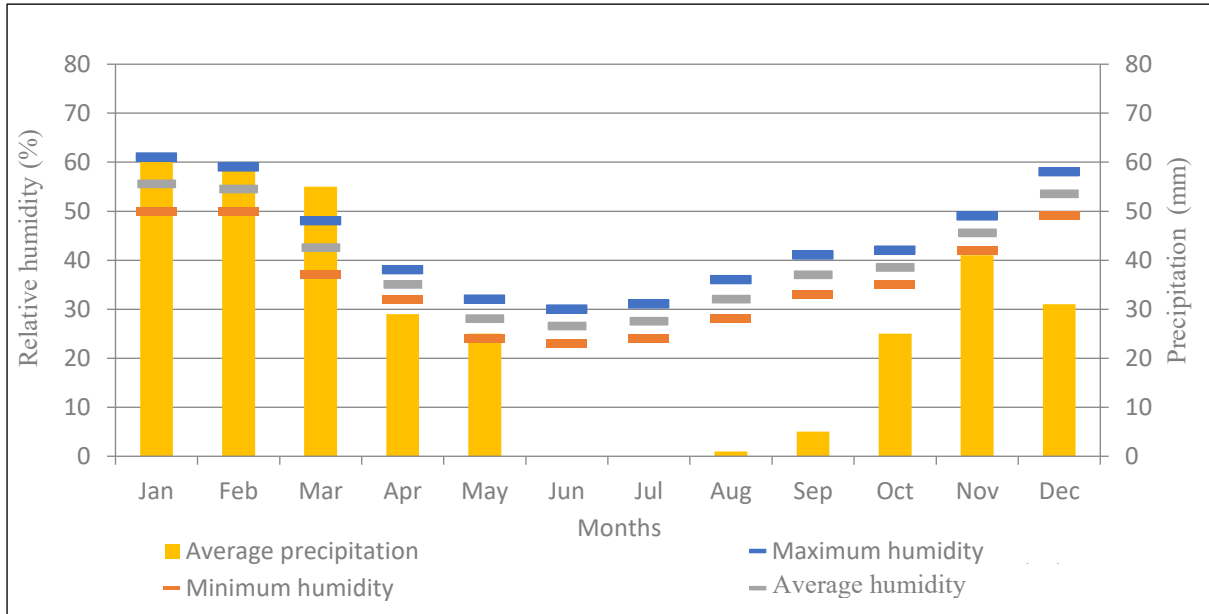


Figure 2-6: Mean minimum, maximum and average relative humidity and average precipitation in Amman. Source of weather data: “AMMAN JO” weather file from Meteonorm 7.

• Wind direction and speed

As illustrated in Figure 2-7, the average wind speeds in Amman vary from 1.6 m/s to 3.7 m/s throughout the year. The highest mean wind speed occurs in July, while the lowest average wind speed occurs in October. Amman is mainly influenced by two wind systems: the north-westerly wind during the summer and the north-easterly wind during the winter. But, during the months of July and August Jordan is hit by dry winds and dusty winds from the southeast. Bring the country its most uncomfortable weather, locally these winds are called Khamsin (Meteonorm 7, 2018).

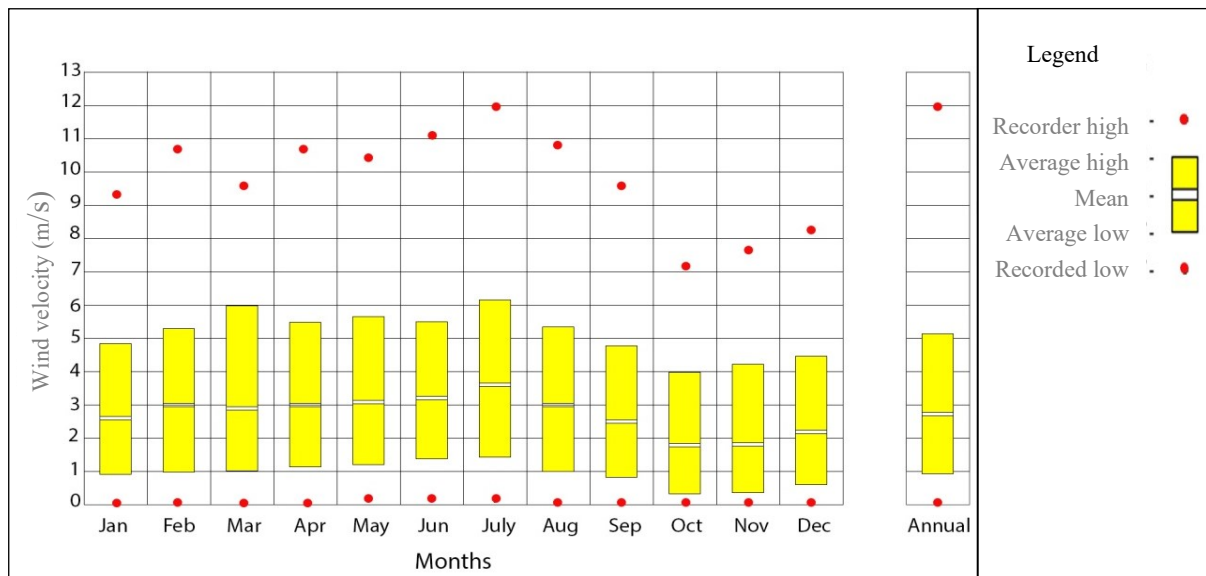


Figure 2-7: Wind velocity range in Amman, Jordan. Source of weather data: “AMMAN JO” weather file from Meteonorm 7.

- **Solar radiation**

The annual global radiation in Amman is 2,049 kWh/m². Figure 2-8 below, illustrate the monthly solar radiation in Amman, the highest average direct solar radiation in Amman is 855 W/m² in June, while the lowest average solar radiation is 573 W/m² in January. While, the highest diffuse solar radiation is 200 W/m² in April, while the lowest diffuse solar radiation is 130 W/m² in October. On average there are 3,602 hours of sunshine per year in Amman, as illustrated in Figure 2-9, the lowest means hours of sunlight are in February and December with about 6 hours each day, while the highest means hours of sunlight are in July with about 13 hours per day (Meteonorm 7, 2018).

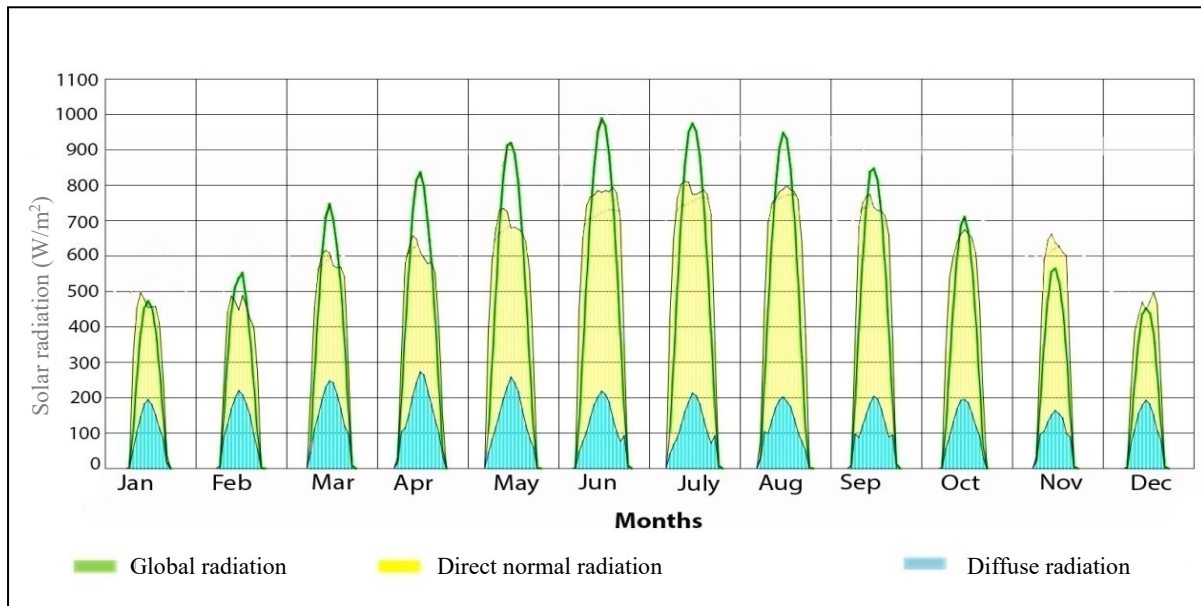


Figure 2-8: Monthly average diurnal solar radiation in Amman. Source of weather data: “AMMAN JO” weather file from Meteonorm 7.

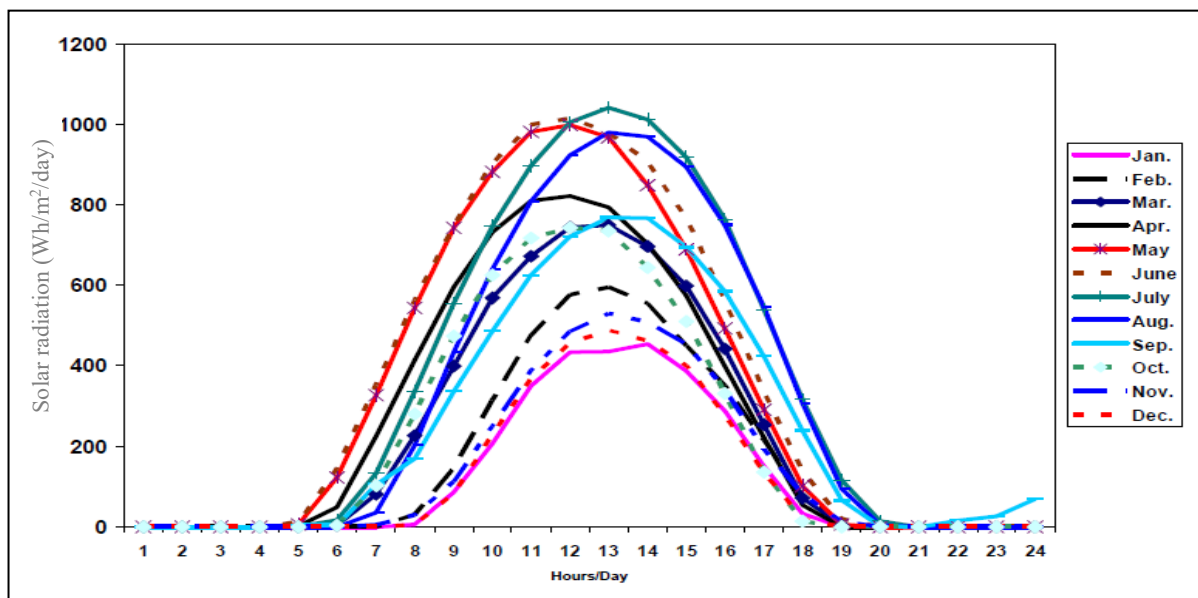


Figure 2-9: Daily solar radiation profile for Amman for each month. Source: (Jordan Climatological Handbook, 2003).

- **Sun path diagram for Amman**

The sun path diagram is a key concept when designing a solar system to determine the most efficient orientation of the solar technology, it gives the sun location (azimuth and altitude) on any given date and time for a given location. Figure 2-10 below, illustrates the sun path diagram of Amman and the solar altitude in Amman for the summer solstice (21 of June), the winter solstice (21 of December), and equinox (March and September). The sun spends most of its time in the south, the highest altitude at the summer solstice in Amman is very high about 81° . Therefore, the horizontal surfaces receive a high amount of solar radiation especially around midday on summer days. While in winter the sun doesn't climb very high in the sky, the maximum sun altitude on December 21 is only 34.3° , therefore vertical surface, particularly south-facing surfaces, receive enough solar radiation for passive heating purpose in winter.

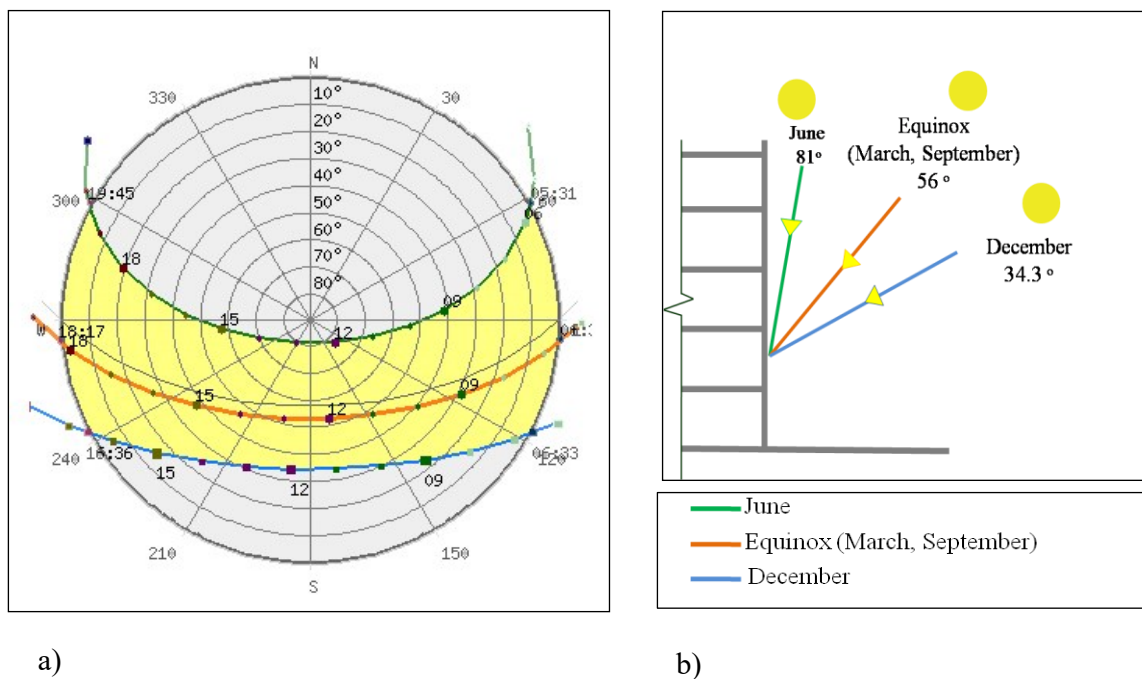


Figure 2-10: a) Sun path diagram for Amman. Source: The Climate Consultant Tool 2016. b) Sun altitude at 12:00 pm in different season in Amman. Source of weather data: "AMMAN JO" weather file from Meteonorm 7.

For the building-integrated photovoltaic and solar thermal technologies, it is important to analysis the available solar radiation in a different direction and slope surfaces, more analyses are presented in Chapter 7.2.

2.4 Energy in Jordan

Overview

Jordan is lacking indigenous energy resources and relies on imported gas and oil from foreign countries. According to the ministry of energy and mineral resources, Jordan imports around 97% of its energy needs in 2015, which causes a financial burden on the national economy in Jordan (MEMR, 2017). The annual energy consumption has been rapidly increasing over the past few years due to rapid population growth with about 2.3%/year and an increase in industrial activities, and this consequently led to increasing environmental pollution and economic difficulties (Jaber and Probert, 2002). As illustrated in Figure 2-11 below, the energy demand in Jordan has doubled during the last 20 years, and is expected to continue at the same rate, or even higher with growth right around 5% (NEPCO, 2016; MEMR, 2017, 2018).

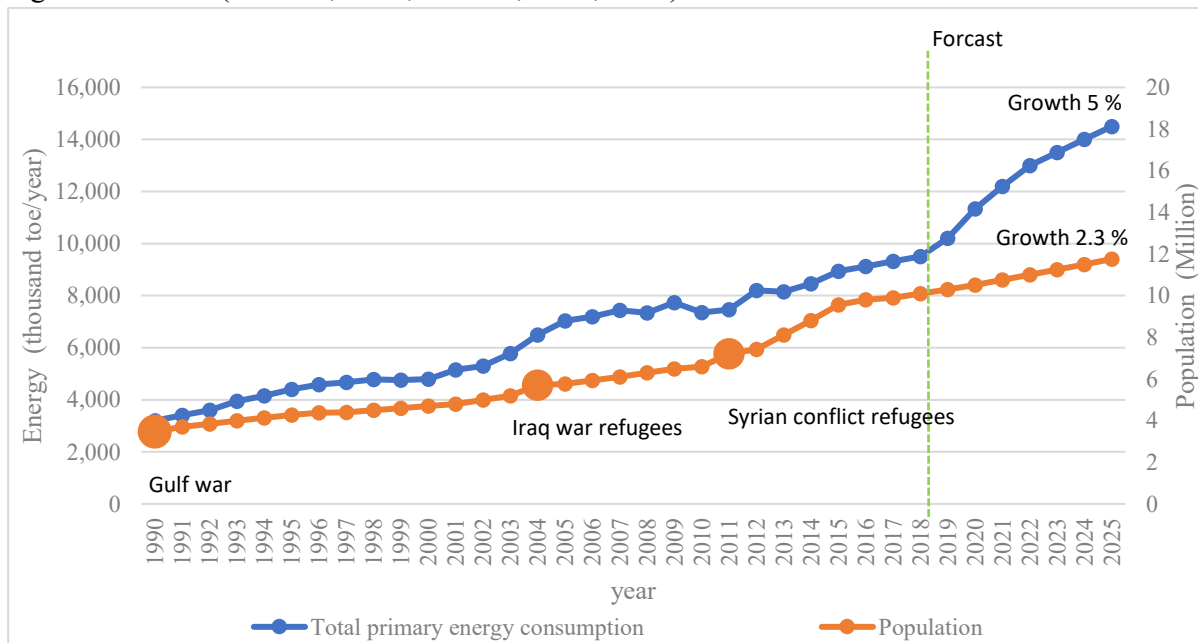


Figure 2-11: Energy consumption and population trends in Jordan from 1992 to 2018 and energy demand forecast from 2019 to 2025. Source of data : (MEMR, 1997, 2003, 2011, 2017, 2018; Jordanian Department of Statistics, 2015; IEA, 2019b)

Jordan's energy mix

According to the ministry of energy and mineral resources (MEMR), the relatively low local energy resources force the country to import most of its needed; 97% of Jordan's energy is imported from foreign countries, as oil products contribute about 71% of the total energy mix and natural gas contribute 22% of the total energy mix, while the imported electricity contribute to about 1% and the renewable energy about 2% of the total energy mix in 2015. However, the national energy strategy has been published by the ministry of energy and mineral resources which aims that by 2020 renewable energy should contribute 10%, oil shale about 5%, nuclear energy about 5%, and by 2025 renewable energy should contribute 6%, oil shale about 10%, nuclear energy about 22%. This means 80%, 52% of Jordan's energy supply will be imported in 2020, 2025 respectively instead of 97% in 2015 (MEMR, 2017, 2018). Figure 2-12 below, show the energy mix components from 1990 -2015 and gives the government plan for 2020, 2025.

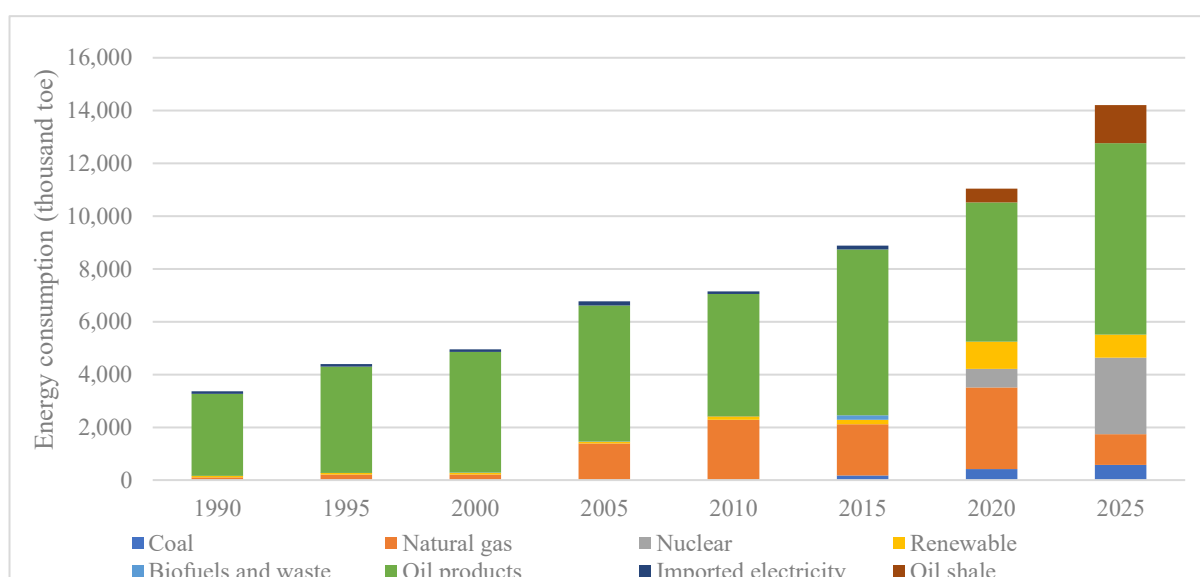


Figure 2-12: Primary energy consumption mix in Jordan from 1990 to 2015 and the government plan for 2020, 2025. Source of data : (MEMR, 1997, 2003, 2011, 2017, 2018; Jordanian Department of Statistics, 2015; IEA, 2019b).

Energy consumption by sectors

As illustrated in Figure 2-13 below, the transportation sector recorded the highest energy consumption rate with about 37% in 2017, followed by the household sector with about 24% of the total energy consumption in Jordan (MEMR, 2018).

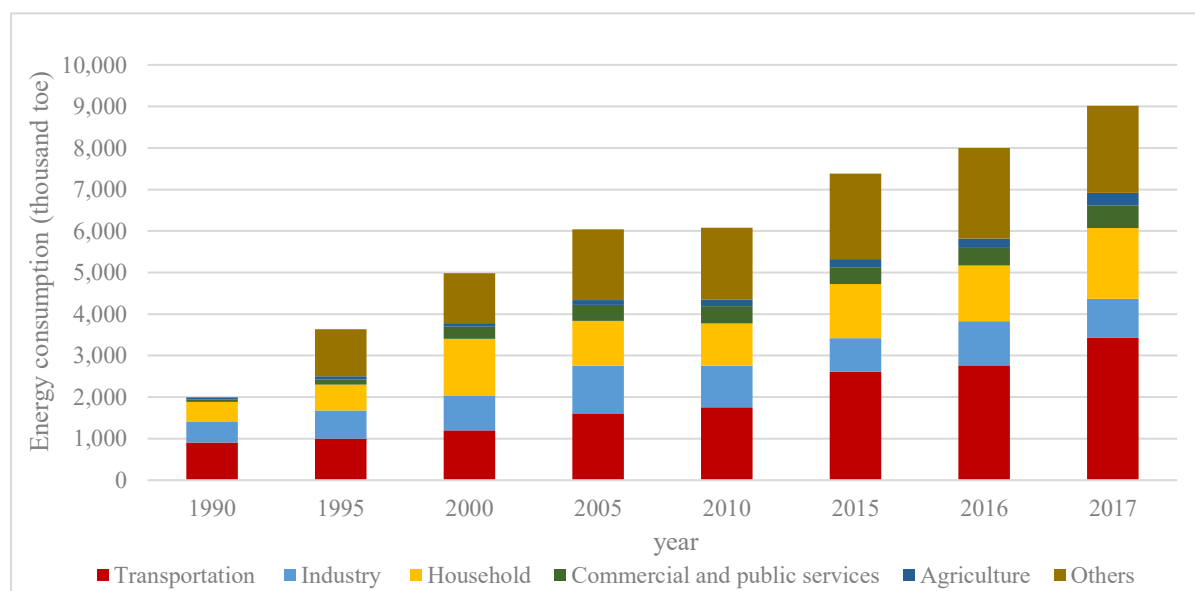


Figure 2-13: Primary energy consumption by sector in Jordan from 1990 to 2017. Source of data: (MEMR, 1997, 2003, 2011, 2017, 2018; Jordanian Department of Statistics, 2015; IEA, 2019b).

However, regarding the electricity consumption, as illustrated in Figure 2-14, the household sector consumed the highest amount of electricity in Jordan, and it increased by about 5.0% in 2017 compared with 2016, it is also expected to increase with the same growth rate in the next years. It is clear that the household sector recorded the highest electricity consumption rate since 2000, with about 45% of the total electric power consumption in 2015, 2016 and 2017, recorded the highest electricity consumption rate in 2015 (NEPCO, 2016, 2017; MEMR, 2017, 2018; IEA, 2019b). This is one of the reasons for selecting the residential sector in this research, this is followed by the industrial sector industrial sectors with about 25% of the total electricity consumption.

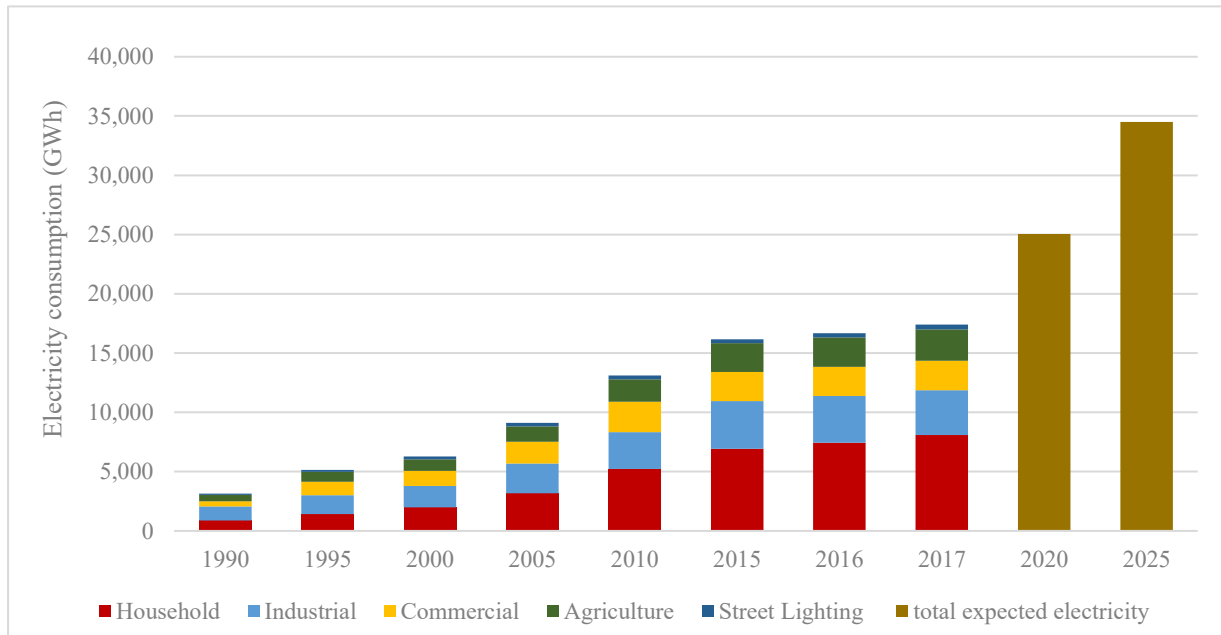


Figure 2-14: Electricity consumption in Jordan by sector between 1990-2017 and the total expected electricity consumption in 2020,2025. Source of data: (NEPCO, 2016, 2017; MEMR, 2017, 2018; IEA, 2019b).

Electricity tariff and energy prices

Prices of energy are relatively high in Jordan; this is because most of its energy consumed is imported. Jordan has a relatively high electricity tariff rate, compared to other countries in the region, even with government subsidies, Jordan's electricity prices in the residential sector are more than ten times higher than its oil-rich Arabian Gulf neighbors (Fattouh, 2010).

Table 2-1 below, shows the electricity price in residential sector and the range of fuel price during the last year, fuel prices in Jordan are set by the government and reviewed on a monthly basis to reflect international prices on the local prices, only the electricity price for the residential sector is mentioned here, as this research is only focused on the residential sectors (NEPCO, 2016; MEMR, 2017).

Table 2-1: Electricity price and fuel average price in Jordan. Source of data: (NEPCO, 2016; MEMR, 2017).

Electricity consumption (kWh/month)	Electricity price (€/kWh)
Residential	
First block: from 1-160	0.040
Second block: from 161-300	0.088
Third block: from 301-500	0.100
Fourth block: from 501-600	0.140
Fifth block: from 601-750	0.190
Sixth block: from 751-1,000	0.230
Seventh block: more than 1,000	0.320
Fuel prices	
Gasoline (90)	0.73-0.81 €/l
Gasoline (95)	0.82-1.04 €/l
Kerosene	0.500-0.62 €/l
Diesel	0.62 €/l
Fuel oil	323-459.75 €/ton
Liquefied gas	671-820 €/ton

2.5 Jordan renewable energy strategies and regulations

In view of the situation explained in the previous section (high population growth rate, lack of local resources and high energy price), the ministry of energy and mineral resources (MEMR) has set a Jordan energy strategy for 2020 to reduce the dependency on imported energy from 97% to 80%, the main goals of this strategy are (MEMR, 2017):

- Decreasing the reliance on imported oil by maximizing using domestic resources (oil shale, natural gas, etc.).
- Diversifying the energy resources and expanding the share of local resources in the energy mix (solar, wind and nuclear energy).
- Enhancing environment protection and achieving sustainable development by enhancing the exploitation of renewable energy.

In this strategy, the government of Jordan is giving considerable attention to the utilization and implementation of renewable energy resources, by setting a renewable energy target of 10% of Jordan's energy mix by 2025. This is expected to comprise 15-20% of electricity consumption, and is to include about 600-1,000 MW of wind energy, 300-600 MW of solar energy and 30-50 MW of energy from waste (Jaber, 2016; MEMR, 2017). It is worth mentioning that the capacity of renewable energy developed and/or underdeveloped projects (solar and wind) amounted to 1,755 MW, completed generating capacity for the renewable energy projects reached by the end of the year 2016 is 544 MW, out of which 347 MW as solar energy projects and 197 MW wind energy. In addition that the capacity of renewable energy net metering and wheeling systems amounted to 200 MW (NEPCO, 2017; MEMR, 2018). To support this renewable energy target, the government has implemented a legal framework and introduced different laws and regulations, as described below:

Renewable energy and energy efficiency law

This law is issued in 2012 (law no.13), includes key supporting measures for encouraging renewable energy, and allows investors for the direct proposal submissions of projects for generating electrical power and connecting to the grid, the main goals for this law are (NEPCO, 2016, 2017; MEMR, 2017, 2018):

- Provide a legal mandate for government and a regulatory framework for renewable energy and energy efficiency development.
- Diversify energy sources in Jordan.
- Reduce greenhouse gases.
- Encourage private sector investment in renewable energy.
- Establish Jordan renewable energy and energy efficiency fund (JREEEF) to provide support for improving energy consumption efficiency studies, and support for awareness campaigns and training programs, as well as loan guarantee for energy efficiency and renewable energy projects. This fund is funded by the government, donors and investment returns.

This law form the basis for supporting other schemes and incentives, the two main supporting schemes feed-in tariff and energy wheeling an overview of this schemes are presented below(NEPCO, 2016, 2017; MEMR, 2017, 2018):

Energy wheeling

This law allows the user to generate renewable energy electricity in one place and use it at another. As illustrated in Table 2-2 below, the total monthly produced energy (sent out energy) from a renewable energy system (RES) shall be subjected to a physical losses reduction as follows:

- 2.3% only - if RES connection direct with transmission network to feed the same customer connected with the transmission network.
- 6% only - if RES connection directly with a distribution network to feed the same customer connected with the distribution network.
- 2.3% plus 6% - if RES connection directly with the transmission network to feed the same customer connected with the distribution network.

Table 2-2: Cost of using a different type of network connection in Jordan. Source of data: (NEPCO, 2016).

Type of network connection	Electrical loss (%)	Cost of using the network (€/kWh)
To transmission	2.3	0.056
To distribution	6	0.087
To distribution and transmission	2.3+6	0.056+0.087

Feed-in tariff

The feed-in tariff system also adopted under the renewable energy law, this law allows any renewable energy producer to sell the excess electricity to the grid at a specific tariff. This excess electricity that is credited can be used to offset electricity used at other times, when there is little or no PV electricity production (e.g. at night).

By-laws and regulations for investment (selling tariff)

By-laws and regulations regarding renewable energy projects for electricity generation have been released by the electricity regulatory commission, specifying the pricing of the purchase electrical power from renewable energy source, “selling tariff” is differentiated by technology but not by installation size, and an extra 15% is added to installations “of fully Jordanian origin”. Current selling tariffs are shown in Table 2-3 below:

Table 2-3: Price of purchase electricity from a different type of renewable energy in Jordan. Source of data: (Graillet et al., 2014; NEPCO, 2016, 2017).

Renewable energy technology	Reference price (€/ kWh)
Wind energy	0.11
Concentrated solar power	0.17
Solar photovoltaic	0.15
Waste	0.11
Biogas	0.075

Energy efficiency by-law

This law issued in April 2013, which outline that the solar water heating systems (SWH) are mandatory for new buildings, including offices, apartments and detached houses of more than 100, 150 and 250 m², respectively. It also includes a basis for energy appliance labeling, and smart metering (MEMR, 2017). However, this law, not implemented until now. As most of the investors claimed that this will lead directly to raising the costs of apartments or offices and reduce the demand for buildings (Jfranews, 2013).

Tax exemptions by-law

This law has been issued recently in law no.10 (2013), exempting all systems and equipment's for renewable energy and energy efficiency projects from sales tax and customs duties (MEMR, 2017).

2.6 Photovoltaics and solar thermal technology market in Jordan

Photovoltaics technology market in Jordan

According to the recent study done by the United States Agency for International Development in Jordan, many PV companies were launched recently in Jordan, reaching 500 companies in one year, after the release of the renewable energy & energy efficiency law in 2012. However, most of them are relatively small companies, working as EPC (Engineering, Procurement, and Construction) contractors, and many of them deal with international companies. According to the Jordanian Royal Scientific Society which is responsible to evaluate the work and the competency of these companies, only 5% of these companies work with professionals and equipped with a local experienced team (USAID, 2014). Currently, Philadelphia Solar Company is the first and only PV module producer in Jordan and exported its products to over 35 countries with the biggest customers being in the UK, Holland, and Germany. The company produces mono and multi-crystalline solar modules using state-of-the-art (automated) robotic assembly lines, with a maximum power of 320Wp (Meza, 2015; Tsagas, 2015; Philadelphia Solar, 2018). As mentioned before, most of the Jordanian companies import their PV modules and components from foreign producers. With the absence of any standards or guidelines for quality control of solar PV products and services in Jordan, most of PV suppliers are imported cheap and low-quality products (Aberg *et al.*, 2014). As illustrated in Table 2-4 below, the most popular is the Chinese solar modules due to their cheap price and mass availability, the next popular imported PV modules are from European countries that make the market and the prices for PV systems do not differ much from international market especially with the absence of import taxes (Antonello, Alawneh and Basha, 2015).

Table 2-4: The percentage origin of imported PV components in Jordan. Source of data: (Antonello, Alawneh and Basha, 2015).

Origin of imported PV component in Jordan	Percentage (%)
Europe	30
Asia	60
Africa	0
USA	10
Australia	0

Solar thermal technology market in Jordan

Regarding the solar thermal collectors, there are few applications for space cooling and heating, it is widely used for domestic solar water heating (SWH) in Jordan (AlShamaileh, 2010; Etier, Al and Ababne, 2010; Sakhrich and Al-Ghandoor, 2013; Abdelhai, 2014). The SWH technology has been known since the Royal Scientific Society (RSS) designed and produced solar systems in its workshop since the early 1970s and the systems were installed for testing all over Jordan (Jaber, 2012). There are several solar systems companies established in Jordan, 10 retailers, and 13 installers, and only three are big companies, in addition to several small shops (Hanania, Nur, and Millennium Energy) producing solar thermal collectors according to defined quality standards under the supervision of Jordanian Royal Scientific Society, and could supply parts of high quality collector production (plastic, metal industries, isolation materials, etc.) (Abdelhai, 2014; Gharas, Menichetti and Cottret, 2014).

Hanania energy company is the first company in Jordan to manufacture solar thermal collectors since 1973, Hanania energy company has been contacted by email and they confirm that they also installed high standard photovoltaics, either by buying them locally (from a local manufacturer or importer) or they import high standard products directly from the manufacturer in Europe or China (Hanania, 2016). It is estimated that more than 30% of total solar collectors products are imported, mainly from China in addition to other countries such as Germany, Austria, Russia, Italy, China, and Turkey (Jaber, 2012; Abdelhai, 2014; USAID, 2014).

Although the solar thermal collector technology for water heating is widespread and approved, there is little knowledge about the opportunities of using these technologies and the distinctive features of the available systems which are also reflected in the prices. Also, there are no quality control regulations for solar thermal appliances, nor standards for products. Systems are not guaranteed by the suppliers. Nevertheless, the country has its own testing laboratories at the Royal Scientific Society (RSS), but without effective regulations to enter into the market (Abdelhai, 2014).

In the Jordanians market, different types of solar thermal technologies are available; flat Plate collectors and recently evacuated tube collectors were introduced which produce a higher energy than flat plate collectors for the same effective installed area, however, only one local company manufacture evacuated tube collectors in Jordan (Hanania) the total installed capacity of solar thermal at the end of 2014 is 882 MW_{th}, corresponding to installed area of 1.26 km² (IEA, 2016). Flat plate collectors dominate the market with about 75% of the total installed collectors (Abdelhai, 2014).

Most of the conventional domestic water system is a decentralized thermosiphon system, consists of approximately 1 m² of solar module per person and a 40-70 l hot-water tank per m² of the solar module. A solar heating system provides up to 80% of the annual energy requirement for hot-water generation (Shariah et al., 1998; Abdelhai, 2014), and this solar water heating system is connected to the backup heater, 50% of homes use diesel boilers for water heating as a back up to the solar water-heating system, 35% use electrical heaters and 15% use LPG boiler (Maaytah, Nsour and Heffner, 2015). The hot water demand for the typical Jordanian family is estimated to be 50 l/person/day with an average temperature of 55 °C (Attia, 2014). Combined domestic water and space heating systems may be considerably larger, e.g. up to 9 m² of solar module per person, and may cover quite a significant portion of the overall heat energy requirements of the household (Taher *et al.*, 2011; Kawkabuna, 2013).

The typical collector design produced in Jordan consists of a metal sheet casing with aluminum film at the back, rock wool as back and side insulation, a carbon steel pipe absorber with non-selective coating and one glass cover (Taher et al., 2011).

2.7 Photovoltaics and solar thermal technology cost in Jordan

Prices of PV systems

In Jordan, prices for PV systems are rather competitive and do not differ much from international market prices. The absence of import taxes, compulsory local content requirements, competitive labor cost lead to internationally competitive end-consumer prices for PV installations. There is no official price index for PV systems in Jordan, however, under “Enabling PV” project, which is coordinated by “Deutsche Gesellschaft für Internationale Zusammenarbeit (GIZ)” in 2014, some interviews done in Jordan to find the price range of photovoltaic systems in Jordan, and the results indicate that the end consumer PV System price is ranging between 1,750 €/kWp for a very small installation and 1,000 €/kWp for very large ones, and for operation and maintenance costs are considered to be annually between 1.5 and 3.5 €/kWp of the total cost, depending on the size of the system (Knaack *et al.*, 2014). Hardware costs (module, inverter, racking, wiring, etc.) account for 75% of the total costs, whereas soft costs (installation, customer acquisition, profit, permitting, contracting, financing) account for about 25% of the total costs. The modules account for about 70% of the hardware costs (Knaack *et al.*, 2014).

As mentioned before, multi-crystalline and poly-crystalline photovoltaic cells are available and manufactured locally in Jordan only by Philadelphia solar company in Jordan, more data on Philadelphia photovoltaics technologies and prices of these technologies are available online at: (goo.gl/wFQn5a) (Philadelphia 2016).

Prices of solar thermal systems

According to Jordan national energy research center (NERC), the average cost for the solar thermal system for heating water is around 750 €, this system is consisting: (flat plate local fabricated (3 collectors) + hot water tank+ cold water tank+ stands for tanks). Solar collectors represent 55% of the total cost of the system and the tank represent 38% of the total cost of the system if the evacuated tube used instead of a flat plate collector the average cost of the system will be 1,250 € (Siebert, 2011; Abdelhai, 2014).

The international market is discussed in Chapter 3.2.2, as there is no official price index for PV technology in Jordan and few undetailed published data, and as mentioned before because the price does not differ much from international market prices.

2.8 Solar energy application in Jordan

Despite the high solar potential of Jordan, solar energy technologies are not extensively used, except for solar water heaters (SWH), which are used for domestic water heating. It is an economically feasible technology to use, compared to all other conventional water heating systems (Kiki *et al.*, 2008). PV and ST technologies in Jordan are commonly mounted onto buildings' roofs as pure technical elements. Roofs are usually out of sight, especially in multi-story buildings, and by placing the PV and ST, the designers tried to hide them to avoid negative impacts on the building's aesthetic. Recently, most of the buildings are multi-floor with a small floor area. The floor area is usually used for many purposes such as water tanks, dishes, etc.

Therefore, there is not enough space for installing solar heating and cooling systems for all residences (Abdelhai, 2014; Aberg *et al.*, 2014).

Most of the solar heating system for space and/or water in Jordan are installed in private homes, as approximately 30% of the houses in Jordan use solar family systems for heating domestic water (Aboushi and Raed, 2015; Antonello, Alawneh and Basha, 2015). There are few applications for collective solar water systems used in large-scale systems (swimming baths, hotels, and camping sites industries, hotels, hospitals) in Jordan with extensive hot water use and in very large-scale collective systems connected to district heating plants. In these plants, solar energy is often used in combination with biomass heating systems (Jaber, 2012; Aboushi and Raed, 2015).

Solar heating is thus used primarily for heating water in hot-water tanks. Therefore, it is very simple to use with other energy sources in homes (natural gas, oil furnaces, fuel furnaces, heating pumps or electric heating). It is also possible to use solar heating systems for heating of homes, e.g. in the form of underfloor heating (Aboushi and Raed, 2015).

Figure 2-15 below, represents the current application trend of solar thermal collectors in Jordan.



Figure 2-15: Installation of solar thermal collectors in multi-family residential building roof in Jordan. Source: (Zawaydeh, 2016).

Regarding the photovoltaics application in Jordan, it is still a new technology, and it is still not as spread as it should be in the kingdom. The research center for renewable energy sources, together with international funding agencies, installed several photovoltaic off-grid systems, mainly in remote regions to supply electricity for water pumping, powering radio and/or telephone stations and for supplying electrical energy for health centers, schools and a few small villages mainly in the south of Jordan, and there are few rooftop solar PV systems installed in Jordan (Aberg *et al.*, 2014; Knaack *et al.*, 2014). Figure 2-16, shows some applications of photovoltaic in Jordan.



Figure 2-16: Application of photovoltaic in a residential building in Jordan. Source: (Zawaydeh, 2015).

2.9 Solar renewable energy barriers and recommendations

Many researches, projects and studies analyzed the main reasons for low take-up of solar technologies and give a recommendation to improve the renewable energy situation in the middle east countries including Jordan (Kiki *et al.*, 2008; GTZ, 2009; Motasem, 2011; Siebert, 2011; Taher *et al.*, 2011; Jaber, 2012; Alex, 2014; Gharras, Menichetti and Cottret, 2014; USAID, 2014; Graillet *et al.*, 2014; Zawaydeh, 2016; Probst, 2017). There are some fundamental barriers in the energy sector that lead to low take-up of renewable technology, these barriers are relating to the technical, economic, social, political framework and market. Below the main barriers and recommendations according to the previously mentioned researches are discussed.

Technical barriers

- The high cost of high specification materials/components such as double-glazing, selective coating material, sheet metal, pipes. This results in hindering the development of designs and quality.
- Lack of experience in solar energy systems installation and operation & maintenance.
- Absence of professional calculation tools or technical handbooks for the design and sizing of large solar systems.
- Absence of compulsory testing regulations that forces the manufacturers and importers to test their collectors, although a national testing facility to test solar collectors exists at the royal scientific society.
- Inadequate use of solar energy research projects results. Even though some of these researches are supported by industries, their work has not been aimed at commercialization.

Figure 2-17 below, shows some examples of the technical barriers for solar technologies in Jordan due to the lack of experience in solar energy systems installation and maintenance. In the first picture at the left, the height of the bottom of the storage tank is beneath the collectors' water outlet. While the right photo is the solar water heating system installed near a chimney that contaminates the system with soot and other combustion gases.



Figure 2-17: Lack of experience in installation of solar energy system in Jordan. Source: (Jaber, 2012).

Figure 2-18 below, illustrates a solar water heating system installed without consideration to safety measures and easy maintenance in Jordan.



Figure 2-18 : Solar energy system installed without consideration to safety and easy maintenance in Jordan. Source: (Zawaydeh, 2015).

Policy barriers

- Absence of regulations, rules and energy provisions to control the quality and the effectiveness of the locally manufactured, imported or used equipment.
- Lack of national standards, testing and certification schemes.
- Generally, no standards or labels are being used for renewable energy products.
- Lack of data/documentation and monitoring, most often, data on the solar technology market are not gathered or access to these data is difficult.

Economical

- The main barrier to the development of the market is the weak buying power of the consumers, due to its high initial cost.
- Solar technologies require adequate space on roof or ground as well as the structural integrity of buildings to be able to mount modules, resulting in increased installation costs.

Market barriers

- Lack of incentives & financing options.
- The lack of local providers for material and components makes the installation of the solar energy systems difficult.
- Most manufacturers are in Amman which makes it difficult and more expensive for people living in other cities to install solar collectors and have periodic maintenance.

Social barriers

- Recently, most of the buildings are multi-floor within small floor area. The roof area is usually used for many purposes such as water tanks, dishes, etc, as illustrated in Figure 2-19, therefore, there is no enough space for installing solar water heating systems for all residences.
- Consumer resistance towards change in behaviors and attitudes because harnessing renewable energy has in general been more expensive per unit of energy than that obtained from conventional energy sources.
- Lack of environmental conscience and confidence in new technologies.



Figure 2-19: Multi-family residential building roof used for many purposes. Source: (Jäger et al., 2012).

Recommendations

- Create intelligent and substantial financing mechanisms to promote the application of solar systems.
- Continue to raise awareness and provide enough information for promoting solar energy to the concerned target groups: public costumers, contractors, and building designers.
- Develop a national marketing plan, including media campaigns and information dissemination.
- Setting up the minimum technical standards for energy efficiency for imported and locally manufactured solar technologies.
- Hold the design of solar system training courses for building designers, contractors, and suppliers.
- Jordan engineer's association should acknowledge the architect and designers of building to emphasis on the implementation of energy efficiency measures and renewable energy in their design.
- The need for establishing standards and specifications for renewable equipment.
- Building regulation to promote passive solar energy efficiency should also be studied and developed in the short term.
- Awareness campaigns for users to buy only labeled energy efficiency equipment.

2.10 Residential stock in Amman, Jordan

During the last two decades, the building and construction sector in Jordan has accelerated at a high rate, and 75% of the growth is resulted from the residential sector due to natural population growth and migration (RSS, 2007). As mentioned earlier, Amman is the city where 45% of the new construction in Jordan is taking place, the multi-family apartment buildings in the country form 75% of the total housing stock and more than 80% of all buildings in Jordan (Younis, 2017). So basically, this research is dealing with the apartment building as a studying model. This makes sense in terms of covering most of the construction and ensure reliability. The typical floor plan and view of a typical middle-class apartment building in Jordan are presented in Figure 2-20 and Figure 2-21 below. The floor layout is rectangular, with 6 floors (including the basement floor), contains 10 residential apartments as each floor accommodates two facing apartments, so one flat has three exterior facades. Table 2-5 below, illustrate the average area of residential buildings and its zones in Amman, Jordan.

Table 2-5: Area and zones of the apartments in Amman, Jordan. Source of data: (MEMR, 2013).

	Apartment	Bedrooms	Guest and living rooms	Kitchen	Corridors	Bathrooms
Average area (m ²)	155	55	45	16	12	13

The main factors affecting the area of houses in Jordan are socio-economic, such as the number of family members and their financial status (MEMR, 2013). According to the survey conducted by the department of statistics in Jordan, as part of a national census, the average number of occupants per apartment is 5.8, it was noted that most of the family houses were occupied by parents aged between 45 and 65, with two adults aged between 18 and 25 and two children aged under 18 (Department of Statistics, 2016).

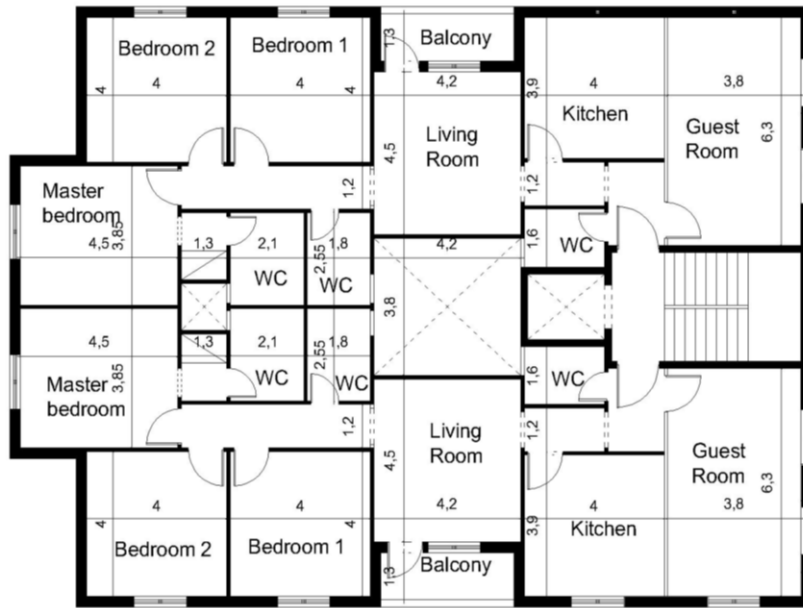


Figure 2-20: A typical floor plan for multi-family residential buildings in Jordan. Source of plan layout: (Goussous, Siam and Alzoubi, 2014a).



Figure 2-21: A view for a multi-family building in Jordan. Source: (Goussous, Siam and Alzoubi, 2014; Attia and Al-Khuraissat, 2016)

Reinforced concrete skeleton structures are the dominant structural system in a contemporary residential building in Amman. Exterior walls are considered as non-structural elements (Jäger *et al.*, 2012), final ceilings are usually flat. Almost 60% of the Jordanian housing is built from concrete and building blocks and stones. In addition, 90% of the roofing for such buildings is made from concrete. 20% of the wall in the residential buildings are insulated, and regarding the roof, around 40% of the residential buildings' roofs are insulated (MEMR, 2013). The commonest types of construction, layers thickness, and U-values of the different building parts of the typical multi-family building in Jordan are presented in Table 2-6 (Al-Asir *et al.*, 2009).

Table 2-6: Proprieties of construction used in the multi-family buildings in Jordan. Source of data: (Al-Asir et al., 2009).

Building element	Materials	Thickness (mm)	U-value (W/m ² K)
Outer wall	Stone cladding	50	2.47
	Plain concrete	100	
	Hollow Block	100	
	Plaster	25	
Inner wall	Plaster	25	2.88
	Hollow concrete block	100	
	Plaster	25	
Internal floor	Cement tiles	20	1.85
	Low weight concrete	30	
	Concrete	200	
	Render	25	
Roof	Tiling(cement)	20	0.84
	Gravel	30	
	Waterproof Asphalt	5	
	Low weight concrete	100	
	Reinforced concrete	200	
	Render	25	

In contemporary residential buildings, most windows in Amman still builds with single glazing and a simple rectangular hollow aluminum profile. Both are highly conductive due to high heat transmission. And highly criticized by weak airtightness. Furthermore, this type of window offers a 50% maximum opening (Jaber and Ajib, 2011b; Jäger *et al.*, 2012). The specifications and characteristics of a single-glazed window are illustrated in Table 2-7 below.

Table 2-7: The glazing properties and specifications for a building in Jordan. Source of Data: (Jaber and Ajib, 2011b).

Glazing properties	Specification
Glass thickness	6 mm, single glazing
Solar transmittance	0.83
Visible transmittance	0.89
Window frame	Aluminum
U-value	5.92 W/m ² K
Solar heat gain coefficient	0.87
Integrated shading device	No

Most apartments in Jordan are naturally ventilated. However, natural ventilation is achieved by opening windows. It is also very common for multi-family buildings to have a ventilation shaft in the middle of the building. This shaft is as high as the building and serves as a passive stack. There are openings between the bathroom and the shaft (Al-Asir et al., 2009).

Urban zones and regulations

Table 2-8 and Figure 2-22 show the regulations of buildings for the residential building sector, setbacks, buildings height, maximum building percentage on the plot (Amman Municipality, 2018). Type C residential zoning (Figure 2-23) is the most common type (Al-Asir et al., 2009; Awadallah, 2015), taken the inflation in land prices this type became common as it provides the minimum area that can be used to build proper residential building and at the same time is economical because of its low area (Awadallah, 2015). Other important regulations including (Amman Municipality, 2018):

- Building projections are only allowed for aesthetic purposes or as solar shading.
- Balconies are not allowed to exceed the permitted building line.
- Reflective materials that might disturb the neighbors or might be public safety hazards are forbidden.
- Not more than 20% of the exterior elevations can be painted with colors other than the color of stone or white.

Table 2-8: Zoning provisions of housing sectors A, B, C and D. Source of data: (Amman Municipality, 2018).

Residential sector	zone	Max area (m ²)	Setback (m)			Max. building height (m)	Max. building percentage (%)
			Front	Side	Back		
A		1,000	5	5	7	16	39
B		750	4	5	6	16	45
C		500	4	3	4	16	51
D		300	2.5	2.5	3	16	55

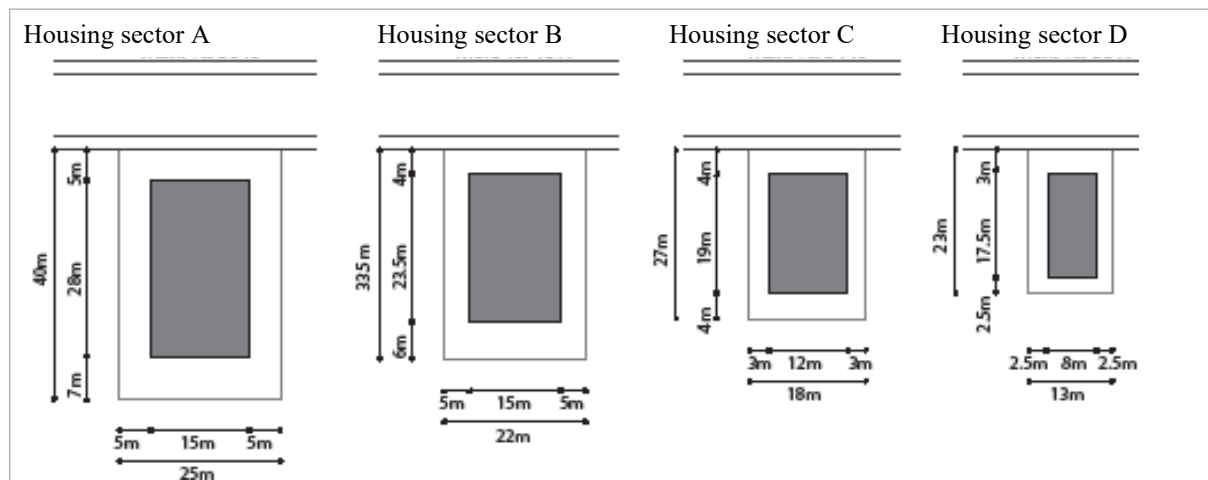
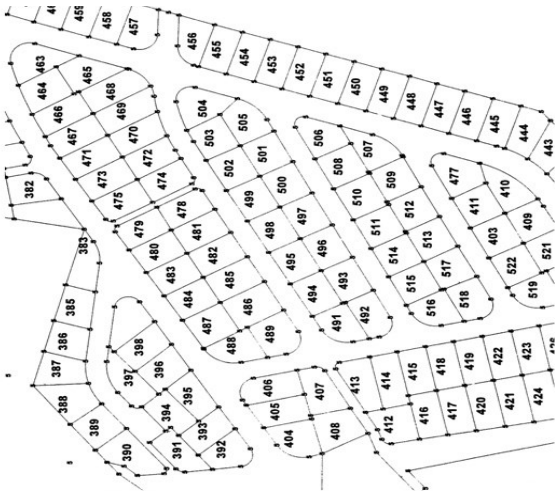


Figure 2-22: Regulations of plot size, building percentage, and setbacks for housing sectors. Source:(Al-Asir et al., 2009).



(a)



(b)

Figure 2-23: a) Land divisions according to residential land use for type C. b) Residential multi-family blocks under zone sector C. Source: (Alzoubi and Alshboul, 2010).

3 Literature review

3.1 Introduction

The developing interest for nearly-zero energy buildings is quickly contributing to change the building skin from being a passive barrier towards a sensitive and active interface. Building-integrated photovoltaics (BIPV) and building-integrated solar thermal (BIST) are unique solutions for delivering clean, safe, affordable and decentralized electricity and energy (Bonomo, Frontini and Chatzipanagi, 2015; Cannavale *et al.*, 2017). The concept is distinctive from regular solar energy applications since the PV/ST functions are integrated into the building envelope instead of mounting them on the roof, creating aesthetic challenges, space availability issues and envelope integrity problems (Berenschot, 2015; Osseweijer *et al.*, 2017).

This section gives an overview of BIPV and BIST and their technical features, prices, technologies and shows the most common solutions on the building roofs and facades. In addition, previous studies and researches related to the energy performance of the BIPV and BIST are reviewed. As buildings are usually designed to last for many years, the importance of life cycle assessment is also emphasized. Solar thermal and photovoltaics are treated independently, since one technology is intended to change the solar radiation into heat, while the other is intended to change it into electricity: two distinctive energies, with different transportation, storage, and safety issues. This brings different formal and operating constraints, leading to different integration possibilities (Kayali and Dr. Halil Alibaba, 2017).

Even a comprehensive market overview can never be complete, this analysis is helpful to identify the relevant possibilities the market today offers and the multiple benefits for PV and ST integration, in addition to the identification of the knowledge gap.

3.2 Building-integrated photovoltaic (BIPV)

3.2.1 BIPV definition

BIPV refers to the integration of PV materials into building envelopes, hence providing it with multiple functions, for example, to act as part of the building structure by replacing traditional building materials and to produce electricity on-site (IEA, 2001, 2013; Jelle, Breivik and Drolsum Røkenes, 2012; Berenschot, 2015; CENELEC, 2016). According to the technological ‘multifunctionality’ concept, the PV systems can be divided into building-integrated systems (BIPV) and building-applied PV systems (BAPV), the former is suitable for new buildings during the early design stage, by replacing conventional building materials with PV modules, while the latter is easily applied to existing buildings by adding PV modules to some parts of their envelopes (Montoro, Vanbuggenhout and Ciesielska, 2011; CENELEC, 2016; Zhang, Wang and Yang, 2018). BIPV has shown its potential to be a multifunctional and effective building energy technology that can bring many advantages to the building (Zhang, Wang and Yang, 2018). Besides of being a source of electricity, several other purposes can be achieved, such as, insulation from winter cold and excessive summer heat, regulation of users’ comfort, while reducing the use of non-renewable energies, noise protection, regulation of the visual relations inside/outside and outside/inside, etc. (Montoro, Vanbuggenhout and Ciesielska, 2011; CENELEC, 2016).

Additionally, the possible advantage of this multi-functionality concept is the reduction of the overall cost due to the reducing the material costs and labor expenses in comparison to traditional PV solutions (IEA, 2013; Frontini et al., 2015). Another advantage of BIPV is its appearance. When it is compared with conventional materials, besides being an energy producer, BIPV can add esthetic value to the buildings (Zhang, Wang and Yang, 2018). BIPV technologies can be transparent, flexible, colorful, and visually arresting, which providing a great opportunity for innovative architectural design and making future buildings more aesthetically appealing (IEA, 2013; Zhang, Wang and Yang, 2018). Moreover, the integrated PV system in a new building from the very first stage commonly guides to better aesthetic results (Martín-Chivelet et al., 2018). Indicates to the architectural concept, its appearance, these are harder to characterize in a unique way, as often perceived as subjective (IEA, 2013; Frontini et al., 2015). For instance, some architects enjoy presenting a BIPV roof as a roof giving a clear visual impression, whereas others need the BIPV roof to see as much as a standard roof as possible (Jelle, Breivik and Drolsum Røkenes, 2012).

It is usually accepted that there are no universal principles applicable to all contexts referring to “good architectural design” (Martín-Chivelet et al., 2018), but some architectural criteria are suggested in the framework of the international energy agency project solar energy and architecture task 41 “Solar Energy and Architecture” (Munari Probst and Roecker, 2012; IEA, 2013), and they are summarized below :

- Naturally integrated: the PV system is a natural part of the building. Without PV, the building would be lacking something;
- Architecturally pleasing: based on good design, the PV system gives eye-catching features to the architecture;
- Good composition: the color and texture of the PV system are in harmony with the other materials;
- Grid, harmony, and composition: the sizing of the PV system matches the sizing and the grid of the building, the total image of a building is in harmony with the PV system;
- Innovative new design: the PV system adds value to the building.

3.2.2 BIPV markets

Currently, BIPV solutions are positioned as a niche product in the market. In 2017, BIPV makes up about 1% of the total PV market with a total installed capacity worldwide of about 5 GWp (IEA, 2017b, 2018a; Osseweijer *et al.*, 2017; Passera *et al.*, 2018). However, the global BIPV market experienced fast growth in recent years and it is expected to grow in the upcoming years (Berenschot, 2015; Transparency Market Research, 2015; Global Industry Analysts Inc, 2016). A roadmap study by Berenschot (2015) shows that in 2020 the global BIPV capacity is expected to exceed 9 GW (Berenschot, 2015; Global Industry Analysts Inc, 2016). Also, as reported by transparency market research, the annual global BIPV installation is promised to be 1,150 MWp in 2019, with a compounded annual growth rate (CAGR) of 18.7%, compared with the 343 MWp in 2012 (Transparency Market Research, 2015).

Tabakovic et al. detailed the status and viewpoint of global BIPV installations from 2014 to 2020 by region, the global installation was estimated to be 2.3 GW in 2015. While the market was only 1.5 GW in 2014, in this way the increasing rate almost reaches 50%, the annual global BIPV installation in 2020 is expected to be 11 GW, with an average global CAGR of 40% during 2014-2020 (Tabakovic et al., 2017). In 2015, Europe was the leader for BIPV installations, accounting for 40% of the whole market (Tabakovic et al., 2017; Passera et al., 2018), 65% of applications concerned as the rooftop integration, the remaining part considered as façade installation (Passera et al., 2018).

In the future, BIPV market will be subject to continuous growth worldwide due to advances in technology, the reduced cost of PV materials, and the increase in incentive policies for renewable energy technologies in some countries, such as Germany, USA, China (Zhang, Wang and Yang, 2018).

3.2.3 BIPV systems classifications

As illustrated in Figure 3-1, BIPV systems can be classified according to the power supply and the storage modes (Yudha, 2018; Zhang, Wang and Yang, 2018), PV cell technology (Jelle, Breivik and Drolsum Røkenes, 2012; Cerón, Caamaño-Martín and Neila, 2013), envelope part (possible area for installation) (Berenschot, 2015; Frontini et al., 2015), BIPV product (Jelle, Breivik and Drolsum Røkenes, 2012; Cerón, Caamaño-Martín and Neila, 2013; Shukla, Sudhakar and Baredar, 2016) and transparency (Zhang, Wang and Yang, 2018).

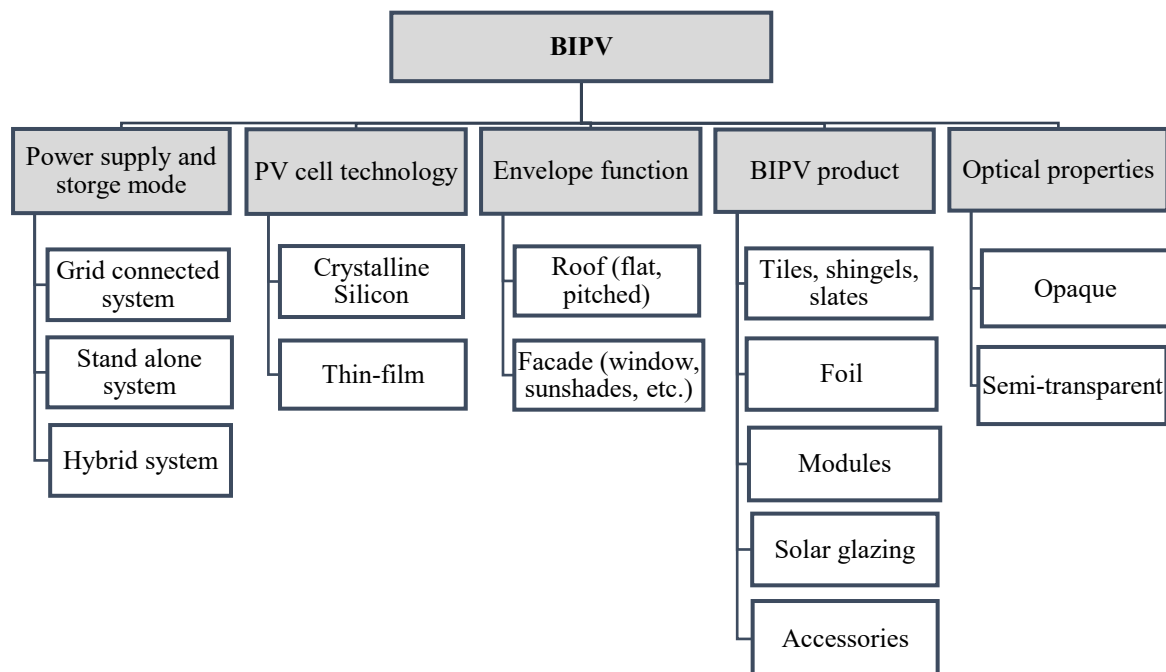


Figure 3-1: BIPV system classifications. Source of data: (Jelle, Breivik and Drolsum Røkenes, 2012; Cerón, Caamaño-Martín and Neila, 2013; Berenschot, 2015; Frontini et al., 2015; Shukla, Sudhakar and Baredar, 2016; Zhang, Wang and Yang, 2018).

Power supply and storage mode

According to the power supply and storage modes, there are mainly two types of PV systems: the grid-connected system and the stand-alone system (off-grid). The former is usually connected to a utility grid that serves as a storage component in the BIPV system and the PV system receives back-up power from a utility grid when the PV system is not producing enough power. The latter type, on the other hand, employs batteries for surplus power storage. The battery also helps to ensure the stable power supply for the fluctuating power generation (Yudha, 2018; Zhang, Wang and Yang, 2018). There is also a hybrid system where the system not only depends on the PV system but also with another type of electricity generator such as wind turbines (Yudha, 2018).

PV cell technology

Usually, a distinction is made between two types of PV technology (Jelle, Breivik and Drolsum Røkenes, 2012; Cerón, Caamaño-Martín and Neila, 2013).

Crystalline silicon (c-Si): PV elements of this kind consist of interconnected Si-wafers. The main advantages are relatively high efficiency and high reliability (Asfour, 2018). Specific efficiencies are dependent upon the composition of the cells in the module. Mono-crystalline silicon cells (mono-Si) have high purity and therefore a relatively high efficiency of typically 14-19%. The efficiency of polycrystalline silicon (poly-Si) is typically 12-15%, due to lower silicon purity since a range of Si-materials is mixed (Twidell and Weir, 2015).

Thin-film (TFSC): These PV elements make up about 5% of the total installed PV capacity in 2017 (Fraunhofer Institute for Solar Energy Systems, 2018). They consist of thin layers of semiconductor material (not necessarily silicon), providing a thin PV element that can be either rigid or flexible. The main advantages are a lower thickness, lightweight and high flexibility (Twidell and Weir, 2015). However, from the overall point of view, the energy conversion efficiency of thin-film PV technologies are generally low (Zhang, Wang and Yang, 2018). Different types of TFSC are Amorphous silicon (a-Si), Cadmium telluride (CdTe) and Copper indium gallium selenide (CIS/CIGS) (Twidell and Weir, 2015).

It needs to be mentioned that a higher degree of integration of PV within the building envelope generally decreases the efficiency of the system. This can be the result of various causes, such as complex geometry, higher temperatures, loss of solar gain area, the use of TFSC instead of c-Si or the requirement of transparency reducing the module density. For both technologies the efficiency will therefore likely be lower in practice and when used as BIPV (Cerón, Caamaño-Martín and Neila, 2013).

Bonomo et al. in their study “BIPV PRODUCTS OVERVIEW FOR SOLAR BUILDING SKIN” found that the dominant PV technology used in BIPV is crystalline silicon (c-Si) with about 75% of the total BIPV products, since it is the most mature technology in the market (Tyagi et al. 2013), and it represents about 80% of the overall PV market in 2017 (Fraunhofer Institute for Solar Energy Systems, 2018), another reason makes the Crystalline silicon very popular for BIPV applications, is because the conventional modules can be easily adapted for building integration; in fact this is the most economical approach to BIPV (Montoro, Vanbuggenhout and Ciesielska, 2011; Bonomo, Zanetti and Frontini, 2016).

Envelope function

Basically, any building component can be replaced by BIPV (Berenschot, 2015). However, two common main application areas are distinguished: roofs and façades (Jelle, Breivik and Drolsum Røkenes, 2012; Berenschot, 2015; Frontini et al., 2015). This two main area includes many alternatives; roof integration or mounting, façade integration or attachments, windows, sunshade integrations, rain-screen integrations, and integration into atrium/skylights, claddings, railings, etc. (Zhang, Wang and Yang, 2018). In the current BIPV market, the roofing market is currently wider than the façade market (Bonomo, Frontini and Chatzipanagi, 2015; Bonomo, Zanetti and Frontini, 2016; Zhang, Wang and Yang, 2018), about 80% of BIPV systems are based on roof integrations, while the rest (20%) are based on façade integrations (Zhang, Wang and Yang, 2018). However, façade BIPV systems are expected to gain importance. As façade PV systems are essential to meet building energy demand, especially in the buildings where the roof is simply not large enough to install solar technologies (Cerón, Caamaño-Martín and Neila, 2013).

Roof integrated photovoltaics usually have little shadowing (Maturi and Adami, 2018) and can be flexibly oriented towards the sun (Jelle, Breivik and Drolsum Røkenes, 2012; Tripathy and Sadhu, 2015), in addition, it is easily accessible which makes the installation and maintenance easier (Tripathy and Sadhu, 2015). The most common product group used for roof integration is solar tiles followed by the opaque roof solution (modules) and solar glazing (Bonomo, Frontini and Chatzipanagi, 2015; Bonomo, Zanetti and Frontini, 2016). Examples of roof-integrated PV are presented in Figure 3-2.



Figure 3-2: Example of roof-integrated PV. a): Typical framed in-roof installation, Sumiswald (Switzerland), the installation achieves a homogeneous appeal through the fact that both, the frame and the modules, share the same color. Source: (Heinstein, Ballif and Perret-Aebi, 2013) b) Frameless c-Si in-roof installation, (Switzerland): 32 modules (Surface: 35 m², Energy output: 5.12 kWp. Source: (Heinstein, Ballif and Perret-Aebi, 2013) c): Semi-transparent photovoltaic integrated to the skylight. Source: (Asfour, 2018).

Regarding PV facade integration, PV modules are visible for people, which may be considered as a visual added value. However, one of the main challenges, in this case, is the issue of shading, which significantly depends on building massing, this issue has to be considered in the early design stage (Asfour, 2018). Façade integrated solar photovoltaic requires thermal and noise insulation, load-bearing and weatherproofing (Frontini et al., 2015).

Different levels of transparency and insulation are available in the market (Cerón, Caamaño-Martín and Neila, 2013). The most common PV product used for façade integration is solar glazing, where the photovoltaic module is used as a building cladding and windows (Cerón, Caamaño-Martín and Neila, 2013; Bonomo, Frontini and Chatzipanagi, 2015; Bonomo, Zanetti and Frontini, 2016). Some of the façade glazing products have electrically operated fittings technology so they can be slid or swung to aid the natural ventilation of the building, and assist heating and cooling as illustrated in Figure 3-3 (a) (Tominaga, 2009). Examples of facade integrated PV are presented in Figure 3-3.

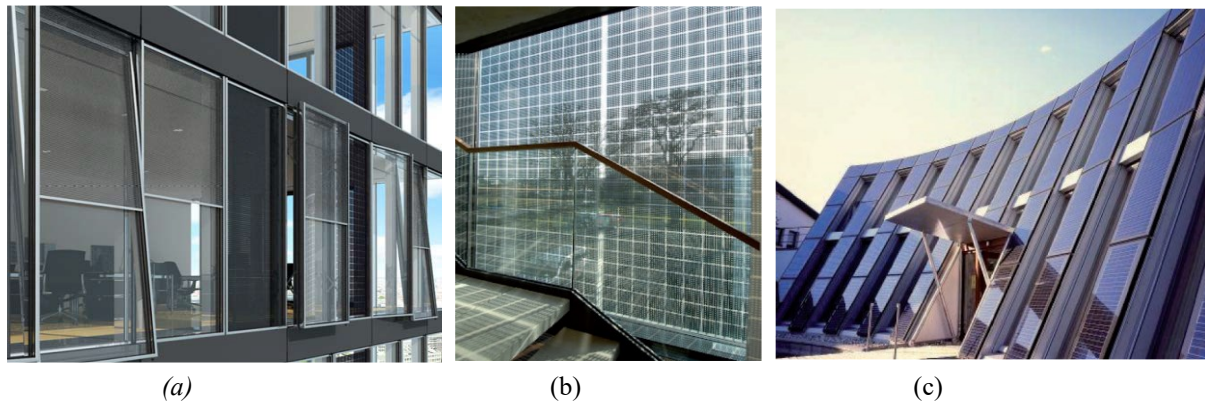


Figure 3-3: Example of BIPV facades. a) Transparent PV integrated to windows. Source: (Bonomo, Frontini and Chatzipanagi, 2015) b) The Energiewürfel (Energy Cube), the customer center for Stadtwerke Konstanz GmbH (Germany): semi-transparent c-Si solar cells with an overall transparency level of 22% provided by the perforated c-Si wafers. Source: (Heinstein, Ballif and Perret-Aebi, 2013) c) Juwi Head Office, Bolanden (Germany): ideal façade inclination with large-scale PV modules to harvest a maximum of solar energy (Surface: 70 m², Energy output: 7.2 kWp. Source: (Heinstein, Ballif and Perret-Aebi, 2013).

BIPV products

BIPV tiles

The BIPV tiles can be either flat or curved as shown in Figure 3-4, with the latter being generally more aesthetically pleasing, but less efficient in catching solar radiation (Jelle, Breivik and Drolsum Røkenes, 2012). Commonly only part of the roof is covered by BIPV tiles, or the BIPV tiles blend with the conventional roof tiles (Frontini et al., 2015). The mono-Si technology is mostly used for these types of solar cells, providing relatively high efficiencies (Cerón, Caamaño-Martín and Neila, 2013).



(a)

(b)

(c)

Figure 3-4: Examples of BIPV tile products. a) Curved BIPV tiles. Source: (Jelle, Breivik and Drolsum Røkenes, 2012) b) Flat BIPV tiles. Source: (Tominaga, 2009) c) Solar tiles solution in Italy to meet with Mediterranean roof tradition. Source: (Heinstein, Ballif and Perret-Aebi, 2013)

BIPV foil

BIPV foil or BIPV membranes are rolls of thin-film PV on soft plastic which can be bonded to roofing materials and structures, see Figure 3-5. Although they do not replace the roof, they are easily installed with electrical connections made under the roof and no additional structural support is required (Tominaga, 2009). The major advantages of BIPV foil are its flexibility and lightweight (Jelle, Breivik and Drolsum Røkenes, 2012). However, BIPV foil products are less efficient than other BIPV products (Frontini et al., 2015).



(a)

(b)

(c)

Figure 3-5: a) Examples of BIPV foil product. Source: (Jelle, Breivik and Drolsum Røkenes, 2012) b) BIPV foil embedded in a flat roof using amorphous silicon cells. Source:(Frontini et al., 2015). c) Transparent light-weight solution. Source: (Heinstein, Ballif and Perret-Aebi, 2013).

BIPV modules

BIPV modules are somewhat like conventional PV modules, sometimes leading to uncertainty whether they are BIPV or BAPV. The difference, however, is that the BIPV solar modules should be able to fulfill a few basic prerequisites when considering their properties of being mechanically stable, fire-resistant, weather-resistant, giving sound and thermal insulation, etc. (Jelle, Breivik and Drolsum Røkenes, 2012; Shukla, Sudhakar and Baredar, 2016; Zhang, Wang and Yang, 2018).

PV modules can be integrated into different parts of building envelope, including roofs, walls, windows, and shadings and replace the conventional material (Frontini et al., 2015; Zhang, Wang and Yang, 2018). Standard PV modules are commonly utilized in BIPV applications, particularly for existing building retrofitting (Frontini et al., 2015; Zhang, Wang and Yang, 2018). The standard PV modules composed of top layer which is transparent and is usually made from hardened or tempered glass in order to protect the PV, at the backside PV modules are usually sealed using Tedlar or glass. Additionally, a frame which is usually made from aluminum is used to ensure the mechanical stability of the PV modules for mounting and fixing. However, this typical standard PV module not always suitable for building integration (Zhang, Wang and Yang, 2018). Recently, various types of PV modules are developed, including PV laminates (frameless PV modules) and semi-transparent modules (Frontini et al., 2015; Zhang, Wang and Yang, 2018). Standard opaque PV laminates are suitable for roofs, walls, and shading systems, but cannot be used for windows. Semi-transparent PV modules can be used in walls, façades, windows, and shadings. Additionally, custom-made modules can be ordered for different BIPV systems before constructing these systems (Zhang, Wang and Yang, 2018). Examples of BIPV modules are presented in Figure 3-6.

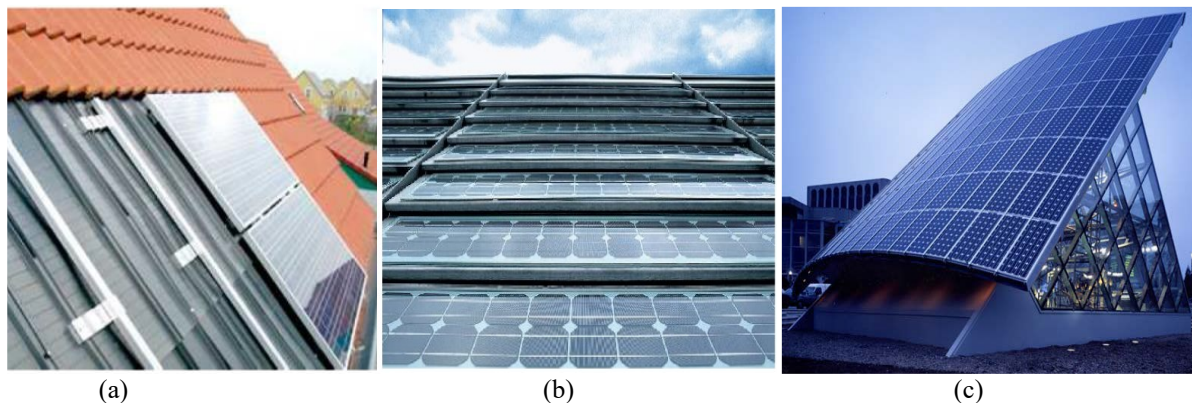


Figure 3-6: Example of BIPV modules, a) PV modules integrated in sloped roof. Source: (Frontini et al., 2015) b) BIPV module for semi-transparent façade (glass-glass module). Source: (Jelle, 2016) c) PV integration on the curved roof of BP solar Showcase in Birmingham. Source: (Basnet, 2012).

BIPV glazing

BIPV glazing is used in all building elements, a great variety of options for windows, facades and roofs are available in the market with a range of different colors and levels of transparency, which can provide many opportunities for aesthetically pleasing design (Jelle, Breivik and Drolsum Røkenes, 2012; Shukla, Sudhakar and Baredar, 2016). Application of transparency is particularly desirable in windows, curtain walls, atria, shading devices and balconies (Frontini et al., 2015). Currently, a typical semi-transparent PV product consists of a layer of PV cells sandwiched between 2 glass sheets. These glazed PV laminates are often made by crystalline silicon cells with adjusted spacing between the cells (usually 3-50 mm), the distance between the cells determines the degree of light transmission, or by laser grooved thin-film which provides filtered vision (Jelle, Breivik and Drolsum Røkenes, 2012; Zhang, Wang and Yang, 2018).

The solar PV cell glazing modules transfer sunlight and serve as water and sun protection. Subsequently, both shading and natural daylighting are provided while producing energy (Frontini et al., 2015). The combination of glass and photovoltaics seems to match well in terms of both aesthetics and functionality of the building's skin (Berenschot, 2015; Shukla, Sudhakar and Baredar, 2016). Examples of BIPV glazing are presented in Figure 3-7.

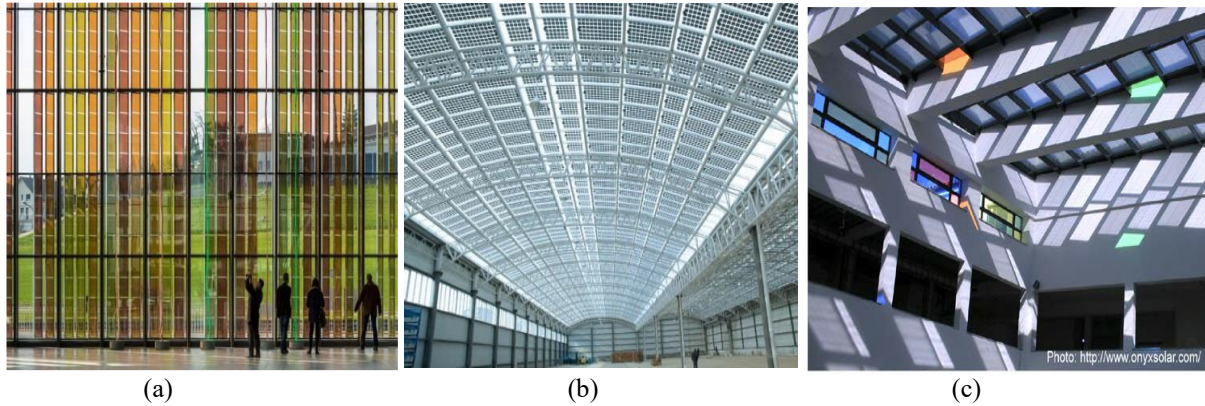


Figure 3-7: Examples of solar glazing a) Coloured BIPV glazing integrated to curtain wall (b) BIPV glazing integrated to skylight. Source: (Berenschot, 2015) c) PV on colored skylights at Bejar Market, Salamanca, Spain. Source: (Basnet, 2012).

BIPV accessories

Both roofs and façades can be integrated with accessories such as balconies, shading systems or decorating. Shading systems are the most commonly used accessory, and it provides the possibility of controlling the temperature and amount of natural light inside a building (Frontini et al., 2015). Figure 3-8, shows an example of a BIPV accessory.



Figure 3-8: Example of BIPV accessory a) PV used as shading in the energy research centre, Netherlands ((Basnet, 2012) b) Solar rail integrated in apartment balcony. Source: (Isa Zanetti et al., 2017) c) PV sliding shades at company HQ, Bitterfeld-Wolfen, Germany. Source: (IEA, 2013).

Transparency

According to the transparency, BIPV systems can be classified as opaque systems and semi-transparent systems (Zhang, Wang and Yang, 2018), which are already described under the product classification.

3.2.4 Life cycle cost assessment

As mentioned in the previous section, many BIPV products have been developed. However, none of these products is mass-produced (Passera et al., 2018). This results in that the price of BIPV is considerably higher than that of the high-volume standard PV modules. However, the price of PV modules has dropped 10-fold since the 1980s, from 30 €/W to 3 €/W (in 2010) (Sharma et al. 2012), and decreased by about 35% from the end of 2017 with the average of 0.50 €/W to the end of 2018 with the average of 0.35 €/W (PV magazine, 2019; PVinsight, 2019). Rapid decreases in the price of PV materials over recent years have resulted in price decreases for BIPV modules (Tominaga 2009; Hammond et al. 2012). This price decrease has been the result of increased production efficiencies and volumes, and improvements in PV technology (Bizzarri et al. 2011). Since PV technology is still under development and the application has increased in the last years, the prices are expected to decrease further in the future (Berenschot, 2015; Jelle, 2016; Yang and Zou, 2016). When considering BIPV these costs can vary in a very wide range depending on many factors such as the materials and the complexity of the solution, system size, location, BIPV product type, and technical specification and it is influenced by the specific country market and by supporting schemes if existing, as well as electricity costs (Hammond et al., 2012; Yang and Zou, 2016; Baxter et al., 2017; Isa Zanetti et al., 2017). Generally, the whole system can be roughly the same as a standard system (when a very simple structure for the installation is designed), and can be 5-12.5% higher than commercially-available PV systems (Baxter et al., 2017; James et al., 2017). Not many studies have been published regarding the cost of BIPV products and integration in buildings, and most of them are country-based.

Previous research generally used case studies to analyse the cost and revenue of BIPV systems by examining short-term data or simulating life cycle operations. They either provide a lump sum cost for the entire system (such as (Tominaga, 2009; Bizzarri, Gillott and Belpoliti, 2011; Li et al., 2012)) or break the costs down into the components of the system, in terms of either €/W or €/m², which is the end-user PV system cost calculated over the area that the PV systems covers on the roof or façade. Using this unit of €/m² it is possible to directly compare various PV technologies to conventional building materials. There are a few studies identified cost breakdown components of BIPV systems (Cucchiella et al., 2012; Rahman, Haur and Rahman, 2012).

Recent study by Passera et al. give the price for different BIPV façade system type, semi-transparent system and opaque system, according to this study, the cost of a BIPV glazing system, including installation, can range between 195 €/m² and 445 €/m² depending on the complexity of the solution, the cost of the transparent PV modules 50 €/m² (5% efficiency) and 225 €/m² (15% efficiency). While the cost of the opaque BIPV system can range between 195 €/m² and 325 €/m². The cost of silicon opaque PV modules (15% efficiency) has a cost in the range of 70 €/m² and 200 €/m² (Passera et al., 2018).

Building owners are often price-sensitive and their decisions are often based on the initial cost that does not consider maintenance and replacement costs in use or the effect of future increases in electricity prices (Jelle, 2016). A way to change the current scenario will be to consider the long-term energy costs, including the savings in electricity benefits (Bhandari et al., 2015; Rauegi et al., 2017), also the avoided costs related to the replacement of building materials and to the additional functions performed by the PV components (Yang and Zou, 2016).

For evaluating the economic performance of PV modules in their lifetime, life cycle cost analysis (LCCA) is needed (Reidy et al., 2005; Yang and Zou, 2016). The BIPV cost-benefit examination should include not only initial costs but also continuing maintenance and repair costs all through the building life costs associated with the maintenance and operations during the lifecycle of the system. According to (Knaack et al., 2014; Rodrigues et al., 2016), the maintenance cost is estimated between 1% and 3% of the initial investment per year and 9% and 13% of the inverter replacement (Yang and Zou, 2016).

No research considered the cost of demolishing the BIPV system at the end of its lifespan. As PV system recycling is currently not viable because waste volumes generated are too small (Hammad and Ebaid, 2015). There were only a few studies that provided information on the transport and monitoring costs. Cucchiella et al. (2012) carried out a simulation on performance evaluation of a rooftop BIPV system in Italy. The transport and mounting costs were identified as 19% of the total cost (Cucchiella et al., 2012). In contrast, although in a similar location, Bakos et al. came up with less than 3% for transportation based on the analysis of a system in Greece. They also allocated a small percentage (2.6%) to the monitoring costs, which mainly comes from management and inspection activities during the system's operation (Bakos, Soursos and Tsagas, 2003).

Recently, Wu et al. investigated the financial benefits of building-integrated photovoltaics (BIPV) facilities and equipment by studying the net present values (NPV) and a payback period of the BIPV façade of a shopping mall in Taiwan over its lifecycle. The NPV and payback period analysis indicated that the BIPV façade in the case study reached its breakeven point within 10 years of payback period and within 16 years of NPV during a life cycle of 20 years (Y. W. Wu et al., 2017).

3.2.5 Carbon and energy life cycle assessment

Nowadays, PV is recognized as one of the cleanest technologies for electricity generation, but there are still arguments that PV technologies may consume additional energy during their life cycles (Zhang, Wang and Yang, 2018). Therefore, a life cycle analysis (LCA) is helpful to evaluate the life cycle performance of PV systems (Fthenakis and Kim, 2011), starting with the resource extraction, the fabrication of PV modules and other system components, the operation and maintenance, and closing with the consideration of an end-of-life (Peng, Huang and Wu, 2011; Lenz *et al.*, 2012).

The international energy agency (IEA) developing methodology guidelines for a PV system LCA. It also structures the guidelines into three main areas: (1) recommendations for technical characteristics related to PV systems; (2) aspects regarding modeling in both LCA inventory and impact approaches; (3) aspects about reporting and communication (Frischknecht et al., 2016).

Commonly used indicators for the LCA of PV systems are the energy payback time (EPBT) and greenhouse-gas emissions (GHG). EPBT is the required period in which the PV system achieves an electricity balance, i.e., the system generates the same amount of electricity as the electricity consumed over its lifetime (Frischknecht *et al.*, 2016; P. Wu *et al.*, 2017). Regarding the GHG emissions, PV systems offer great potential for mitigating GHG emissions compared with conventional power systems (Fthenakis, Kim and Alsema, 2008; Fthenakis and Kim, 2011). Fthenakis et al. found that PV-based electricity generation systems produce notably lower GHG emissions than the classical fossil fuel stations, and the variance could be as high as 89% if the PV-based electricity generation systems are linked to the grid (Fthenakis, Kim and Alsema, 2008).

A few studies on the energy and carbon LCA found focusing on the LCA of BIPV (Lu and Yang, 2010; Ng and Mithraratne, 2014; Bhandari et al., 2015; Zhang, Wang and Yang, 2018). However, most of these studies have either presented a limited data set or used outdated data without considering the continues improvement in the PV technology's efficiency and the process used in manufacturing them (Bhandari et al., 2015). Moreover, to an overall investigation, for BIPV applications, the thermal performance of BIPV systems and building material replacement should also be counted for the energy and environmental LCA estimation (Lu and Yang, 2010).

The LCA results from different studies have varied a lot, influenced by many factors, such as, solar radiation level, installation location, climate conditions, and other parameters that affect the system's electricity output (Lu and Yang, 2010; Zhang, Wang and Yang, 2018). The local electricity mix also affects the LCA results, which should be taken into account (Lu and Yang 2010; Ng and Mithraratne, 2014).

Ng et al. inspected the life cycle environmental and economic performance of six commercially available semi-transparent BIPV modules for a window application under the tropical conditions of Singapore. Energy simulations were assumed to perform a life cycle evaluation to decide long-term performance regarding energy and carbon emissions, as well as cost considerations. The performance of semi-transparent BIPV windows not only included electricity generation capabilities but also the effects on the cooling load and artificial lighting requirement. The results indicate that the major life cycle stages that require significant primary energy use are the manufacturing of photovoltaic modules and the balance of systems. The energy payback time EPBT was less than two years ranged from 0.7 years to 2 years, while energy return on the investment ranged from 12 to 35 years. After considering government allowance, some modules cost lower than traditional windows, while half of the remaining modules completed payback periods of 1 to 13 years (Ng and Mithraratne, 2014).

Lu and Yang investigated the energy payback time (EPBT) and the carbon payback time (CPBT) of the BIPV system in Hong Kong. The embodied energy of the whole system in the lifespan was estimated to be around 70% of the PV modules and 29% of the balance of system (BOS). Nearly half of the embodied energy is for silicon purification and processing. The EPBT of the PV system was estimated to be 7.5 years, and the CPBT was estimated to be 5 years by considering the fuel mixture composition of local power stations, however, these figures could be much lower if the utility power plants generate power by 'non-clean' fuel. This paper also studied the EPBT for BIPV systems with different orientations, ranging from 7 years (optimal orientation) to 20 years (west-facing vertical PV façade). The outcomes demonstrated that the 'sustainability' of a PV system was influenced by its installation orientation and location (Lu and Yang, 2010).

Perez and Fthenakis performed an environmental LCA for façade PV systems, the life cycle inventory data used were based on the detailed bills of material and construction data directly from the designers, architects, and supply chain partners involved in the construction of curtain-wall façade arrays in New York city. The findings indicated that replacing an alternative cladding system with a BIPV façade system had a competitive EPBT of 4 years (Perez et al., 2012).

3.2.6 Energy performances of BIPV systems

As afore-mentioned, BIPV systems provide multiple benefits to buildings, including on-site electricity generation and improve the building energy efficiency. BIPV systems affect building energy demand through solar heat gain, daylighting and electricity production. Accordingly, the effect of the BIPV system on the power output and building energy performance, optical performance and thermal performance, should be considered (Lu and Law, 2013; Ng, Mithraratne and Kua, 2013; Cannavale et al., 2017). This section reviews the latest research outcomes which have considered the performance of BIPV systems.

Some studies have pointed out that the electrical performance of the BIPV systems can be influenced by many designs and installation parameters (orientation, slope of PV, internal gains), as well as by the PV module properties, including the module efficiency, shading effect, incident and azimuth angles, orientation, etc. (Cannavale et al., 2017; Zhang, Wang and Yang, 2018). Some researches investigate the effect of ventilation on PV electricity production, Gan concluded that an air gap in the range of 12-16 cm could improve reduce overheating and increase the PV electricity generation (Gan, 2009; Ritzen *et al.*, 2017). Ritzen et al. compared the electrical performances of ventilated and non-ventilated PV rooftops in the Netherlands, based on the results, the power output of the ventilated PV rooftop was 2.5% higher than that of the non-ventilated type (Ritzen et al., 2017).

Peng et al. experimentally investigated the thermal and power performances of a double-skin semi-transparent PV (PV-DSF) façade under different ventilation modes, based on the tested results the electricity generation under the ventilated mode was more than that under the non-ventilated mode by 3%, in accordance with the lower operating temperature. A conclusion was pointed out that the ventilation design can not only decrease the heat gain of PV-DSF but also enhance the energy conversion efficiency of PV modules by reducing their operating temperature (Peng et al., 2015). Later in 2016, Peng et al. numerically examined the overall energy performance and energy-saving potential of this ventilated PV system in a Mediterranean climate zone. The simulation results marked that using a south-facing PV-DSF in an office assessed to save the net electricity use by about 50% compared with other commonly utilized glazing systems and can block solar radiation while still giving daylighting illuminance. The system was able to generate 65 kWh/m² electricity yearly and to cut down the net electricity demand of the room to 55 kWh/m² (Peng et al., 2016).

The overall energy performance of semi-transparent PV is investigated by few researchers, Xu et al. performed a parametric analysis to find out the optimal PV cell coverage ratio for semi-transparent PV façade systems in terms of the overall energy demand of office buildings in central China. The results verified that with the increasing PV cell coverage ratio, the indoor daylight illuminance decreased linearly, the electricity demand increased, and the heating and cooling electricity demand decreased. The use of the optimal PV cell coverage ratio could obtain overall energy demand savings of 13% (on average) compared to the least favorable PV cell coverage ratio (Xu et al., 2014). Recently, Tian et al. investigated the overall energy performance of semi-transparent photovoltaic (STPV) windows in southwest China, based on the test and simulation research work. This study focuses on the overall energy performance of different windows, the interactional effect was studied among air conditioning energy demand, lighting energy demand and energy generation. The results of the experimental test concluded that STPV windows could provide 0.25 kWh/day and save 29% on comprehensive building load on a typical sunny day.

Furthermore, buildings installed with STPV windows in four typical cities with various climate conditions in southwest China were simulated and analyzed. The cooling load of all the buildings was decreased, while the heating energy demand and lighting energy demand slightly increased, owing to the partially blocked solar radiation by STPV windows and different climatic conditions. The energy-saving potential of STPV windows was ranged from 25% and 55% of all cases (Tian et al., 2018).

Cannavale et al. studied the effect of the replacement of standard clear glass windows with new windows integrating semi-transparent photovoltaic modules, and the change of the original transparent shading system with high-performance opaque cells, they carried out simulations of a real office building located under Mediterranean climate in Bari (Italy). The overall energy demand for heating, air conditioning, and artificial lighting, estimated against the overall energy yield provide by building-integrated photovoltaic modules were analyzed. Results demonstrated that under ideal conditions (no obstructing buildings) yearly savings up to 15% for semi-transparent PV window, and up to 22% horizontal PV shades could be obtained compared to the reference case. In the presence of nearby buildings, cast shadows significantly reduced the energy yield. In particular, PV window on the ground floor become mostly ineffective (the energy yield reduced by more than 50%), and from the visual comfort point of view, they do not contribute to reducing glare as direct sunlight is shaded by buildings (Cannavale *et al.*, 2017).

PV Shading devices can decrease daylight availability, increase artificial light needs, block the beneficial winter solar radiation, and produce on-site electricity. Mandalaki et al. done several studies during 2012 and 2014 in Mediterranean climatic conditions on the visual and energy performance of PV-integrated with fixed shading devices. It was found out that shading devices with integrated south-facing PV can produce electricity to be used for lighting (Mandalaki et al., 2012), and found that the Brise-Soleil (horizontal louvers) system is the most efficient system where it ensures visual comfort and sufficient energy production (Mandalaki, Tsoutsos and Papamanolis, 2014).

BIPV has a significant effect on the amount of heat transfer through the building fabrics and could affect the indoor air temperatures and the comfort of the occupants since it changes the thermal resistance of the building envelopes (Ekoe A Akata, Njomo and Agrawal, 2017). Tina et al. studied the thermal sensation of Italian occupants sitting or standing near BIPV systems and reported that it corresponded to a slightly uncomfortable but acceptable condition (Tina *et al.*, 2013).

3.3 Building-integrated solar thermal (BIST)

3.3.1 BIST definition and advantages

BIST is defined as the multifunctional construction element, which can be integrated into a building envelope element (e.g. wall, window, shading, or roof), and differs from conventional solar collectors in that it offers a wide range of solutions in architectural design features (i.e., color, texture, and shape). It has flexible functions of buildings' heating/cooling, hot water supply, power generation and simultaneously improving the insulation and overall appearance of buildings (Zhang, Shen, Campus, *et al.*, 2015; Zhang, Shen, Lu, *et al.*, 2015; Maurer, Cappel and Kuhn, 2017). BIST can also deliver many more features that are also available in some conventional building envelopes. BIST products that allow solar gains to be removed from the building envelopes thus reducing the buildings' cooling load; can supply to mechanical resistance and stability; protection against noise, energy efficiency and the sustainable use of natural resources (A.Kalogirou, 2015; Maurer, Cappel and Kuhn, 2017).

The integration of solar thermal collector systems in buildings can equally add to the aesthetics like that posed by the photovoltaic systems. Integrating these systems into building means that not only should they respond to the technical limitations of their particular solar thermal technology, they should also become architectural components designed to be integrated into the building skin, similar to PV integration (Basnet, 2012). There must exist some level of flexibility in all the system characteristics affecting the building appearance, these include collector material and surface texture, absorber color, shape, size and type of jointing (Basnet, 2012; Munari Probst and Roecker, 2012; Maurer, Cappel and Kuhn, 2017).

3.3.2 BIST market

Unlike the BIPV market, the solar thermal market provides a limited variety of products suitable for architectural integration and this is the major barrier to the widespread solar thermal systems in the building practice (IEA, 2012; Munari Probst and Roecker, 2013). Unfortunately, there are no available data concerning the number of BIST installations, unlike the BIPV market. According to Cappel *et al.* this number is very small (Cappel *et al.*, 2015). Therefore, the evolution of the solar thermal market, in general, is presented here to give a general frame of the state of the art of solar thermal collectors.

The international energy agency published an annual global solar thermal statistics report “ solar heat worldwide: markets and contribute to the energy supply ” (IEA, 2018b). The 2017 edition reports that in 2016, solar thermal technologies produced 375 TWh. The global solar thermal capacity of unglazed and glazed water collectors in operation grew from 62 GW_{th} (89 million square meters) in 2,000 to 470 GW_{th} (675 million square meters) in 2017 (Figure 3-9). The corresponding annual solar thermal energy yields amounted to 51 TWh in 2,000 and 388 TWh in 2017.

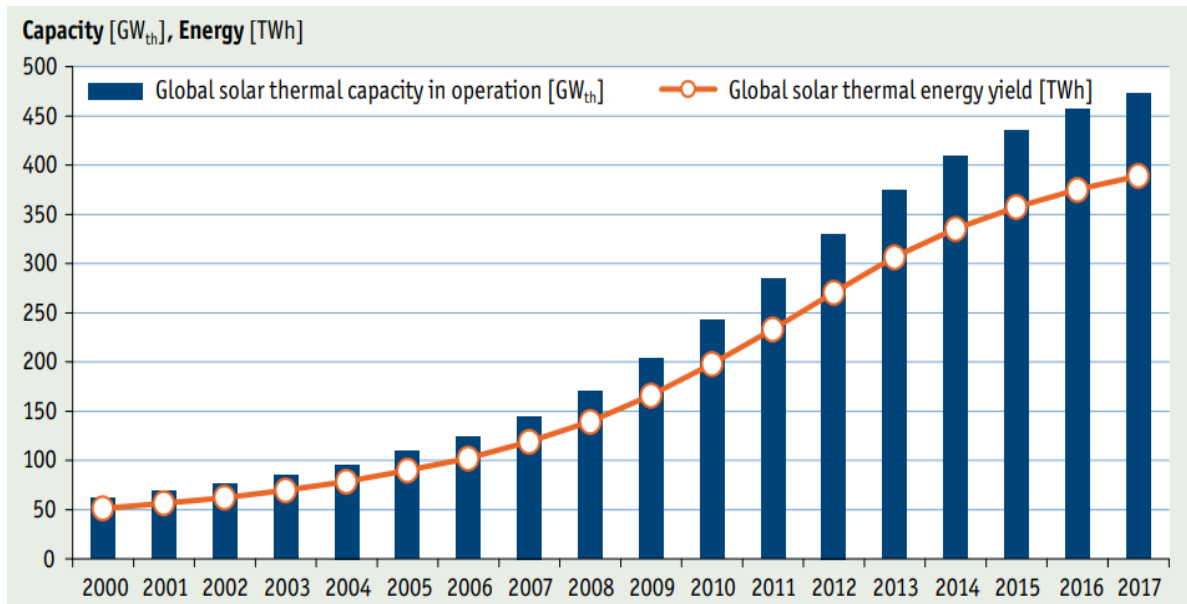


Figure 3-9: Global solar thermal capacity in operation and annual energy yields 2000-2017. Source: (IEA, 2018b).

In 2017, photovoltaics had the highest global growth rate with 33% added capacity and was followed by wind, which increased its installed capacity by 11%. With a 4% added capacity, solar thermal was significantly behind the other two technologies. Solar thermal systems are facing challenging times. This is reflected in the continuous shrinking of the annual added collector capacity, which declined from 18% in the period 2010/2011 to 4% in the period 2016/2017. Compared to the year 2016, new installations declined by 4.2% in 2017. The most dramatic development was in China, where for the fourth year in a row the market declined, after a 17% decline in 2014 and 2015 and a 9% decline in 2016, this trend continued 2017 with a 6% decline (IEA, 2018b).

By the end of 2016, 650 Million square meters of water-based solar thermal collectors corresponding to a thermal peak capacity of 450 GW_{th} were in operation worldwide. Most of the total capacity in operation was installed in China (325 GW_{th}) and Europe (51 GW_{th}), which together accounted for 82% of the total installed capacity. The total installed capacity in operation in 2016 was divided into flat plate collectors (FPC): 101 GW_{th} (144.4 Million square meters), evacuated tube collectors (ETC): 327 GW_{th} (467 Million square meters), unglazed water collectors 27.7 GW_{th} (39 million square meters), and glazed and unglazed air collectors: 1.2 GW_{th} (1.7 Million square meters). With a global share of 71.5%, evacuated tube collectors were the predominant solar thermal collector technology, followed by flat plate collectors with 22% and unglazed water collectors with 6% (Figure 3-10). However, flat plate collectors are most common in Europe (83%) (IEA, 2018b).

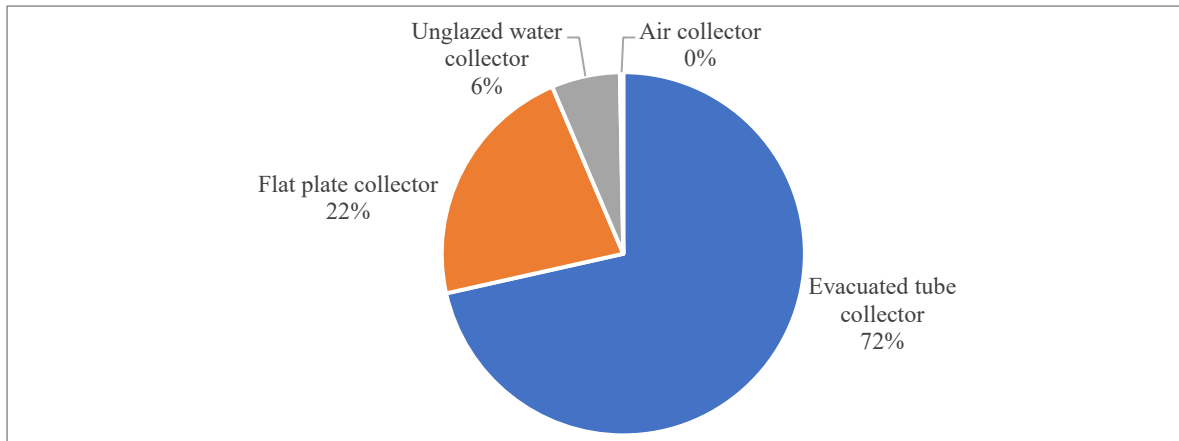


Figure 3-10: World distribution of the total installed capacity in operation by collector type in 2016. Source: (IEA, 2018b).

Worldwide, more than three-quarters of all solar thermal systems installed are a thermosiphon system and the remaining solar heating systems are pumped solar heating systems. In 2016, 89% of the newly installed systems were a thermosiphon system while pumped systems only accounted for 11%. Generally, thermosiphon systems are more popular in warm climates, such as in Africa, South America, southern Europe, and the MENA countries. In these regions, thermosiphon systems are installed with flat plate collectors, while in China the typical thermosiphon system for domestic hot water preparation is installed with evacuated tubes (IEA, 2018b).

3.3.3 BIST classifications

Building-integrated solar thermal systems (BIST) have been categorized in a variety of operating characteristics, system features and mounting configurations which are briefly illustrated in Figure 3-11. The main classification criteria are based on: final application for the energy collected (A.Kalogirou, 2015; Zhang, Shen, Lu, *et al.*, 2015; Maurer, Cappel and Kuhn, 2017), method of transferring collected energy (A.Kalogirou, 2015), thermal collection typologies (O'Hegarty, Kinnane and McCormack, 2016), heat-transfer medium (A.Kalogirou, 2015; Zhang, Shen, Campus, *et al.*, 2015), envelope function (possible area for installation) (Basnet, 2012; A.Kalogirou, 2015; Zhang, Shen, Campus, *et al.*, 2015; Zhang, Shen, Lu, *et al.*, 2015; Maurer, Cappel and Kuhn, 2017), as well as transparency (Munari Probst and Roecker, 2013; A.Kalogirou, 2015; Zhang, Shen, Campus, *et al.*, 2015; IEA SHC Task 51, 2016).

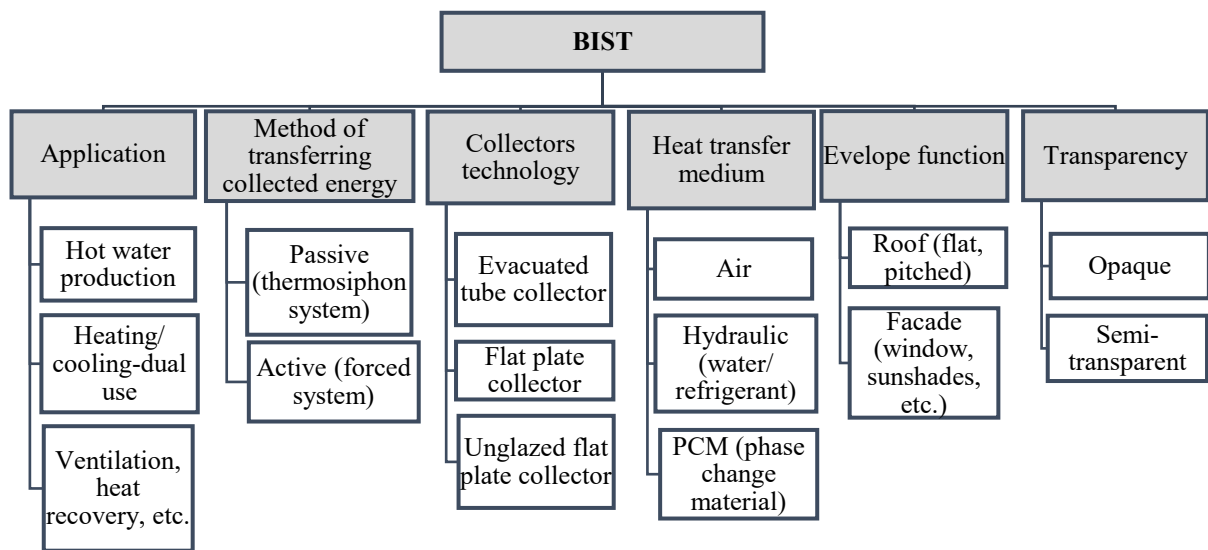


Figure 3-11: BIST system classification. Source of data: (Basnet, 2012; Munari Probst and Roecker, 2013; A.Kalogirou, 2015; Zhang, Shen, Campus, et al., 2015; Zhang, Shen, Lu, et al., 2015; IEA SHC Task 51, 2016; O’Hegarty, Kinnane and McCormack, 2016; Maurer, Cappel and Kuhn, 2017).

Application

In general, BIST system can be used to supply thermal energy for different applications, when it works well in a system, that typically involves piping, a thermal storage tank, a pump and a membrane expansion vessel (A.Kalogirou, 2015). The most common application of solar thermal systems is domestic hot water supply (Maurer, Cappel and Kuhn, 2017), instead of oil, gas, biomass or electricity, the sun is used to heat the water. Typically, the domestic hot water should provide a minimum temperature between 40 °C and 65 °C. If the BIST collectors cannot provide the minimum temperature, they can still be used in combination with a back-up system, to preheat the fresh water to reduce the demand for non-renewable energy sources (R2CITIES Project, 2014; Maurer, Cappel and Kuhn, 2017). Solar thermal can be also used for domestic hot water and space heating, so-called “combi-systems”. The solar combi-system has a larger collector area and generally larger storage to meet the space heating needs (R2CITIES Project, 2014). Solar thermal can be also used for space cooling, for example, thermally driven heat pumps (adsorption and desorption), can be used for space cooling, however, electrically driven heat pumps more common for space cooling with photovoltaic integration (Maurer, Cappel and Kuhn, 2017). Another possible application for solar thermal including dehumidification, process heat, swimming pools, ventilation, etc. (R2CITIES Project, 2014; Maurer, Cappel and Kuhn, 2017).

Method of transferring collected solar energy to the application

The solar collecting methodologies that can be applied in buildings are the thermosiphon (passive) and pumped (active) systems (R2CITIES Project, 2014; A.Kalogirou, 2015). Thermosiphon systems using thermal buoyancy for fluid transport (natural convection or circulation), common in frost-free climates (A.Kalogirou, 2015). This avoids the need for pumping and the associated costs but means that the heat storage needs to be placed on the roof above the collector, limiting its size because of its weight (R2CITIES Project, 2014). Pumped circulation systems utilize pumps or fans to circulate the thermal transfer fluid to a point of demand or storage (forced convection or circulation) (R2CITIES Project, 2014; A.Kalogirou, 2015). Many façade solar air heaters use thermal buoyancy to induce airflow through the vertical cavities which if necessary can be further increased by in-line fans (A.Kalogirou, 2015).

Collector technology

In terms of collectors technology, the solar thermal systems can be classified into the evacuated tube collectors; glazed flat-plate collectors; unglazed flat-plate collectors (Probst and Roecker, 2011; Zhang, Shen, Lu, *et al.*, 2015; Maurer, Cappel and Kuhn, 2017), concentrating collectors also exist but are not really relevant to the topic of building-integrated treated here.

The popular element of all these collectors technology is the solar absorber made of a thin metal or polymeric sheet covered with a chosen coating material to maximize its solar absorption rate and minimize the infrared loss to the surroundings (Probst and Roecker, 2011; Zhang, Shen, Lu, *et al.*, 2015).

The sandwich structure of glazed flat plate collectors makes them well suited for the integration into the opaque part of the building envelope layers. The collector layers can be merged with the envelope ones, so as to provide multifunctional components able to fulfill the traditional envelope functions, and in addition capable to produce energy (Munari Probst and Roecker, 2013). In the case of unglazed collectors, the absorber is not protected by a glass layer and has then to take over correctly all the protection functions of the cladding or roofing element, ensuring water tightness when needed (Munari Probst and Roecker, 2013; Zhang, Shen, Lu, *et al.*, 2015). Differently, than glazed and unglazed collectors, the integration possibilities of vacuum tube collectors in the building envelope are hence very different than the ones seen for the sandwich structured flat plates (glazed and unglazed). The main difference is that the assembled tube modules are not watertight and are visually semi-transparent, making them less suitable for multifunctional applications in the opaque envelope parts, but more suitable for windows, shading devices, and balcony (Munari Probst and Roecker, 2013). Evacuated tube collectors are composed of several individual glass tubes, each containing an absorber plate bound to a heat pipe, surrounded by a vacuum. The possibility to orient the single tubes (and their absorber) independently from the tilt of the whole collector (see Figure 3-12), opens the way to new applications, allowing, in particular, the horizontal mounting, less suitable for flat plates (Probst and Roecker, 2011).

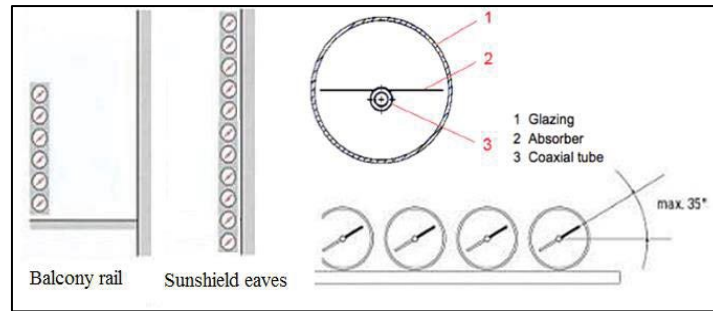


Figure 3-12: Evacuated tube collectors' structure and the possibility to orient the absorbers. Source: (Zhang, Shen, Campus, et al., 2015)

Heat-transfer medium

In terms of heat-transfer medium, the BIST collector can be classified into the air, hydraulic (water/heat pipe/refrigerant) and PCM-based types (A.Kalogirou, 2015; Zhang, Shen, Campus, *et al.*, 2015). Air systems have the features of anti-freezing or anti-boiling operation, non-corrosive medium, simple structure and low costs (Probst and Roecker, 2011), this means that a larger wall or roof area is needed to deliver the same amount of heat. This system generally utilizes the collected solar heat to pre-heat the intake air for ventilation building purposes and space heating (A.Kalogirou, 2015; Zhang, Shen, Campus, *et al.*, 2015).

Hydraulic systems are commonly used for building-integrated solar thermal that allows the striking solar radiation to be collected effectively and converted into heat for warm water supply and space heating purposes. The heat collection efficiency of the water is higher than by air and therefore the water-based system is small-sized in both container and piping compared to the air systems. For this type of system, the potential risk of piping freezing is in existence, but this could be removed by charging a certain amount of antifreeze liquid (Zhang, Shen, Campus, et al., 2015). The PCM-based type is usually worked in combination with air, water or other hydraulic measures that allow the storage of part of the collected heat during the high solar radiation period, which is then released to the passing-through fluids (air, water, etc.) during the low solar radiation period, thereby achieving a long period of BIST operation, however, it has several disadvantages like difficult to operate and complex behavior (Zhang, Shen, Campus, *et al.*, 2015; Zhang, Shen, Lu, *et al.*, 2015).

Envelope function

In terms of building function, the BIST can be classified as facade (wall, window, balcony, shading device, etc.) and roof-based type (Basnet, 2012; A.Kalogirou, 2015; Zhang, Shen, Campus, *et al.*, 2015; Zhang, Shen, Lu, *et al.*, 2015; Maurer, Cappel and Kuhn, 2017).

The roof has great popularity for the installation of BIST systems. It has many advantages, including high solar thermal yield, convenient installation methods and improving the roof thermal insulation (Zhang, Shen, Campus, *et al.*, 2015; Zhang, Shen, Lu, *et al.*, 2015; O'Hegarty, Kinnane and McCormack, 2016). Flat-plate structures are the most promising in the roof-integrated solar thermal with either modular rectangular or tile geometry, it could either be a glazed or unglazed structure (Zhang, Shen, Lu, et al., 2015). Some examples of roof-integrated solar thermal are presented in Figure 3-13.

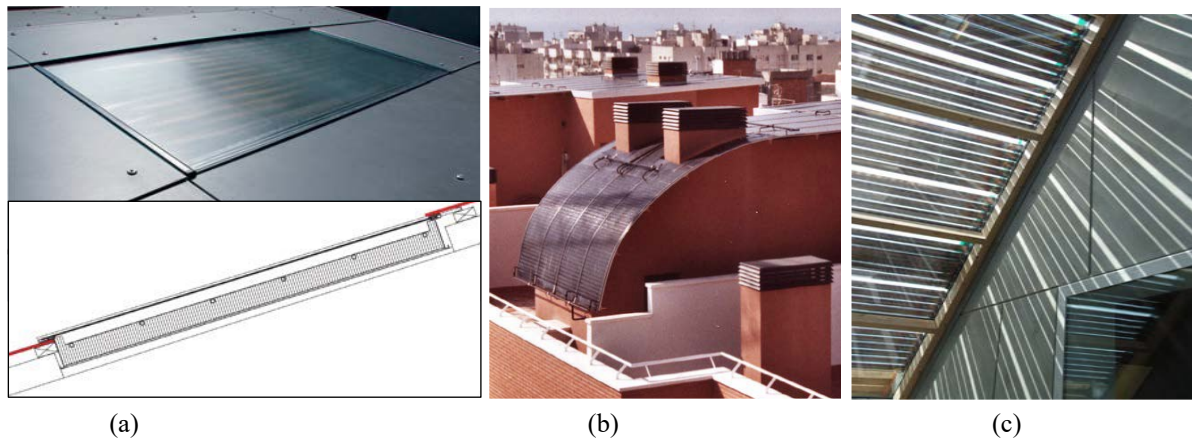


Figure 3-13: a) Integration of a glazed flat plate collector as part of the multilayer roofing system, picture and details (Credits Eternit / Soltop, www.eternit.ch; www.soltop.ch). Source: (Munari Probst and Roecker, 2013) b): Roof integration of unglazed flat plate collectors used as roof covering. (Credits Energie Solaire SA.). Source: (Munari Probst and Roecker, 2013) c): Evacuated tubes collectors used as glazed roof sun shading. Source: (Basnet, 2012).

Façade integrated collectors are becoming more and more popular mainly since they are visible and in turn enhancing the overall look of the building. The other advantage of façade-integrated collectors is the uniform irradiation of sunlight over the year, which is due to their vertical installation. This is very beneficial as a lot of irradiation can be used even in winter when the highest heat demand occurs for space heating (Basnet, 2012). Further, arguments for installing solar thermal collectors on the façade are that there is often not enough space on the roof, or no suitable oriented roof area is available. This is typically the case for multi-family apartment buildings with a relatively high number of floors (Basnet, 2012; Munari Probst and Roecker, 2013). In comparison to BIPV systems, BIST may suit to façades mainly because of the fact that they are considerably more tolerant of shading (Munari Probst and Roecker, 2013). Façade-integrated collectors fulfill several functions: first of all, they function as energy generators for heating water, they improve the building's thermal insulation, and they act as a weather skin for the façade through the glazing and are at the same time a structural element of the façade (Basnet, 2012).

The typical solution of a wall integrated solar thermal collector consists of the usual parts found in stand-alone flat plate collector systems without the casing and the whole construction is set up in front of the normal wall. The collector can be installed directly on the wall, as shown in Figure 3-14 (a), or by leaving an air gap between the insulation and the building structure (brick, masonry, concert), to avoid migration of moisture into the building (Figure 3-14 (b)) (Basnet, 2012; A.Kalogirou, 2015). Integrating the collector directly to the wall insulation decreases the heat loss through the back of the collector resulting in efficiency increases (O'Hegarty, Kinnane and McCormack, 2016). The same construction can be used for sloping roof applications (A.Kalogirou, 2015; Zhang, Shen, Campus, *et al.*, 2015).

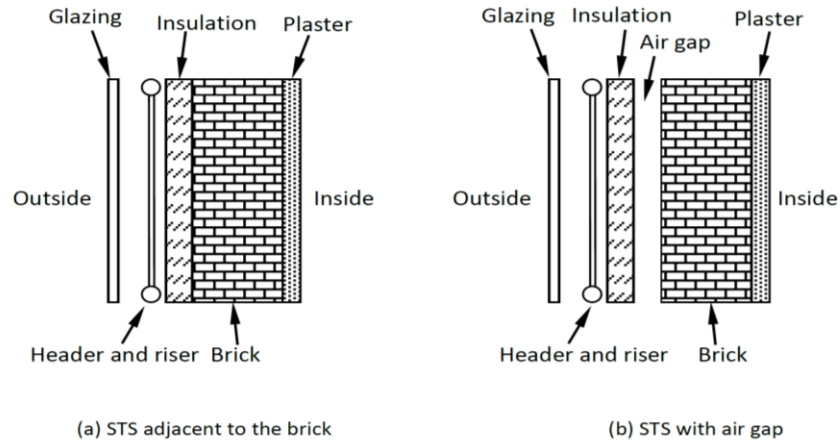


Figure 3-14: Two typical solutions of façade building-integrated flat plate collectors. Source: (A.Kalogirou, 2015).

On the contrary, due to the characteristics of their absorbers, flat plate collectors seem to be less compatible with the functions of transparent envelope parts, but possible implementations such as shading devices should not be excluded (Figure 3-16 (c)), however the thickness and dimensions of the flat plate collectors restrict them to fixed sun shading (Probst and Roecker, 2011; Li, Qu and Peng, 2016). The partial transparency of evacuated tube collectors allows using them as a balcony eave, or as sun shading devices in front of exposed glass surfaces (Figure 3-15). Of course, vacuum tubes can still be applied also in the opaque building parts, as added solar elements. The collector won't become a multifunctional envelope element, but good composition results can still be achieved also with this more traditional approach (Probst and Roecker, 2011).

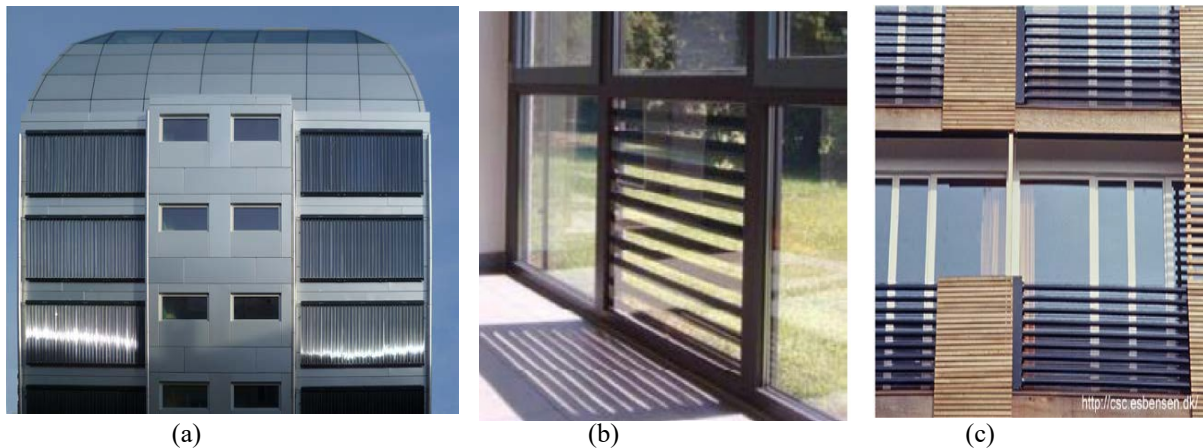


Figure 3-15: Example of façade integrated evacuated collectors' system. a) Evacuated Tubes collectors in front of metal cladding (Hotel Swissnights Lausanne). Source: (Munari Probst and Roecker, 2013) b) Integration of evacuated tubes into a window. Source: (Munari Probst and Roecker, 2013) c) Use of evacuated tube collectors as balcony railings. Residential building in Zurich. Source: (Probst and Roecker, 2011).

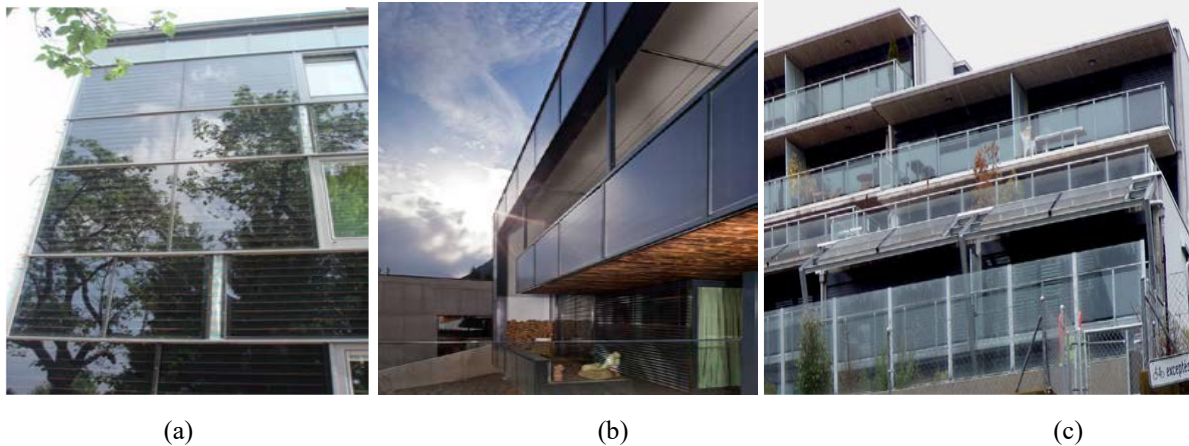


Figure 3-16: Example of a façade integrated flat plate collector's system. Source: (Munari Probst and Roecker, 2013)
a) Façade collectors systems in Austria (credits: www.solar.at) b) SIKO INTEGRAL collectors as balcony fence c) Glazed flat-plate collectors used as sun shading systems (credits EPFL-LESO)

Transparency

In terms of transparency, the BIST system can be classified as opaque and semi-transparent types (Maurer, Cappel and Kuhn, 2017). The semi-transparent type offers the dual functions of solar control in order to reduce the cooling demand or overheating of the building (Kuhn, 2017) and daylight transmission, also provide visual contact between the interior and the exterior of the building (Mertin et al., 2014; Zhang, Shen, Lu, et al., 2015). Some examples already presented in Figure 3-13, Figure 3-15 and Figure 3-16.

3.3.4 Life cycle cost assessment

As mentioned before, only very few installations of the BIST system are known, and most of them are prototypes, in addition, a very few studies available regarding the cost estimation of BIST system, accordingly it is difficult to get reliable data on the cost of such systems (Cappel et al., 2014; Maurer, Cappel and Kuhn, 2017). Unlike solar thermal systems installed on the roof without any integration criteria, the cost of façade adapted solutions depends strongly on the façade typology (lightweight or heavyweight structure) and the solar thermal application (DHW, combi-systems) and on the boundary conditions e.g. energy prices. The other crucial aspect is the climate of the location (Cappel *et al.*, 2015; Zhang, Shen, Lu, *et al.*, 2015).

In terms of the economic evaluation, BISTs can be assessed by using simple payback time and life cycle analysis (Zhang, Shen, Lu, *et al.*, 2015; Maurer, Cappel and Kuhn, 2017). Which are dependent on the initial investment and the cost of alternative energy (Zhang, Shen, Lu, et al., 2015). Since solar façades represent a new frontier, many uncertainties regarding manufacturing, materials, and installation can occur during economic estimations. These can lead to underestimated or overrated costs. Furthermore, the cost of fossil fuels and electricity varies from country to country, so payback periods and life cycle cost cannot be extended even in the same climate zone (Maurer, Cappel and Kuhn, 2017; PASSERA, 2017).

According to the Cappel et al. façade integrated solar thermal collectors had a cost of 250- 360 €/m² which is 25% to almost 50% cheaper than standard installed collectors (480 €/m²), and the cost of the piping and the tank 1,000 €/m² for both cases (Cappel et al., 2015). Maurer et al. found that the solar thermal system has provided investment cost reductions of about 40% compared to a conventional solar thermal installation, and has been shown that 45-65% higher than the conventional building walls. This means that the additional investment cost of building a solar thermal building envelope instead of building a conventional building envelope plus a conventional solar thermal collector can be 40% cheaper per m² collector (Maurer, Cappel and Kuhn, 2017). One reason for the savings can be the direct supply from the manufacturer to the installer without an intermediate wholesaler. Another reason is the synergetic effect of installing the BIST facade in one attempt instead of completing the building envelope first and then altering it for the solar thermal installation again which result in labour and material saving (Cappel et al., 2015; Maurer, Cappel and Kuhn, 2017).

Cappel et al. (2014) estimated the cost of some solar thermal façades, starting from the prices (including labor costs, excluding VAT) of standard passive solutions. The costs are 90 €/m² for a regular composite insulation system and 240 €/m² for a wooden façade with vacuum insulation modules. The prices with integrated absorbers behind customized glazing are 390 €/m² and 600 €/m² respectively. This gives an investment for integrated solar thermal façades that is between 150% and 300% higher than for standard wall constructions. They also noted that the area of an STF would need to be increased by a factor of between 1.5 and 2.0 when compared with tilted solar thermal collectors (Cappel et al., 2014).

Life cycle costs analyze is carried out by Kotic to evaluate the economic feasibility of building-integrated solar thermal collectors to supply hot water to a multi-family residential building in the settlement Konjarnik in Belgrade, Serbia. Four scenarios of position of solar thermal collectors on building envelope were taken into consideration (Figure 3-17), a) solar modules mounted on the roof and tilted at 40°; b) solar modules integrated in the parapets (vertical position-90°; c) solar modules integrated in parapets and tilted at 45°; and c) solar modules integrated as sun shadings (horizontal position-0°). The economic analysis includes the capital cost, energy costs and life cycle costs of the building, including operating, maintenance, repair costs and saving cost over the lifetime of an installed solar system. The results indicated that the thermal collectors positioned on the roof have a better financial advantage compared to other BIST scenarios. life cycle cost for solar thermal collectors on the roof is higher with about 75%, 27%, and 188% than scenarios b, c and d, respectively. And the simple payback was 8 for scenario a, 17 for scenario b, 10 for scenario c and 61for scenario d (Kotic, 2015).

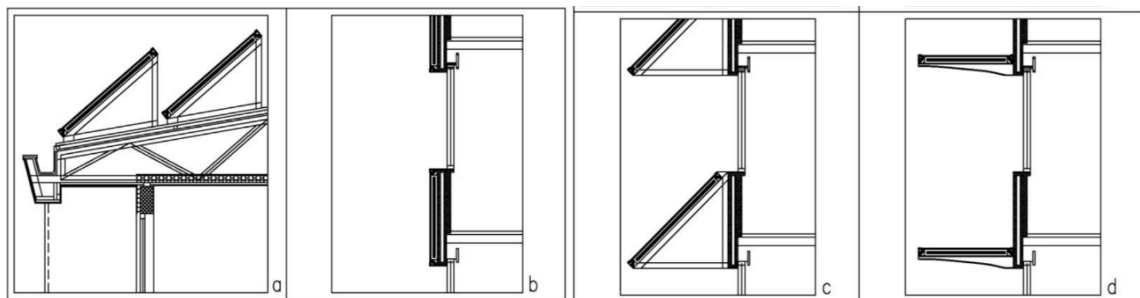


Figure 3-17: Design variants 1– 4 (a - d) cross-sections. Source: (Kotic, 2015).

Palmero and Oliveira (2006) assessed the economic viability of the solar thermal collectors integrated into the louver shading device of a south-facing window for water heating in temperate and Mediterranean climatic conditions of Lisbon in Portugal and Tenerife in Spain. For different configurations, a numerical model for the integrated solar collector has been developed and the collector efficiency is quantified for each configuration. The economic analysis for a solar louver system providing 200 l of hot water per day, led to a payback period of 6.5 years in Lisbon and 5.5 years in Tenerife (compared with conventional heating with gas). The life cycle analysis showed that the louver area that leads to maximum savings (in costs) is equal to about 9 m² for a system life of 20 years (2,290 € for Lisbon and 1,364 € for Tenerife) (Palmero-Marrero and Oliveira, 2006).

3.3.5 Carbon and energy life cycle assessment

Concerning studies which examine the environmental profile of the systems by means of life cycle analysis (LCA), most of them are about roof-mounted solar thermal collectors and very few literatures addressing the LCA works relating to the BIST systems (Lenz *et al.*, 2012; Lamnatou *et al.*, 2014, 2018; Lamnatou, 2015).

An LCA study about solar thermal for façade-integration into high-rise buildings conducted by Lenz *et al.*, they followed a “Cradle to Grave” approach, considering the various stages of the product life cycle process including construction, in-use (operation, maintenance), and end-of-life. Moreover, primary energy issues were also examined. Preliminary results for a transparent solar thermal collector in two different façade layouts (integrated into a double skin facade and a single skin facade), were presented. The major environmental impact was found in the production phase due to the use of energy-intensive materials (e.g. metals, glazing). The adoption of recycling for metals reduced the overall lifecycle impact of up to 30%. The maintenance phase had almost no influence on the overall life cycle impact. It was noted that the transparent solar thermal collector in different layouts and different façade integrations seems to offer advantages from an environmental point of view if the component is applied to the south façade. In addition, for the case where the heat produced by the solar system substitutes the conventional heat production (for example, a condensing gas boiler) while the building is in operation, remarkable energy savings (in terms of non-renewable primary energy) can be achieved (Lenz *et al.*, 2012).

Lamnatou *et al.* conducted an LCA study about a real building-integrated active solar thermal system (integration into building gutters). Three alternative configurations were examined, based on the life cycle impact assessment methodologies of embodied energy (EE) and embodied carbon (EC). Two databases, as an inventory of carbon & energy and Alcorn, and multiple scenarios (related to material recycling, electricity mix France’s vs. Spain’s electricity mix), etc., were adopted. The results demonstrated that by recycling, the energy payback time of the reference system was approximately 1.5 years while by utilizing collectors in parallel connection this value decreased to around 0.5 years, the EE of the systems was around 3 GJ/m² and around 0.4–0.5 GJ/m² by recycling, the EC of the configurations was approximately 0.16 tCO₂/m² without recycling and around 0.02–0.03 tCO₂/m² with recycling, which were strongly related to the electricity mix (Lamnatou *et al.*, 2014; Lamnatou, 2015).

Recently in 2018, Lamnatou et al. studied the life cycle assessment of different options of a BIST system under the Mediterranean climatic conditions: Ajaccio and France. Two configurations in terms of the collectors (with and without PCM component) have been examined. The environmental profile of the studied configurations is evaluated using CED (cumulative energy demand), GWP (global warming potential) and EPBT (energy payback time). Concerning life cycle results, the configuration without PCM (scenario without recycling) shows 0.67 MJ/kWh and 0.06 kgCO₂/kWh, while the configuration with PCM presents 0.74 MJ/kWh and 0.08 kgCO₂/kWh. Regarding EPBT, if the inputs for pumping/auxiliary heating are not taken into account, both configurations (with/without PCM) have nearly the same EPBT (about 1.3 years). On the other hand, if the auxiliary heating inputs are considered, EPBT is lower for the system with PCM (Lamnatou et al., 2018).

3.3.6 Energy performance of BIST

When a solar collector is integrated as a part of a building envelope, the thermal performance of both the collector and the building component is changed. The building envelope influences the collector back heat losses and consequently alters its efficiency; on the other hand, the heat fluxes of the building envelope must be re-evaluated considering the solar collector as part of the envelope itself (Beccali *et al.*, 2016; Leone and Beccali, 2016). The majority of the BIST studies focuses on the influence on the solar system performance when integrated into buildings, whereas there are just a few studies that analyze the influence in the building envelope (Chr Lamnatou *et al.*, 2015; A. Moreno *et al.*, 2017).

Li et al. (2017) evaluated the performance of a BIST shading system applied to a medium office building in Los Angeles. The BIST louvers mounted on the south, east, and west façades were used to collect solar energy to supply the building with domestic hot water, space heating and/or cooling for the building. Solar fraction and solar useful efficiency were estimated through simulation software, and a recommended operation strategy was proposed. The results revealed that: either 10 m² BIST on the south façade or 33 m² BIST on the east and west façades are required to achieve the economic optimum 75% of solar fraction for domestic hot water heating. It is recommended that the BIST on the south façade provide space heating and/or cooling. South-facing collectors deliver similar year-round solar gains comparable constant solar gains all year round, leading in increased load coverage and solar useful efficiency. By using solar power, 65% (7,080 kWh/year) of the heating demand and 20% (9,770 kWh/year) of the cooling requirement can be potentially met by using solar energy (Li, Qu and Peng, 2017).

Buonomano et al. introduced a novel flat plate solar collector made up of inexpensive materials to be integrated into buildings. The overall energy, comfort, the environmental and economic performance of the system was evaluated considering diverse climatic conditions in different regions. They found out that remarkable energy saving was achieved mostly regarding solar heating water production. Significant outcomes were also obtained through the passive effect analysis. The free heating effect allows a remarkable reduction of heating loads and demands in cold winter climate zones. Conversely, for the hot summer areas, the relevant superheating effect was observed (in these cases, the standard stand-alone layout can be preferred to the vertical building integration by also selecting the optimal collectors' slope). In many cases by also accounting the solar heating

water production through the investigated façade integration layout remarkable energy savings and avoided CO₂ emissions are achieved vs. traditional buildings (Buonomano *et al.*, 2015).

Beccali *et al.* (2016) evaluated the yearly performance of a low-cost BIST configuration (solar wall) by means of a TRNSYS model. The effects of a south façade integrated solar air collectors analyzed for a typical Italian building for shape and thermal characteristics. Transient simulations were then performed for two different sites in Italy, characterized by opposite climatic conditions (Milan and Palermo). The result showed that the BIST positively affects the yearly energy balance of the climate where heating demand is prevalent (Milan): reduction of heating demand was always higher than the rise of cooling demand. Positive effects on heating demand were ensured by the fact the energy transfer through the solar façade generally is more than doubled. The overall energy demand reduced by 13% in Milan (from 100 kWh/m²/year to 90 kWh/m²/year) and 9% (from 35 kWh/m²/year to 32 kWh/m²/year) in Palermo (Beccali *et al.*, 2016).

3.4 Summary and identification of knowledge gap

In urban areas, arguments for installing solar thermal collectors on the façade are that there is often not enough space on the roof, or no suitable oriented roof area is available. This is typically the case for multi-family buildings with a relatively high number of floors.

From an overall point of view, when the photovoltaic and thermal collector technologies are integrated into the building envelope (as a roof covering, façade cladding, sun shading, balcony fence), it acts as a multi-functional integral element. As they not only have a technical energy purpose (i.e. heating, cooling, and power) but also contributes to the building fabric from architectural and materials perspective. Also, it has a significant influence on the amount of heat transfer through the building envelope and could affect the energy demand in the building, since it changes the thermal resistance of the building envelope. In addition, integrating PV & ST into the building envelope, eliminating the need for new land and an additional support structure provides a further advantage of cost-saving. However, when the photovoltaic and thermal collector technologies are integrated into the building envelope, easy maintenance and replacement of the components should be considered.

The building integration of PV and ST technologies represent a real challenge to the architects to achieve multifunctional roles, as various factors must be considered, such as the photovoltaic module temperature, shading, installation angle and orientation, effect of PV and ST integration on building thermal performance, aesthetic, installation and maintenance cost, etc.

Most of the studies have been made in the field of building integration of photovoltaic and solar thermal are focused on the performance and technical aspects of the system itself, neglecting the architecture integration aspects and the influence of these systems on the building energy demand. Also, there is a gap in the literature regarding the economic and environmental LCA of building-integrated solar thermal and photovoltaic systems.

Given the fact that architectural integration is an important issue in the spreading of solar technologies, there is a need for further investigations, including information that not only includes the performance of the system itself, but also its implications and impacts on the building. The environmental and economic lifetime performances which provide building designers with additional first-hand information on BIPV's and BIST's energy efficiency to increase and enhance widespread adoption. In addition, to promote the application of BIPV and BIST systems, design and informative graphs that can be easily adopted in the early stages of building design to aid in decision-making should be available. These tools can aid architects and building designers to compare and adopt an alternative, depending on the criteria of the user.

From the background information along with the identification of the knowledge gap as discussed thus far, the next chapter formulates this research methodology.

4 Methodology

In this chapter, the research methodology is presented. First, the research approach is discussed to provide an overview of the research work. After that, the individual stages of research are explained.

4.1 Research approach

To make reasonable solutions concerning the integration of PV and ST technologies into the building envelope, a holistic assessment must be performed at the early design stage of the building, considering all benefits and losses. Therefore, a holistic evaluation method for the assessment of the performance of building-integrated photovoltaic is considered in this research. An overview of the methods adopted for this research is presented below.

- Literature and market review:
Market and previous related research have been reviewed in order to identify the relevant possibilities and the aesthetical solutions the market offers, and the multiple benefits for PV and ST integration.
- Computer simulations:
Different simulations software has been used in this research, IDA ICE 4.8 is used for building energy demand estimation, and to predict the effect of the shading from the surrounding building, while Polysun 11 simulation software is used to predict the systems energy demand and the energy production of the PV and ST systems. In addition to SketchUp pro2017, Autodesk Ecotect analysis 2011 and Meteonorm 7 simulation software. The arguments for choosing this simulation software are presented in the next section.
- Life cycle assessment:
Energy, carbon and cost life cycle assessments of the proposed solutions of the solar integration systems have been made based on current manufacturing practices.
- Develop a decision-support matrix in the form of a radar chart acting serves to include environmental, economic, aesthetic (formal, functional), and energy benefits criteria. This acts as a tool to assist building designers, architects, clients, etc., in their early building design decisions.

The energy performance of the typical multi-family building in Amman, Jordan has been improved through architectural, passive and energy-efficient strategies. After that, the installation of the solar systems (PV & ST) into the improved building envelope under different cases have been evaluated using multi-assessment evaluation criteria, the evaluation criteria are presented below.

Evaluation criteria:

By analyzing related research, documents, literature five main critical factors have been found and used as evaluation criteria. These four critical criteria are, overall energy performance, life cycle economic performance, life cycle environmental performance, formal (aesthetic) and functional performance, see Table 4-1 below.

Table 4-1: Evaluation criteria and the research method used in this research.

	Main criteria	Individual sub criteria	Method
Quantitative criteria	Overall energy performance (OEP)	Energy generation Reduction in energy demand for heating, cooling, and lighting	Simulation software (IDA ICE) Improved an overall energy index
	Economic (25-year lifetime benefit)	Capital cost (initial cost) include the potential of battery installation Running cost (cleaning, maintenance,) Profit and payback	life cycle assessment Improve spreadsheet-based calculations and previously available data
	Environmental performance (25-year lifetime benefit)	Energy Carbon	life cycle assessment Improve spreadsheet-based calculations and previously available data
Qualitative criteria	Formal (aesthetic)	Identity, easy to recognize	Based on the literature review
	Functional	Functional: substantial functions that PV & STC can have like waterproof, heat insulation, Maintainability: to evaluate the the convenience of the maintenance and management of the technology	Based on the literature review

4.2 Software selections

Various building and energy system simulation software is currently available in the market, such as TRNSYS, DesignBuilder, Polysun, IDA ICE, PV*SOL, T*Sol, Ecotect, SOLTOP, etc., and Modelica building simulation library (Witzig, Foradini and Probst, 2009; IEA, 2010). However, integrated software that can support the architects in the early design stage for the development of building architectural design aspects together with the PV and ST systems design is clearly lacking (IEA, 2010; Ruyssevelt, 2014). As most of the available simulation software simulates the thermal behavior and energy demands of buildings have immature or non-implementation of solar active systems, on the other hand, solar energy system simulation software is very specialized and accurate, but not well linked to building models (Witzig, Foradini and Probst, 2009).

There are several important criteria should be considered to select appropriate software such as, the need of a library of standardized ST and PV products as most of the designers and architects are not experts in the active systems design and need access to a wide range of pre-designed products with known properties, easy to follow user guide for a person with architectural background, comprehensive database of various building construction materials, in addition to accurate, user-friendly software tools (Román 2015).

The selection process of the simulation software also included consultation with other professionals and colleagues using various simulation software. Furthermore, making the correct choice involved a review of other papers that compared some of the more recent buildings and energy simulation software.

In this research, more than one simulation software has been used, the mainly used software is IDA ICE 4.8 and Polysun simulation software (version 11). This will allow the use of detailed modeling of IDA ICE to determine the most important architecture treatments and passive strategies to reduce the energy demand of multi-family apartment buildings in Amman, Jordan.

In addition to estimating the effect of installation the solar technology onto the façade on the building energy demand, and to estimate the reduction of the PV production due to the shading effect of the surrounding buildings. While Polysun simulation software is used for the analysis of PV and ST energy productions under different scenarios, and to estimate the energy demand of different energy supply systems to find out the most energy-efficient one.

IDA ICE simulation software

The latest version of indoor climate and energy, IDA ICE 4.8, has been used to perform the dynamic multi-zone simulation to study the building energy demand. The software is developed by the EQUA simulation AB in Sweden. The software provides detailed results on the energy use and on the parameters affecting the thermal behavior of the studied cases (EQUA, 2016). Multi-zone models can be created, defining each room of the building with different conditions (equipment, lighting, occupants, shading, etc.). Besides, it gives the possibility to import to all common 2D and 3D CAD models used today in architecture. Geometry can be also imported from SketchUp or other geometry tools. A benefit with IDA ICE is the open-source code. This makes it possible for the user to understand the governing equations used for the simulation. One of the major benefits of IDA ICE is the 3D-visualisation of the building (EQUA, 2018). The 3D-view can be used for presenting simulation results, which makes it easier for designers, engineers, and clients to visualize the consequences of design choices (Baranda and Sartori, 2014; EQUA, 2018). The program is commonly used in European countries for research and consulting purposes (Baranda and Sartori, 2014; Vadiée, Dadoo and Gustavsson, 2018).

IDA ICE is one of the well-validated building energy simulation software (Ryan and Sanquist, 2012; Milić, Ekelöw and Moshfegh, 2018), as it can give accurate calculations of buildings' energy demands and indoor climate performances in comparison to other simulation software (Molin, Rohdin and Moshfegh, 2011; Baranda and Sartori, 2014; Vadiée, Dadoo and Gustavsson, 2018). Validation of IDA ICE has been performed out during the development and comparisons have been made with other software and measurements over the years by several studies, examples are applied in (Karlsson, Rohdin and Persson, 2007; EQUA Simulation AB, 2010, 2010b; Molin, Rohdin and Moshfegh, 2011; Hesarakı and Holmberg, 2013; Liu et al., 2014; Liu, Rohdin and Moshfegh, 2015; La Fleur, Moshfegh and Rohdin, 2017).

Polysun simulation software

Polysun allows performing very detailed energy system simulations. It is also relatively user-friendly and offers valuable support to design, analysis, and calculation of installations in the field of renewable energies. The designer license makes it possible to build new unique systems using components from the Polysun library. The software offers a large number of system templates with component data enabling them to access the relevant physical parameters without the need to deal with various datasheets from the manufacturers (Vela solaris, 2018).

Polysun is relatively easy to use compared to Matlab, Modelica, and TRNSYS (Persson et al., 2016), and it offers reliable and accurate results (Carbonell, Haller and Frank, 2014; Persson et al., 2016; Graefenhain, Fiedler and Tsanakas, 2017; Simonetti et al., 2017; Witzig et al., 2017).

In both simulation software, IDA ICE and Polysun, the same climate data provided by the Meteoronorm 7 software are used as input, to allow the simulation software to make a realistic simulation of the surrounding environment for every hour during a whole year. “AMMAN JO” weather data file for Amman city is used in all simulations.

Other used simulation software in this research are SketchUp and Ecotect analysis simulation software. The building body is created in SketchUp and then imported into IDA ICE and Ecotect analysis simulation software. The Ecotect analysis simulation software is used to analyze the incident solar radiation on the building envelope components.

4.3 Building energy improvement

The possibility of reducing the energy demand of the typical multi-family building in Amman, Jordan by means of architecture and passive design strategies are investigated through a parametric simulation study using IDA ICE 4.8 simulation software. Figure 4-1 presents the main steps adopted to reduce the building energy demand. More details are presented in Chapter 5.

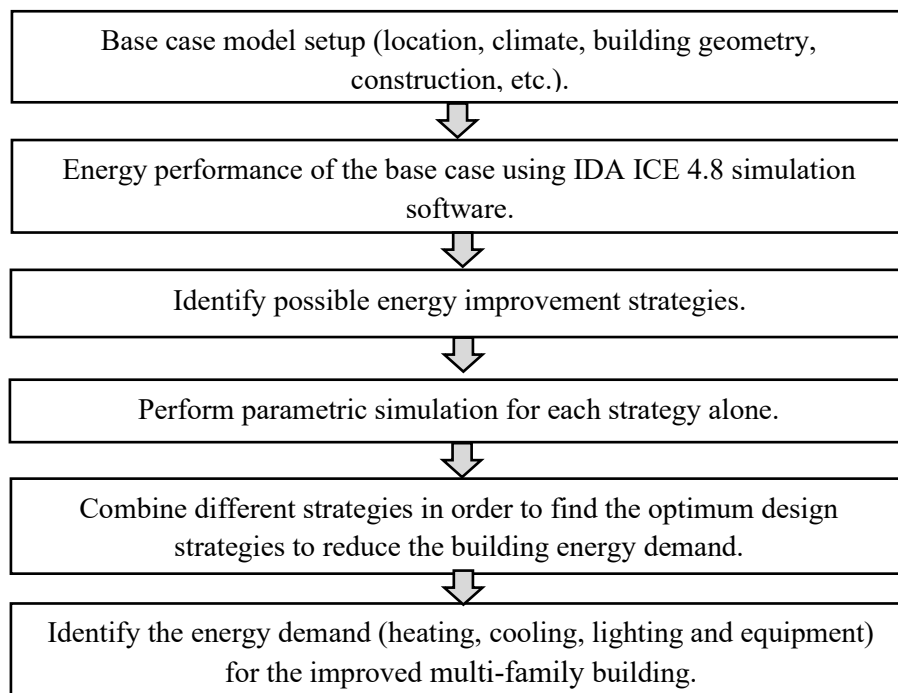


Figure 4-1: The main steps adopted in this research to reduce the energy demand of typical multi-family building in Amman, Jordan.

4.4 Energy supply system improvement

Polysun simulation software (Version 11) is used to simulate and study the proposed systems energy performance, and to calculate the energy output of the solar thermal and photovoltaic systems. Different solar energy supply systems have been proposed and compared with each other, and with a reference system (a conventional Jordanian energy supply system without solar technologies).

The energy demands profiles of the improved multi-family residential building in Amman, Jordan, which is obtained from the IDA ICE simulation software is used in Polysun simulation software, more details are presented in Chapter 6. Figure 4-2 presents the main steps used for energy supply systems selection.

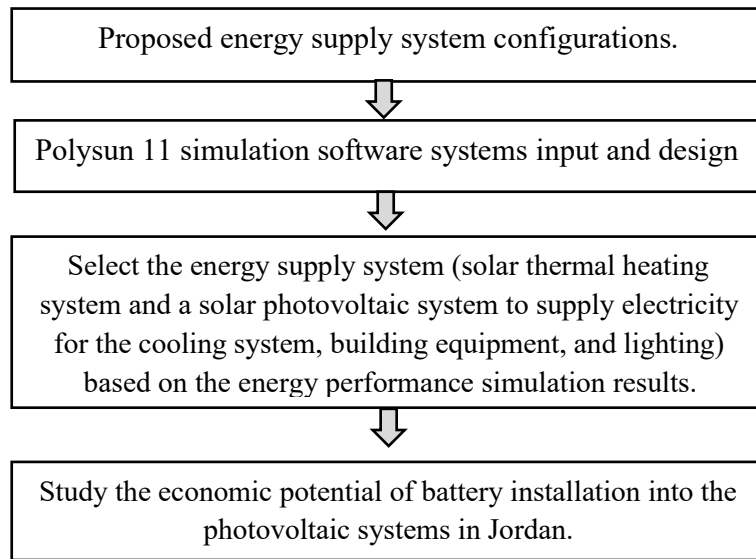


Figure 4-2: The main steps used for energy supply systems selection for improved multi-family building in Amman, Jordan.

4.5 ST and PV applications performance evaluation

The potential of implementing the solar systems on the roof and facades are investigated using multi-assessment criteria, including energy performance, life cycle environmental and economic performance, in addition to formal and functionality performance. All the simulation and analysis of the PV applications are carried out on a new improved multi-family building in Amman, Jordan, with an energy-efficient heating and cooling systems based on section 2.3 and 2.4. The main steps followed to study solar systems performance for different proposed cases are illustrated in Figure 4-3.

It must be mentioned that this research is considering the installation of solar photovoltaic modules to the building façade (in addition to the roof installation), while the solar collectors are only installed on the roof. Based on the literature review analysis and the arguments discussed in Chapter 3.

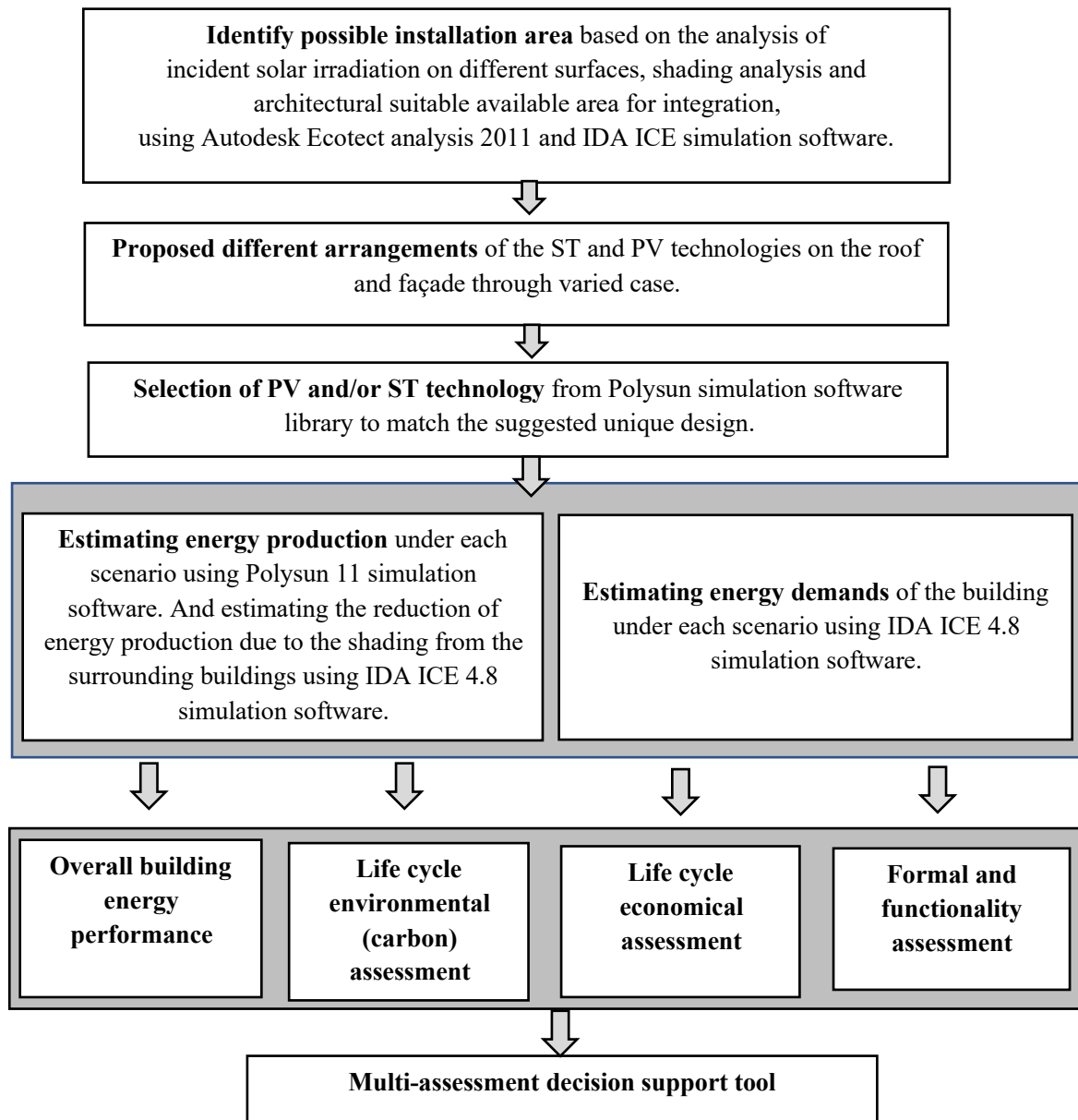


Figure 4-3: The main steps followed to evaluate the performance of different proposed solar systems cases, in multi-family building in Amman, Jordan.

4.5.1 Overall energy performance (net primary energy demand)

Due to the multi-functional role that solar PV integration facade systems have, evaluation of energy performance of the integrated PV should be carried out in terms of the overall energy performance, considering the annual net energy production of the solar systems and the annual primary energy demand (heating system, cooling system, lighting and equipment) of the building. In order to define the overall energy performance of the different solar systems proposed cases, all the energy demands must be converted into primary energy, as there is no published information about the local primary energy factor in Jordan, in the case of heating (the used fuel is oil) the international values for oil and gas are used in this research, where the primary energy conversion factor of oil is equal to 1.1 (Hitchin, 2019). While in for the electricity (including, cooling system, building lighting and equipment electricity demand), the primary energy factor is generated by the 2015 energy mix of Jordan (IEA, 2019a), through dividing the input (production & imports) energy to the output energy (demand), accordingly the conversion factor of electricity to primary energy is 2.71.

The overall energy performance (net primary energy demand) is defined based on Equation 4-1.

$$OEP = (C + H + L) - EG \quad (4-1)$$

Where:

OEP is the overall energy performance (net primary energy demand) (kWh/year), C is the primary cooling demand (kWh/year), H is the primary heating energy demand (kWh/year), L is the light savings (kWh/year) and E is the primary energy saved due to the solar systems installation (kWh/year).

4.5.2 Environmental life cycle assessment

Life cycle assessment (LCA) is a tool for systematically analyzing the environmental performance of products or processes over their entire life cycle, starting with the manufacturing of solar system components from raw materials, and end with disposal/recycling of the waste. Hence, LCA is often considered a “cradle-to-grave” approach in evaluating environmental impacts (Peng, Huang and Wu, 2011; Lenz et al., 2012). In this research, the environmental performance evaluation considered both energy and carbon.

The IEA framework for BIPV LCA assessment is used with the latest Ecoinvent database (version 3.3) (Jungbluth et al., 2012; Frischknecht et al., 2016) along with secondary database from literatures (Fthenakis and Kim, 2011; Fu, Liu and Yuan, 2015; Hou et al., 2016), in order to determine the life cycle energy and material requirements of BIPV systems (including modules, BOS and installation).

Eco-invent is the leading supplier of consistent and transparent life cycle inventory data of renown quality and their databases have often been updated regularly (Jungbluth et al., 2012). While the IEA framework for BIPV LCA assessment provides guidelines includes, photovoltaic-specific parameters used as inputs in LCA, choices, assumptions in the life cycle inventory data analysis and implementation of modeling approaches, etc. (Fthenakis et al., 2011). The information obtained from the database has been modified to represent the actual scenario.

The used indicators for evaluating the environmental impacts of PV systems are the cumulative primary energy demand (CED), greenhouse-gas emissions (GHG), energy payback time (EPBT) and carbon payback time (CPBT), which are very common for the LCA (Frischknecht *et al.*, 2016; P. Wu *et al.*, 2017). Energy payback time is defined as the period required by a renewable energy system to generate the same amount of energy (in terms of the equivalent primary energy) used to generate the system itself (Frischknecht *et al.*, 2016). The EPBT is calculated as defined by Bhandari et al. and Wu et al. in Equation 4-2 (Bhandari *et al.*, 2015; P. Wu *et al.*, 2017).

$$EPBT = \frac{E_{input}}{E_{output}} \quad (4-2)$$

Where:

Einput is the embodied primary energy input during the system life cycle (MJ).

Eoutput is the annual primary energy savings due to electricity generation by the PV system (MJ).

The greenhouse-gas (carbon emissions) payback time (CPBT) is estimated according to Equation 4.3 (Lu and Yang, 2010).

$$CPBT = \frac{GHG_{input}}{GHG_{output}} \quad (4-3)$$

Where:

CHGinput is the embodied carbon emissions of the system during the system life cycle (kg CO₂).

GHGoutput is annual GHG produced by the local power plant for the power generated by the PV system (kgCO₂).

The details of the environmental life cycle assessment including the assumptions and values adopted in this research are presented in Chapter 8.3.

4.5.3 Life cycle economic assessment

The life cycle cost assessment (LCCA) method is used in order to investigate the economic performance of the solar roof and façade PV system under different integration scenarios. The life cycle cost of PV covers all system life stages including, the capital cost (initial cost), the running cost (maintenance cost) and the profit in term of energy production and energy saving (Knaack et al., 2014; Bhandari et al., 2015; Rodrigues et al., 2016; Raugei et al., 2017). As illustrated in Figure 4-4.

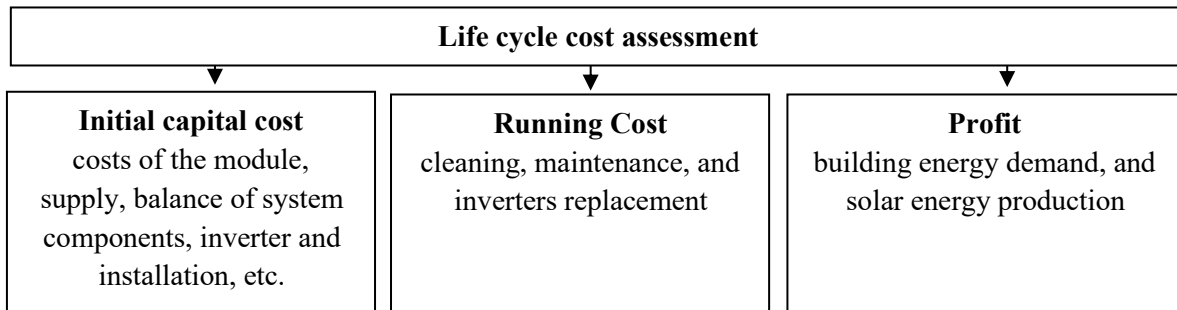


Figure 4-4: Life cycle assessment stages adopted in this research for the PV systems. Based on: (Knaack et al., 2014; Bhandari et al., 2015; Rodrigues et al., 2016; Raugei et al., 2017).

The cost-profit is estimated based on the electricity production and energy saving considering the change in the building energy demand due to the installation of the PV modules into the façade. The current electricity tariff in Jordan is used to estimate the saved electricity costs. For future estimations, the increase in the electricity price has been considered, in addition to the inflation rate and the discount rate. The inflation rate represents the escalation trend in the costs over the all system life, while the discount rate represents the decrease in the components cost with future mass production (El Shenawy, Hegazy and Abdellatef, 2017).

The economic performance assessed through payback time (PBT). Payback time is defined as the number of years expected to recover the initial investment (Jaber and Hawa, 2016). The PBT is calculated according to Equation 4-4.

$$\text{Payback Time (PBT)} = \text{Initial capital cost} + \left(\frac{\text{Runing cost}}{\text{Annual saving}} \right) \quad (4-4)$$

Assumptions and values related to the life cycle cost assessment are presented in Chapter 8.4.

4.5.4 Qualitative criteria

Regarding the qualitative criteria as mentioned in the literature review (Chapter 3), there are no universal criteria for solar systems integration architectural quality evaluation, these are harder to define in a unique way, as often perceived as subjective (IEA, 2013; Frontini et al., 2015). However, recent studies have confirmed the existence of potential criteria shared by the architect's community and resulting to improve the architectural integration quality perception (Munari Probst and Roecker, 2007, 2012; IEA, 2013).

Several architectural criteria have been defined in the framework of the International Energy agency project Task 41 "Solar Energy and Architecture" for BIPV formal integration quality, (Munari Probst and Roecker, 2012; IEA, 2013). Based on these criteria and previous literature (Munari Probst and Roecker, 2007, 2012, 2013, 2019; Dessì, 2011; Probst and Roecker, 2011), two evaluation aspects are proposed in this research; formal and functional aspects.

The analysis processes are fully logical and not affected by the preferences of individuals. They also enable cross-comparisons of the quality between separate cases, each aspect has a different level with a different score and each score represents the different degree of function or performance; in the end, the scores have been summed up as a basis to evaluate the quality level of BIVP. Below is the description of each proposed quality aspect.

Formal aspect (aesthetic)

This aspect refers to the term "visibility" or "visual impact" (Munari Probst and Roecker, 2012; IEA, 2013). The visual impact can be expressed by the visibility of the solar installation from the viewpoint of an observer (Dessì, 2011; Munari Probst and Roecker, 2019). Different factors affect the visibility of the solar installation such as building height, observer's height, tilting angle and observer distance, etc. (Dessì, 2011). In this research, the only consider factors are the tilt angle and the place of the solar installation (roof or façade), Table 4-2 gives a description of the formal criteria evaluation under different levels (score).

Table 4-2: Formal aspect evaluation criteria under different level.

Factors	Level	Explanation
Visibility	1	The roof-mounted system with different tilts angles
	2	Roof integrated system with different tilts angles
	3	Façade integrated the system with 30° tilt angle
	4	Façade integrated vertical PV technology (90°) tilt angle

Functionality

The purpose here is to emphasize the substantial function of BIPV. It not only has the advantage of electricity generation but also can replace current building materials. It is also evaluated by the convenience of management and maintenance, see Table 4-3 below.

Table 4-3: functionality aspect evaluation criteria under different levels.

Factors	Evaluated content	Level	Explanation
Functionality	To evaluate substantial functions that PV can have in lighting, heat insulation, and waterproof, shading, etc.	1	It meets at least one requirement (roof mounting system)
		2	It meets at least two requirements (roof-integrated)
		3	It meets at least three requirements (façade mounting)
		4	It meets at least four requirements (façade integrated)

In order to be able to compare the quantitative and qualitative data all the calculated results for the previous factor are normalized. In order to do so, the worst and best values of given performance indicators are first identified to form a range before placing the remaining ones as percentage values. As presented below:

- Step 1: Best value of the category
(X) = 100%
- Step 2: Worst value of the category
(Y) = 0%
- Step 3: Range obtained
(Y – X) = O
- Step 4: Position remaining modules within range and determine the percentile
(R)% = 100% - [(R – X) / O × 100%]

4.6 Decision support matrix

A decision-support matrix is developed in the form of a radar chart. The criteria within the tool include environmental performance (CPBT, EPBT), economic performance (capital cost, PBT), overall energy performance, qualitative performance (formal and functional performance). This acts as a tool to assist building designers, such as architects in their early building design decisions pertaining to BIPV application. Users can make their decisions based on their criteria or emphasis on environmental or economic performance, etc. Also, if occupant preference and aesthetic considerations are important, the inclusion of formal and aesthetic performance can also assist in picking a choice. To plot the values on the proposed matrix, which is in the form of a radar chart, the data must be first normalized. In order to do so, the worst and the best values of a given indicator represent the range, and all data are shown as relative percentage values, as previously described in section 2.5.4.

Figure 4-5 presents the proposed matrix with an example of two cases to describe the evaluation method. As can be seen, case 1 has much better environmental performance, which is observed from the higher scores for CPBT and EPBT. However, in case 2 the economic performance is significantly better with a higher value for payback time. This information allows architects or building designers to decide on the criteria that they like to pay more emphasis on. If there are regulations considering environmental performance, case1 is likely to be chosen. In the case of cost limitations and a short-term view on the cost benefits, case 1 may be chosen instead. In addition, with the aesthetic and functional information included, the architect or the clients can also make an informed decision on the effect of the qualitative.

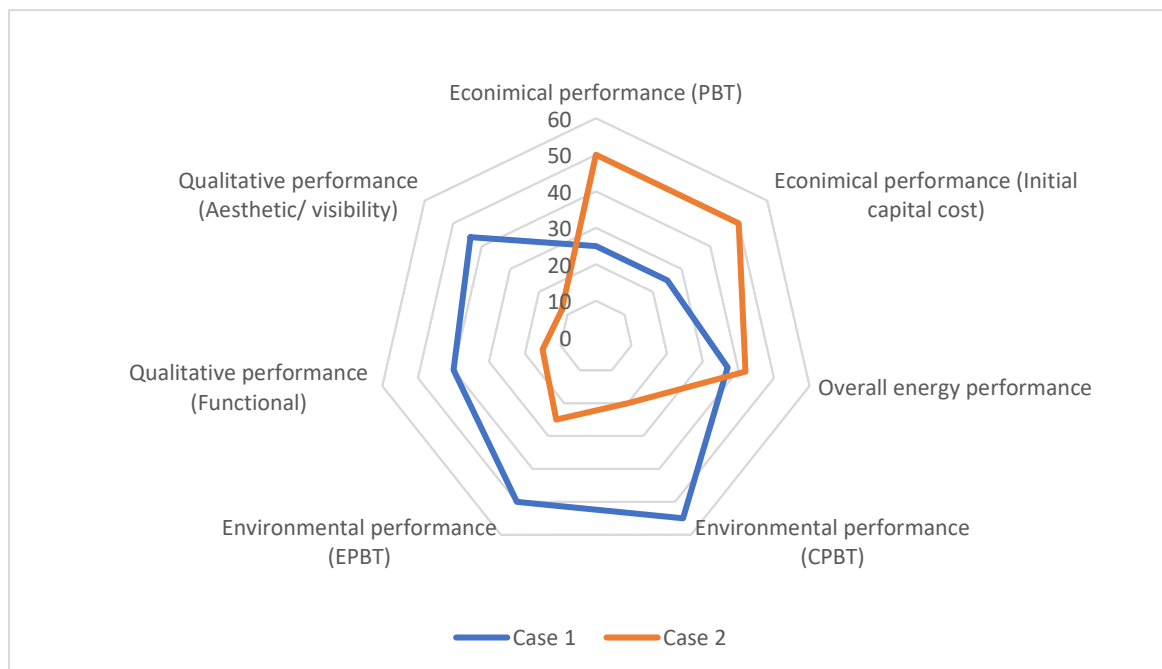


Figure 4-5: The proposed decision-making matrix, with two examples.

5 Improving energy performance of the typical multi-family building

5.1 Introduction

In this chapter, the possibility of reducing the energy demand of the typical apartment building in Amman, Jordan by means of passive design strategies are investigated. The building performance simulation program IDA ICE 4.8 is a dynamic multi-zone simulation software used to conduct the energy simulations for this research (the argument for choosing IDA ICE is presented in Chapter 4). The chapter starts with the description of the base case model input data then the energy demand results for the base case model are analyzed. After that, several design strategies have been applied to the base case. The effect of each strategy on the building energy demand is investigated and compared to the base case alone and then in combination with the other strategies, to find the optimum solution to reduce the energy demand of the base case simulated building.

It is important to mention that the values regarding the cooling and heating demand are thermal demands, while the equipment and lighting are electricity demands.

5.2 Base case model setup

This section describes the input data to the IDA ICE 4.8 simulation software. The building body is created in SketchUp and then imported into IDA ICE. Each room is modeled as a space of its own. All spaces have separate internal loads (occupancy, light, and equipment) with different schedules, in order to achieve realistic and accurate variable demands of the rooms according to the room type. The energy demand is calculated on an hourly basis (8,760 hours) for a period of a whole year.

Input data for the modeled building, including building site surroundings, architecture, floor plans, and specifications of walls, roof, and windows are based on the typical apartment building practice in Amman, Jordan (highlighted in Chapter 2.10). Other input data such as lighting, occupants and equipment's internal gains and schedule are based on standardized values or assumptions. The fundamental input data of the building is presented below:

Location and climate

As mentioned in Chapter 0, Amman is the city where 46% of the new construction in Jordan is taking place (Jordanian Department of Statistics, 2015), therefore the model used in the simulation for this research is located in the city of Amman in Jordan. The latitude is 31°95' North and the longitude is 35°93' East. The elevation considered is 788 meters above sea level. Moreover, Amman has a time zone of +02:00 hours that must also be defined.

Regarding the climate conditions, which allow the program to make a realistic simulation of the surrounding environment for every hour during a whole year, the "AMMAN JO" weather data file created by Meteonorm 7 software for Amman city is used in all simulation models. Climate analysis has been already presented in Chapter 2.3.

Building site and orientation

It is assumed that the simulated building is located in a residential urbanized area classified as C class urbanized context (the most common type), which obliges 6 m side offset, and 8 m back offset, and considering one side is facing the main street. All the surrounding buildings have a maximum allowable height in this zone, which is 15 m. Figure 5-1 illustrates the building model within the urban context. However, in IDA ICE only the buildings close to the simulated case are considered (see Figure 5-2 and Figure 5-3), as the other building does not have a significant shadowing effect on the energy demand of the simulated building, and this takes less time in the simulation process. Regarding the site orientation, there is no specific orientation of the buildings, as many factors affecting the building orientation, such as main street orientation, land shape, number of apartments on each floor, it is not easy to achieve the best orientation for each apartment. However, it is assumed that the most occupied zone, the living room for both apartments is oriented toward the south and least occupied zone bedrooms to the north orientation (zones and floor layout is presented in the next section).

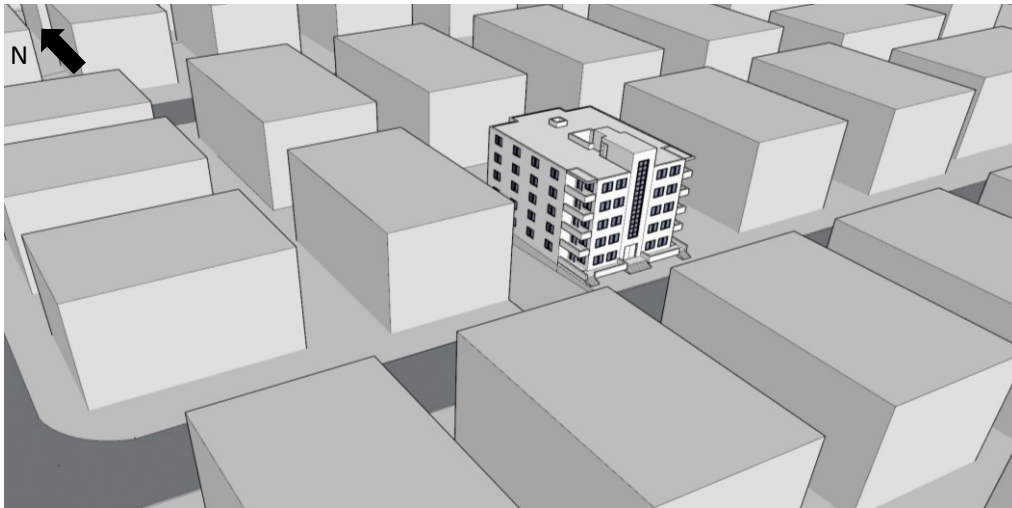


Figure 5-1: 3D view of the base case building within the typical urban context in Amman, Jordan.

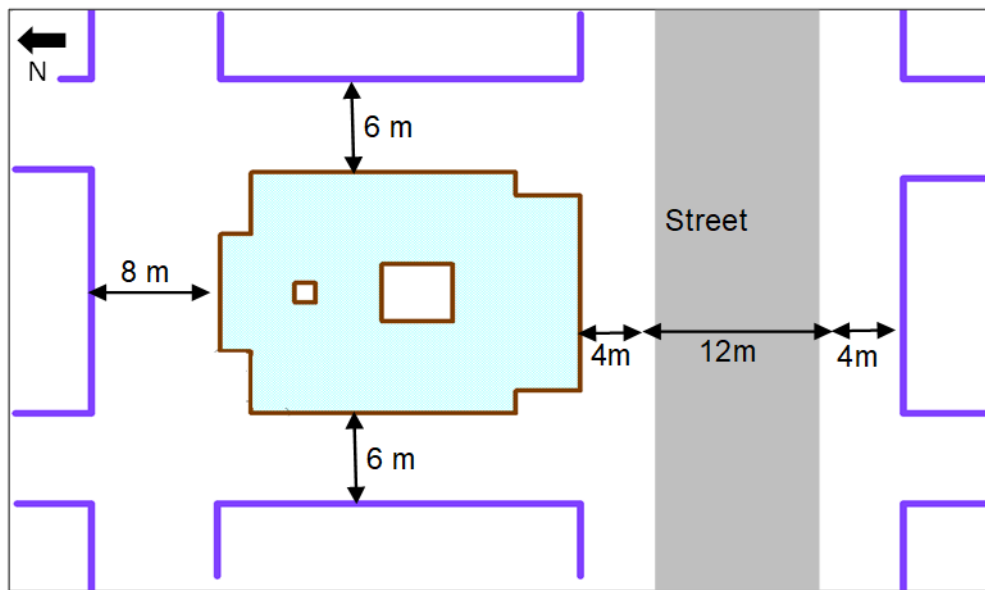


Figure 5-2: Site plan and the assumed surrounding building modeled in IDA ICE 4.8.



Figure 5-3: 3D view of the base case building and surrounding buildings modeled in IDA ICE 4.8.

Geometry, area, and zones

The simulated apartment building, shown in Figure 5-3 is based on a typical middle-class apartment that is found in most Jordanian residential building blocks (details Chapter 2.10). The model consists of 6 floors, 5 identical floors with 2 apartments on each floor and basement floor, the floor height is 3 m. Each apartment is about 150 m² consists of a living room, a kitchen (including a dining area), 3 bathrooms, and three bedrooms. The basement floor, including parking and storages area. As mentioned before, the zone arrangement is modified to orient the most occupied zone (living room) toward the south; the typical floor plan is presented in Figure 5-4. The common areas in the apartment building include elevator, staircase and basement floor and does not consider for energy demand analysis.

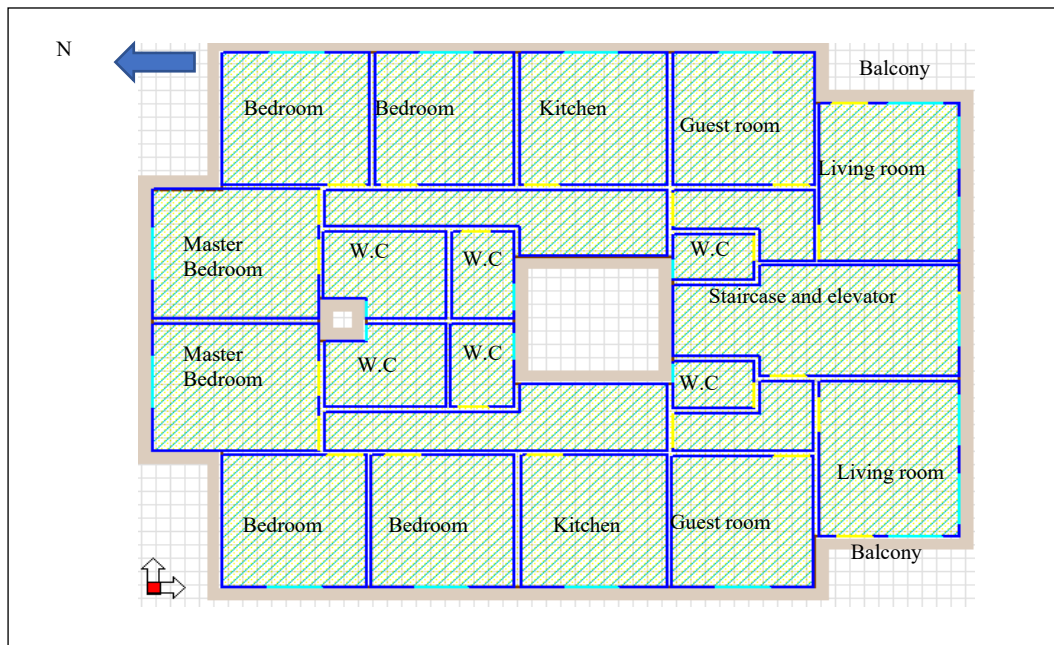


Figure 5-4: Typical floor plan for the simulated multi-family building in Amman, Jordan

Construction features

The commonest types of construction, layer thickness, and U-values of the different building parts of the typical apartment building in Jordan have been presented in Tables 2-6 and 2-7.

Generally, the building construction is of concrete and column structure with a hollow block envelope and stone veneer as an external finish and has no thermal insulation. The overall heat transfer coefficient (U-value) is $2.47 \text{ W/m}^2\text{K}$ and $0.84 \text{ W/m}^2\text{K}$ for the wall and ceiling, respectively. All windows are a single glazed window with aluminium-framed ($U\text{-value} = 5.92 \text{ W/m}^2\text{K}$) and without shading device.

Parameters related to occupants

- Occupant number and schedule

Based on Chapter 2.10, it is reasonable to assume that each apartment is occupied by 6 persons, the parents and 4 kids, parents aged between 45 and 65 years, two adults aged between 18 and 25 years and two children aged under 18 years (Department Of Statistics, 2016).

On weekdays, it is assumed that most of the occupants are out of the apartment at work, school or university except for mothers, due to their roles as housewives. After 14:00, young children come home from school, while adults stay at work or university until 18:00, after which all family members tend to stay at home. Until 20:00, they are likely to stay in the living room and then after this, the school kids will go to their bedrooms, and after 22:00 the other family member will go to their bedrooms with two members per room. However, at weekends, i.e. on Fridays and Saturdays, all occupants are assumed to be at home and most of the time in the living room and in the dining area in the kitchen from 08:00 until 12:00. The occupancy schedules in a different zone in the apartment are illustrated in Figure 5-5.

About the guest room in Jordan, it is not mentioned in the previous diagram, however, most relatives visit each other on the weekend and so it is assumed that the guest room is occupied from 16:00 until 18:00 on Friday and Saturday. However, in most of the family in Jordan, the men and women are not set in the same room so in this study it is assumed that there are 6 occupants in the guest room and 6 occupants in the living room including the family member.

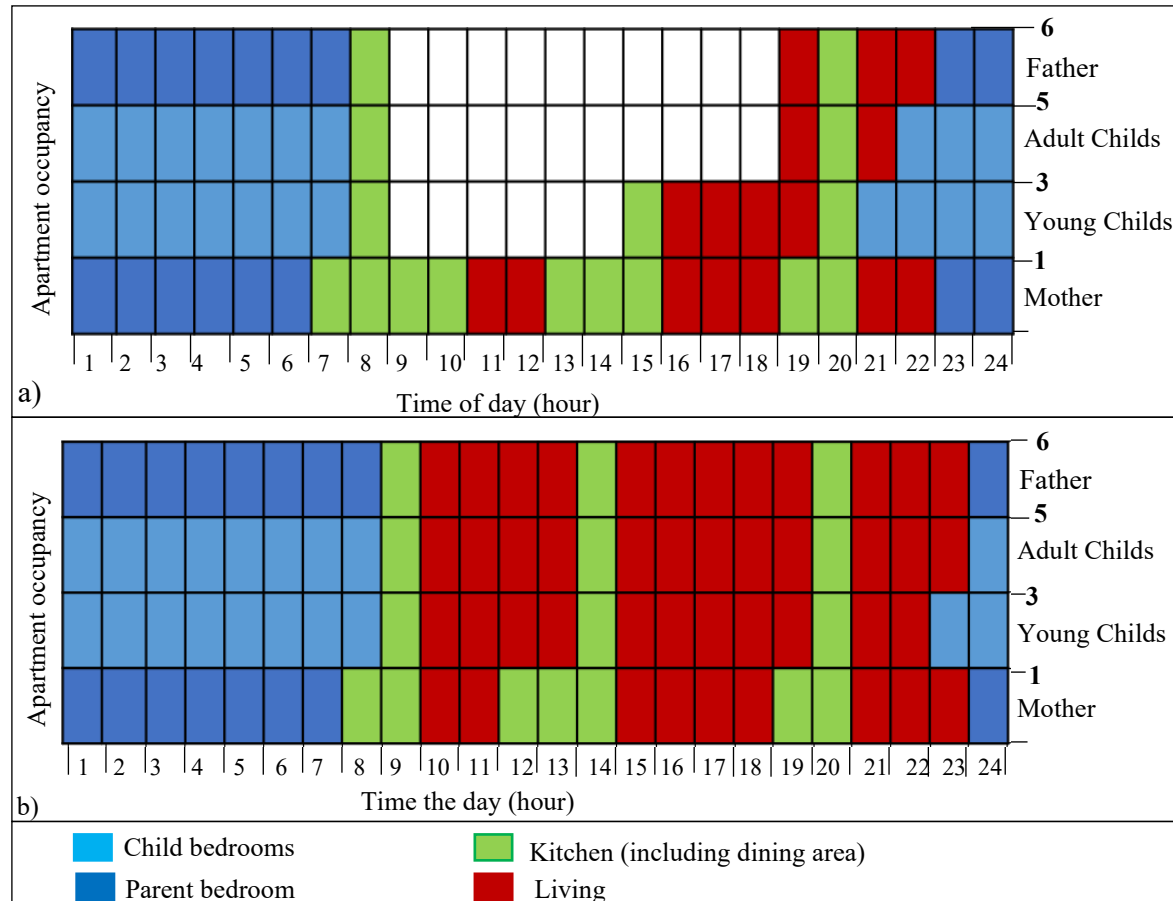


Figure 5-5: Apartment occupancy schedules: a) weekdays, b) weekends.

- Metabolic rate

It has been considered that the main activity level of each person is 1 MET, which corresponds to 58.2 W/m² of the body surface, which is the amount that an inactive person (one sitting person) is assumed to emit. However, in the bedrooms, the activity level is set 0.7 MET, which corresponds to a 72 W/m² of heat loss from the sleeping occupant (ASHRAE, 2004).

- Clothing insulation

Another input value that is added for the occupants is their clothing level, defined in CLO. The ISO-standard for clothing insulation (ISO 9920) provides lists, including different types of clothing. These could be added together into a combination of a suitable and reasonable dressing. A value of 0.57± 0.25 CLO is used as the reference value in the performed simulations in IDA ICE. The CLO-value of 0.57 corresponds to the occupants wearing underpants, a shirt, and trousers (ASHRAE, 2004).

Equipment

Regarding the equipment, it is assumed that each apartment has basic electrical appliances such as a refrigerator, washing machine, water heater, and television, etc. Some of these appliances are not in constant use, so daily operating hours and schedules for each device have been estimated by the author, as illustrated in Table 5-1 below. The specifications for the equipment are taken from the academic literature and guides (Nadel, 2002; CIBSE, 2006; ASHRAE, 2004).

Table 5-1: The main appliances and their heat output in different zones in an apartment building in Jordan

Zone	Appliance	Heat output (W) (operating)	Heat output (W) (standby)	Operating (hour/day) time
Living room	Television	315	20	6 hour/day
	Receiver	140	5	11:00-12:00, 16:00-17:00, 20:00-22:00
	Iron	1500	-	2 hour/day Saturday: 10:00-12:00
	Vacuum cleaner	630	-	0.15 hour/day 10:00-10:15
	2 laptops	120		2 hour/day 20:00-22:00
Kitchen	Refrigerator	350	10	24 hour/day
	Washing machine	512	10	2 h/week Saturday: 8:00-10:00
	Kettle	1200	5	0.15 hour/day
	Microwave	800	5	6:00-6:05, 13:00-13:05 18:00-18:05
Bedroom (in each)	Laptop	60	-	1 hour/day 21:00-22:00
	Hair dryer	250	-	1 hour/day 6:00- 7:00

Lighting:

the installed power and the distribution of the light units in the modeled apartment are presented in Table 5-2 below, based on the previous research conducted by AL-Salaymeh (Al-Salaymeh et al., 2010), two considerations have been considered:

- There are two kinds of lighting units, light bulbs with an electrical power of 60 W and fluorescents with an electrical power of 40 W.
- The convective fraction for every unit is 0.4.

Table 5-2: Electric power for the apartment lighting, source of data:(Al-Salaymeh et al., 2010).

Room	Number of lights unites	Power (W)
Guest room	1 chandelier (6 lamps 60 W each)	360
Kitchen	2 light bulbs 60W each and 1 florescent lamp	160
3 bathrooms	3 light bulbs	180
3 bedrooms	2 bulbs each	360
2 corridors	2 bulbs each	240
Living room	1 chandelier (6 lamps 60 W each)	360

The artificial lighting is controlled according to the “setpoints and schedule” strategy. The setpoints are considered according to the recommended light values in lux by CIBSE lighting code, (see Table 5-3.) (CIBSE, 2013). For example, in the living room when the indoor daylight intensity is higher than 300 lux, artificial lighting is turned off. On the contrary, the artificial light is starting to work when the natural light is lower than 100 lux. Regarding the schedule, in the living room, guest room and kitchen zones the lighting schedule follow the presence of the occupants. However, in the bedrooms it is assumed that the occupant turns the light on (when the light level below the setpoints) 2 hours in the early morning during the weekdays and two hours daily in the night, the lighting schedules in the bedrooms are presented in Figure 5-6. For the corridors, the light schedule is set on from 5:00-7:00 and from 20:00-23:00.

Table 5-3: Lighting setpoints used in the simulated model based on a recommended light level by (CIBSE, 2013).

	Living room	Kitchen	Bathroom	Bedroom	corridors
Light level (lux)	100-300	150-300	150-200	100-150	100-150

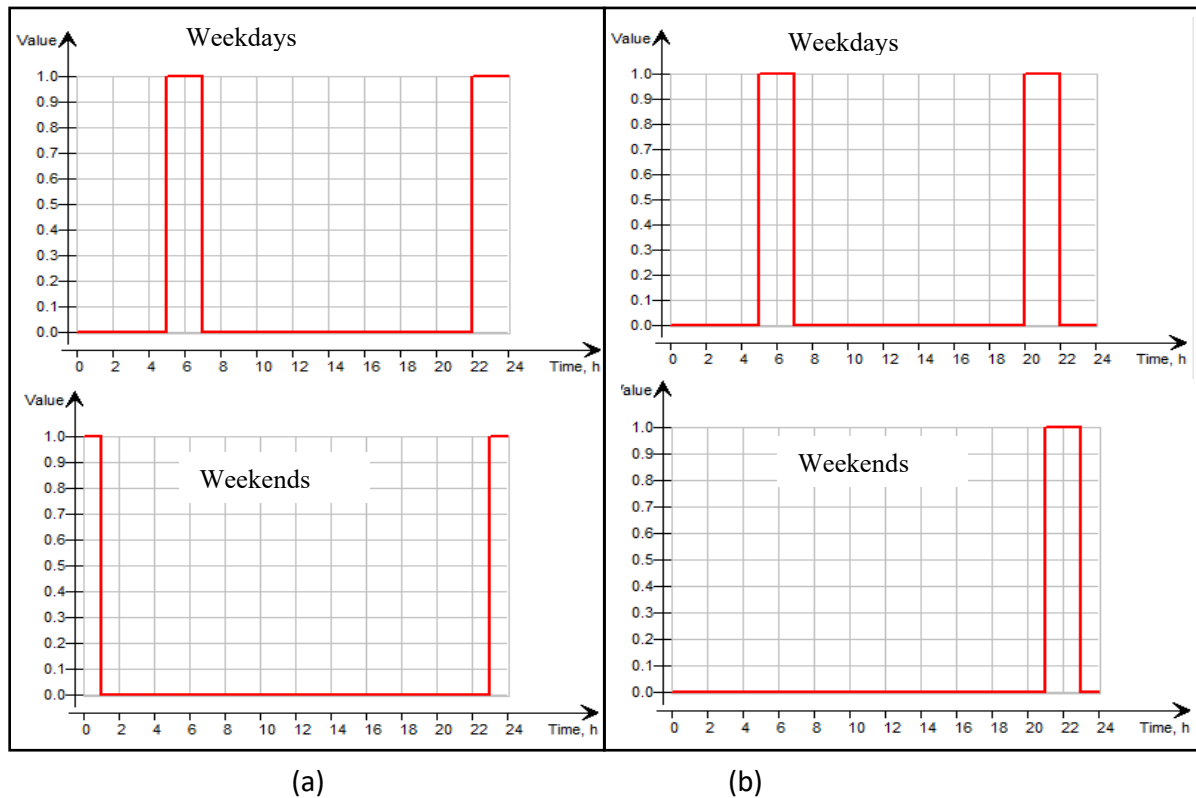


Figure 5-6: Bedrooms lighting schedules: (a) master bedroom, (b) children's bedrooms.

Infiltration:

The assumed infiltration rate is 0.5 ACH (air change per hour) at a differential pressure of 50 Pa (Pascal), based on ASHRAE Standard 62.2- 2016 (ASHRAE, 2016).

Ventilation:

Regarding the ventilation, in winter, the occupants revealed that opening windows is not desirable except just for fresh air intake for a short time in the morning. For simulation analysis reasons, this limited-time was approximated to be one hour in the morning (from 8:00 to 9:00). On the other hand, in summer, the windows are opened if cooling is needed and the occupants are at home.

The opening and closing of the windows are modeled using an on/off temperature control macro with a dead band 4 °C (Figure 5-7). This means that the windows would open when the room temperature raised 2 °C above the setpoint temperature, and close when it is dropped 2 °C under the setpoint temperature. In this case, the setpoint temperature is set 25 °C ensuring window opening at 27 °C and closing at room temperature under 23 °C. It is also connected to the outdoor temperature, as the windows would open if the outdoor temperature is only under the indoor temperature and it is connected with the zoning occupancy. Then it is multiplied by a fresh air schedule from 8:00 to 9:00 in winter.

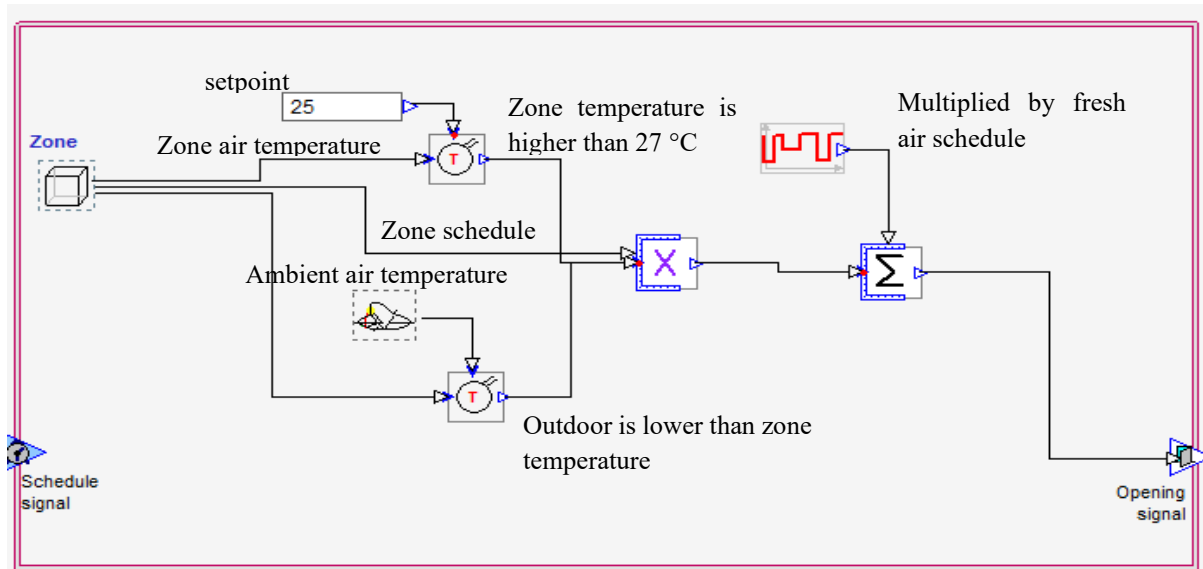


Figure 5-7: Windows opening control macro in IDA-ICE used in simulations. The window are opened if the zone temperature exceeds the cooling setpoint $t_{cool} + \Delta t/2$, and the outdoor temperature is lower than the room temperature. The window are closed when the zone temperature drops below $t_{cool} - \Delta t/2$. Δt is defined as dead band value.

Regarding the ventilation in the bedrooms, the windows are assumed to be open every day for fresh air, for one hour from 08:00-09:00.

Heating and cooling units

An “ideal heater” and “ideal cooler” are assumed as the devices for heating and cooling the rooms in IDA-ICE. Regarding the heating and cooling setpoints, according to ASHRAE comfort standard 55, the recommended temperature range of residential buildings, where the relative humidity is 60%, is between 23 °C and 26 °C in summer and 20 °C and 23 °C in winter (ASHRAE, 2004). But summer humidity in Amman, Jordan, is less than 50%, as the country is mainly characterized by hot and dry weather. Therefore, summer temperatures range from 23.5 °C to 27 °C, assuming that relative humidity is 30%. However, different setpoint temperature has been found in the previous studies and literature as shown in Table 5-4.

Table 5-4: Comfort temperature range, setpoints for active buildings in Amman, Jordan.

Source	Winter (°C)	Summer (°C)
(ASHRAE, 2004)	20-23	23.5-27
(Qawasmeh et al., 2017)	19-21	21-24
Adapted from Jordanian thermal insulation codes		
(Bataineh and Alrabee, 2018)	20	24.5
(Shariah, Tashtoush and Rousan, 2002)	20	27
(Attia, 2014)	20	25.5
(Al-Asir <i>et al.</i> , 2009)	January: 17-24	April: 19.5-26.5 July: 22.5- 29.5 October: 27.5
This research	20.00	27.00

In this research, the proposed setpoints are 20 °C for heating and 27 °C for cooling. The advantages of a higher upper limit (27 °C) during the summer and lower limit during the winter season (20 °C) are less thermal shock on entering or leaving a building, and less energy needed for air-conditioning. A series of simulation is done with different thermostat cooling setpoints for one apartment (top floor apartment with 135 m² heated area) to examine the effect of temperature on the cooling demand. As illustrated in Table 5-5, with 27 °C thermostat cooling setpoints, the energy demand is less by 36% compared to the case with a 24 °C thermostat cooling setpoint. This is a costless strategy that also brings down the investment cost for the cooling system since the peak power decreases by 13%.

Table 5-5: Simulation results for the base case apartment building with different thermostat cooling setpoints. The heated area for the apartment is 135m².

Cooling setpoint temperature (°C)	Cooling demand (kWh/year)	Cooling peak demand (kW/m ²)
24	5,800	6.9
25	5,130	6.5
26	4,410	6.3
27	3,740	6.0

5.3 Energy performance of the base case model

In this section, the base case building energy demands, and energy balance are estimated by IDA ICE simulation software, based on the above-mentioned input conditions, in order to understand the energy performance of the typical apartment building in Amman, Jordan and suggest possible solutions to reduce its energy demand. In the discussion below, the apartment (Apt.1) refers to the apartment on the east side and apartment 2 (Apt.2) refers to the west side of the building (see Figure 5-9).

The total annual energy demands for all the apartments in the base case residential building are 27,545 kWh/year (20 kWh/m²/year) for cooling, 59,247 kWh/year (44 kWh/m²/year) for heating, 34,552 kWh/year (26 kWh/m²/year) for equipment and 12,350 kWh/year (9 kWh/m²/year) for lighting. Figure 5-8, illustrates the energy demand, including heating, cooling, lighting, and equipment of each apartment on different floors. Generally, the simulation results show that both cooling and heating demands are present, however, the heating demand is dominant. It is also clear that the top-floor apartments have the highest heating and cooling energy demand among all other apartments with about 3,730 kWh/year (27 kWh/m²/year) and 6,990 kWh/year (52 kWh/m²/year) for annual cooling and heating demand respectively. While for other apartments the annual heating demand ranges from 5,136 kWh/year (38 kWh/m²/year) to 5,576 kWh/year (41 kWh/m²/year) for third-floor apartment and ground floor apartment respectively. According to Figure 5-10 and Figure 5-11, the main source of heating losses in the heating period is the building envelope and it is the highest for the top floor. This is because of the roof, which is connected with the outdoor environment, while in the cooling period the main source of heat gain is windows and solar. Regarding the electricity demand for lighting and equipment, annual lighting demand range from 1,235 kWh/year (9 kWh/m²/year) to 1,355 kWh/year (10 kWh/m²/year) for top floor apartment 1 and ground floor apartment 2 respectively, while the required energy for equipment is constant among all apartments with 3,450 kWh/year (26 kWh/m²/year).

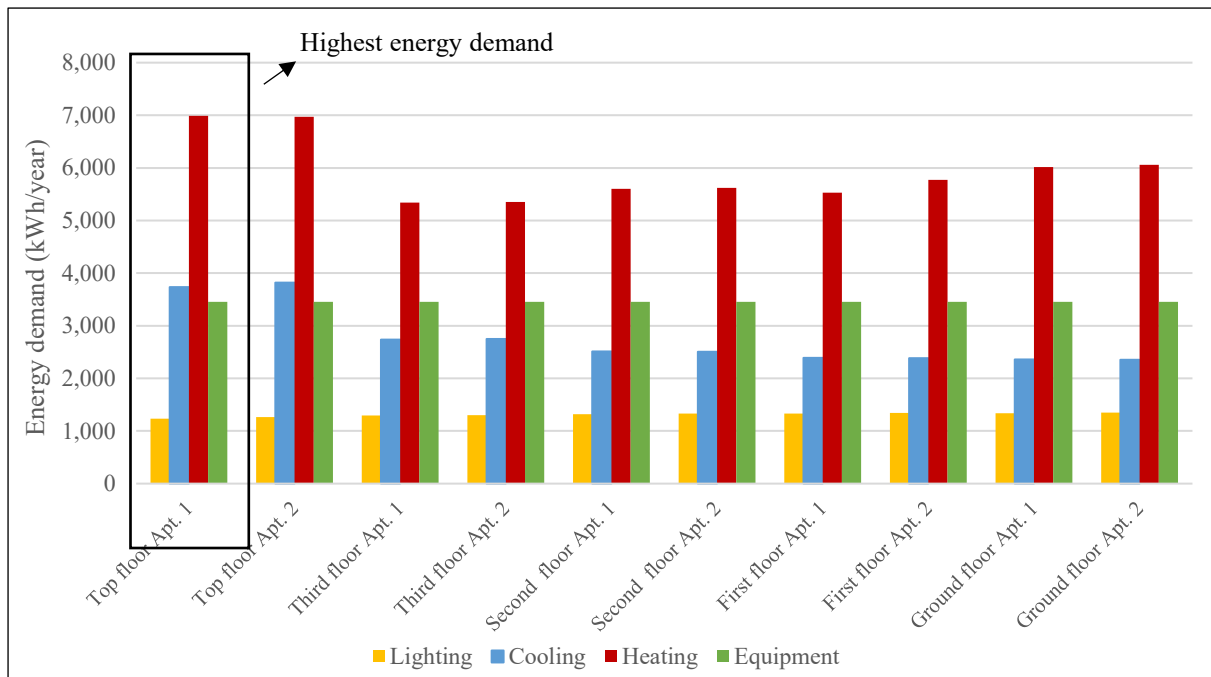


Figure 5-8: Annual energy demand for different apartments of the base case model representing a typical residential apartment building in Amman, Jordan. The heated area for each apartment is 135 m².

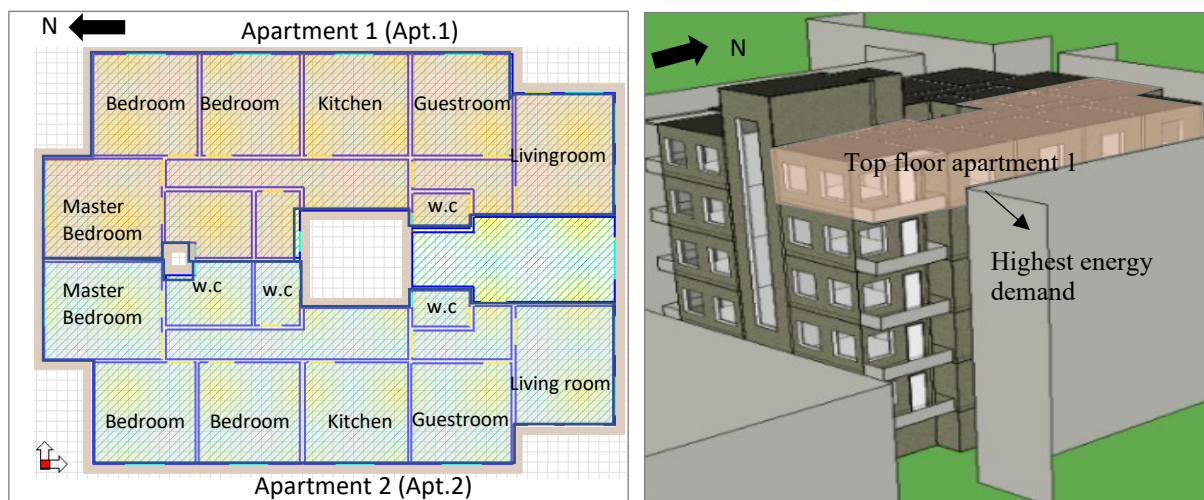


Figure 5-9: Floor plan and 3d view of the simulated apartment building.

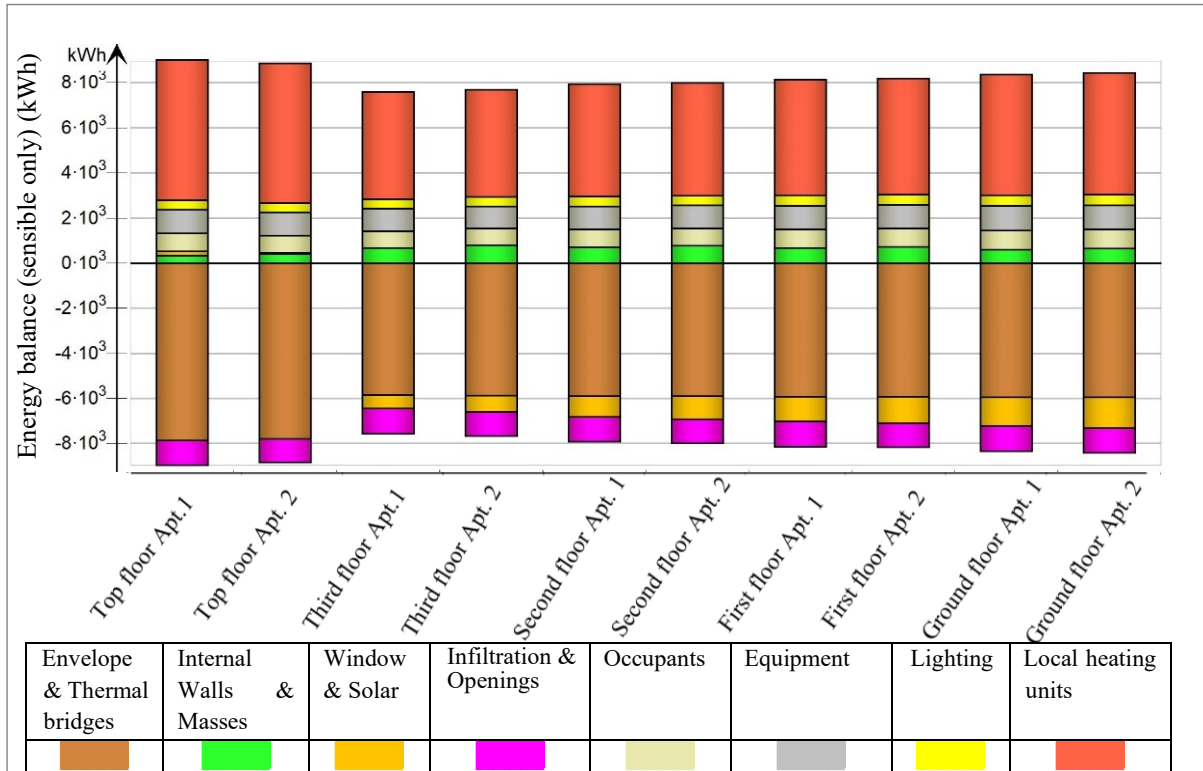


Figure 5-10: Annual energy balance (sensible only) result during the heating period for the base case simulated apartments in multi-family building in Amman, Jordan. The heated area of each apartment is 135 m².

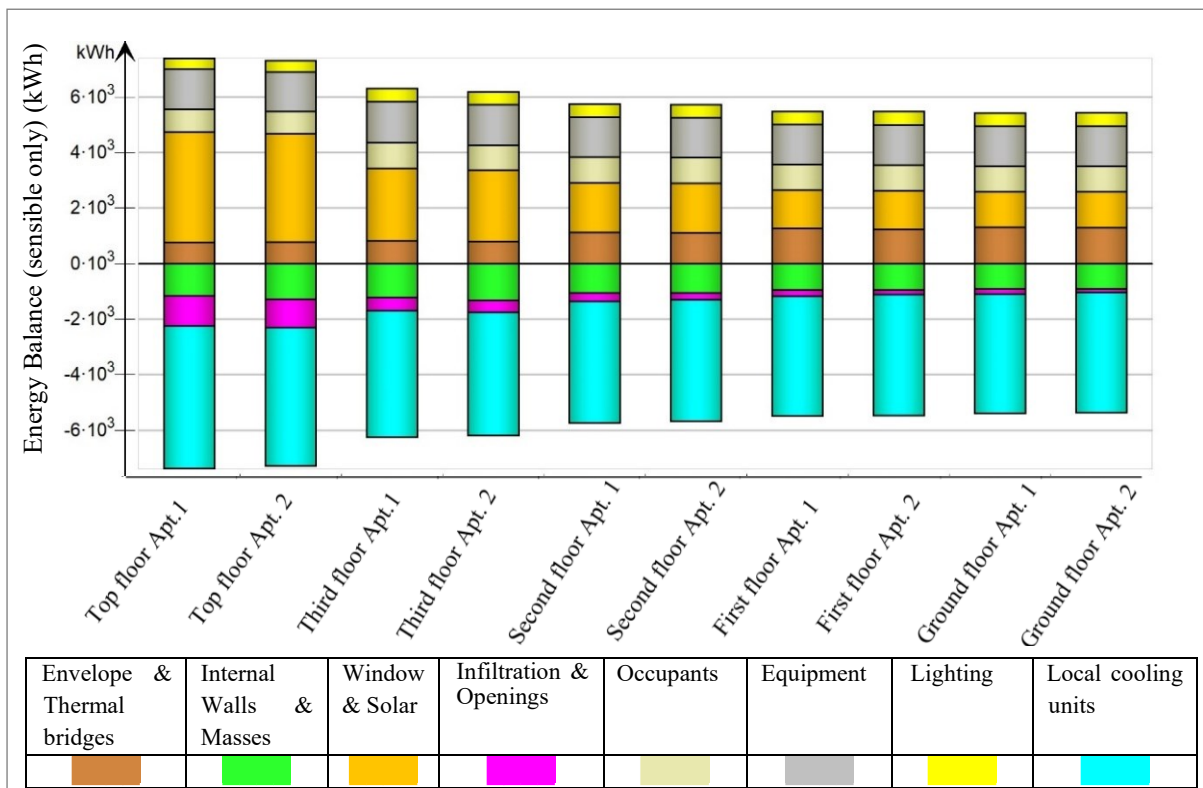


Figure 5-11: Annual energy balance result during the cooling period for the base case simulated apartments in residential building in Amman, Jordan. The heated area of each apartment is 135 m².

For further analysis in terms of monthly energy demand and energy balance, top floor apt.1 is selected, assuming it is the critical case.

As illustrated in Figure 5-12, the heating months start from December and last until the end of March, the highest demand is in January with 2,550 kWh, while the cooling months begins in May and ends in October, also, a small cooling load is occurring in April. The highest amount of energy consumed for cooling is in July with around 1,060 kWh.

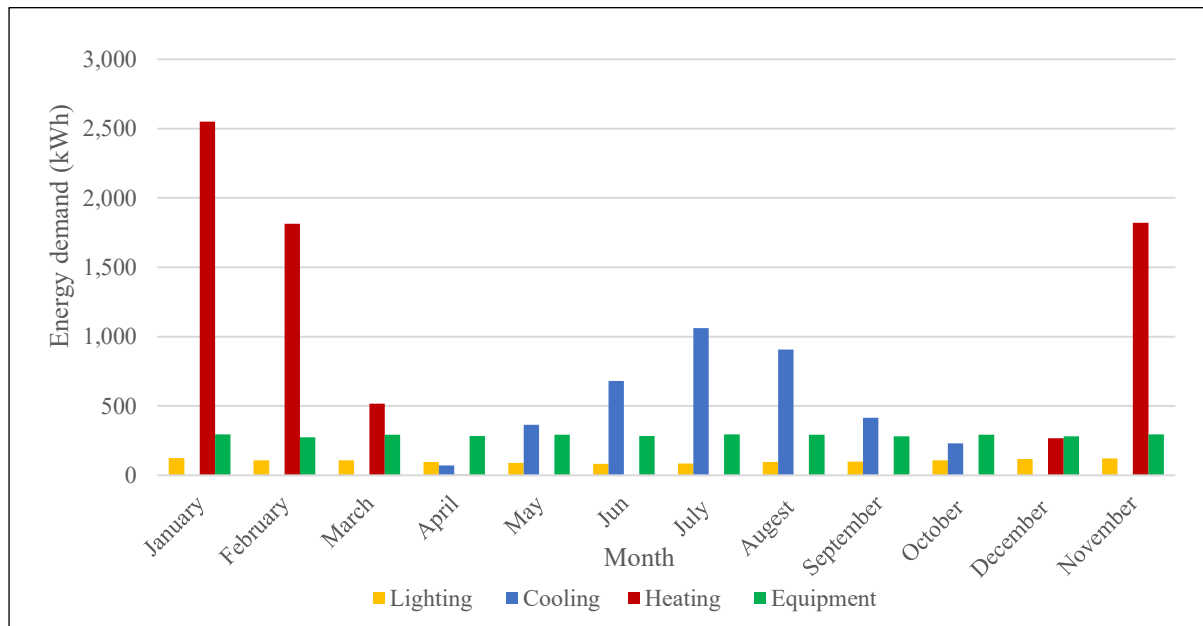


Figure 5-12: Monthly energy demands of the top floor apartment 1, in the base case typical apartment building in Amman, Jordan. The heated area of the apartment is 135 m².

Figure 5-13 shows the monthly energy balance (sensible only) throughout the year for the top floor apartment 1. Simulation results show that during the cooling period, the cooling energy demand is high due to high solar radiation through glazing (980 kWh in July) and the building envelope (1,240 kWh in July). On the other hand, during the heating period, the main source of heat loss is the building envelope (2,549 kWh in January) followed by infiltration and openings with 345 kWh in January. Internal heat produced by equipment, lighting, and occupants is mostly constant throughout the year.

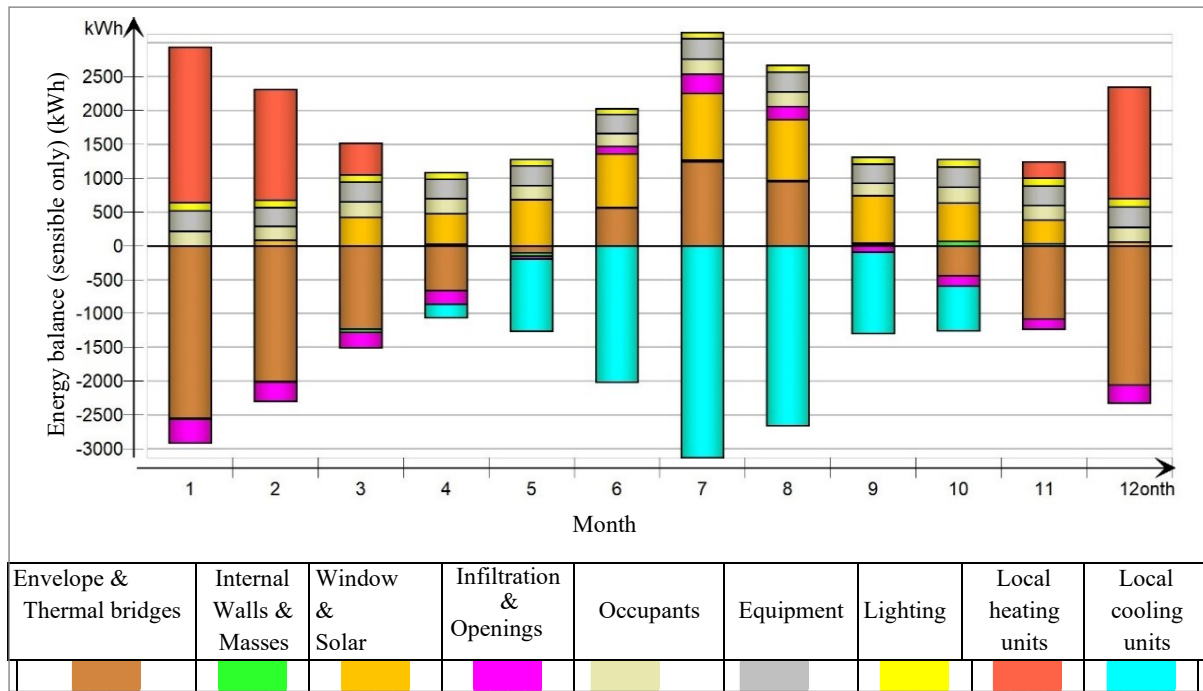


Figure 5-13: Monthly energy balance (sensible only) results for the base case top floor apartment 1 in residential building in Amman, Jordan. The heated area of the apartment is 135 m².

Figure 5-14 illustrates the heat transmission losses and gains through the building envelope elements and Figure 5-15 shows the percentage of transmission losses in the heating period and transmission gains in the cooling period. The highest transmission loss during the heating period occurs through the walls, with more than half of the total losses, followed by the windows with 26% and then the roof by 16%. Regarding the heat gain in the cooling period, the main source of heat gain from the roof and then from the walls.

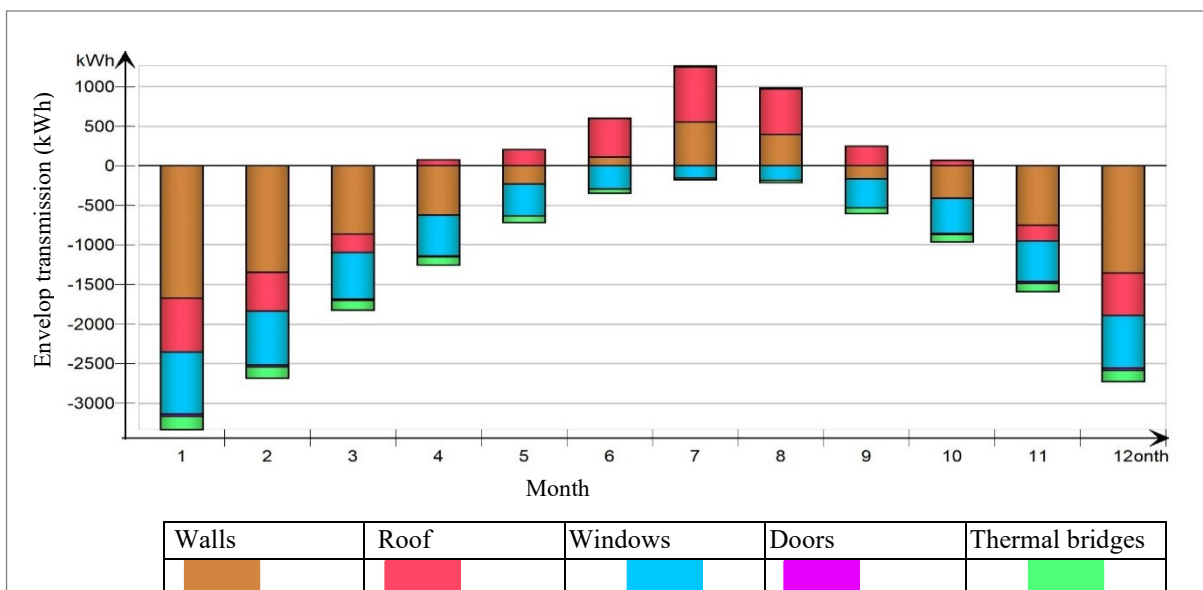


Figure 5-14: Monthly envelop transmission results for the base case top floor apartment 1 in residential building in Amman, Jordan. The heated area of the apartment is 135 m².

By analyzing the results of the simulation for the base cases in IDA ICE, it could be concluded that the walls and roof and windows account for the major part of the total heat loss and gains.

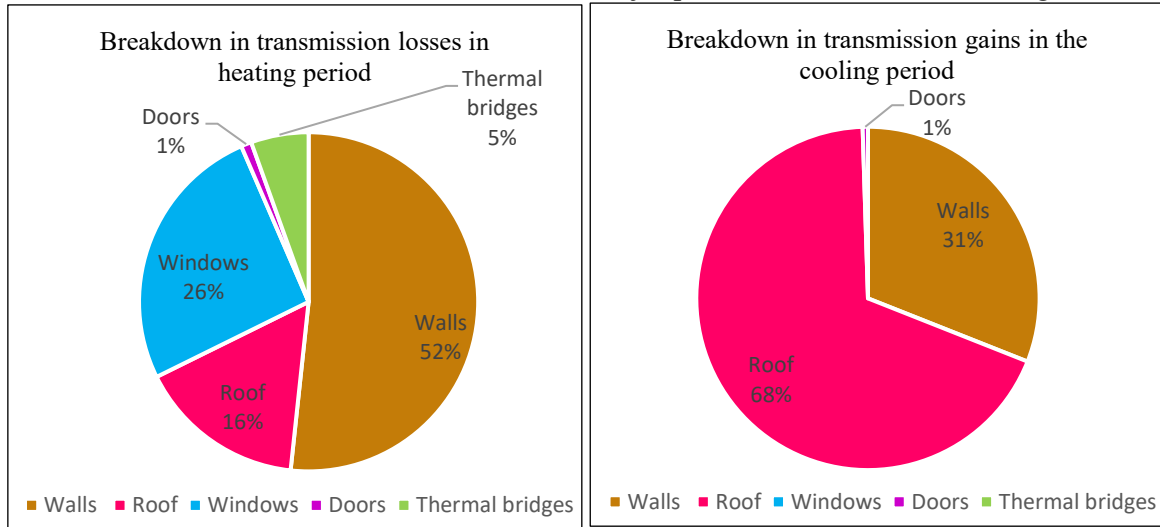


Figure 5-15: Break-down of transmission losses in the heating period and transmission gains through the building envelope elements for the base case top floor apartment 1.

5.4 Energy demand optimization strategies

The most important passive strategies that have the potential to reduce the energy demand of the typical apartment building (base case) in Amman, Jordan are defined based on the base case simulation results in the previous section, also different scenarios of each strategy have been proposed to determine the optimum solution with the aim of minimizing building annual energy demand. Although this chapter is mainly about passive strategies, installing energy-efficient lighting is also suggested to mainly reduce the building electricity demand. The proposed strategies are as follows:

Strategy 1: Walls insulation

The average heat flow through the wall construction can be reduced by wall insulation, which consequently can contribute to reducing heating demand, however, this could also affect the cooling demand. Therefore, the effect of adding thermal insulation to the external walls with different thicknesses (from 1 cm to 10 cm) on annual heating and cooling energy demands of the base case is investigated to find the best insulation thickness that can contribute to the energy saving of the base case. The heat conductivity of the insulation is $0.67 \text{ W/m}^2\text{K}$.

Strategy 2: Roof insulation

During summer, roofs are generally more exposed to solar radiation than walls due to the different angles of solar beams in winter and summer (see Figure 2-10 in chapter 0). Inadequate roof insulation, results in heat transfer from the roof into the building (see Figure 5-14 and Figure 5-15) and consequently undesirable hot indoor air during summer and increasing the cooling energy demand. The effect of roof insulation is investigated, considering a thickness range from 1 cm to 10 cm.

Strategy 3: Window type and recess depth

The effect of replacing single-pane windows with U-values of $5.92 \text{ W/m}^2\text{K}$ in the base case with two windows types; double clear glazing windows with U-value of $2.86 \text{ W/m}^2\text{K}$, and low-emission double glazing window with U-values of $1.59 \text{ W/m}^2\text{K}$, in different façade orientations are investigated in term of energy-saving potential. Another possible strategy related to the window design is the window recess depth with respect to the façade, 2 cases are proposed, in addition to the base case, see Figure 5-16.

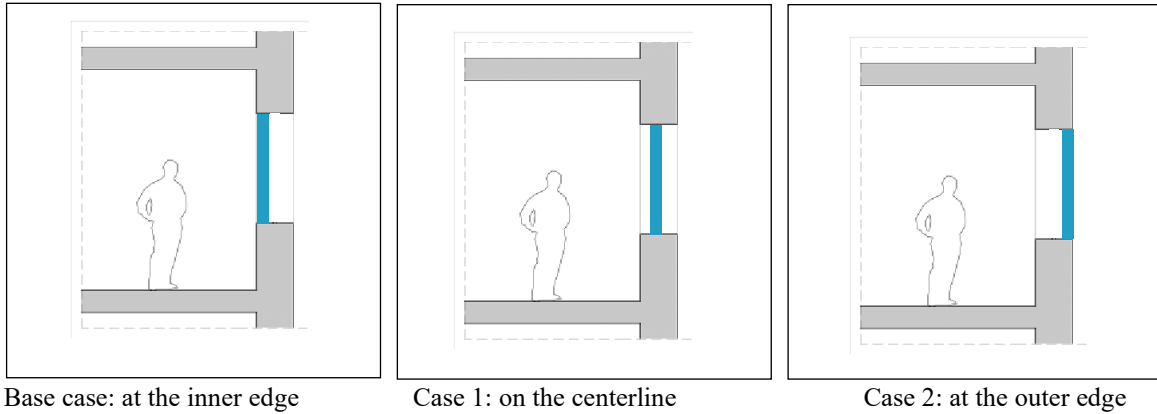


Figure 5-16: Proposed cases of windows recess depth with respect to the façade.

Strategy 4: shading device

Adding shading devices can contribute to avoiding the solar gains in the apartment and consequently reduce the cooling demand. Shading devices in winter should allow the low-angle sun in winter when passive heating is required, screen the sun in summer when overheating is a risk. Different types and sizes of shading devices in different orientations on the building energy demands are suggested.

The current status of the apartment in the base case model is without any shading devices for windows. Horizontal overhang, vertical side-fins, and ventilated blind are the three proposed cases of shading devices, see Figure 5-17. Overhang and side-fins are simulated with different projections; ranging from 20 cm and 140 cm. While, the ventilation blinds are simulated with different operating strategies, as mentioned below:

- Case 1: “sun and schedule”. In this case, during the cooling period from May to October, the ventilation blinds are down when the occupants are present in the zone and the sun penetrates through the windows.
- Case 2: “day cooling”. In this case, during the cooling period from May to October, the ventilation blinds are down during the day from 06:00 to 18:00.
- Case 3: “all day cooling”. In this case, the ventilation blinds are down through all day in the cooling period from May to October.
- Case 4: “night heating”. In this case, the ventilation blinds are down in the heating period from December to March during the night from 18:00 to 06:00.

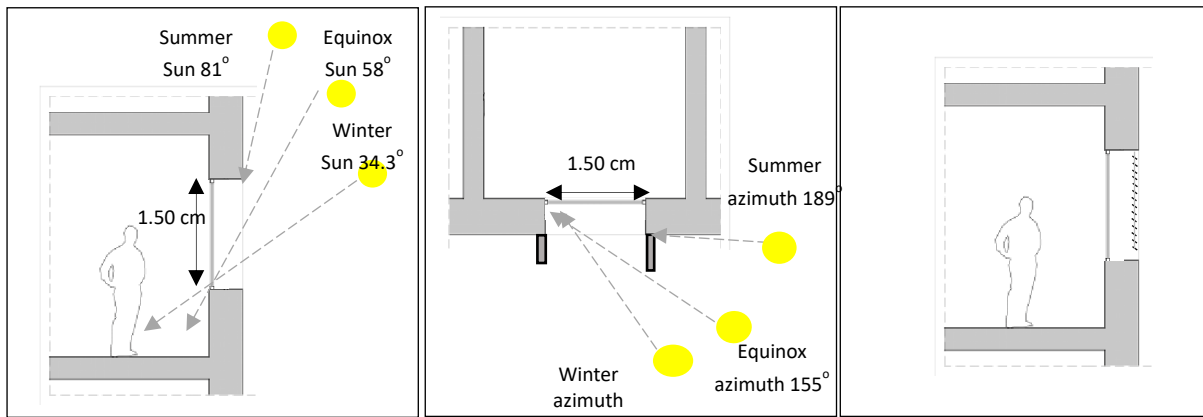


Figure 5-17: Proposed shading device types.

Strategy 5: Natural ventilation

As mentioned before, in the base case the windows are already assumed to be opened during the day when the cooling is needed, and the outdoor temperature is lower than the indoor temperature. In addition to the day ventilation which is assumed in the base case, the natural ventilation strategy during the night and evening is proposed in order to reduce the cooling demand in cooling periods from May to October, different cases are proposed as mentioned below:

- Case 1: “bedrooms 2 hours night ventilation”, in this case, the windows are open during the cooling period from May to October in the bedrooms at the evening two hours before sleeping from 18:00 to 20:00, in order to avoid the undesirable flow of air during sleeping time.
- Case 2: “all night ventilation”, windows are open in the living room, guest room, kitchen during the evening and night from 18:00 to 6:00.
- Case 3: include both case 1 and case 2.

Strategy 6: Energy-efficient lighting

LED light bulbs are proposed to replace the lighting bulbs in the base case. The used power of LED lighting bulbs is 12 W (ENERGY RATING, 2018).

5.5 Results and discussion

In this section, the benefit of each strategy is assessed by comparing the annual energy demand simulation results before and after the implementation of each strategy separately, and then in combination with other strategies. The aim is to provide suggestions about the best design options when trying to achieve a high energy performance building as PV and solar thermal technologies sizing and performance strongly depend on energy demand. The top-floor apartment 1 in the base case is used as a reference, however, at the end of this chapter, the effect of the best-selected strategies on energy demand for all apartments is presented.

Strategy 1: Walls insulation

Figure 5-18 illustrates the effect of the wall insulation thickness on the cooling and heating demands compared to the base case (no insulation) for top floor apartment 1 in a residential building in Amman, Jordan. It is obvious that higher insulation thickness leads to lower heating demand. However, most of the energy savings are achieved through the first 4 cm thickness, and after that, increasing the insulation thickness has no important impact on the heating demand, which proves that there is no need for huge insulation thicknesses. The wall insulation leads to lower cooling demand compared with the uninsulated case, but the reduction is not high as in the heating demands. Thus, it can be said that the use of insulation is more important for the reduction of the heating demand than the cooling demand.

Accordingly, with 4 cm insulation thickness the annual saved energy is about 46% (3,230 kWh/year) and 3% (100 kWh/year) in terms of total heating and cooling demand respectively, compared to the base case.

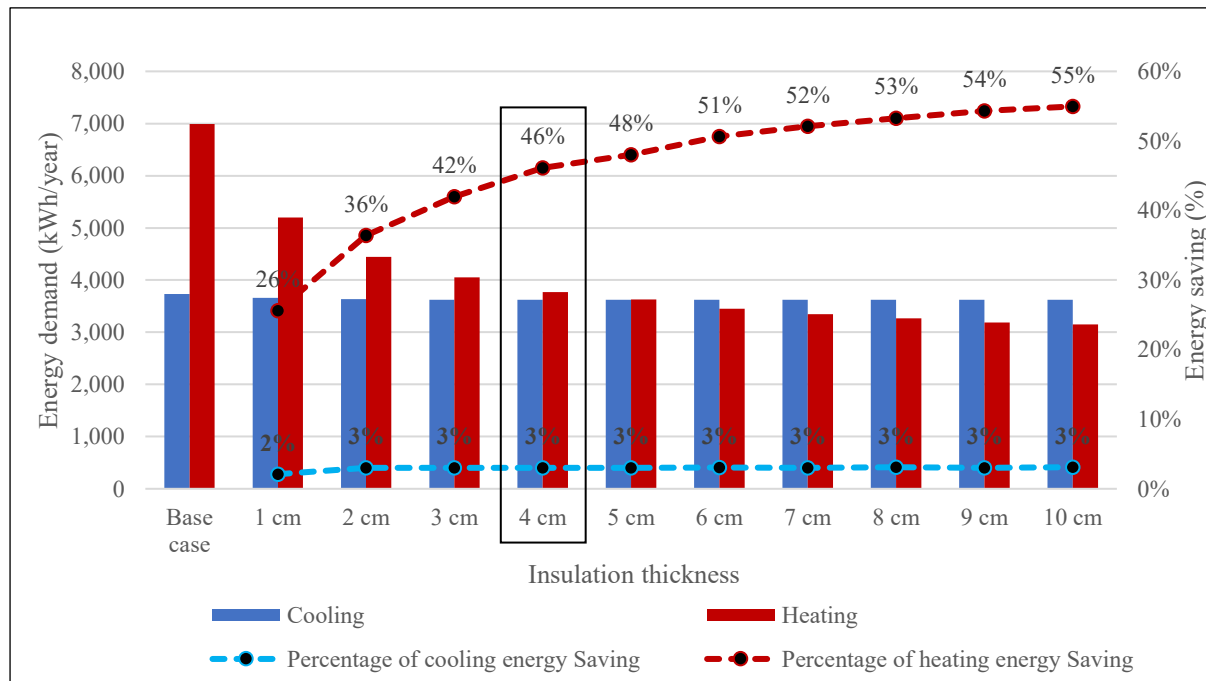


Figure 5-18: The effect of thermal insulation thickness applied to the wall on heating and cooling energy demand for the top-floor apartment 1, and the energy-saving percentage in comparison with the base case model. The heated area of the apartment is 135 m².

Strategy 2: Roof insulation

Figure 5-19 demonstrates the effect of the roof insulation thickness on the annual energy demand of the base case apartment model. Different thicknesses of insulation have been examined from 2 cm to 10 cm. It can be stated that the roof insulation leads to lower heating and cooling demands compared with the base case (uninsulated case), the effect on the heating demand is higher than on the cooling demand, however, the roof insulation has a more significant impact on the total cooling energy demand than the wall insulation. Generally, insulation thickness over 4 cm has a low impact on the results. Accordingly, with 4 cm roof insulation thickness, the total saved energy is 13% (879 kWh/year) and 8% (302 kWh/year) for heating and cooling respectively.

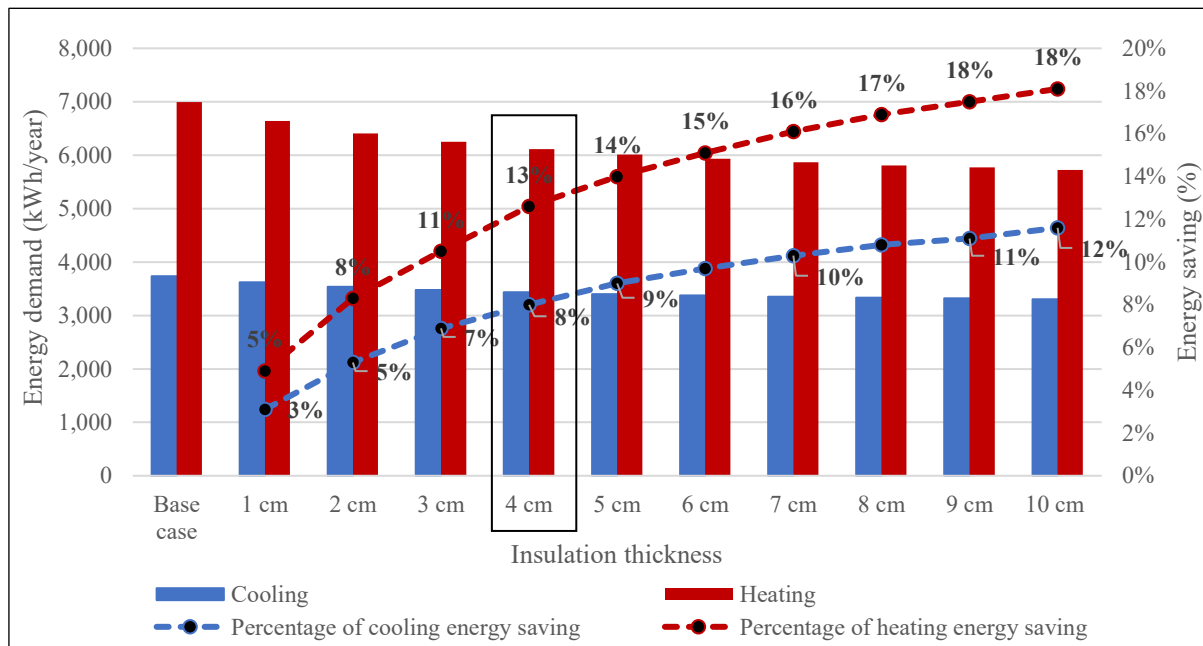


Figure 5-19: The effect of thermal insulation thickness applied to the roof of the top floor apartment on heating and cooling energy demands, and the energy-saving percentage in comparison with the base case model. The heated area of the apartment is 135 m².

Strategy 3: Window type and recess depth

Figure 5-20 and Figure 5-21 illustrate the impact of installing double clear glazing windows and low-emission double glazing windows, respectively, with different orientations compared to the base case model (single glazed windows) in terms of annual energy demands. From the results, it can be noticed that both windows types on the east orientation results in a higher heating and cooling demand saving than in the north and south orientations. In the eastern orientation cooling demand is reduced by 14.7% (551 kWh/year) in case of low-emission double glazing windows, and 6.1% (118 kWh/year) in case of double clear glazing windows, the heating is reduced by 2.1% (144 kWh/year). In contrast, lighting demand is increased slightly, and it reaches its highest value in the east orientation by 3.2% (37 kWh/year).

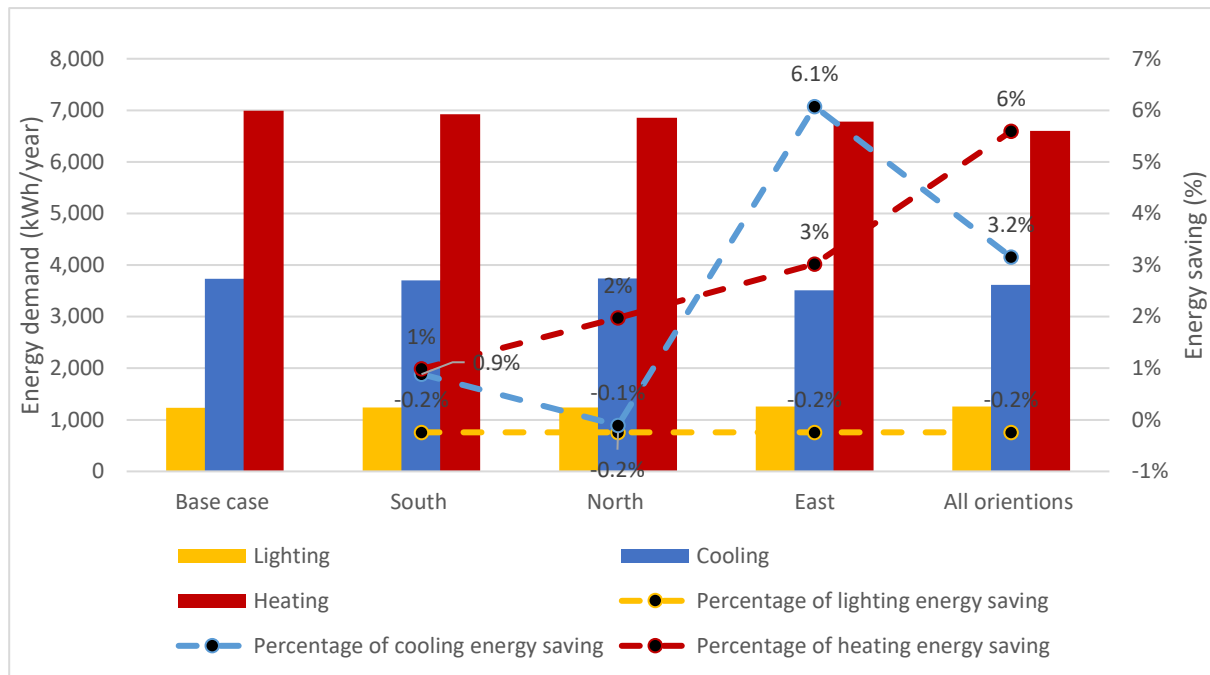


Figure 5-20: The effect of installing double clear glazing windows with U-values of 2.86 W/m²K, on different orientations on the heating, cooling, and lighting energy demands, and the energy-saving percentage in comparison with the base case model. The heated area of the apartment is 135 m².

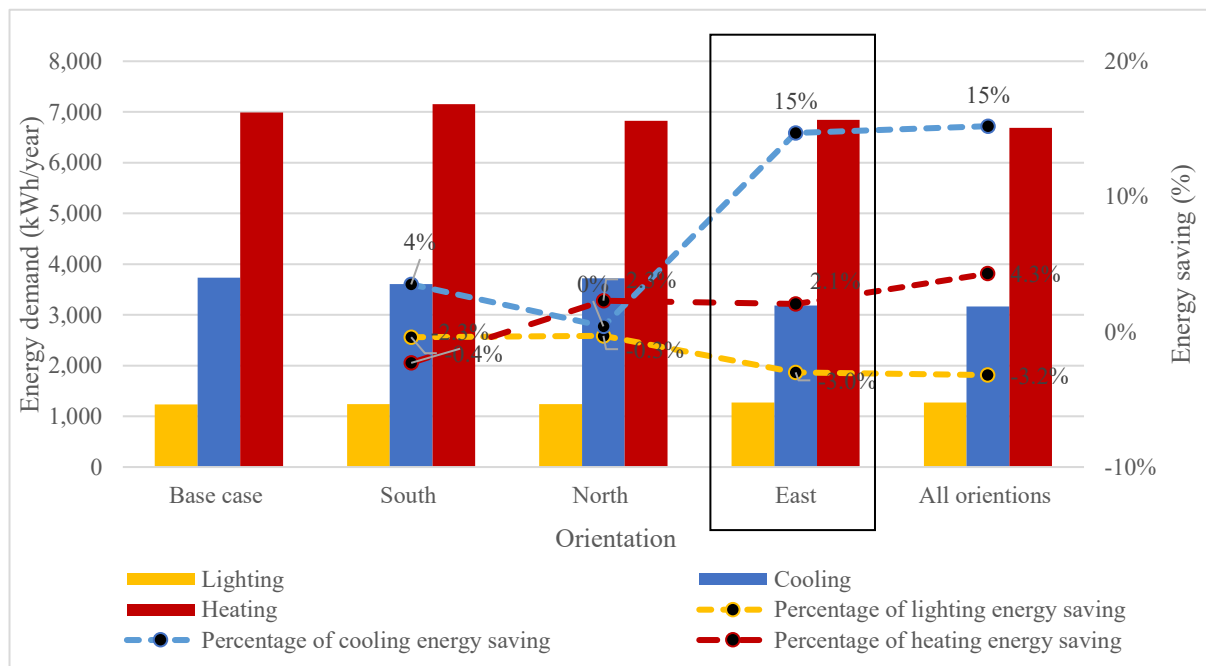


Figure 5-21: The effect of installing low-emission double glazing windows with U-values of 1.59 W/m²K double glazing windows on different orientations on the heating, cooling, and lighting energy demands, and the energy-saving percentage in comparison with the base case model. The heated area of the apartment is 135 m².

Regarding the window recess depth, the simulation shows that there is no big impact of this parameter on the energy demands, see Figure 5-22, therefore, the typical practice of positioning the windows on the inner edge is selected (base case).

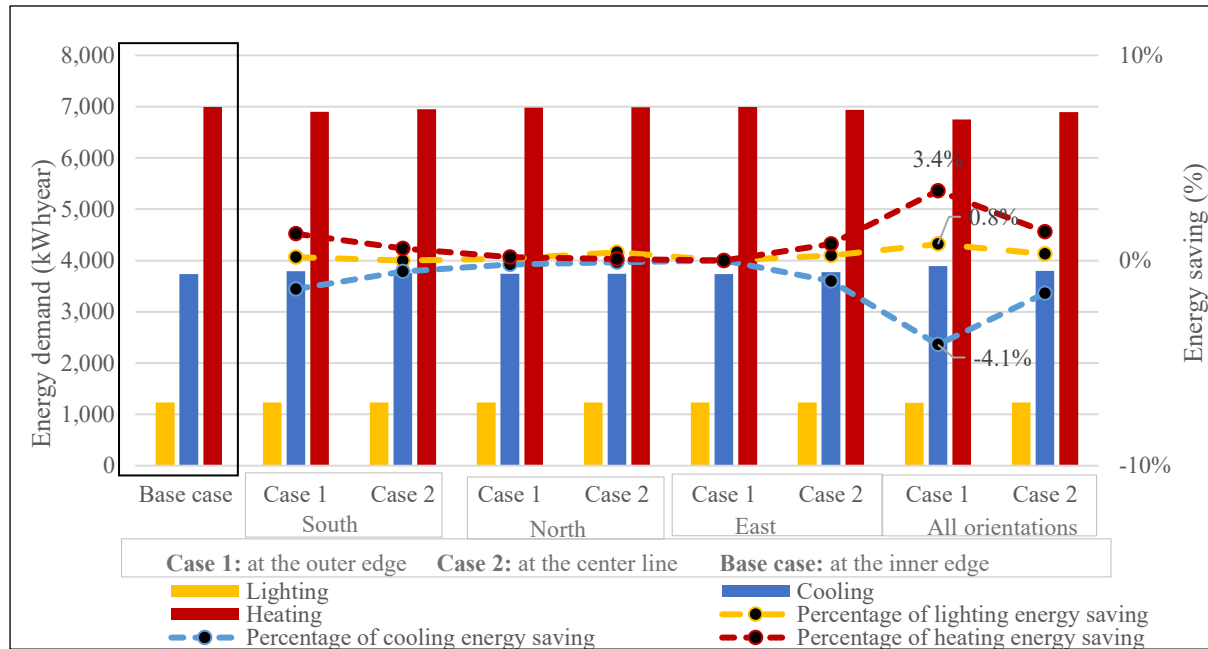


Figure 5-22: The effect of window recess depth with respect to the facade (at the outer edge, on the center line, at the inner edge) on the heating, cooling and lighting energy demands, and the energy saving percentage in comparison with the base case model. The heated area of the apartment is 135 m².

Strategy 4: Shading device

In this section, the effect of different types of external shading devices in different orientations on the annual energy demands is investigated. Figure 5-23 and Figure 5-24 illustrate the annual energy demands of the multi-family building with overhangs on the south orientation and side-fines on the east orientation of different sizes and compared with the same building without shading devices (base case). Generally, both overhang shading devices on south-facing windows and side-fines on the east-facing windows reduce the cooling energy demand and increase the heating and lighting energy demands. Increasing the size of the shading devices increase this effect. However, the increase in heating energy demand is more than reducing the cooling energy demand of the building. This is because southern overhangs and western side-fines limit the solar gains in winter. While the decrease in cooling energy demand is approximately equal to the increase in lighting energy demand. Therefore, using the overhang for south-facing windows and side-fins for east-facing windows will increase the total energy demand.

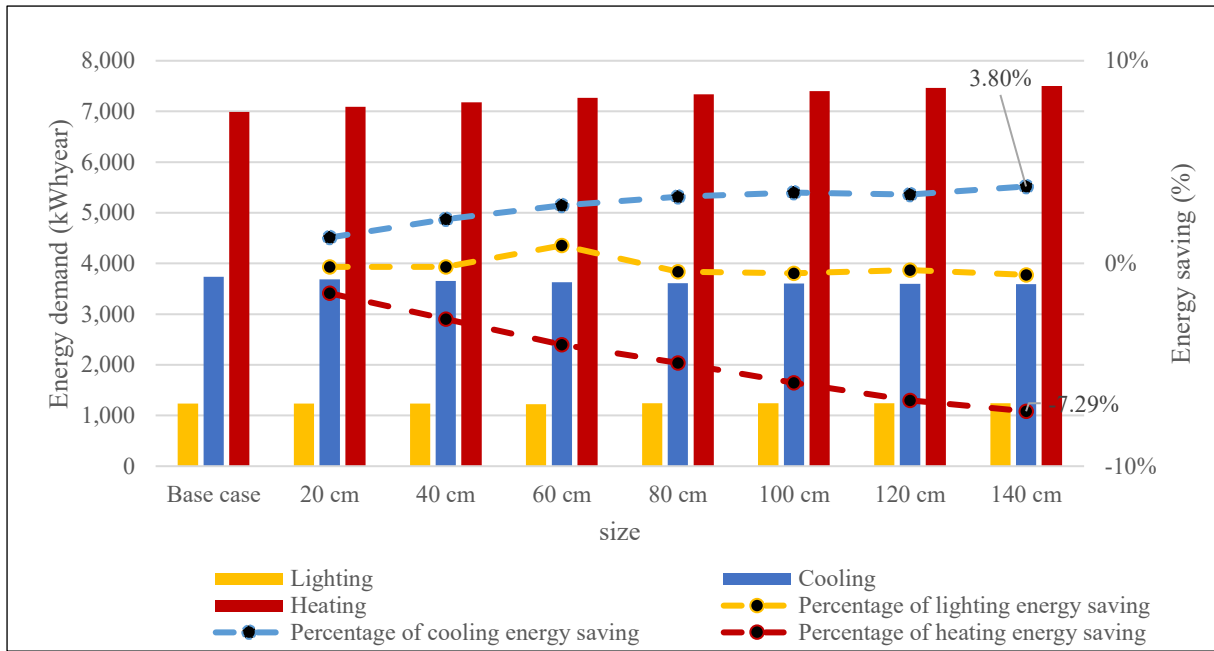


Figure 5-23: The effect of overhang with a different projection on the south elevation on the heating, cooling, and lighting energy demands, and the energy-saving percentage in comparison with the base case model. The heated area of the apartment is 135 m².

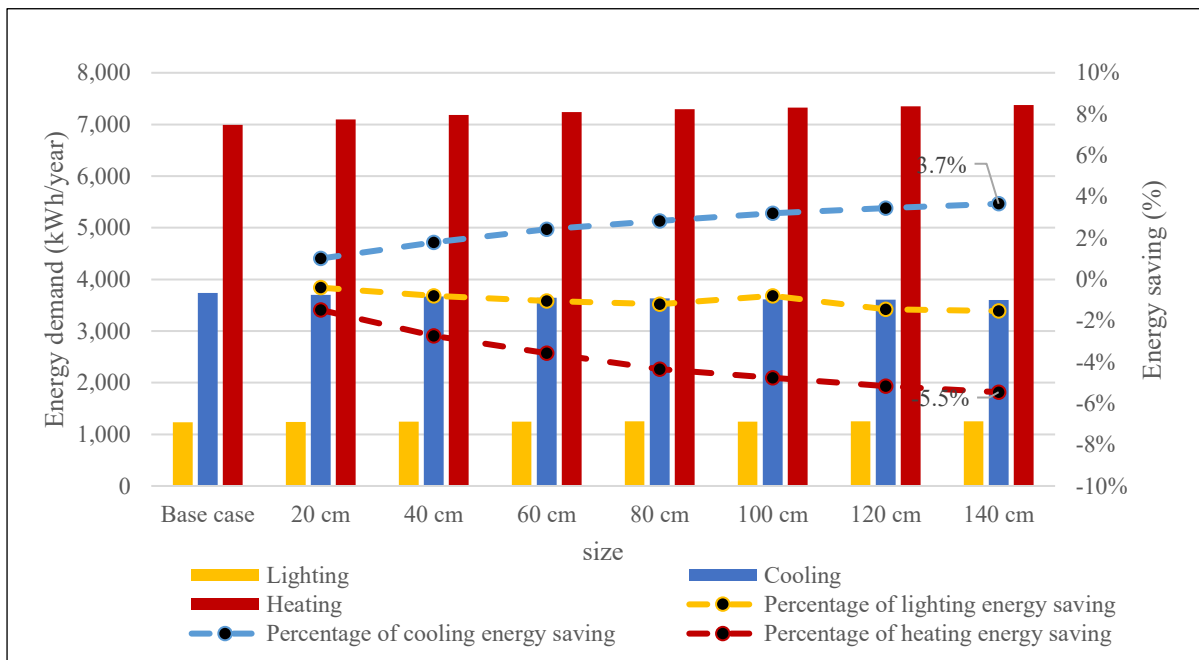


Figure 5-24: The effect of side-fines with different projections on the east elevation on the heating, cooling, and lighting energy demands, and the energy-saving percentage in comparison with the base case model. The heated area of the apartment is 135 m².

In order to study the effect of ventilation blinds and the strategy of controlling them on the energy demands of the multi-family building in Amman, Jordan. The apartment without any shading devices (base case) and with external ventilation blinds with different operating strategies is simulated.

For south and east-facing windows, movable ventilation blinds have more effect on the energy demands, when it is correctly controlled by users, see Figure 5-25 and Figure 5-26. In case 1, case 2 and case 3 the ventilation blind is kept down during the heating period; therefore, these cases have no effect on the heating demand, however, the cooling demand is decreased with the highest cooling energy saving in case 2 when the ventilated blind is kept down during all day in the cooling period. In case 2, the cooling energy decreased by 4.3% (160 kWh/year), 17% (640 kWh/year) for south and east-facing windows, respectively, compared to the base case.

In case 4, the ventilation blinds are down during the night (from 18:00 to 6:00) during the heating period. In this case, the heating demand is reduced by 1% (70 kWh/year) and 4.3% (300 kWh/year) for south and east-facing windows respectively in comparison with not having any shading device (base case), because closing the blinds in the winter nights reduce the heat loss to the outdoor environment.

Regarding the lighting energy demand, ventilation blinds on the south elevation have a neglected effect, however, in the east elevation the lighting energy demand reduced by 3.7% (45 kWh/year) for case 2 and 4.3% (55 kWh/year) for case 3.

Based on the results of the simulation of the shading devices, “day cooling” and “night heating” operation strategies are used in this research for both south and east-facing windows.

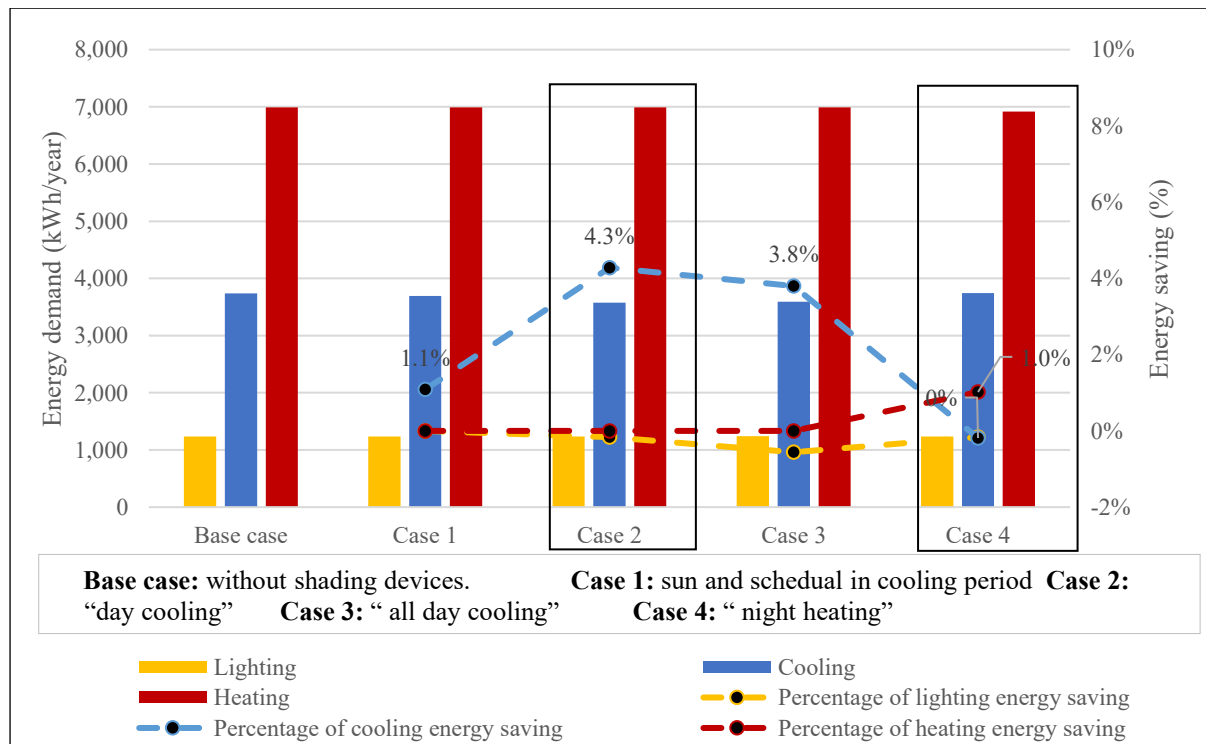


Figure 5-25: The effect of ventilation blinds on the south elevation on the heating, cooling and lighting energy demands, and the energy-saving percentage in comparison with the base case model. The heated area of the apartment is 135 m².

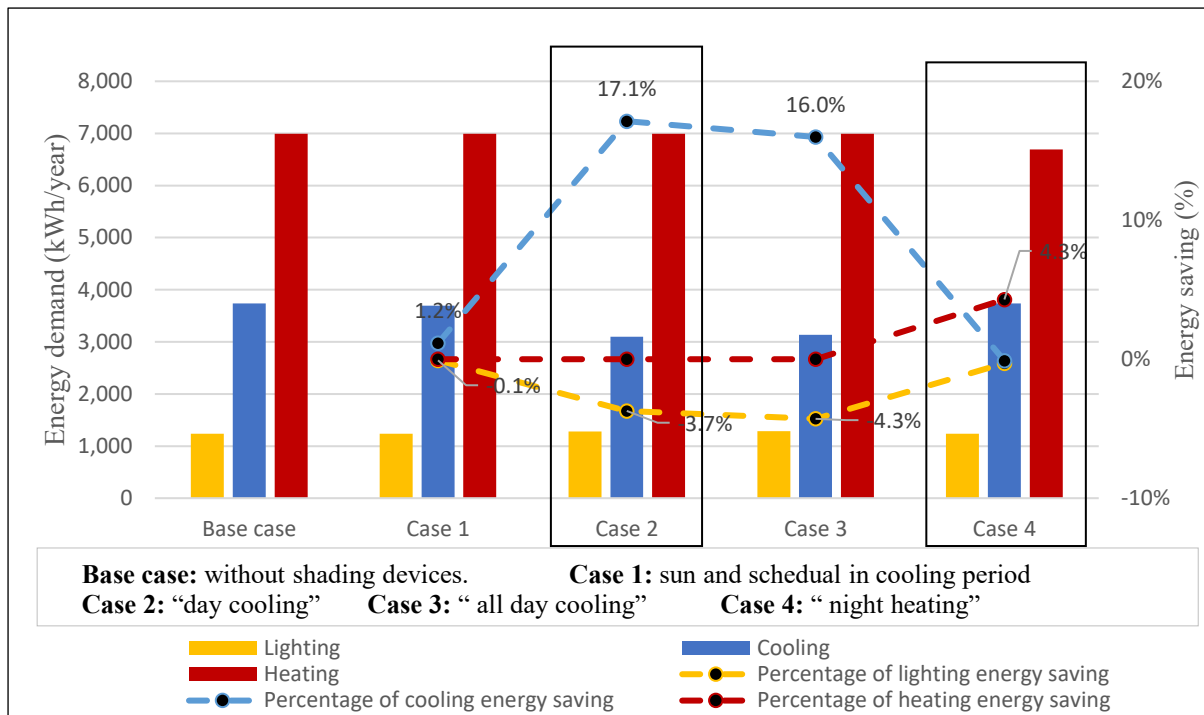


Figure 5-26: the effect of ventilation blinds on the east elevation on the heating, cooling and lighting energy demands, and the energy-saving percentage in comparison with the base case model. The heated area of the apartment is 135 m².

Strategy 5: Natural ventilation

As mentioned before, in the base case, natural ventilation is used during the day when the cooling is needed, and the outdoor temperature is lower than the indoor temperature. Figure 5-27 below, illustrates the effect of night ventilation with different schedules in comparison with the base case (daytime ventilation) in the cooling period. In case 1, when the windows are open in the bedrooms, two hours in the evening, the cooling demand decrease by 1% (46 kWh/year). While in case 2, when the windows are open during the night in the living room, guest room, and kitchen, the cooling demand decrease by 13.9% (520 kWh/year) compared to the base case. If these two ventilation schedules are applied together (case 3), the total saving of cooling energy reaches 14.6% (545 kWh/year).

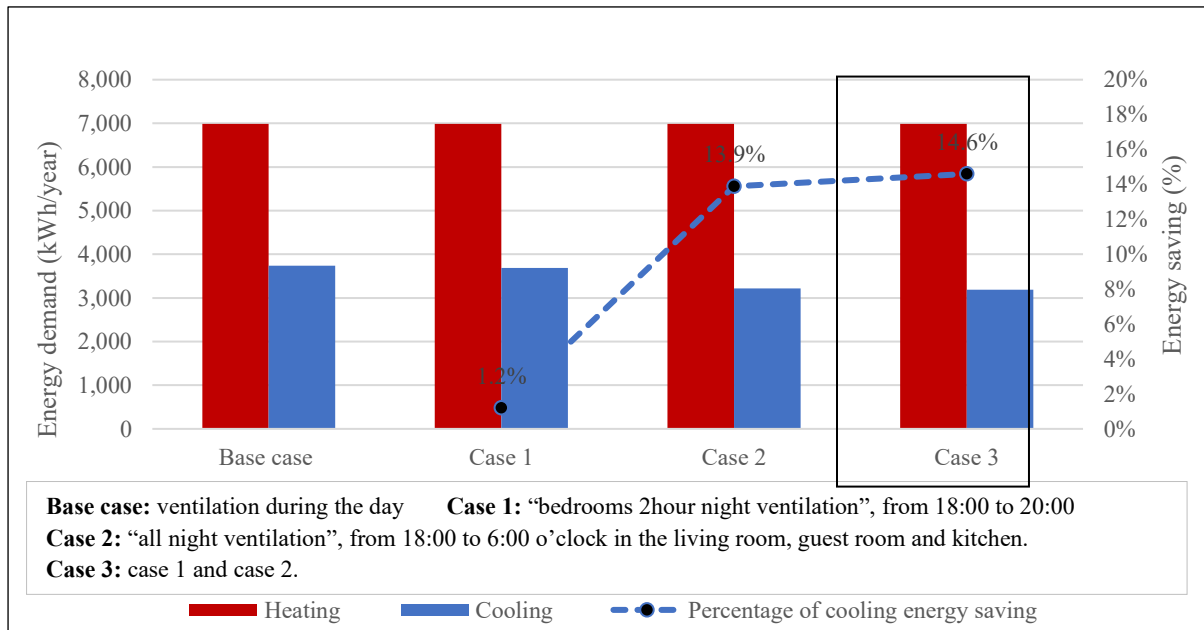


Figure 5-27: the effect of night ventilation from May to October on the heating, cooling and lighting energy demands, and the energy saving percentage in comparison with the base case model. The heated area of the apartment is 135 m².

Strategy 6: Energy-efficient lighting fixtures

When all the light bulbs in the base case replaced by LED bulbs the total annual lighting is reduced significantly by 75% (925 kWh/year). Moreover, the use of LED bulbs generates less of an internal load from light-waste-heat, which results in reducing the cooling demand by 3.2% (120 kWh/year) and increasing the heating demand by 4.7% (330 kWh/year) compared to the base case, see Figure 5-28. However, the increase in heating demand is neglected in comparison with the lighting energy-saving potential.

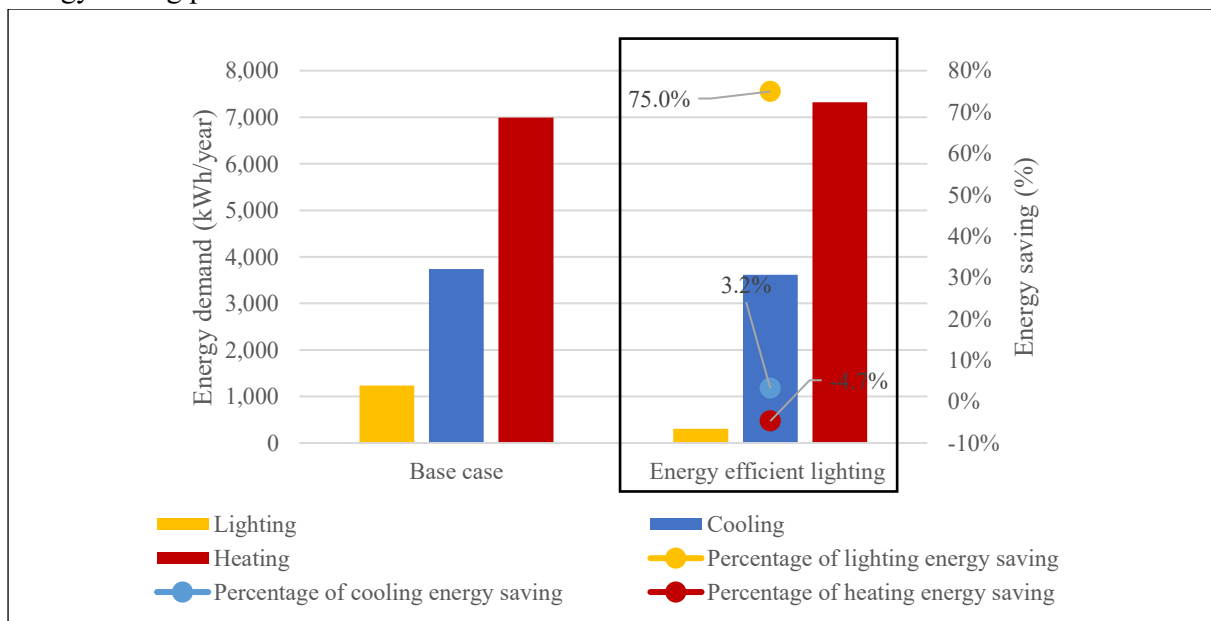


Figure 5-28: The effect of installed energy-efficient light LED bulbs on the energy demands and the energy-saving percentage in comparison with the base case model. The heated area of the apartment is 135 m².

Combinations of all strategies

In this section the best design of all the previous investigated strategies is selected and simulated in combination with each other, to find out the best final proposed design for the multi-family building in Amman Jordan.

The cases simulated in this section are:

- Case 1: adding 4 cm wall insulation to the base case model.
- Case 2: case1 + adding 4 cm roof insulation.
- Case 3: case 2 + double glazing windows on east and north elevations.
- Case 4: case 3 + ventilation blind on the south and east elevations with “day cooling” and “night heating” operation strategies.
- Case 5: case 4 + night ventilation (“bedrooms 2 hours night ventilation” and “all night ventilation” strategies)
- Case 6: case 5 + energy-efficient LED lighting bulbs.

The main results of this study indicated that when combining the all best strategies (case 6), the annual energy demand for the building could be reduced significantly, see Figure 5-29, the estimated saved energy in the top floor apartment 1 is 55.1% (2,059 kWh/year), 64.1% (4,440 kWh/year) and 81.7% (1,009 kWh/year) of the annual cooling, heating, lighting demands respectively, in comparison with the base case model. The final energy demand for the improved top floor is 226, 1,677 and 2,551 kWh/year for lighting, cooling and heating respectively.

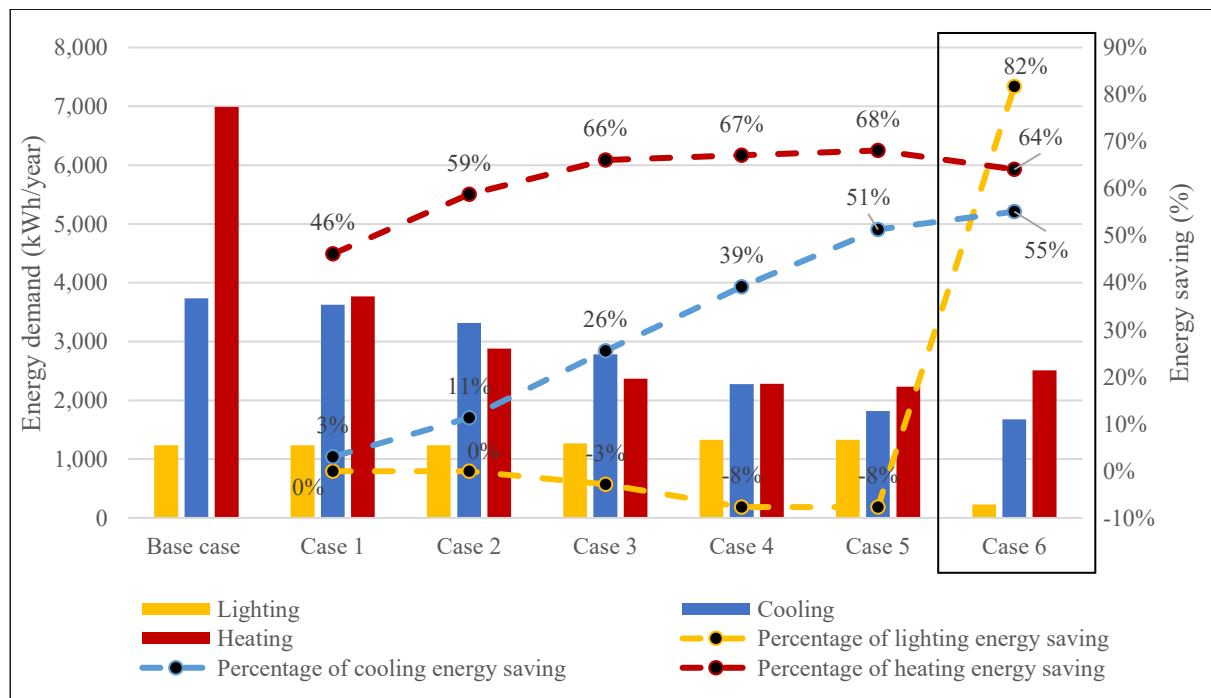


Figure 5-29: Annual energy demands for different energy-saving strategies in comparison with the base case apartment in Amman, Jordan, and the energy-saving percentage in comparison with the base case model. The heated area of the apartment is 135 m².

Energy demand for the improved multi-family building

The total annual energy demands for all the apartments in the residential building are 12,807 kWh/year (9.5 kWh/m²/year) for cooling, 17,160 kWh/year (12.7 kWh/m²/year) for heating and 37,300 kWh/year (27.5 kWh/m²/year) electricity for equipment and lighting (see Figure 5-30).

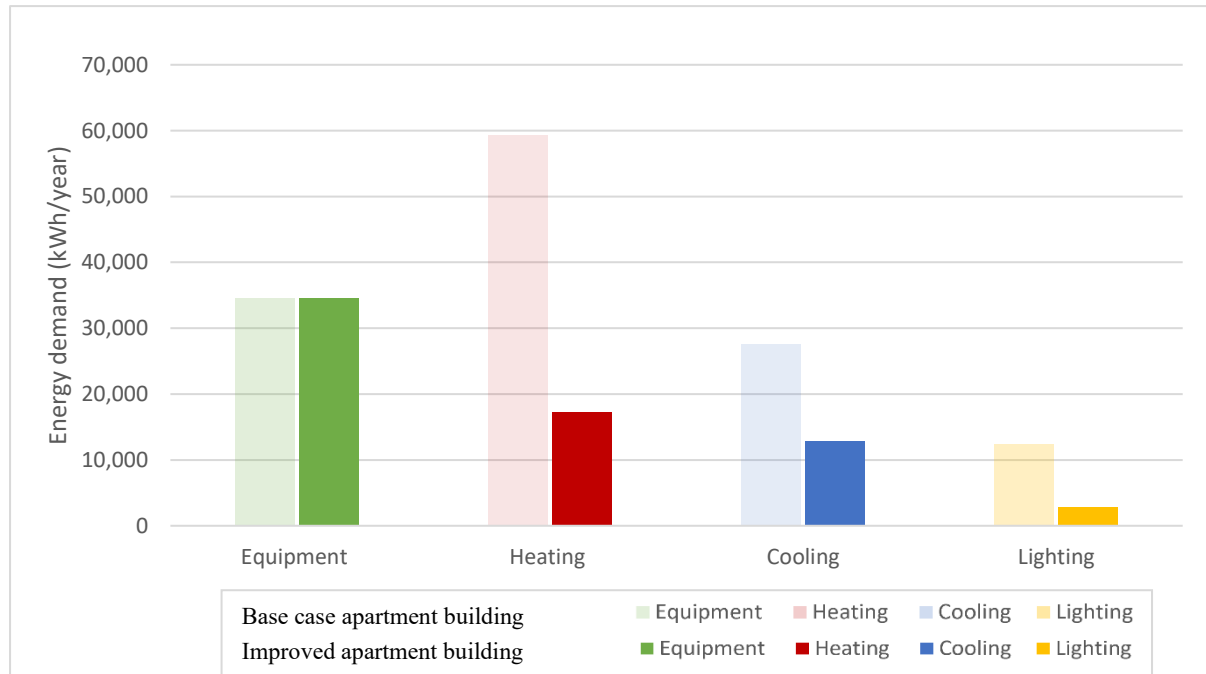


Figure 5-30: Energy demand of the improved apartment building in comparison to the base case apartment building, in Amman, Jordan. the total heated area is 1,350 m².

Figure 5-31 shows the results of energy demand for all apartments after the implementation of the energy-saving strategies (final design). It can be also seen that the heating demand for apartments on the east side (Apt.1) is higher than the apartment on the west side of the building (Apt.2), this is because in the morning when the occupant is out of the apartments the sun is penetrating through the east façade, while during the afternoon, when the occupants are at home the sun is penetrating through the west façade (Apt.2) house which decreases the heating energy demand.

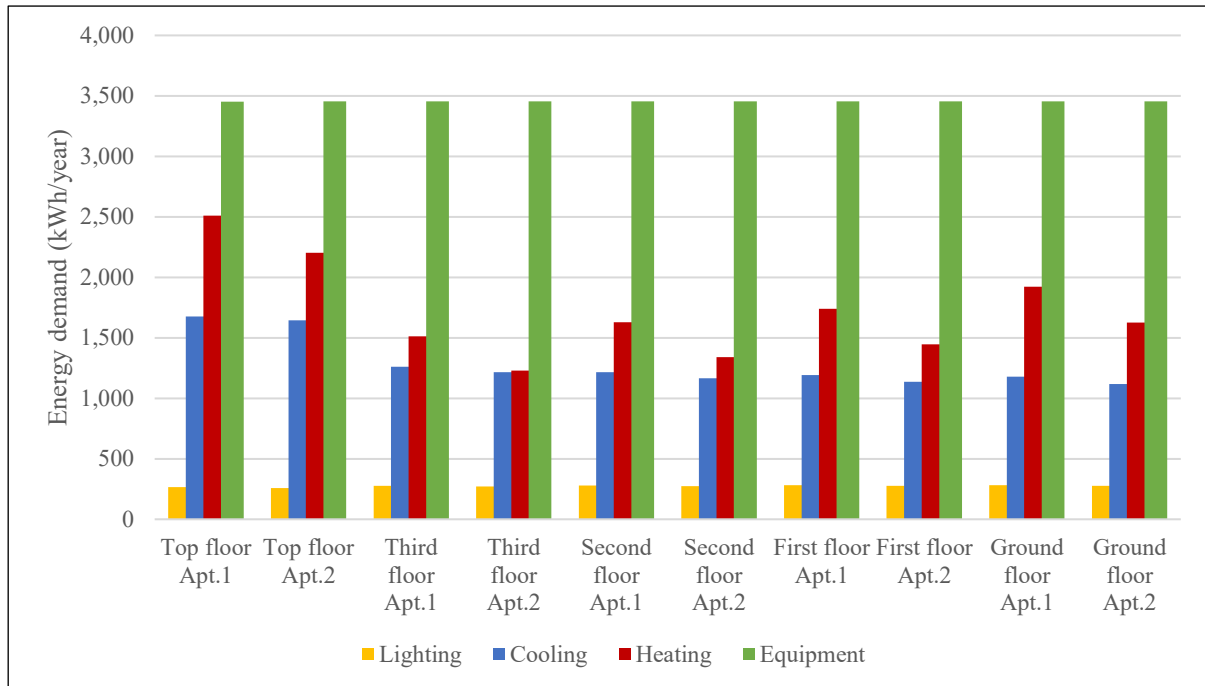


Figure 5-31: Annual energy demand for different apartments of the improved apartment building in Amman, Jordan. The heated area of each apartment is 135 m².

5.6 Summary

In this chapter, the energy demand of the typical multi-family building in Amman, Jordan, is estimated using IDA ICE 4.8 simulation software, after that, the possibility of reducing the building energy demand through different passive design strategies is investigated. The results indicate the energy demand of the typical apartment building in Amman, Jordan can be reduced up to 53% (14,700 kWh/year), 71% (4,440 kWh/year) and 78% (9,600 kWh/year) of the annual cooling, heating, lighting demands respectively, in comparison with the base case model.

6 Energy performance of solar energy systems

6.1 Introduction

In this section, different solar supply energy systems are proposed and compared with each other, and with a reference system (a conventional Jordanian energy supply system without solar technologies). Simulation software Polysun (Version 11) is used to simulate and study the proposed systems energy performance, and to calculate the energy output of the solar thermal collectors and photovoltaics. The systems designed considering the energy demands profiles for the improved residential building design in Amman, Jordan, which are obtained from the detailed energy simulations in IDA ICE 4.8, as described in Chapter 5.

6.2 System configurations

- **Solar thermal heating systems**

Different solar thermal heating system configurations are suggested for covering a part of residential heat demand required for space heating and domestic hot water (DHW), and compared with the conventional heating systems, as shown in Figure 6-1.

System 0: Conventional heating system

This reference system represents the widely used energy supply system for residential buildings in Jordan. In this system, each apartment has a complete system, so all the system components are decentralized. The hot water and space heating demands are met with a de-central oil boiler installed in the basement, for space heating, heat is transferred by radiators into the rooms.

System 1: Decentralized solar water heating system

The thermosiphon system is proposed here to produce DHW, as this system is the most popular used in Jordan (as described in Chapter 2.8). The system is composed of solar thermal collectors, and a tank to accumulate the DHW with an electric boiler to produce DHW when the solar modules cannot. Regarding the space heating system, the system components are the same as the conventional heating system.

System 2: Decentralized solar combi-heating system

In this system, solar energy is primarily used for domestic hot water supply and as partial support for the heating system. Each apartment has a complete system, solar thermal collectors are installed on the roof of the building, the hot water storage is installed in the basement when needed, the back-up oil heating heats up the stand-by volume of the buffer storage to the required set temperature.

System 3: Centralized solar combi-heating system

All apartments have shared the same collector field, storage, and back-up heater. The hot water is produced centrally in the basement of the building with an oil boiler and a thermal solar collector system installed on the top of the building. The hot water is distributed to the space underfloor heating system.

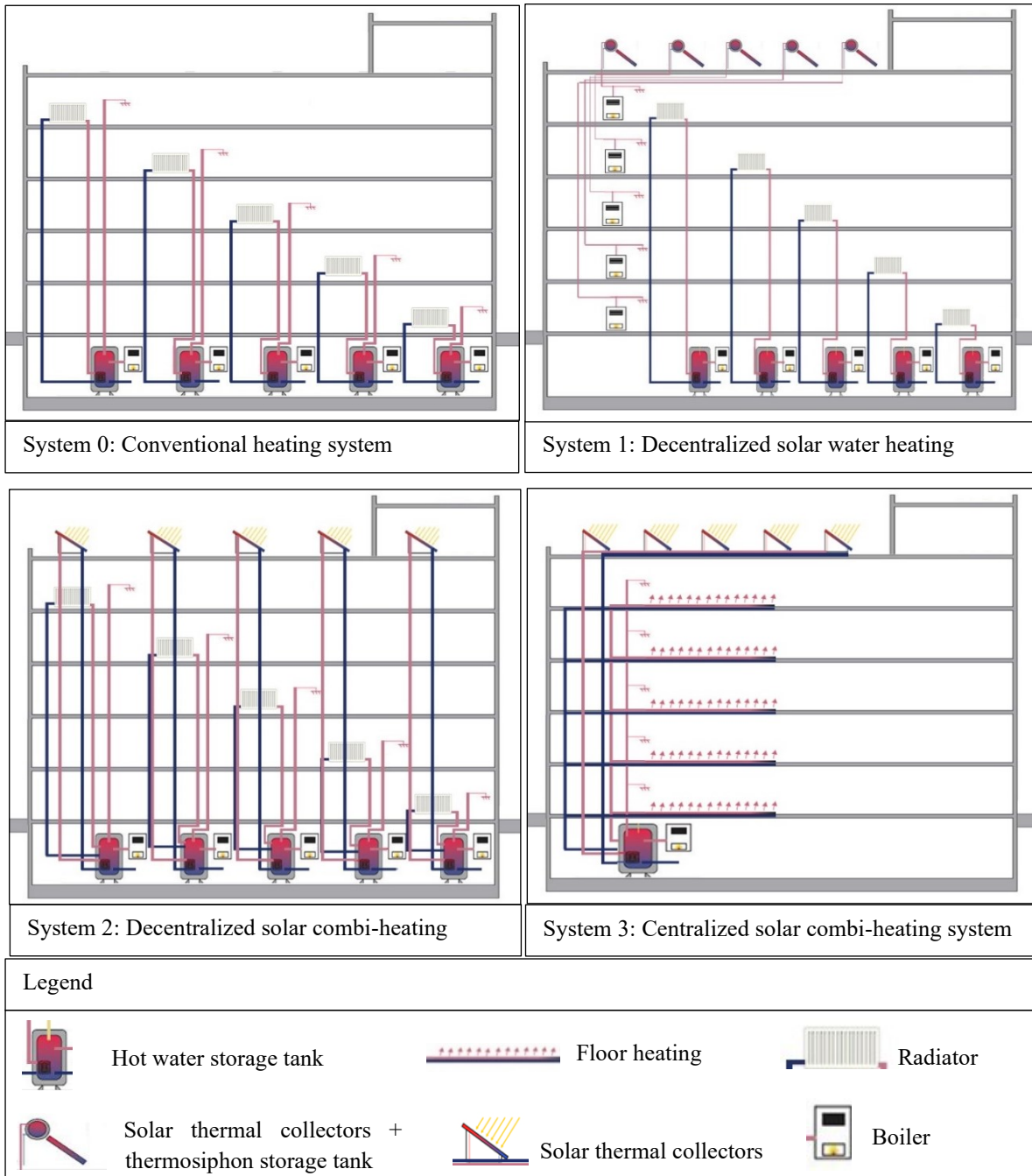


Figure 6-1: Simplified schematic of the proposed solar space and water heating systems and conventional heating system for multi-family building in Amman, Jordan.

- **Solar photovoltaic systems**

Two configurations of photovoltaic solar cooling systems (see Figure 6-2) is suggested for covering a part of residential cooling demands, the photovoltaics also designed to cover part of the building electricity demand for equipment and lighting, in order to decrease the amount of energy purchased from the electric grid. All the proposed photovoltaics systems are grid-connected systems, however, at the end of this research part, the battery need will be investigated for the chosen system. Solar thermal-driven cooling systems are not considered in this study. The investigated cooling systems are:

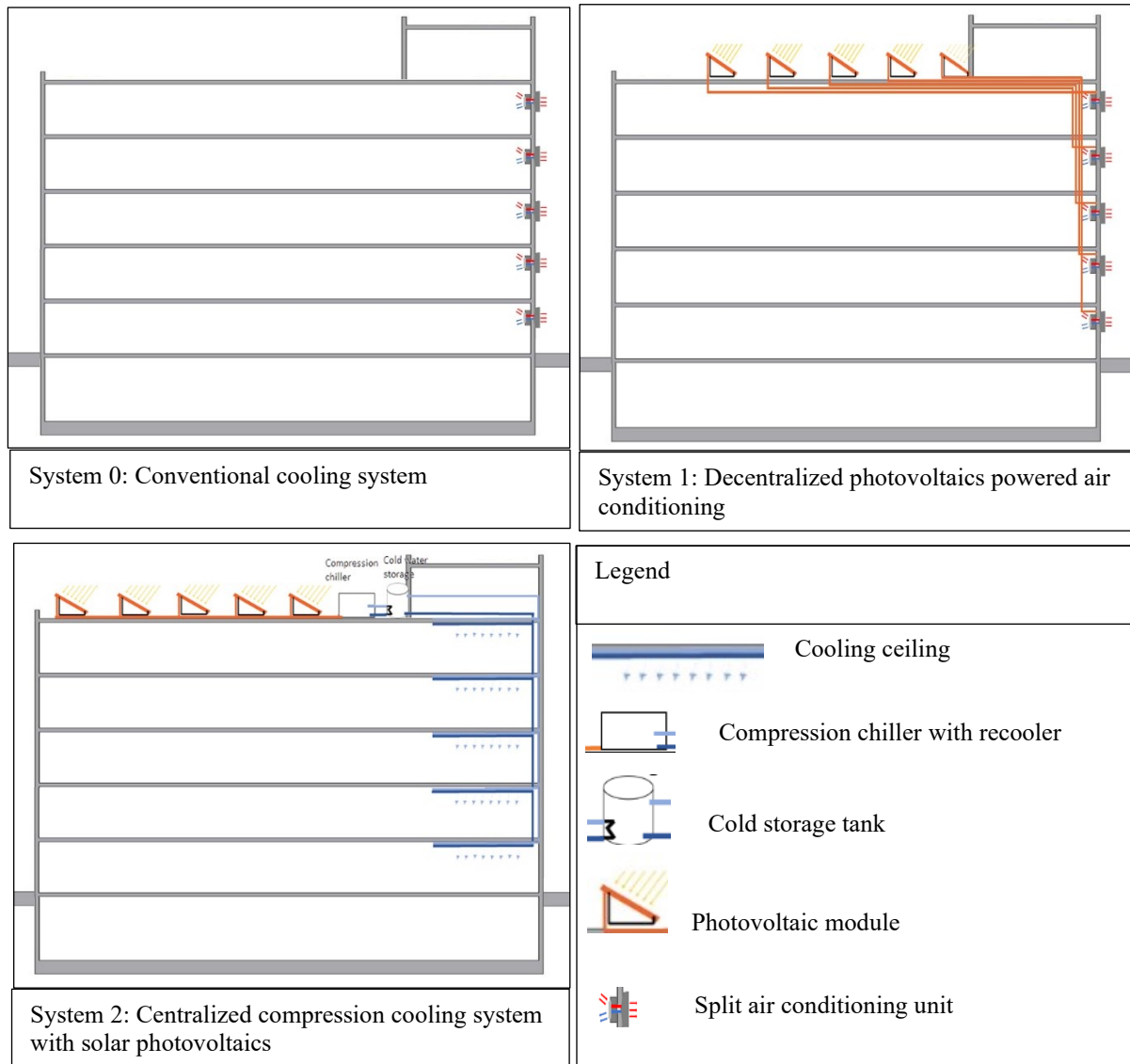


Figure 6-2: Simplified schematic of the proposed solar cooling system configurations and the conventional cooling for multi-family building in Amman, Jordan

System 0: Conventional cooling system without photovoltaic

For space cooling during the summer, a split air conditioner unit is installed on the outer wall of the building.

System 1: Decentralized photovoltaics powered air conditioning

In this system, the photovoltaic modules are installed on the roof to supply part of the energy needed for cooling used by the split air conditioner units (conventional cooling units).

System 2: Centralized compression cooling system with solar photovoltaics

The space cooling is produced centrally on the roof of the building, the conventional air-cooling split units are replaced with a cold-water supply system. Here, the electricity needed for the compression chiller is produced by photovoltaic modules. If an overproduction of electricity occurs, it can be fed into the grid. Dry re-cooling is used as the method of heat rejection. The cooled water transferred to space by ceiling cooling systems.

6.3 Simulation input and systems design

In all the simulated systems, there are constant input parameters such as the solar collectors and photovoltaics module type, tilt angle and azimuth. The same climate data and the same space heating and cooling, hot water demands. However, each system has different components of the design. In this section, the most important parameters, the design considerations and the selection of the system components in Polysun simulation software are described.

- **Constant parameter**

Location and climate

The location for all simulations is Amman, Jordan. The exact location is selected directly from the map tool installed in Polysun, the latitude is 31°95' North and the longitude is 35°93' East. Regarding the climate conditions, the same hourly weather data used in IDA ICE 4.8 simulation (Chapter 5), which is created by Meteonorm 7 software for Amman city, is used for all simulation models with Polysun. Climate analysis has been already presented in Chapter 2.3.

Building energy demand

Regarding the input for the building energy demands in Polysun, the data which has been obtained from the IDA ICE simulation cannot be directly imported to Polysun. As the time step for output files in IDA ICE is set 5 minutes and in Polysun hourly time step is needed, therefore, Python 3.7.2 program is used to convert the time step from 5 minutes (IDA ICE output files) to hourly average values.

The reason for not considering the hourly time step for the output file in IDA ICE is that the result files contain instantaneous and not the average hourly value results (EQUA, 2018), which is resulted in different annual energy demands value in Polysun. Building hourly heating and cooling energy demand are presented in Figure 6-3, it is important to note that is the total heating area is 1,350 m² for all apartments in the building, more details are presented in Chapter 5.

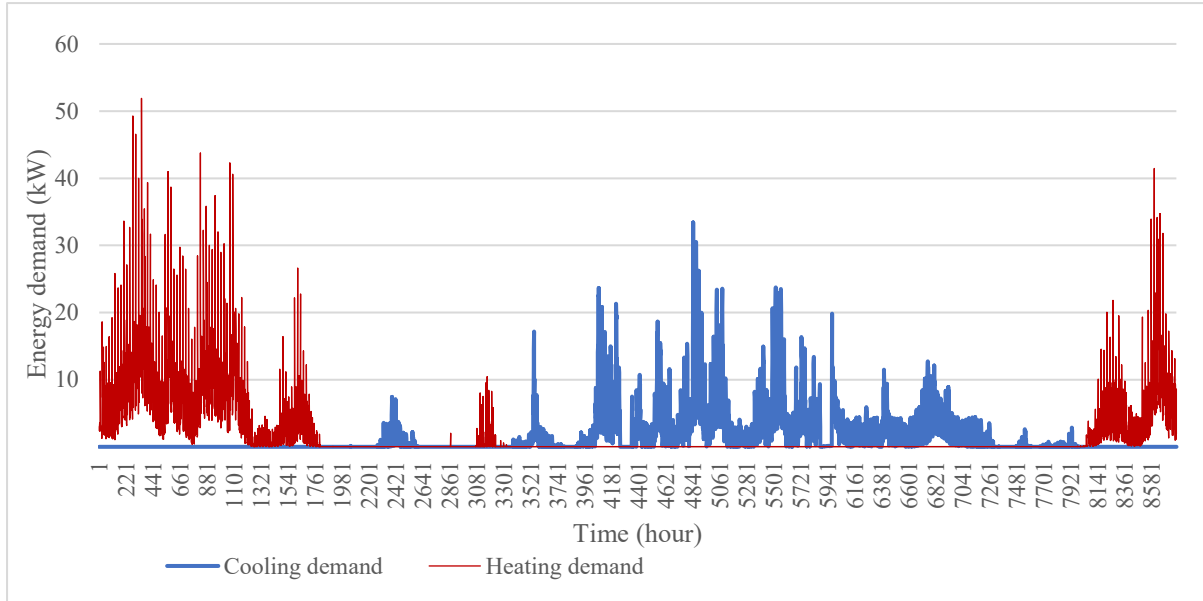


Figure 6-3: Hourly heating and cooling energy demand for an improved apartment building in Amman, Jordan. The total heated area for the apartment is 1,350 m².

Domestic hot water demand

Regarding the domestic hot water (DHW) demand, the average hot water demand for the typical Jordanian family is estimated to be 50 l/person/day with an average temperature of 50 °C (Shariah, Al-Akhras and Al-Omari, 2002; Attia, 2014). As each apartment occupied by 6 persons, the hot water demand for each apartment is 300 l/day.

The daily hot water demand profile examined in this study is shown in Figure 6-4, this hot water daily profile is based on Polysun "multi-family dwelling" water profile and edited to match the occupancy profile. Constant daily demand is assumed for all days in the year. The annual energy demand for hot water is 4,077 kWh/year.

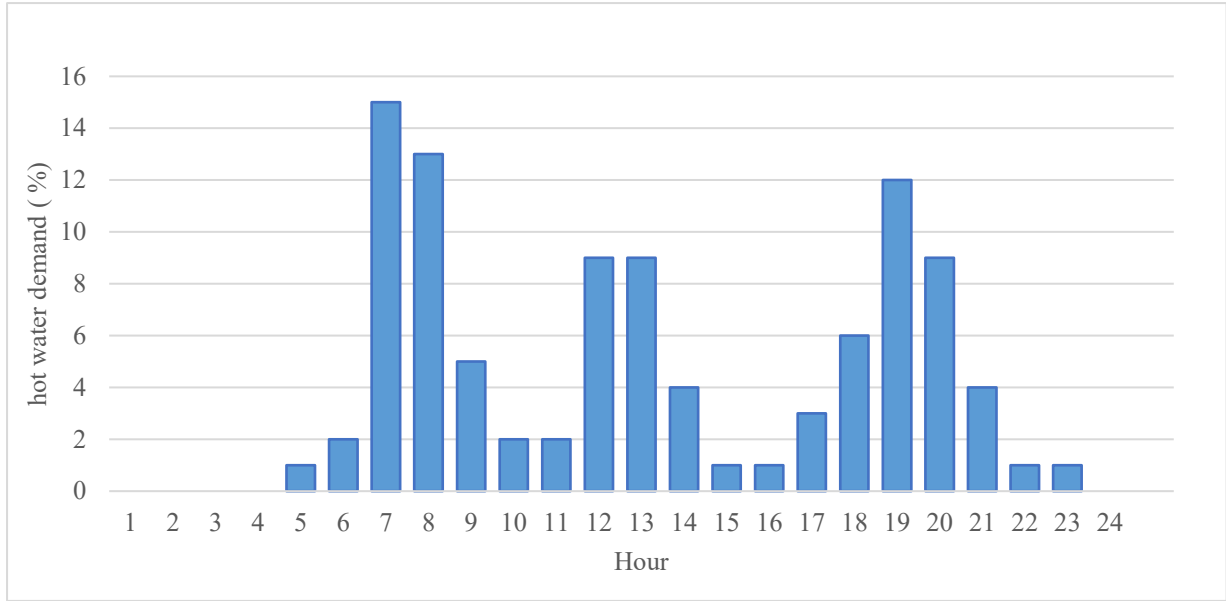


Figure 6-4: Daily hot water demand profile (300 l/day) in percentage for each family in the residential building in Amman, Jordan, used in Polysun simulation software.

PV module/solar collectors tilt angle, azimuth, shading, and the total installation area

In this section, the PV modules and solar collectors are installed directly on the roof, facing the south (azimuth is 0°) with tilt angle 30°, as recommended by the previous research (Fasfous et al., 2013; Goussous and Al-Refaie, 2014; Adas, 2016). However, in the next chapter, the installation on the roof with different tilt angles will be evaluated.

Regarding the area of the installation, the maximum number of PV modules/solar collectors is assumed to be installed on the roof, considering the space between the modules/collectors to avoid shadows on each other. The estimated space between the solar collectors/PV modules rows is around 1.6 m, which is calculated according to Equation 6-1 (Adas, 2016). The length of the solar collector and PV modules used in this part of the research is 2 m, 1.95 m respectively (more details described later).

$$\text{Distance to next array} = \text{length of solar panel} \times \left(\frac{\sin(\text{panel angle})}{\tan(\text{panel angle})} \right) \quad (6-1)$$

The total roof area is about 300 m², however, part of the roof area is used for the installation of the building services such as water tanks, dishes, etc. The assumed area for the building services is near the staircase to avoid the shade into the PV modules and solar collectors. Accordingly, the total area available for solar technology installation is about 200 m², in addition to 25 m² above the staircase roof.

Based on the above-mentioned description, the proposed arrangement for the solar collectors, and the photovoltaic module on the top of the residential building apartment in Amman, Jordan is shown in Figure 6-5 below. This assembly allows the most use of the roof space, the total gross available area for the installation of each of solar collectors and PV module is 60 m². However, regarding the thermosiphon heating system, more area is needed for the hot water tank installation, therefore, the available area for the solar thermal collector in this system is assumed to be 40 m².

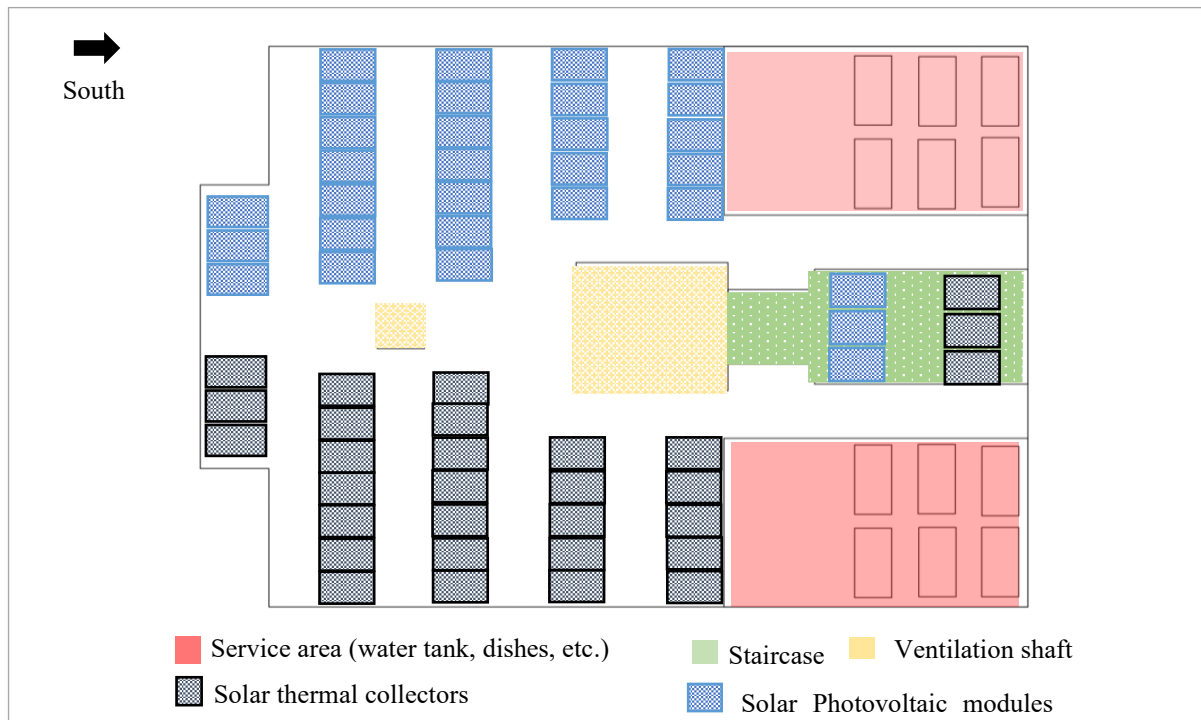


Figure 6-5: Proposed arrangement for the solar collectors, and photovoltaic module on the roof of residential building, in Amman, Jordan

Systems components design

The systems configurations which are presented in section 6.2 are transferred into Polysun simulation software by using the relevant template available in the Polysun library, which are used as an initial design structure of the studied systems. Then several setups have been tried out for each system, such as storage tank volume and type, auxiliary heating and cooling size, control strategies, etc., to find out the design of the optimum system in terms of energy performance (energy demand of the system, building energy deficit, and solar energy fraction). Below is the description of the final proposed systems designed in Polysun:

- **Heating systems design**

The flat plate collector is applied to all solar thermal systems. The selected collector is “Flat-plate, good quality”, which is matching well developed local flat-plate collector in Jordan (Hanania Energy, 2017). The orientation of the solar collectors is to the south, and the tilt angle is 30°. As described before, the total gross area of the installed collectors on the roof for all apartments is 60 m² for 30 solar collectors, however, in the case of the thermosiphon system (system 1) is 40 m² (4 m² for each apartment). An overview of all the heating systems input and design parameters are presented in Appendix A.

The description of heating systems models design in Polysun is presented below:

System 0: Conventional heating system

The simulation model layout for the conventional heating system for each apartment is presented in Figure 6-6, the system consists of oil boiler with maximum capacity of 5 kW for the top floor apartments and 4 kW for other apartments (the peak power and the demand is higher in the top floor apartments, as presented in Chapter 5), 300 l hot water storage tank, pump, mixing valve, cold water supply and how water demand. The boiler is switched on when the tank temperature at layer 8 is lower than 50 C° and switch off when it is higher than 60 C°.

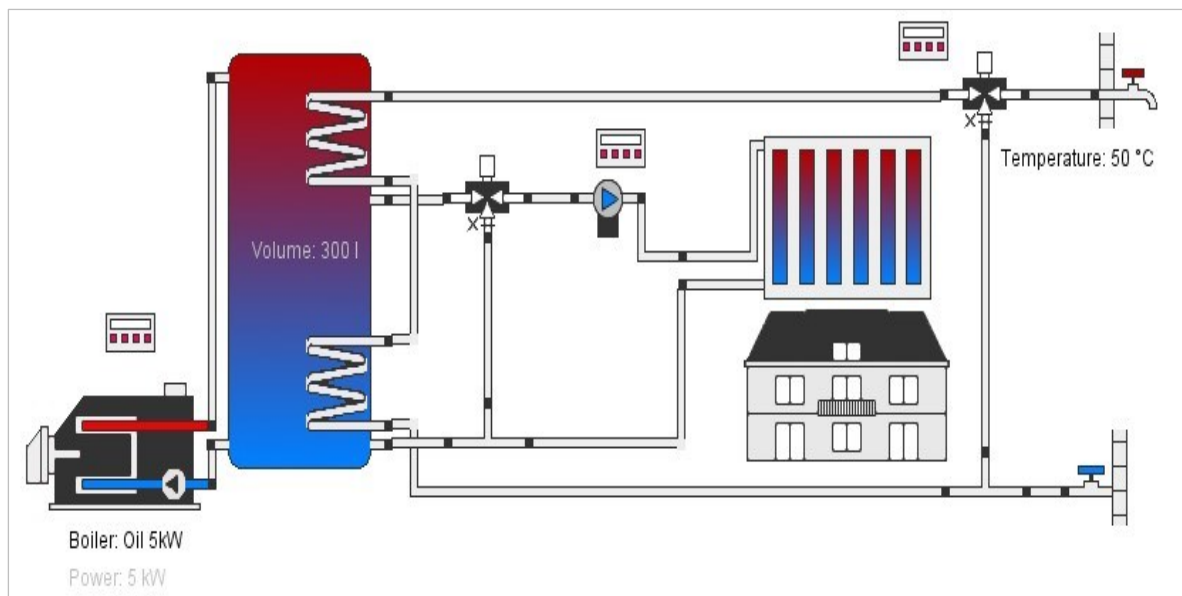


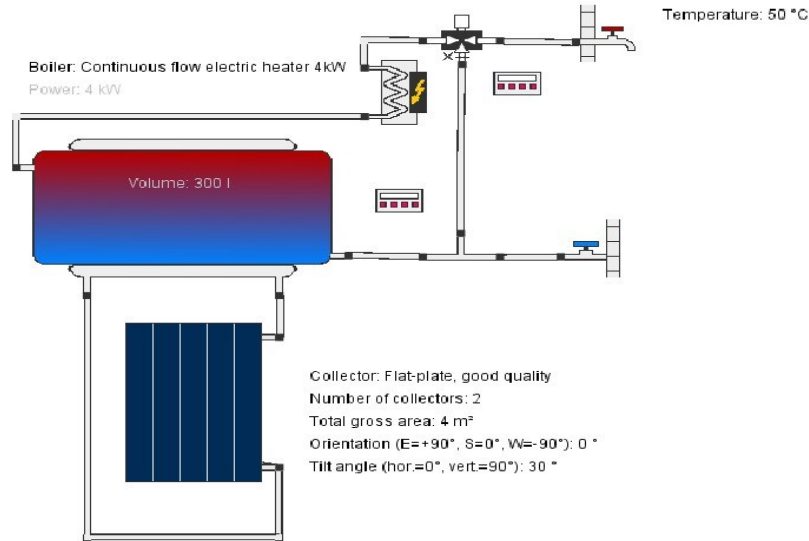
Figure 6-6: Model layout of the conventional heating system in Jordan (system 0).

System 1: Decentralized solar water heating system.

In this system, the domestic hot water is supplied to each apartment through a decentralized thermosiphon system, the system designed based on the description in Chapter 2.8. The system shows in Figure 6-7 (a), basically consists of 4 m² (gross area) flat-plate collectors for each apartment, connected to a storage tank with a volume of 300 l. In winter (from early November until late February), continues flow electric heater with the heating capacity of 4.0 kW, is used for auxiliary heating when the temperature of the hot water is lower than 50 °C, and it is switched off when the temperature is higher than 55 °C.

Regarding space heating, as shown in Figure 6-7 (b), the system for each apartment mainly consists of a 4 kW oil boiler which is connected to a 200 l hot water storage tank. The boiler is switched on in the heating period (from November until late March) when the tank temperature (layer 10th counting from the storage bottom) less than 50 °C and switch off when it is higher than 60 °C at the same tank layer.

(a) System 1: thermosiphon solar hot water system



(b) System 1: conventional heating system

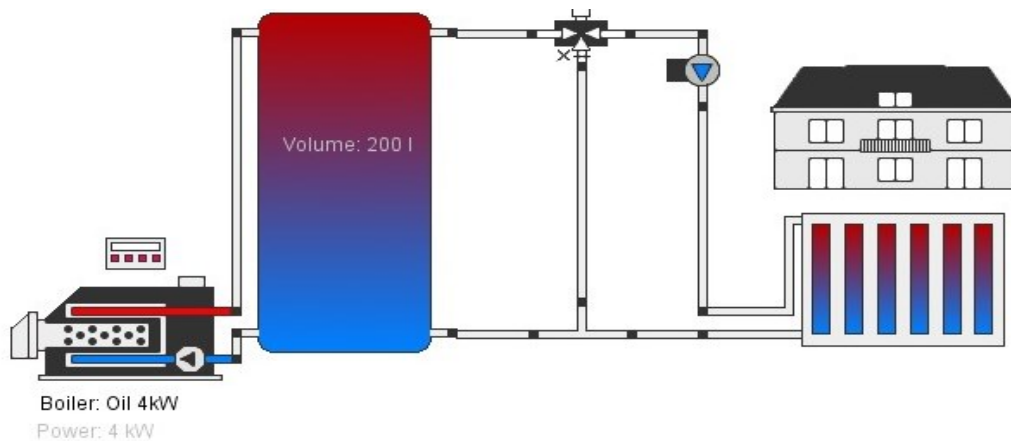


Figure 6-7: Model layout of (a) System 1: thermosiphon solar hot water system (b) System 1: conventional heating system.

System 2: Decentralized solar combi-heating system.

The solar combi-system as shown in Figure 6-8 has been modeled in Polysun. In this system, the main components are solar collectors, the buffer and the boiler. As can be seen, the heat for DHW preparation and space heating is supplied by the 6 m² of flat-plate solar collectors for each apartment. In winter (from early November to late January), the additional heat source (oil boiler), with the heating capacity of 4.0 kW for top floor apartments and 3 kW for other apartments, is used as a backup system.

Both the solar collectors and the boiler are connected to the storage tank of 300 l with a maximum setpoint temperature of 120 °C, above this limit, the storage tank will no longer be loaded with solar energy. The specific flow rate in the solar collector loop is 40 l/h/m² and the maximum temperature at the collector outlet is 140 °C, to avoid overheating of the solar loop.

The oil boiler is switched on when the temperature of the storage tank (layer 7th counting from the storage bottom) is lower than 50 °C and switch off when the temperature higher than 60 °C.

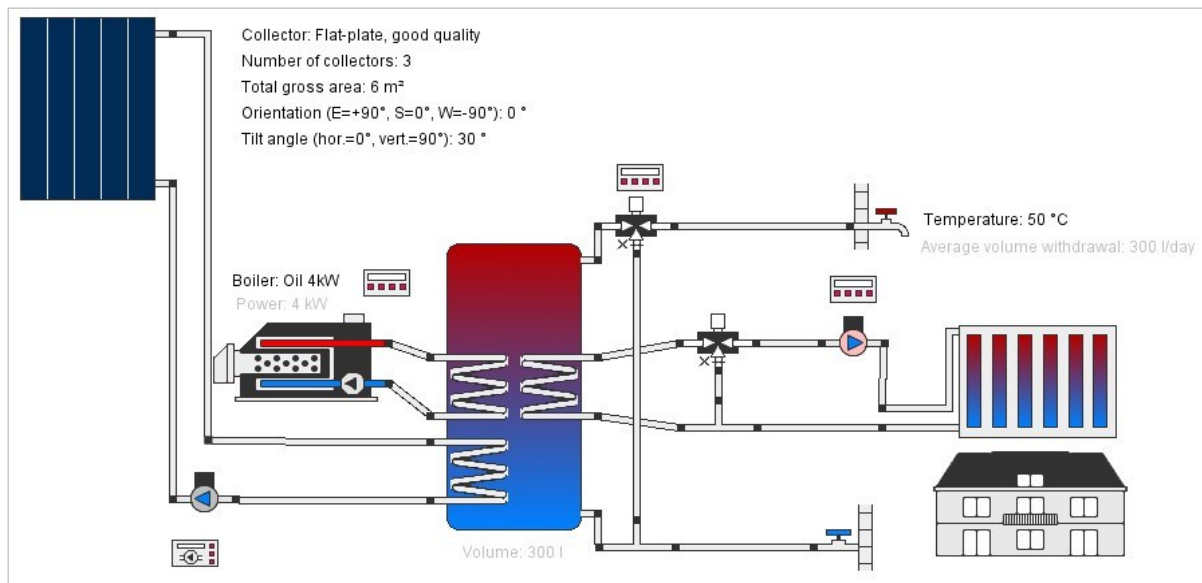


Figure 6-8: Model layout of the decentralized solar combi-heating system (system 2).

System 3: Centralized solar combi-heating system.

The component of this system is the same as the previous system (system 2), however, all apartments shared the same solar thermal collector field of 30 flat plate collectors with a total gross area of 60 m², a storage tank of 3,000 l and oil boiler auxiliary heating with a heating capacity 20 kW. Figure 6-9 illustrates the system layout designed in the Polysun simulation.

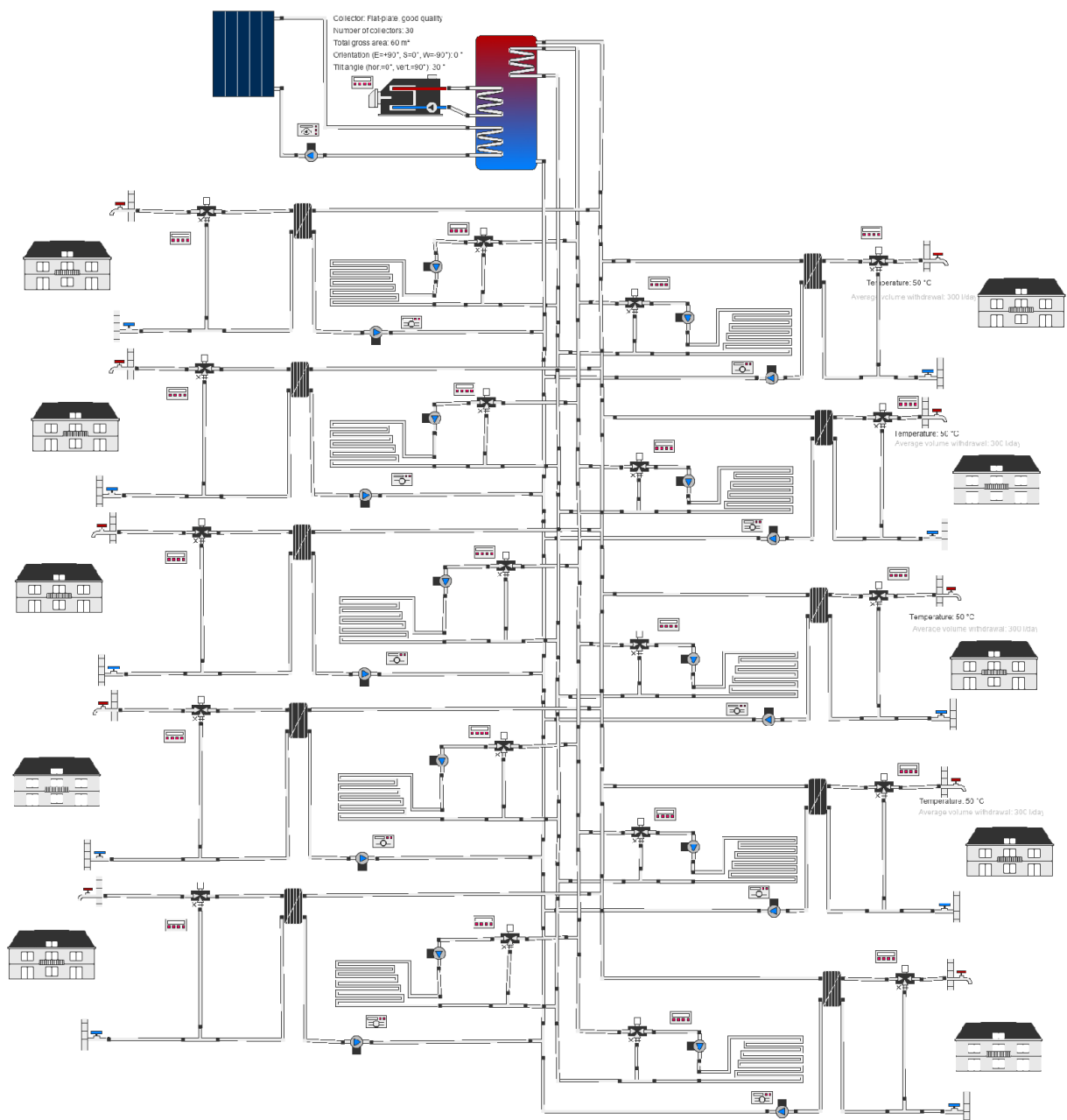


Figure 6-9: Model layout of the centralized solar combi-heating system (system 3).

- **Solar photovoltaic systems design**

As mentioned before, two PV air-conditioning systems have been proposed and compared to the conventional split air condition system (system 0), in order to find out the system with lowest electricity demand to provide the same cooling demand and to evaluate the potential of solar photovoltaic for covering part of the building electricity demand. Both systems (system1 and system 2) are grid-connected systems, the battery need for the selected system will be evaluated at the end of this chapter.

From the list of PV modules in Polysun, it has been selected the modules with the mono-crystalline silicon technology, due to it is a relatively high efficiency and a high reliability (based on the discussion in Chapter 3.2.3), the selected module named: “PS-M 2H-300”, which produced locally in Jordan in “Philadelphia solar” company (Philadelphia Solar, 2018). A PV module has a dimension of 1,965 mm x 990 mm x 45 mm with a 1.95 m² gross area. The maximum power of the PV modules is 300 Wp at standard test conditions and the module efficiency is 15.4% (reflect average typical values). The same as the solar thermal collectors, the orientation of the PV-modules is designed facing south, and the tilt angle is 30° the total number of the installed solar photovoltaic modules on the roof for all apartments is 30 modules with a total gross area of 58.9 m². The arrangement of the PV modules on the roof has been presented in Figure 6-5.

In Polysun models, the assumed wind fraction and rear ventilation are 80% and good, respectively. As the PV modules are mounted on the top of the roof with no surrounded obstacles and with good rear ventilation (without integration). Moreover, it is necessary to choose the percentage of cable losses, which is assumed by 4%. The inverter of both systems has been selected by using “wizard” choice in Polysun; through filtering the configuration of the available inverters according to some electrical parameters of the PV field such as voltage, current, and power levels.

An overview of all the PV and cooling systems input and design parameters are presented in Appendix B.

System 0: Conventional cooling system

As mentioned before conventional split air-condition (electrical driven vapor compression) used in this system to cover the cooling demand of each apartment. Regarding the coefficient of performance (COP) of the traditional air-conditioning system in the residential building in Jordan, different values have been found in the literature which is 2.5 (Jaber and Ajib, 2011a) and 3 (Jaber and Hawa, 2016; Ali and Alzaed, 2017). In this research, the COP value is assumed to be 2.7. The conventional cooling system is modeled in Polysun as illustrated in Figure 6-10. The system mainly consists of the air heat exchanger, compression chiller and fan coils. The nominal cooling capacity of the chiller and air heat exchanger is 3 kWh for each apartment. The number of required fan coils has been calculated automatically in Polysun.

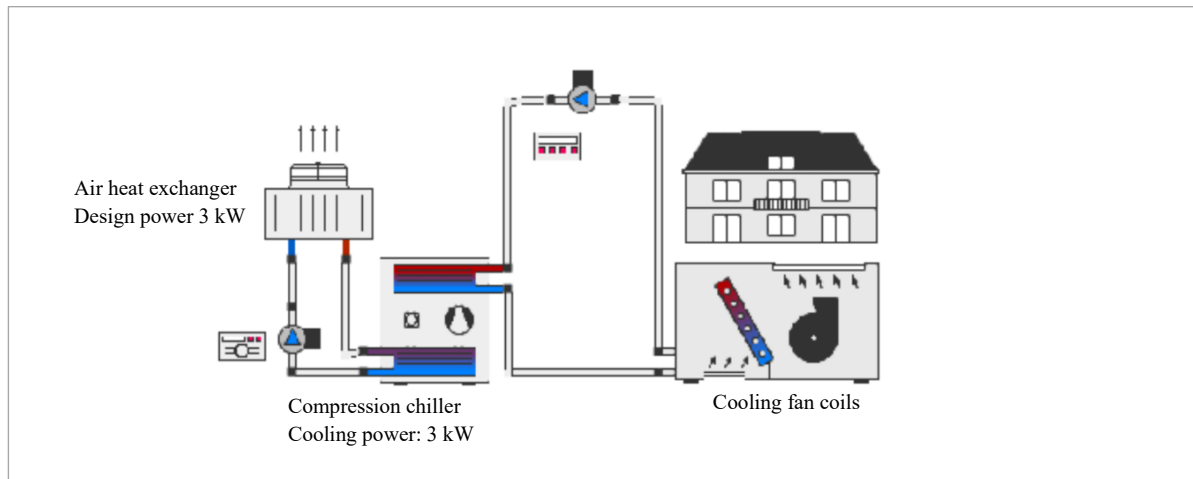


Figure 6-10: Conventional split air condition system in Jordan.

System 1: Decentralized photovoltaics powered air conditioning

This system uses the same cooling devices as the reference conventional cooling system (system 0). However, the electricity demand is supplied by PV modules and from the public grid, if required. If the electricity produced by the PV is higher than the electricity demand, the surplus can be fed into the public grid. The PV system is also used to cover part of the building electricity demand. The main components of this system are the PV module and inverter with the configuration as shown in Figure 6-11. Each apartment is mainly consisting of 3 PV Modules (30 for all apartments) with 0.9 kWp (9 kWp for all apartments). The electric demand profile for building equipment and lighting is also included in the Polysun simulation software.

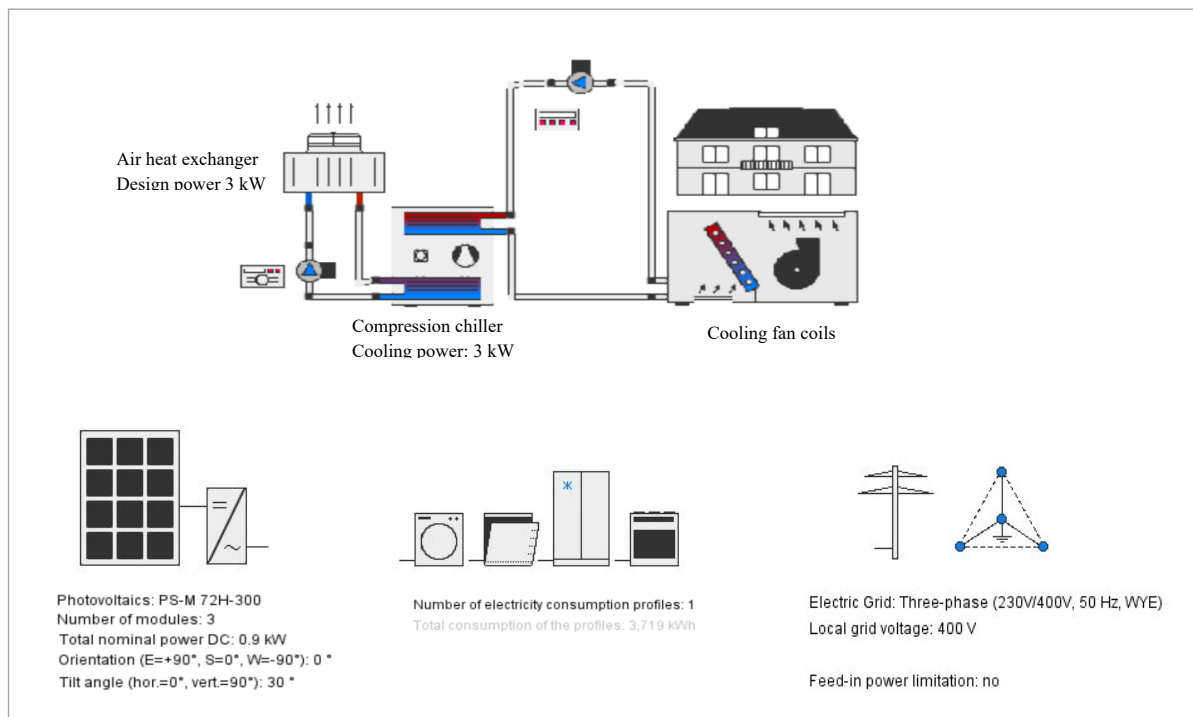


Figure 6-11: Grid-connected photovoltaic system powered conventional cooling system (system 1) and building electricity demand.

System 2: Centralized compression cooling system with solar photovoltaics

As illustrated in Figure 6-12. This cooling system consists of a compression chiller with a nominal cooling capacity of 10 kW and a COP of 4.36, a cooling tower (dry-cooler) to extract waste heat from the chiller as well as a cold-water storage tank which has a volume of 500 l.

The chiller starts to work when the temperature of the cold-water tank (layer 5th counting from the storage bottom) exceeds 10 °C and stops running if the indoor temperature is equal to the cooling setpoint temperature and the cold-water tank temperature is lower than 10 °C.

Regarding the photovoltaic system, it has the same components as the previous system (system 1), the difference here is regarding the electricity demand of the cooling system.

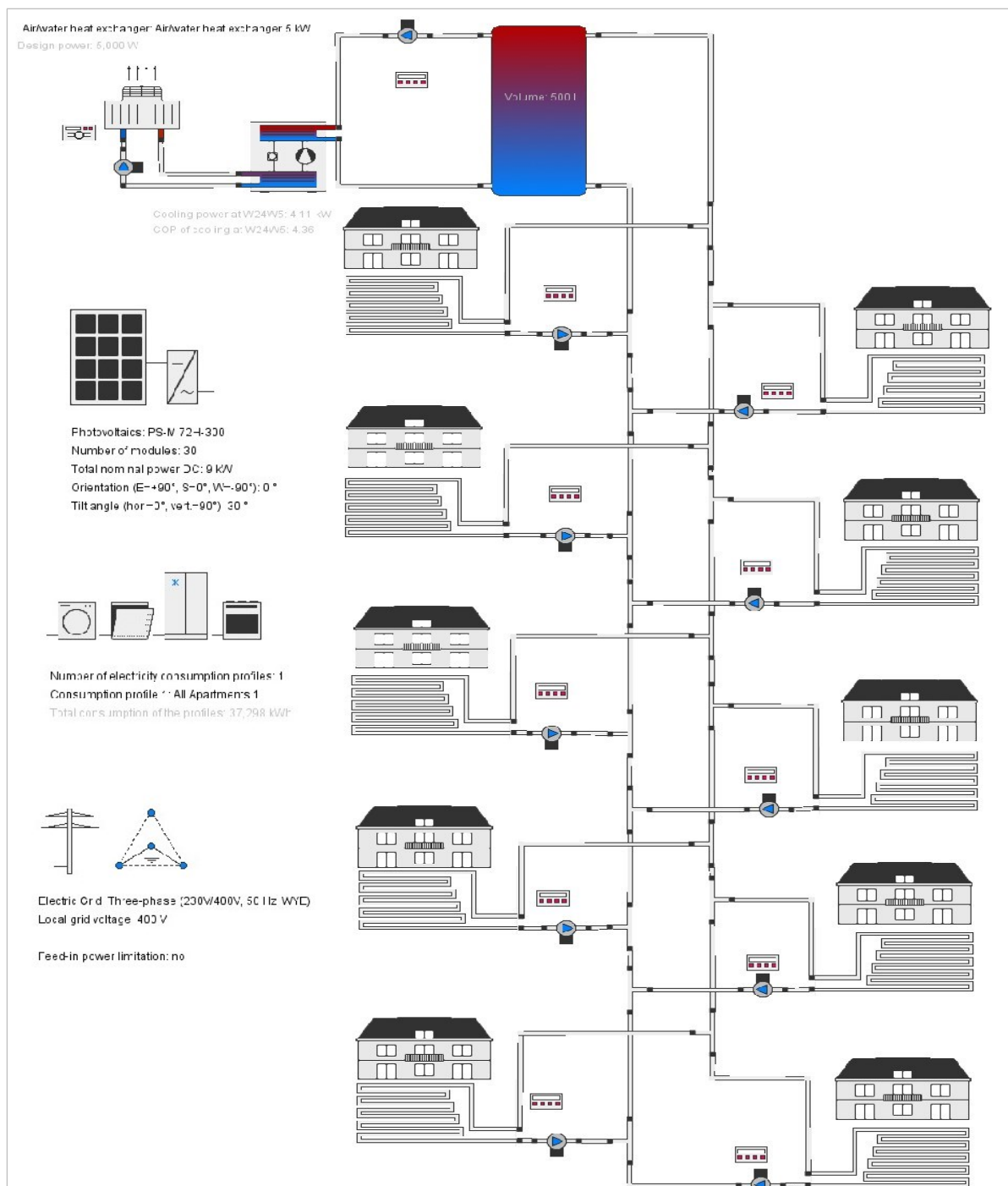


Figure 6-12: Grid-connected photovoltaic system powered centralized compression cooling system (system 2) and building electricity demand.

6.4 Results and discussion

In this section, the Polysun simulation results along with the discussion of the proposed systems are presented. A yearly simulation is carried out based on an optimum system specification described in the previous section.

• Solar heating systems

An overview of the annual energy results obtained from Polysun simulation software for the solar heating systems is presented in Table 6-1.

In order to compare the different heating systems with the reference system, all the energy demand has been converted into primary energy, the conversion factor of electricity to primary energy is 2.71 and the factor of oil to primary energy is 1.1, as described under the methodology chapter (Chapter 4). Table 6-2 presents the primary energy demands of the system, primary energy savings due to the solar thermal collectors, and the primary energy saving in comparison to the reference conventional system (system 0).

Table 6-1: Annual overview of the solar thermal systems results obtained from Polysun simulation software

System overview	Unit	System 0	System 1	System 2	System 3
Total fuel and/or electricity demand of the system	kWh/year kWh/m ² /year	93,000 69	32,180 24	36,190 27	22,230 17
Total electricity demand	kWh/year kWh/m ² /year	1,750 1.3	7,160 5	1,940 1.3	290 0.2
Total oil demand	kWh/year kWh/m ² /year	91,220 77	25,000 19	34,250 25.4	25,000 19
Overview of solar thermal energy (annual values)					
	Unit	System0	System1	System 2	System 3
Collector area	m ²		40	60	60
Solar fraction total	%			70	71
Solar fraction hot water	%		88	76	83
Solar fraction building	%		0	35	33
Total annual field yield	kWh/year		39,630	57,580	49,380
Collector field yield relating to the aperture area	kWh/m ² /year		1,101	1,067	915

Table 6-2: Annual overview of the primary energy of heating systems system.

Parameter	Unit	System 0	System 1	System 2	System 3
Primary energy demand	kWh/year kWh/m ² /year	1,051,000 78	46,930 35	44,900 33	24,452 18
Primary energy saving due to solar thermal collectors	kWh/year kWh/m ² /year	-	43,590 32	63,340 47	54,320 40
Primary energy saving in comparison to the system 0	kWh/year kWh/m ² /year	-	58,160 43	60,200 45	75,880 56
Relative primary energy savings in comparison to the system 0	(%)	-	55	57	77

The energy demand of the studied systems is different from each other, although they have the same profiles of energy demand (as described in the previous section), with 55,415 kWh/year (41 kWh/m²/year) annual space and water heating energy demand. System 3 (centralized solar combi-heating system) has the lowest energy demand follow it by system 2 (decentralized solar combi-heating system), system1 (thermosiphon solar water system and conventional space heating system), and system 0 (conventional heating system), respectively.

As illustrated in Table 6-2 and Figure 6-13, system 3 (centralized combi-solar thermal system) consumed less energy than the other systems with 22,230 kWh/year (17 kWh/m²/year), corresponding to 24,450 kWh/year (18 kWh/m²/year) primary energy. The energy-saving rate is 77% compared to the reference conventional heating system (system 0).

From the simulation results, it's important to note that a solar fraction of 71% of system 3 can be achieved, whereas it's only 33% of space heating and 83% of DHW production. It can also be seen from the results, that the energy demand of the centralized solar combi-heating system (system 2) is 20% lower than the decentralized solar combi-heating system (system 1). System 1 (thermosiphon solar water system and conventional space heating system) can save 55% primary energy demand in comparison to the reference (system 0). Although the installed solar thermal collectors' area (40 m²) is lower than system 2 and system 3 (60 m²). The annual collector field yield relating to aperture area for system 1, system 2 and system 3 is 1, 100, 1,066 and 914 kWh/m²/year, respectively. Accordingly, the thermosiphon solar water heating system (system 1) can have potential, especially if the economic aspects are considered, however, in this research only the energy aspects of the proposed systems are considered. The economic aspects can be considered in further research.

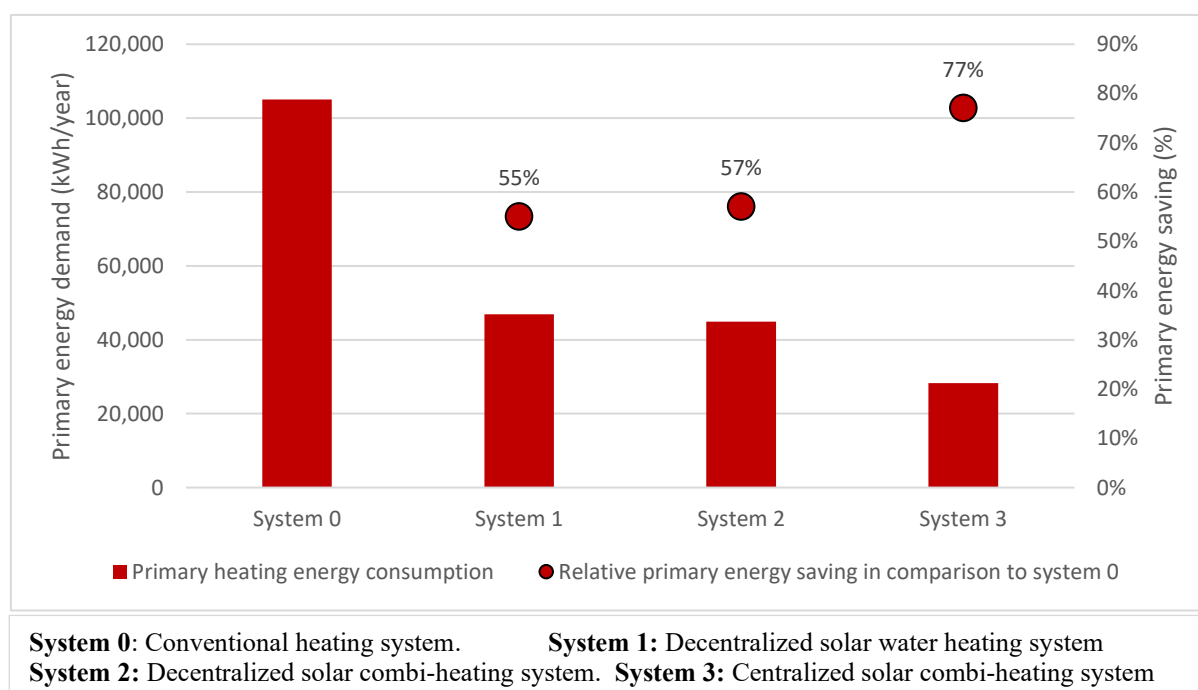


Figure 6-13: The annual primary energy demand for different heating systems (water + space heating), and the primary energy saving in comparison to the system 0, installed for multi-family building with 1,350 m² total heated area in Amman, Jordan.

Based on the above discussion, the centralized solar combi-heating system (system 3) is selected in this research. The monthly energy results of this system are presented in Figure 6-14 and Figure 6-15.

As can be seen from Figure 6-14, the simulated monthly solar fractions are significantly higher during periods of high solar thermal energy and lower building energy demand (no heating demand). from May to October the total solar fraction is 100% and there is no need for auxiliary heating, and this solar fraction is mainly for DHW production, as there is no need for space heating between April and November. Furthermore, the estimated monthly solar fraction in December, January, and February are 40%, 29%, and 37% respectively. Thus, the consumed energy of the system is high during these months to cover the complete heating load of the building, see Figure 6-15.

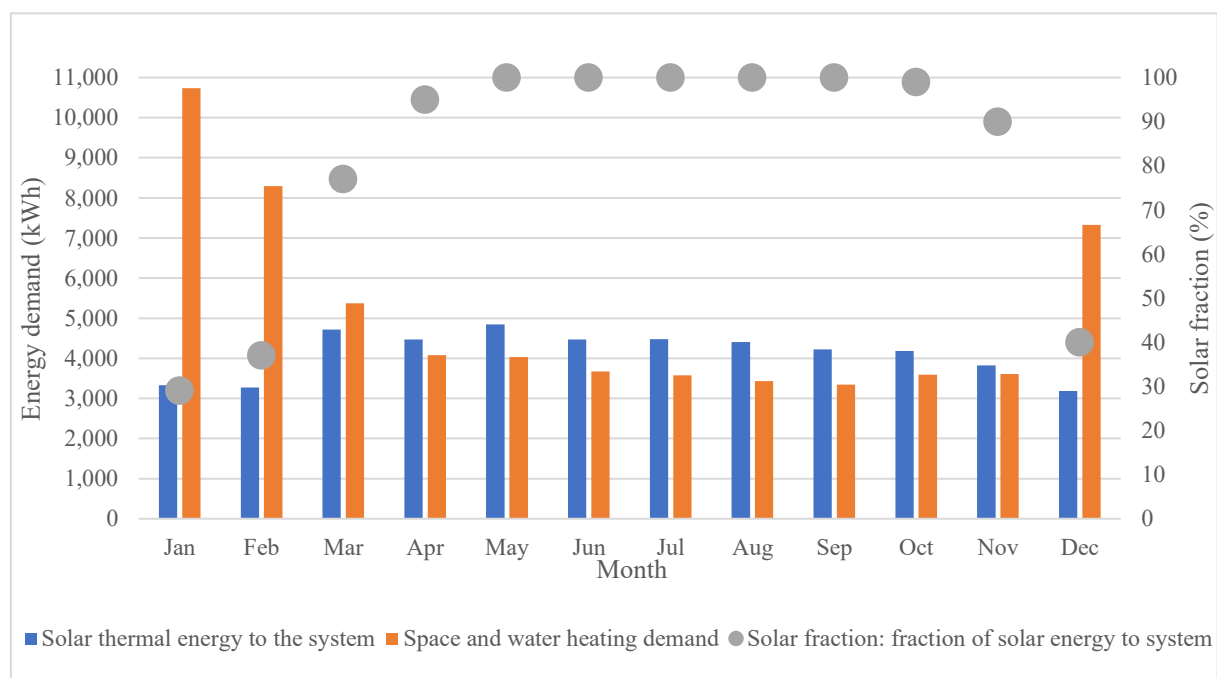


Figure 6-14: The monthly heating demand (water + space heating) for 1,350 m² total heated area in apartment building in Amman, Jordan, and the monthly solar thermal energy yield (for 60 m² solar collector), solar fraction of the centralized solar combi-heating system (system 3) estimated by Polysun simulation software.

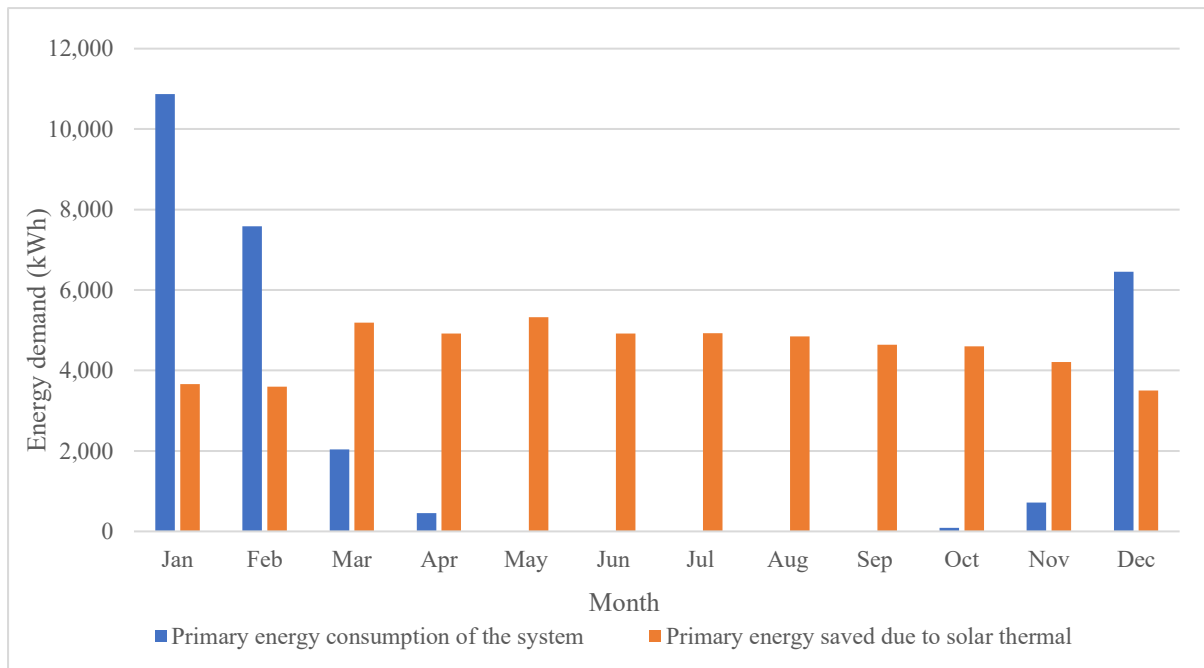


Figure 6-15: Monthly primary energy saved by solar thermal energy and primary energy demand of the centralized solar combi-heating system for a residential building with 1,350 m² heated area in Amman, Jordan.

• Solar photovoltaic systems

An overview of the annual energy results obtained from the Polysun simulation software for the proposed two grid-connected PV systems and the conventional system are presented in Table 6-3. The system energy demand and PV production have been converted to the primary energy values using a conversion factor of 2.71 for electricity, see Table 6-4.

The building electricity demand profile for lighting and equipment is the same for all the systems, with 37,300 kWh/year (27.5 kWh/m²/year) electricity demand. While, the electricity demand of the cooling system 2 is different than conventional cooling system 0 and system1, although they have the same cooling demand profile.

System 2 (centralized compression cooling system with photovoltaic) has the lowest energy demand follow it by system 1 (conventional cooling system with photovoltaic), and system 0 (conventional cooling system), respectively. The energy-saving rate of system 2 in comparison to the conventional cooling system without photovoltaic (system 0) is around 80%.

It can also be seen from the results, that the annual energy production of the photovoltaics in system1 and system 2 is 16,940 kWh/year (1,882 kWh/kWp), however, system 2 consumed less electricity than cooling system 1. Therefore, the photovoltaic can cover 43% in system 2 and 31% in system1 of the total electricity demand for building cooling and equipment. It is important to note that 60% of the solar photovoltaic electricity is directly consumed by the building, while the rest is sold to the grid.

Based on the above discussion, the centralized compression chiller with photovoltaic (system 2) is selected in this research. The monthly energy results of this system are presented in Figure 6-14 and Figure 6-15.

Table 6-3: Annual overview of the studied solar photovoltaic systems results obtained from Polysun simulation software.

System overview (annual values)					
	Symbol	Unit	System 0	System 1	System 2
Total electricity demand (Ebul+Ecol)-(E _{pv})	Etot	kWh/year kWh/m ² /year	47,870 35	30,930 23	22,650 17
Electricity demand for the building (equipment and lighting)	Ebul	kWh/year kWh/m ² /year	37,300 27.6		
Total electricity demand of the cooling system	Eco	kW/year kWh/m ² /year	10,870 12.5	10,870 12.5	2,300 7.6
Overview solar photovoltaic system (annual values)					
		Unit	System0	System1	System 2
Total gross area		m ²		58.5	58.5
Total nominal power		kWp		9	9
Performance ratio		%		84	84
Specific annual yield		kWh/kWp		1,880	1,880
Energy production AC		kWh/year		16,940	16,940
Self-consumption		kWh/year		11,421	13,270
To the grid		kWh/year		5,745	3,670
Solar fraction (to the grid+ self-consumption)		%		31	43
Degree of self-sufficiency		%		27.5	28

Table 6-4: Annual overview of the primary energy of the studied solar photovoltaic systems.

Parameter	Unit	System 0	System 1	System 2
Net primary electricity of building (consumption-PV production)	kWh/year kWh/m ² /year	129,700 95	83,820 75	61,380 45
Relative net primary saving in comparison to the system 0 including saving due to cooling system improvement + photovoltaic production	%	-	39	50
Primary energy demand for cooling system	kWh/year kWh/m ² /year	29.400 21.7	29,400 21.7	6,230 4.6

As illustrated in Figure 6-16, the monthly PV electricity production is less than the building electricity demand during all the months. However, the solar fraction is higher during the summer, where the solar radiation is high, as the estimated monthly solar fraction in June, July and August is around 47%, about 31% is consumed directly by the building and 15% is sold to the grid. While, in winter, the estimated monthly solar fraction in December, January, and February is 32%, 33%, and 37%, respectively. Thus, the consumed primary energy of the system in the winter is higher than in summer, see Figure 6-17.

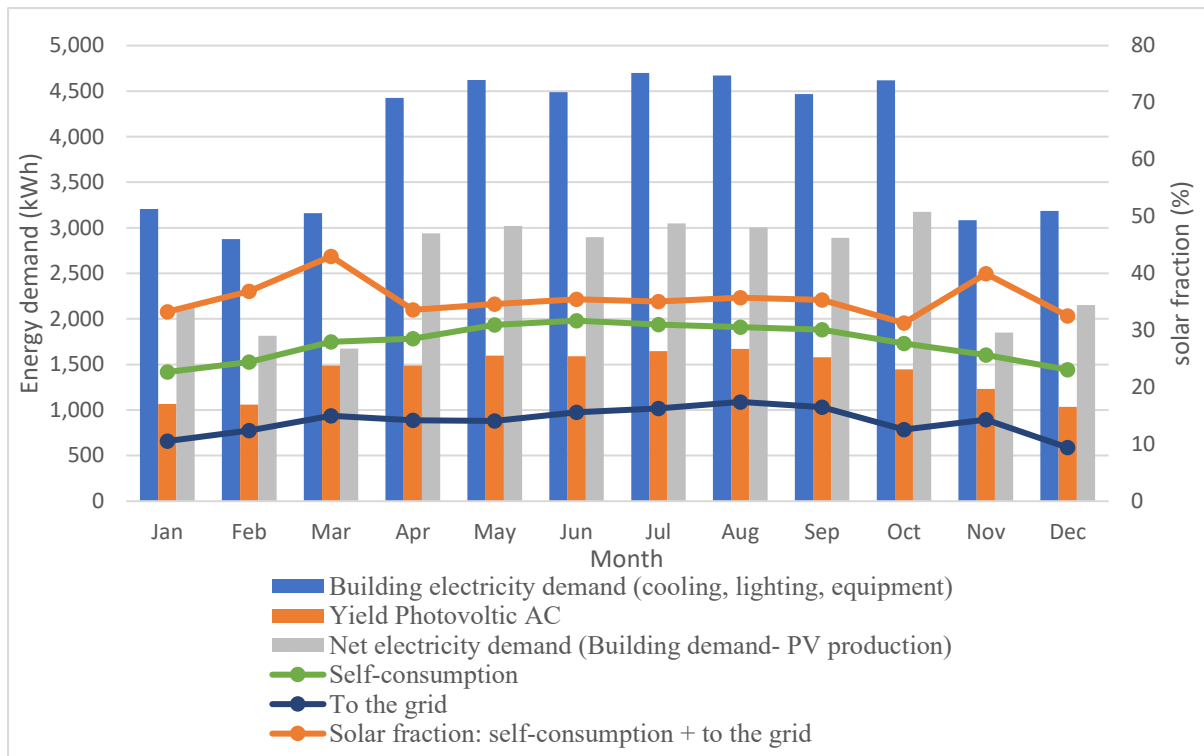


Figure 6-16: The monthly electricity demand (equipment and lighting + cooling) for 1,350 m² total heated area in residential building in Amman, Jordan, and the monthly solar photovoltaic energy yield (for 58.5 m² solar photovoltaic), solar fraction of the photovoltaic system with centralized compression chiller system 2, estimated by Polysun simulation software.

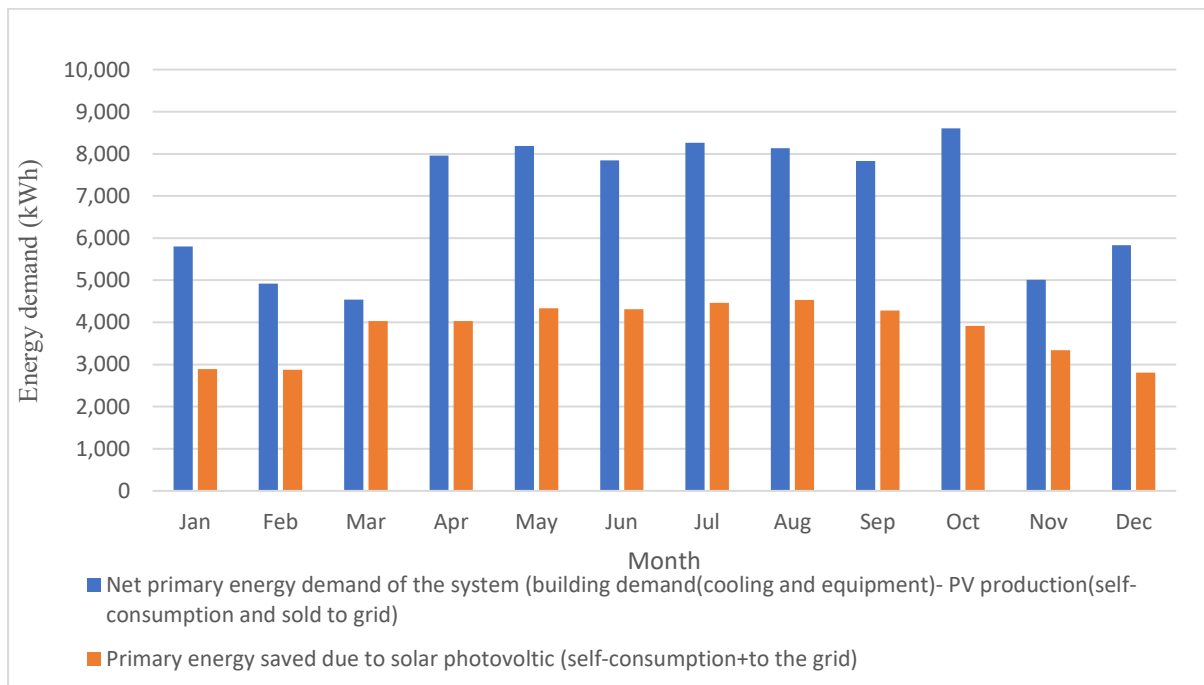


Figure 6-17: Monthly primary energy saved by solar photovoltaic energy and net primary energy demand of the residential building with 1,350 m² heated area in Amman, Jordan.

Also, the building hourly electricity demand (including equipment, lighting, and electricity for cooling system 2) and electricity production of the photovoltaic is presented here, which is helpful to evaluate the need for the battery storage in the next section. The hourly results are presented for two days with the most overproduction days in summer (11th of July) and in winter (11th of January). The results for the two selected days are presented in Figure 6-19 and Figure 6-18. The areas A and B are the total net electricity demand and generation, respectively. The overlapping part in area C is the PV power that is utilized directly within the building, indicated to self-consumption.

It can be noticed that there are two peaks in the hourly electricity demand of the building. The first peak occurs in the morning around 6:00, and the second peak occurs in the evening around 21:00, while during midday the electricity demand is low, as the apartments are empty around midday, with the inhabitants at work or school. On the other hand, the peak energy production of solar modules occurs around midday, which resulted in daily PV overproduction with about 21,700 W and 18,000 W in summer and winter day, respectively.

During off-peak demand hours, the excess PV generation is sold to the grid (as described in Chapter 2.5). Another possibility is to store the excess PV energy in the battery storage, and use it later during the peak demand, in the next section the potential of battery installation will be evaluated using the selected system (system 2) as reference.

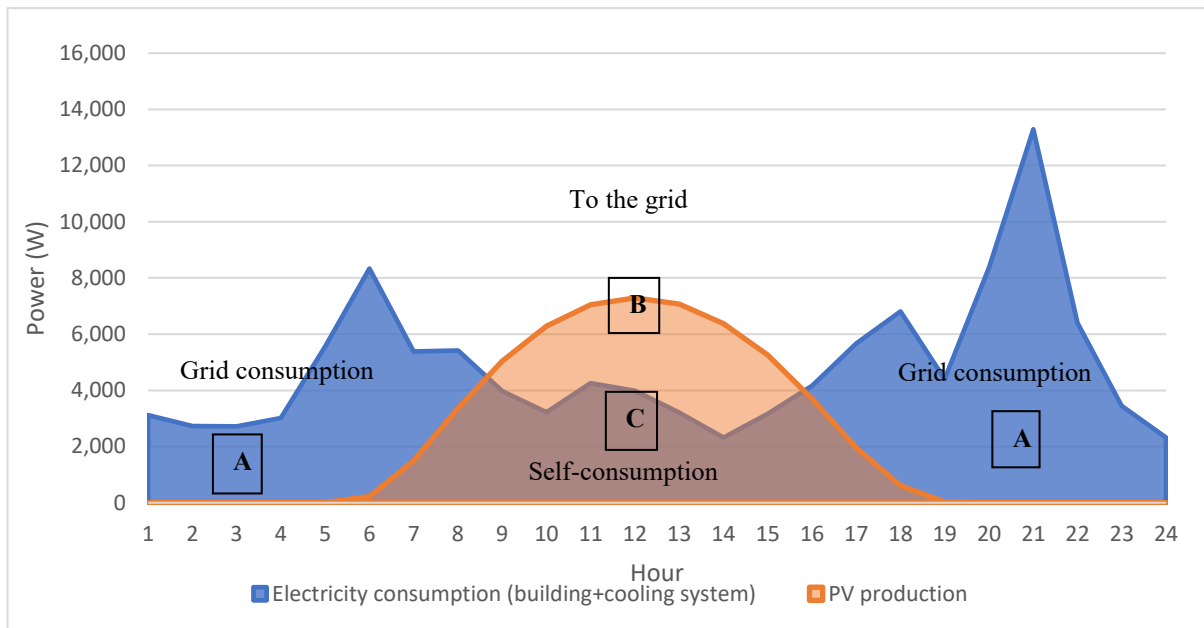


Figure 6-18: Hourly PV production and electricity consumption profiles in 11th of July of multi-family building in Amman, Jordan with 9 kW photovoltaics system and 1,350 m² heated area. results from Polysun and IDA ICE simulation software.

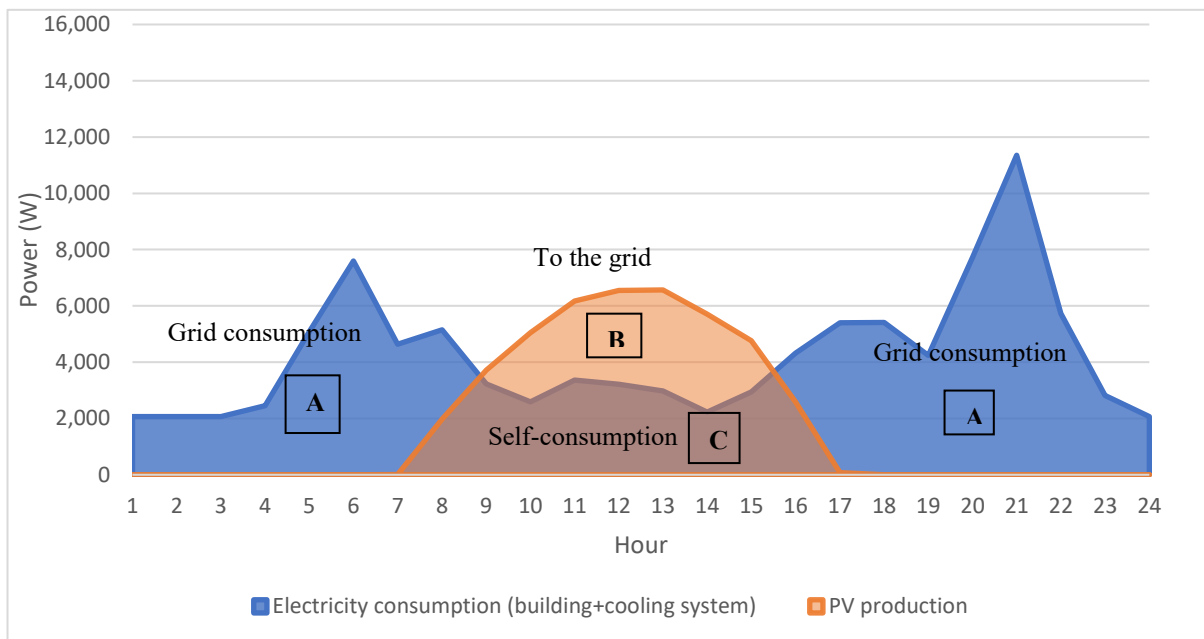


Figure 6-19: Hourly PV production and electricity consumption profiles in 11th of July of multi-family building in Amman, Jordan with 9 kW photovoltaics system and 1,350 m² heated area. results from Polysun and IDA ICE simulation software.

6.5 Potential of battery installation

In this section, the energy and economic feasibility of the battery installation to the PV system is studied and compared to the grid-connected system. The system set up of a PV air conditioning with battery is similar to the system 2, but it additionally has a storage (battery) system and a charge controller.

As can be seen in Figure 6-19 and Figure 6-18, during the early morning hours there is no PV generation; as a result, the electricity demand is entirely bought from the grid. When the photovoltaic modules generate more power, less electricity from the grid is needed. In the middle of the day, the PV power output is at its maximum; an excess of power is sold to the grid. When the day ends, once again the household demand is met fully by the energy provided from the utility grid. However, in the case of battery storage installation, the excess energy is stored in the battery to use it when there is no enough PV generation to cover the electricity demand, and the rest of the needed electricity is imported from the grid to cover the complete building electricity demand.

The battery is designed based on the overproduction criteria taking into account the days of autonomy and the deep of discharge. In this case, the overproduction in the summer is higher than in winter. So, based on the difference between the PV energy production and the load demand for system 2, the size of the battery system has been calculated from the day with more overproduction. From the results obtained in the previous section, see Figure 6-19, the overproduction in summer day is 21,644 W.

Regarding the autonomy, as the average sunshine duration is more than 300 days and 3,602 hours per year in Amman, Jordan (as presented in Chapter 0), the autonomy criteria is considered to be one day. A deep cycle battery is selected; this battery is designed to be repeatedly discharged by 80% of their capacity so they are a good choice for the solar electric system. This means that the battery/batteries with 26 kWh capacity, can store the maximum amount of energy without dumping it to the grid.

To be sure that the battery with 26 kWh capacity is not oversized, several simulations are done in Polysun simulation software. The selected battery type from the Polysun library is a lithium-ion battery with 80% deep of discharge. Figure 6-20 shows the relation between the capacity of the battery and not stored energy (energy to the grid), and the percentage of the stored energy in relation to the photovoltaic overproduction energy. It can be seen that as bigger is the capacity of the battery/batteries, as lower is the energy not stored, however, there is a point where despite increasing the size of the batteries, the energy unused does not decrease fast. As during the months with less production, this ability is not going to be covered at all, and the battery does not compensate for the investment of extra capacity. So based on this curve, 18 kWh capacity (3 batteries, each 6 kWh) is selected, around 97% (5,573 kWh/year) of the photovoltaics overproduction (5,745 kWh/year) can be stored in the batteries.

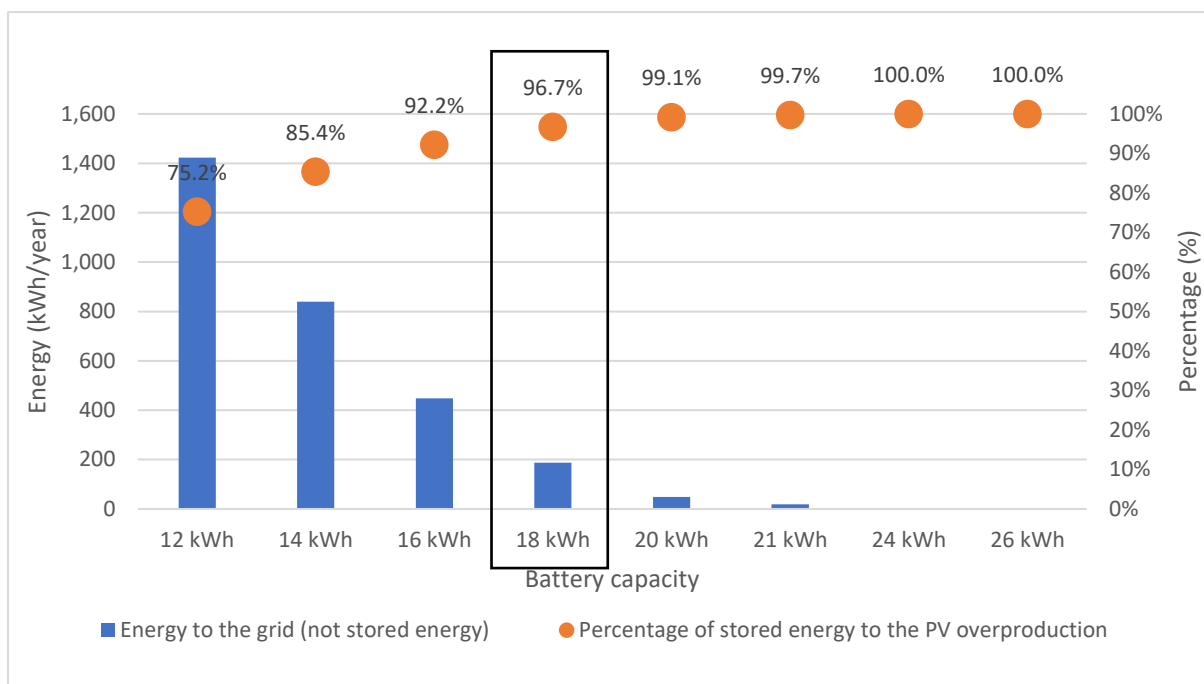


Figure 6-20: The relation between battery capacity and not stored energy (energy to the grid) of 9 kWp photovoltaic system with 5,745 kWh/year overproduction, results obtained from Polysun simulation software.

Table 6-5 shows, the overview energy simulation results for system 2 with and without battery installation, also the estimated energy transmission losses of the sold electricity to the grid. As mentioned before, the annual yield of 9 kWp photovoltaics is 16,940 kWh/year, 11,195 kWh/year is directly consumed by the building, while 5,745 kWh/year is PV overproduction energy, which can be sold to the grid or stored in the batteries. The total electricity sold to the grid without battery installation, after considering the grid losses is 5,613 kWh/year, while in the case of battery installation is only 168 kWh/year (considering grid transmission losses) is sold to the grid, and 5,573 kWh/year is charged to the battery, however, 3,482 kWh/year discharged electricity from the battery. It can be seen, that the losses energy in the case of battery installation is higher than in the case of only grid-connected.

Table 6-5: Overview annual simulation results for 9 kWp photovoltaic system with and without battery, installed in an improved apartment building with 1,350 m² heated area in Amman, Jordan.

	Unit	Grid-connected system	Battery storage with grid-connected
Yield photovoltaic	kWh/year	16,940	
Direct consumption		11,195	
To external grid		5,745	172
From the external grid		28,660	25,180
Battery charge			5,575
Battery discharging			3,480
Grid network losses/ battery losses		132 (2.3%, based on Chapter 0)	4 2,090

Economic analysis is considered here to give an idea if stored the overproduction photovoltaic energy in the battery is more feasibly than sold it to the grid and does compensate for the extra investment of the battery.

The Jordanian electricity system pricing is considered as described in Chapter 0, including the cost of buying electricity from the utility grid due to the PV system does not produce enough energy and the savings earned due to sell overproduction of energy to the grid as well as the saved electricity cost after using the battery instead of the grid. Also, the price of the batteries of a PV system has been considered, however, the rest of the PV installation has not taken into consideration in this part of the research, as it equal in both cases (detail photovoltaics system economic analysis is in Chapter 8.4).

As presented in Chapter 0, the monthly electricity tariff in Jordan is based on the monthly electricity demand, this means that the economic feasibility result is different from the building with different electricity demand. In this research, the net electricity demand of the improved building design in Amman, Jordan in all months after considering the saved electricity due to the direct-consumption of the electricity produced by the PV system (system 2) is between 1,500-2,500 kWh/month for all apartments (10 apartments), see Figure 6-16. Accordingly, the current electricity tariff of the studied apartment building is 0.088 €/kWh. Regarding selling the electricity to the grid, the current electricity selling tariffs to the grid from photovoltaic is 0.15 €/kWh, however, the cost of using the grid-network is 0.056 €/kWh (see Table 2-2 and Table 2-3, Chapter 0), resulting in net electricity selling tariffs of 0.094 €/kWh.

The economic overview result of the current annual electricity cost for the grid-connected photovoltaic without battery case and with battery case is presented in Table 6-6. As can be seen, the net electricity cost when the battery is installed is higher than without a battery by 206 €/year. This is because the cost per kWh of selling the electricity to the grid (under the second block tariff) is higher than buying it from the grid.

Table 6-6: Annual electricity cost of the grid-connected photovoltaic without battery case and with battery case, under current electricity tariff for a residential building in Amman, Jordan.

The grid-connected photovoltaic system, without battery			
	Energy (kWh/year)	Cost	
		€/kWh	€/year
Sold to the grid	5,613 considering the losses	0.094 (selling cost (0.15)- cost of using network (0.056))	527.6
Purchased from grid	28,660	0.088 (second block)	2,522
Net cost (€/year)	1994 (0.07 €/kWh) (purchased from the external grid - sold to the grid)		
Battery storage with the grid-connected photovoltaic system			
	Energy (kWh/year)	Cost	
		€/kWh	€/year
Sold to the grid	168	0.094	16
Purchased from grid	25,178	0.088	2,216
Net cost (€/year)	2,200 (0.087 €/kWh)		

Based on the above results, under the current situation, the battery installation for the studied case is not beneficial, however, the electricity tariff in Jordan is estimated to increase by 5% annually (NEPCO, 2016; MEMR, 2017, 2018), while, the battery cost is estimated to decrease, for example, the lithium-ion battery is estimated to decrease by 50% by 2025, by 75% by 2035 compared to 2018 (Vartianinen, 2018), therefore the life cycle cost analysis is studied.

The battery cost is different depending on the capacity, chemical composite of battery, and its life cycle, etc. (Zerohomebill, 2019). The average battery lithium-ion battery cost with a capacity of 6 kWh in 2018 is 3,000 € (Vartianinen, 2018; Zerohomebill, 2019), accordingly, the estimated initial cost of the 3 batteries (each 6 kWh) is 9,000 €.

Regarding the battery lifetime, different factor can affect the battery life, such as the battery cycle; the more cycles a solar battery can provide, the longer time it can perform normally (Zerohomebill, 2019) taking 80% deep of discharge can result in 7-8 years lifetime of the selected batteries (El Shenawy, Hegazy and Abdellatef, 2017).

Since battery life is considered 8 years, it must be replaced three times in the system's lifetime (25 years). The annual inflation rate in batteries price is considered to be 4% and the market discount rate is 8% (El Shenawy, Hegazy and Abdellatef, 2017); the inflation rate represents the escalation trend in the costs over the all system life, while the discount rate represents the decrease in the components cost with future mass production (El Shenawy, Hegazy and Abdellatef, 2017).

The details life cycle cost analysis has been done in a spreadsheet, Table 6-7 illustrates the net electricity cost saving due to battery installation in comparison to the same system without battery, it is also showing the estimated battery price and the estimated payback time. For more details see Appendix C.

Based on the results of life cycle analysis the total electricity cost over 25 years of the grid-connected system without battery is 122,233 € and in the case of battery installation is 102,234 € resulting in life cycle cost saving of 19,999 €. However, the life cycle cost of the batteries is 16,305 € resulting in a net cost saving of 3,694 € and 23 years payback time. It must be mentioned that battery efficiency degradation has not been considered, which will also result in the cost benefits decreasing. It can be also seen from Table 6-7, that the battery can be more beneficial in the future, after 15 years, based on the mentioned assumptions about the continuous decrease of battery price and increase in electricity cost.

Based on the above discussion the grid-connected system without a battery is chosen in this research.

Table 6-7: life cycle electricity cost benefits and payback time for 18 kWh battery installation to the 9 kWp grid-connected photovoltaic system in a residential building with 1,350 m² heated area in Amman, Jordan.

Grid-connected system with battery saving in comparison to the grid-connected system without battery				
PAYBACK reached in years where cells turn GREEN in accumulative total				
Note	Net electricity cost saving of Battery installation= Net electricity cost grid and battery system - Net electricity cost grid	Yearly discount in battery price	The assumed annual rate of inflation	Total battery cost= Estimated battery cost with inflation and discount in the 1 st year + after 8 the year + after 16 year
		8%	4%	
Year	Net electricity cost saving of battery installation per year (€)	Accumulative total net electricity cost-saving (€)	Estimated battery cost (€)	Total battery cost (€)
1	-101	-101	9,000	8,654
2	-57	-159	7,961	347 the accumulative saving
3	-10	-169	7,324	
4	41	-128	6,738	
5	96	-32	6,199	
6	157	125	5,703	
7	222	347	5,247	4,827
8	292	640	4,827	
9	369	1,009	4,441	
10	451	1,461	4,086	
11	540	2,001	3,759	
12	636	2,638	3,458	5,956 € the accumulative saving
13	740	3,378	3,181	
14	851	4,230	2,927	
15	972	5,202	2,693	
16	1,101	6,304	2,477	
17	1,241	7,545	2,279	17,640 the accumulative saving
18	1,391	8,936	2,097	
19	1,552	10,489	1,929	
20	1,726	12,216	1,774	
21	1,913	14,129	1,632	
22	2,114	16,243	1,502	
23	2,329	18,573	1,382	
24	2,561	21,134	1,271	
25	2,809	23,943	1,169	
Life cycle total	23,943			16,305 €

6.6 Summary

In this chapter the installation of solar thermal systems and photovoltaic systems on the roof of the improved residential building in Amman, Jordan has been evaluated using Polysun simulation software. The building includes 10 apartments with a total heated area of 1,350 m², the building energy demands have been obtained from IDA ICE simulation software. Different solar thermal heating systems to provide space and water heating, and photovoltaic systems to supply electricity to the building cooling system, equipment and lighting have been studied and compared in terms of the energy demand of the system and solar energy production. The battery installation to the photovoltaic system has been also investigated, moreover, the installation of solar thermal collectors on the roof with different tilt angles, azimuth, and installation area have been evaluated. The selected system configurations are presented in Figure 7-10. The typical arrangement for the photovoltaic modules and solar thermal collectors is considered in this part of research, the solar thermal collectors and photovoltaic modules are installed on the roof with about 60 m² total installed area, the tilt angle is 30° and all the collectors and modules are oriented toward the south, more arrangements will be investigated in the next chapter. The centralized solar thermal combi-heating system is selected to supply hot water and heat the space in winter. The results show that the net energy demand of the system is 22,230 kWh/year (17 kWh/m²/year), the total solar fraction is 70% whereas it's only 33% of space heating and 83% of DHW production. The annual field yield of the solar collectors is 49,380 kWh/year (915 kWh/m²/year). Regarding the photovoltaic and cooling system, a centralized compression cooling system is selected, as illustrated in Figure 7-10 b, the photovoltaic system supply electricity to the cooling system, equipment, and lighting. The net electricity demand of the building (including the cooling system, equipment, and lighting) is 22,650 kWh/year (17 kWh/m²/year). The annual energy production of the photovoltaics is 16,950 kWh/year and the specific annual yield is 1,880 kWh/kWp (280 kWh/m²/year), the solar photovoltaic cover around 42% of the building electricity need.

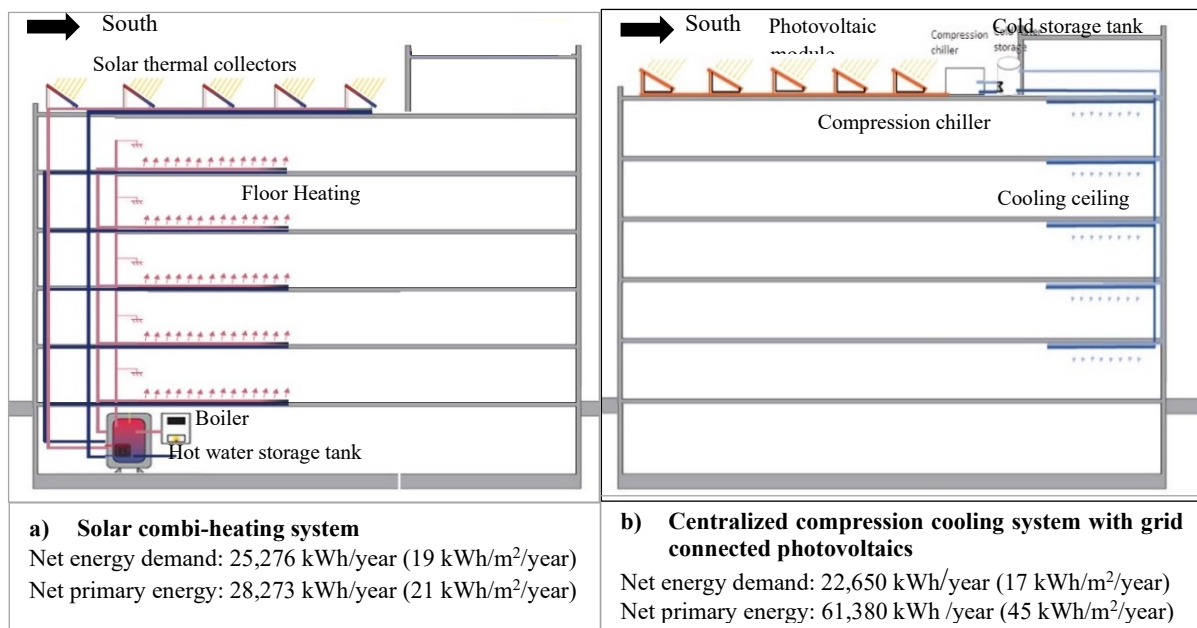


Figure 6-21: Simplified schematic of the selected energy systems for multi-family building in Amman, Jordan a) solar combi heating system b) centralized compression cooling system with grid-connected.

7 ST and PV roof and façade applications

7.1 Introduction

In this chapter, the potential of implementing PV and ST systems on the roof and facades of the new apartment building in Amman, Jordan is investigated. Firstly, the suitable surface areas for the ST and PV installation are determined based on incident solar irradiation on different surfaces, shading analysis and architectural suitable area for integration considering limitations due to the constructions, available surfaces area and use of the available surfaces for other purposes. Afterward, several arrangements of the solar thermal collectors and photovoltaic modules application on the roof and façade are proposed and investigated through varied cases. The resulting impact is analyzed through the estimation of the electricity yield with Polysun simulation software, considering the effect of rear ventilation and shading on the electricity production of the PV modules, and the results are compared to the demand amount that could be covered. Moreover, the impact of the facade PV cases on the energy demand for heating, cooling, lighting in the space have been estimated with simulation software IDA ICE 4.8.

All the simulation and analysis are carried out on a new improved apartment building in Amman, Jordan (based on Chapter 5), with an energy-efficient heating and cooling systems (with traditional solar roof arrangement) as presented in Chapter 6. This case is identified as the base case model, where all the investigated cases in this study are compared to its energy performance.

7.2 Assessment of the PV and ST potential area

In order to define the potential area for installation of the photovoltaic and solar thermal technologies into the facades and roof, it is important to analyze the received amount of solar incident by surfaces, in addition to the shading of surrounding buildings and the architectural available area of the building.

The incident solar radiation on the building surfaces and the building solar exposure analysis of the location of Amman, Jordan is performed with Autodesk Ecotect analysis 2011 simulation software. The building model geometry within the typical urban context is created in “SketchUp”, which is then imported into Ecotect. The hourly climatic data of Amman, Jordan selected is the same ones used for the building simulation in IDA ICE and Polysun simulation software.

Solar radiation analysis

General analysis of the solar radiation in Amman, Jordan has been presented in Chapter 0. In this part, the solar radiation is estimated firstly without considering the effect of the surrounding building, the reason for this is to estimate its actual full potential for solar energy generating. Further analysis is done to determine the exact solar radiation of the studied building within a typical neighborhood context in Amman, Jordan.

Figure 7-1 shows the available annual solar radiation in kWh/m²/year for tilted and vertical surfaces in different directions, and the percentage of annual radiation in comparison with the available global horizontal radiation (2,054 kWh/m²/year) in Amman, Jordan without considering the effect of shading. It is clear that the south 30° tilted surface received higher annual global solar radiation with 2,296 kWh/m²/year, it is also can be seen that the vertical surfaces received lower solar

radiation than the horizontal surface with about 33%, 40%, 43% and 75% in south, east, west and north directions, respectively. Based on this analysis, the south-facing solar technology has higher potential than other directions, without considering the shading from the surrounding building. Moreover, there is also a potential for east and west direction, especially when the south elevation is shaded from the surrounding building. It should be noted that the north direction has very low solar potential, so it is excluded.

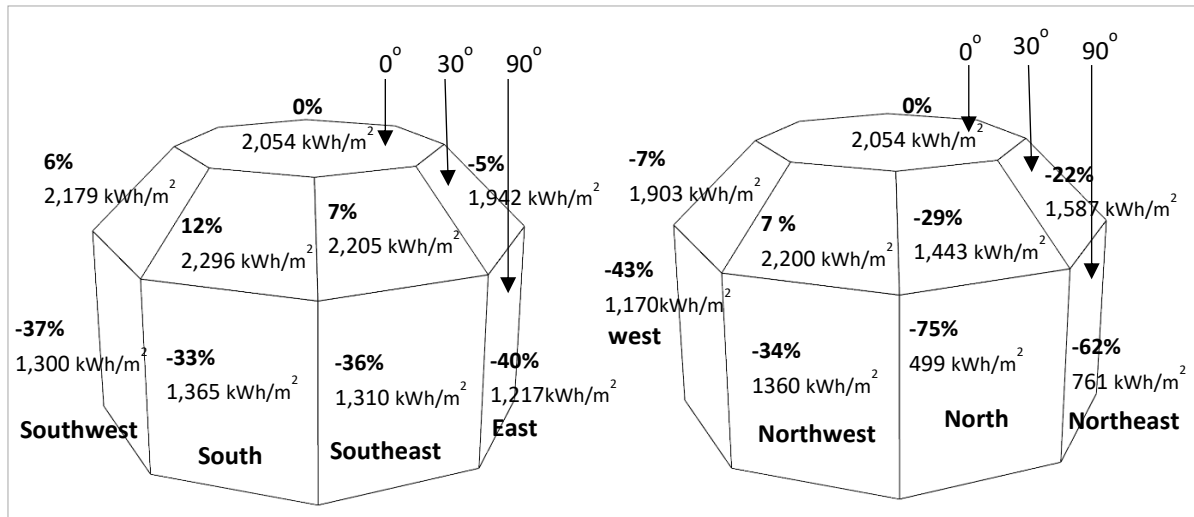


Figure 7-1: Influence of tilt and orientation on the percent of total solar radiation received annually in kWh/m² in Amman, Jordan. Source of weather data: Meteonorm 7.

Regarding the monthly solar radiation, as illustrated in Figure 7-2, the vertical and 60° tilted surfaces in the south direction received more solar radiation than the horizontal surface in winter months when heating is needed, as the sun angle is lower during the winter season. The east and west walls have good potential but only for limited hours as each receives a solar incident for half the day.

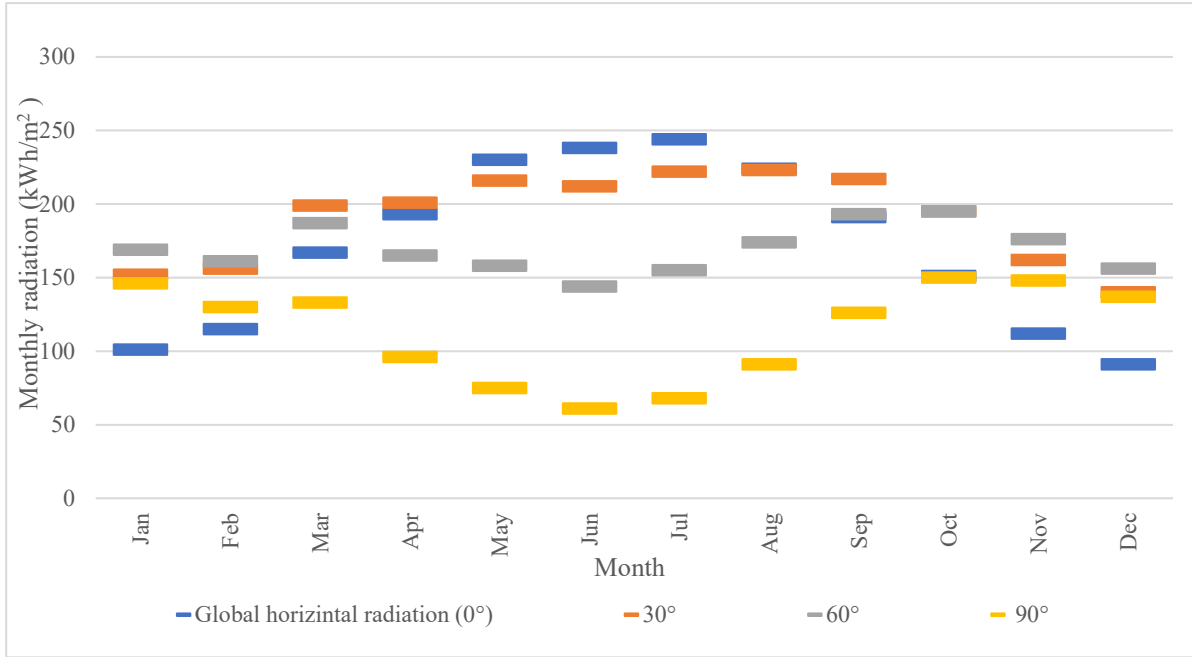


Figure 7-2: Monthly solar radiation available on the horizontal surface, and on 30°, 60° and 90° south exposed a tilted surface in Amman, Jordan. Source of weather data: “AMMAN JO” weather file from Meteonorm 7.

Figure 7-3 and Figure 7-4, illustrate the cumulative and hourly incident solar radiation on different surfaces for the studied building during different time periods, including the whole year, cooling period and heating period, considering the effect of surrounding building on the received solar radiation, for the location of Amman, Jordan.

The highest amount of solar irradiation is received by the roof with 2,050 kWh/m²/year which is the same as in the scenes without shading scenario (Figure 7-1), while the roof area around the staircase received less amount of solar radiation vary between 1,050-1,680 kWh/m²/year. Moreover, it can be observed that the vertical south surfaces, receive approximately 1,300 kWh/m²/year, except the lower part of the facade with around 1,050 kWh/m²/year as it is the most shaded area, which means a reduction of 22% in solar radiation potential. While the east and west elevation received the lowest amount of solar ranging from around 840 kWh/m²/year on the upper part to 210 kWh/m²/year on the lower part, this means the reduction of solar potential due to the obstruction is about 30% in the upper part and 80% in the lower part.

In the cooling period, the roof can receive monthly more than 1,060 kWh/m² as an average, and the peak hours are at noon. During the same period, the south wall does not receive much by comparison, and because of the high sun position. Despite this, the south wall in the heating period can receive around 840 kWh/m². This antithesis between the roof and south wall is clearly apparent in Figure 7-4. However, the south-oriented wall had significant potential and is considered the best of walls to integrate the PV array as it received solar radiation almost all day.

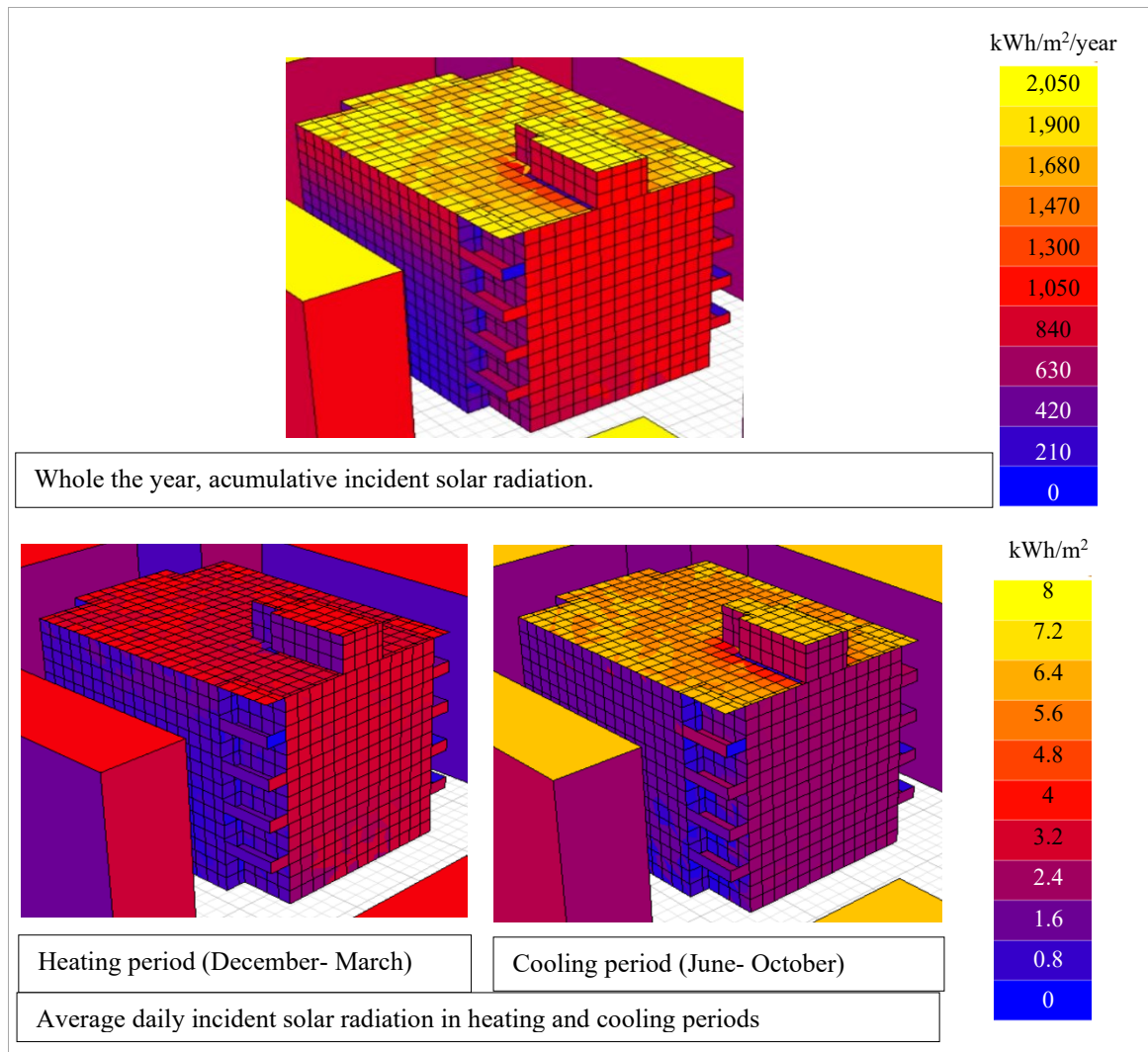


Figure 7-3: Accumulative incident solar radiation through all the year, and average daily incident radiation through heating and cooling periods, on studied multi-family building envelope. Source: Autodesk Ecotect analysis 2011 simulation software.

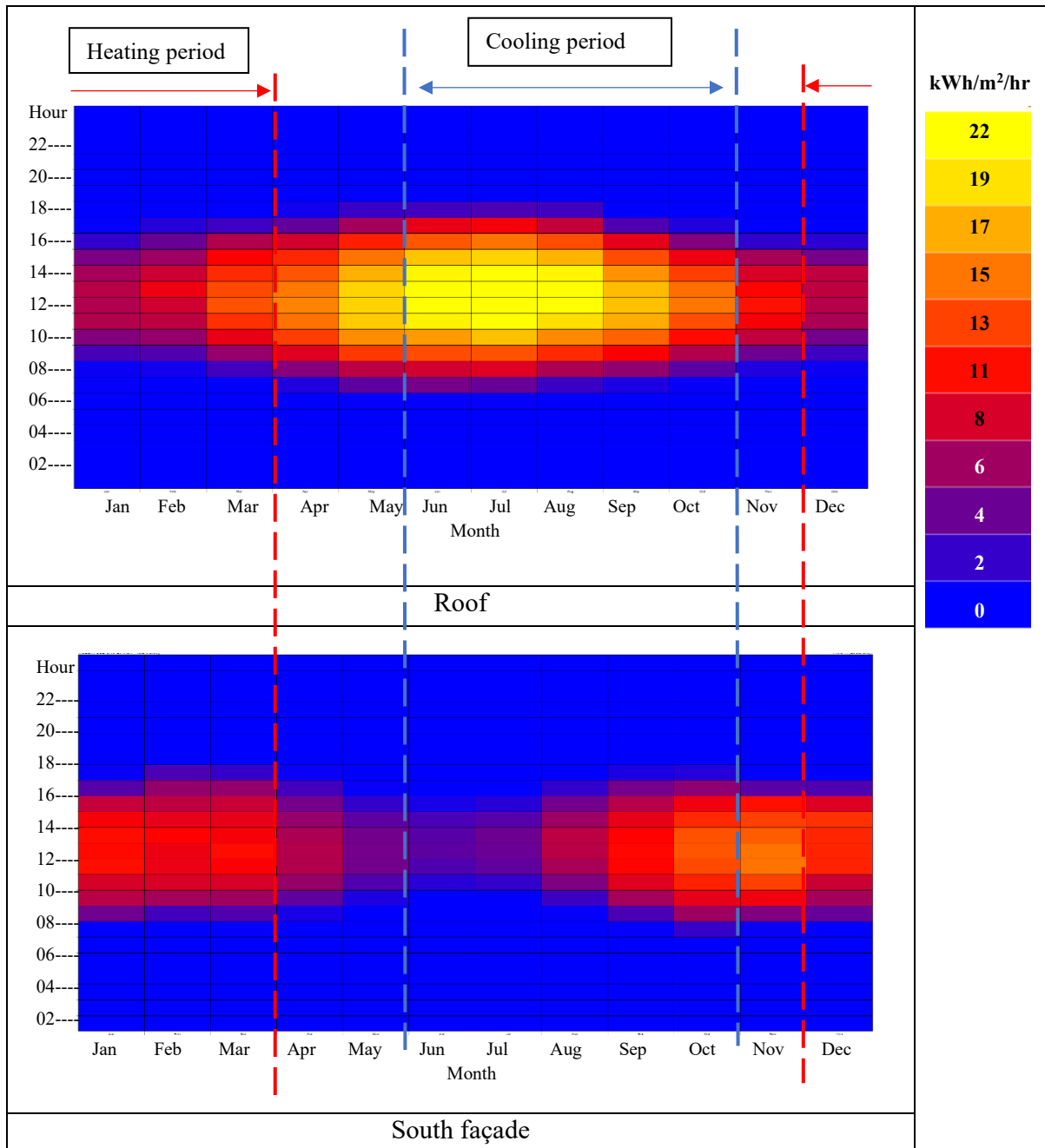


Figure 7-4: Hourly incident solar radiation received by the roof and south façade of the studied multi-family building in Amman, Jordan. Source: Autodesk Ecotect analysis 2011 simulation software.

In general, after analyzing the amount of solar incident radiation received by each of the studied building exposed surfaces, the roof is found as the best surface to receive solar radiation. Moreover, out of all façades, only the south façade is considered suitable for solar energy integration.

Solar exposure and overshadowing analysis

Figure 7-5 below, illustrates the solar exposure percentage of the roof and south façade, as these are the most envelope parts that have the potential for solar installation. It can be noticed that during the mid-day throughout the year the sun is very high, and the roof and south facade have no shading from the surrounding buildings. In the early morning and late afternoon, for a few hours, around 10% (ground floor) to 40% (ground and first floor) of the south facade is shaded, and part of the roof is shaded, especially during summer periods, from the building's own projections (elevator and staircase), see Figure 7-6.

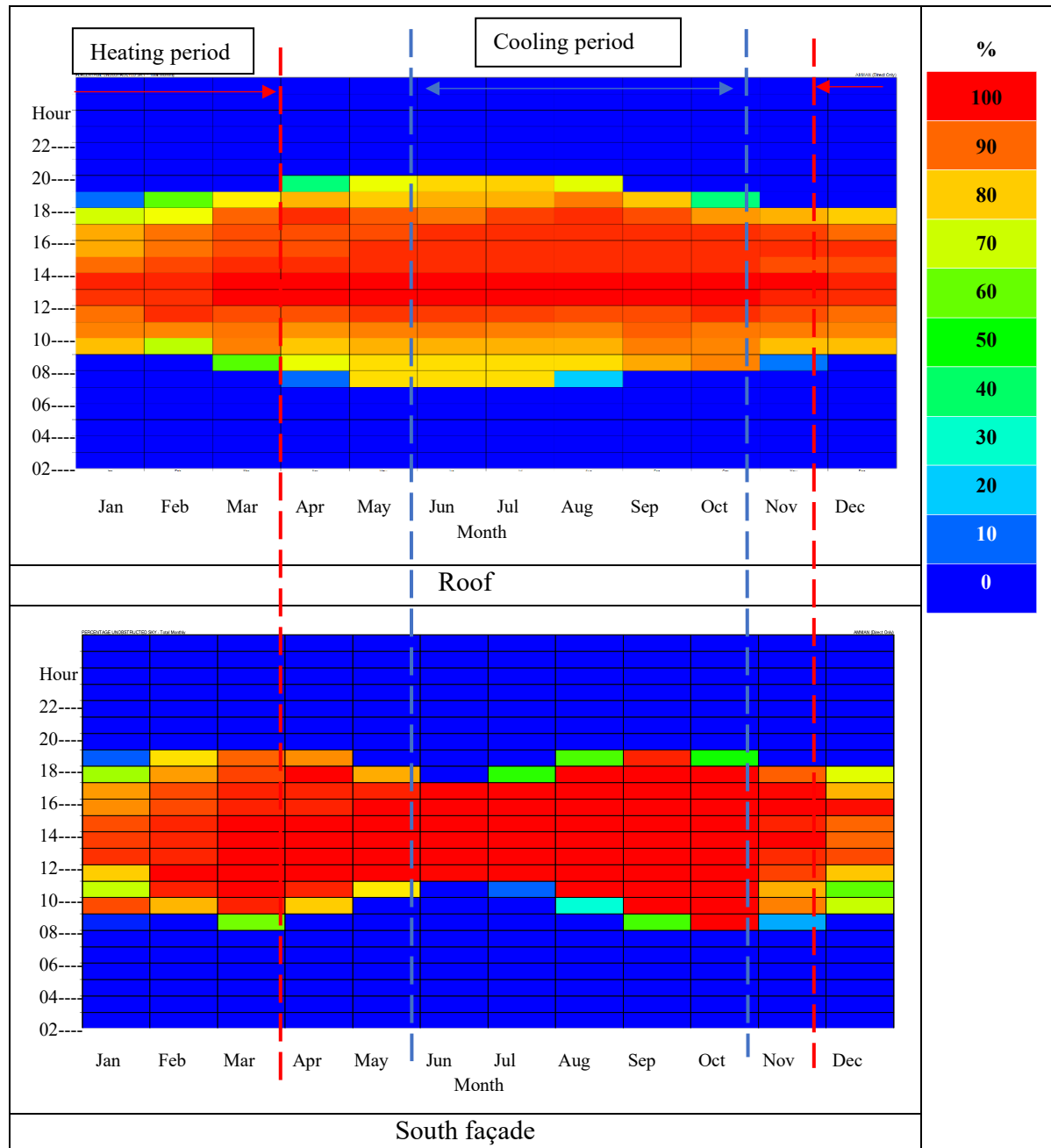


Figure 7-5: Hourly solar exposure analysis in percentage received by the roof and south façade of the studied multi-family building in Amman, Jordan. Source: Autodesk Ecotect analysis 2011 simulation software.

Shadow analysis is also done with IDA ICE, Figure 7-6 illustrates the shadow on the studied building during the different times for three days of the year: winter solstice (21st December), spring equinox (21st March) and summer solstice (21st June). The effect of partial shading in energy production will be estimated later.

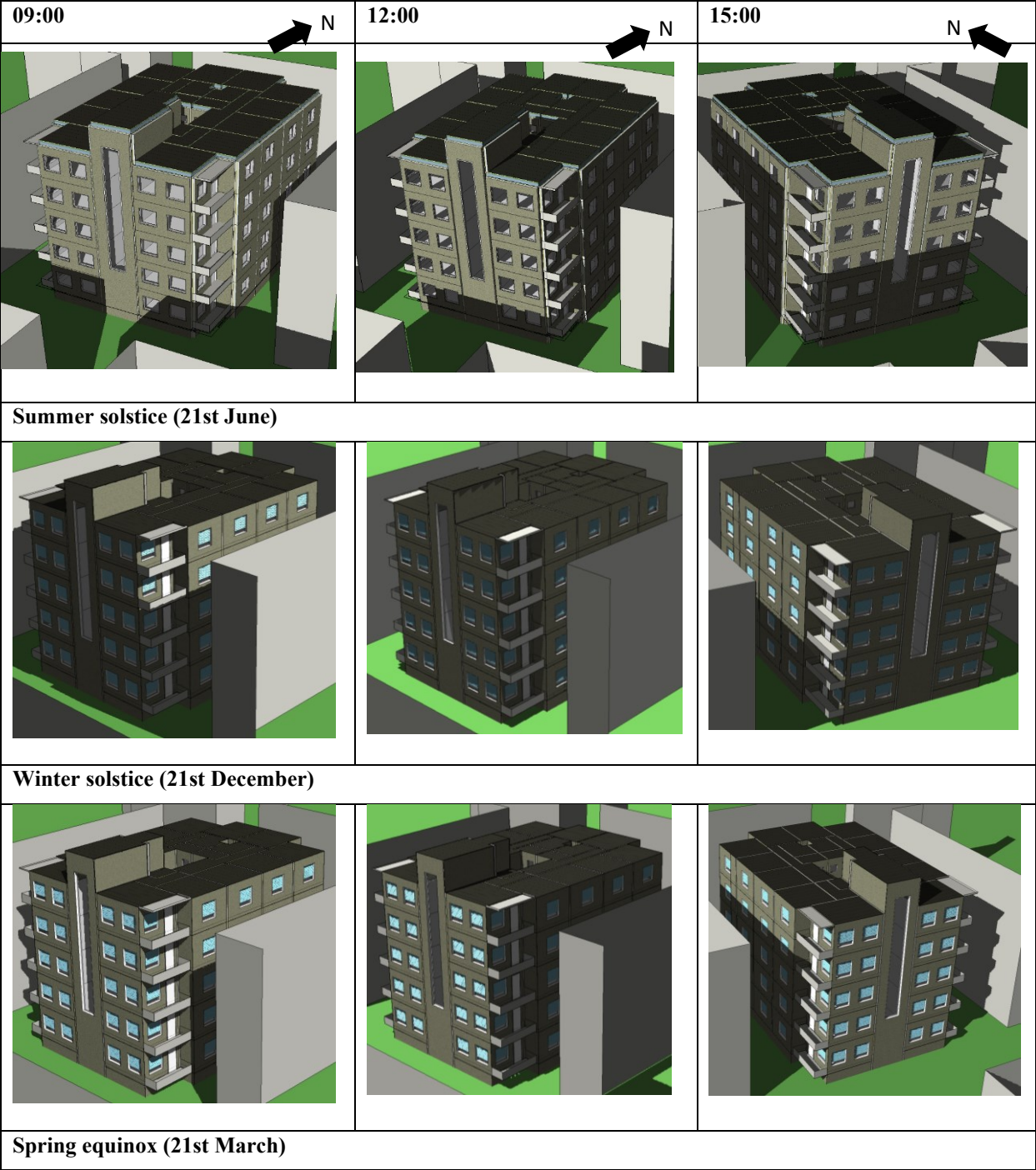


Figure 7-6: Shadow analysis on the studied apartment building in the typical urban context in Amman, Jordan during the different times for three days of the year: winter solstice (21st December), spring equinox (21st March) and summer solstice (21st June). Shadow simulation results are obtained from IDA ICE 4.8 simulation software.

Architectural suitable area

Based on the above discussion the solar suitability area for ST and PV is the roof, followed by the south façade, as they received the highest amount of solar radiation. The total roof area is about 300 m², however, part of the roof area is assumed to be used for the installation of the building services such as water tanks, dishes, etc. The assumed area for the building services is near the staircase to avoid the shade into the PV modules and solar collectors. Accordingly, the total area available for solar technology installation above the roof is about 200 m², in addition to 25 m² above the staircase roof.

Regarding the south elevation, the vertical total available south façade area is 240 m², as mentioned before, the lower part of the south façade (ground floor) is the most shaded part, which is around 50 m² façade area, therefore, the installation of solar technology in this part of façade will be avoided. Accordingly, the available architectural suitable area for solar technology installation is about 190 m², including 57 m² transparent parts (window and staircase glazing).

Another possibility for the installation of solar technology into the façade is as attached components such as an overhang shading device, which increased the potentially available area for solar technology installation.

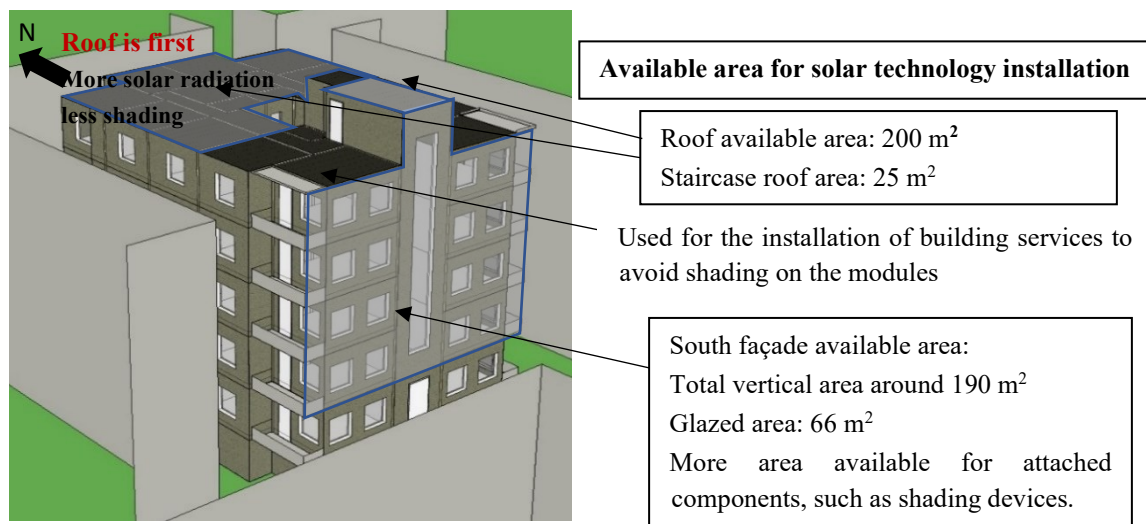


Figure 7-7: Available surfaces area for solar technology installations.

According to the above analysis, the roof has the highest solar potential for PV and ST installation. far behind comes the south wall with a 40% less received solar radiation and more shaded area. Here, and according to that, the potential of installing the solar technologies on the roof to cover part of the building energy is firstly investigated, after that, the potential of solar technology installation into the south façade (in addition to roof application) is investigated to cover part of the rest building needed energy.

7.3 Roof application

In Chapter 6, different solar energy heating and cooling systems with the traditional arrangement of ST and PV on the roof have been investigated. In this section, the energy production of photovoltaic modules and solar thermal collectors installed on the roof with different tilt angles (20° , 10° , 2°) and azimuth (south, east, and west) are investigated and compared to the base case. In the base case the photovoltaic modules and solar thermal installed on the roof with an optimum tilt angle of 30° and oriented toward the south (azimuth 0). The decrease in the tilt angle and orientation toward the east and west requires less row spacing to avoid shading and accordingly more installed area and capacity. All the proposed cases are modeled in Polysun simulation software, and implemented in the selected cooling and heating systems (based on the above discussion), which are centralized combi-heating system (solar thermal system 3) and centralized compression chiller with grid-connected photovoltaic (photovoltaic system 2), the variables between the studied cases are the tilt angle, the azimuth angle, the installed capacity, and area. To obtain a correct layout, it is necessary to calculate the minimum distance between arrays in order to avoid shadowing. The space and the design between array have been calculated using an online tool (available on the web: <https://www.renvu.com/Browse?website=solar#Plan-and-Design/Renvu-Calculators/Inter-row-Spacing-Calculator>).






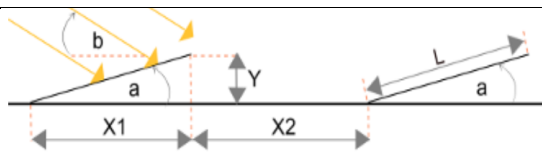
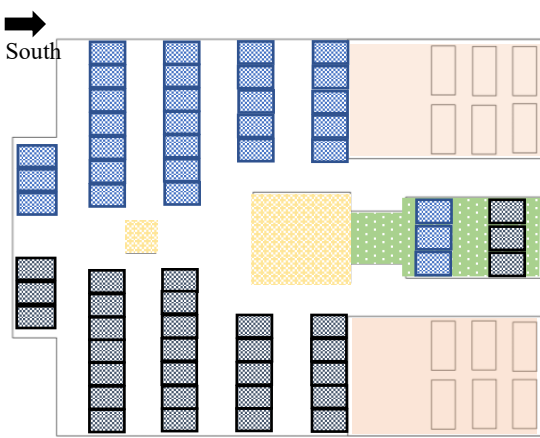

Details of the studied cases, including photovoltaic module and solar thermal collectors arrangement on the roof, installed area, capacity are presented in Table 7-1. Figure 7-8 compares the results of the studied cases, including the total energy production of the photovoltaic modules, and the percentage of the electricity covered by photovoltaic energy production (self-consumption and to the grid), while Figure 7-9 presents solar thermal collectors energy production and the total solar fraction.

As can be seen from Table 7-1 and Figure 7-8, the maximum specific annual yield the photovoltaic modules is $1,882 \text{ kWh/kWp}$, which is obtained in base case where the tilt is 30° and the azimuth is 0° (south orientation), while the lower specific annual yield is obtained in case 4A (tilt is 30° , azimuth east and west) with $1,446 \text{ kWh/kWp}$. However, the maximum total energy provided is in case 3 (tilt is 2° , azimuth south) where the production reach 21.4 MWh/year , which can cover 54% of the building electricity demand (including direct consumption and energy sold to the grid), compared to 42% in the base case. This is because the available installed area for the PV module in case 3 (87.8 m^2) is more than in the base case (60 m^2).

Regarding the solar thermal installation on the roof, it can be clearly seen that the solar fraction and the total solar production results are not very different between the studied cases, the main reason is that the solar fraction is more than 90% during 8 months (from April to November), where only the hot water needed, as has been illustrated in Figure 6-14. Also, solar energy production per m^2 is decreased with a lower tilt angle. Accordingly, increasing the solar thermal collectors' installed area doesn't influence the solar fraction in most months and results in overproduction in summer while slightly improving in winter. The maximum collector field yield relating to aperture area is $915 \text{ kWh/m}^2/\text{year}$, which is obtained in the base case (tilt is 30° , azimuth south). While the maximum solar fraction and total annual field yield are 71% and 45 MWh/year , respectively, which is obtained in case 1 (tilt is 20° , azimuth south), which slightly higher than in the base case where the total annual field yield is (49.3 MWh/year) and the solar fraction 70%. However, in case 1 the

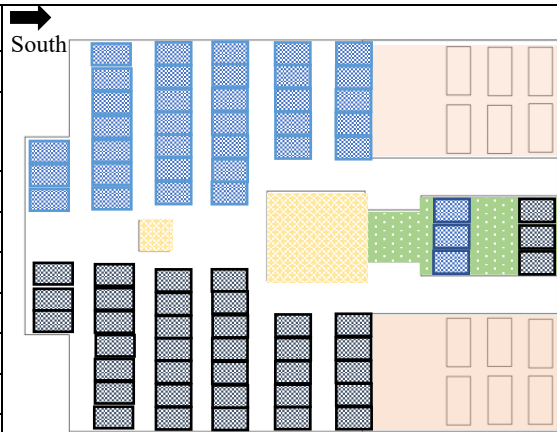
installed area is more than in case 0 with 8 m² (4 collectors) while the solar fraction is only improved by 1%.

Table 7-1: Design and arrangements and results of the photovoltaic modules and solar thermal installation with different tilts and azimuth angle installed on the roof of a residential building in Amman, Jordan. Results obtained from Polysun simulation software.

Legend:  Solar thermal collectors  Solar Photovoltaic modules  Ventilation shaft  Staircase  Service area (water tank, dishes, etc.)		
Design legend: a: Module Tilt Angle (degrees) b: Sun Angle (degrees)= 32 ° L: Module Length, L= solar photovoltaics: 1.95 m, Solar thermal: 2 m X1: Horizontal length below module X2: Distance between rows of modules		
		
		Source: https://www.renvu.com/Inter-row-Spacing-Calculator
Base case: tilt angle (a) = 30° / South (0 °)		
Photovoltaic	Unit	
Azimuth		South (0°)
Design: L/ X1/X2/Y	m	2/ 1.7/ 1.6/ 1
Installation area	m ²	58.9
Nominal capacity	kWp	9
Number of modules	unit	30
Solar thermal		
Azimuth		South (0°)
Design: X1/X2/Y	m	1.7/ 1.6/ 1
Installation area	m ²	60
Number of collectors	unit	30
		
Case1: tilt angle (a) = 20° / South (0 °)		
Photovoltaic	Unit	
Azimuth		South (0°)
Design: L/ X1/X2/Y	m	1.95/ 1.9/ 1.1/ 0.7
Installation area	m ²	66.3
Nominal capacity	kWp	10.2
Number of modules	unit	34
Solar thermal		
Azimuth		South (0°)
Design: X1/X2/Y	m	1.8/ 1.1/ 0.7
Installation area	m ²	68
Number of collectors	unit	34
		

Case 2: tilt angle (a) = 10° / South (0 °)

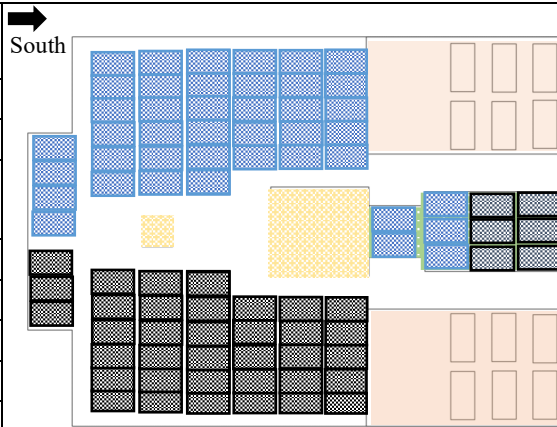
Photovoltaic	Unit	
Azimuth		South (0°)
Design: L/ X1/X2/Y	M	2/ 2/ 0.6/ 0.3
Installation area	m ²	72.2
Nominal capacity	kWp	11.1
Number of modules	Unit	37
Solar thermal		
Azimuth		South (0°)
Design: X1/X2/Y	M	1.9/ 0.5/ 0.3
Installation area	m ²	74
Number of collectors	Unit	37



Case 3: Tilt angle (a) = 2° / Azimuth: South (0 °)

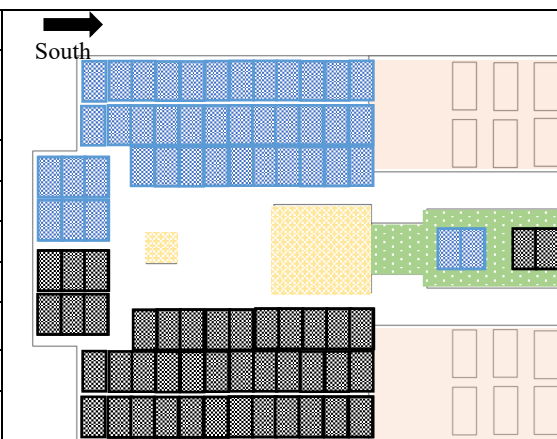
Photovoltaic: It is assumed it is mounted 2.3 m above the roof surface.

Photovoltaic	Unit	
Azimuth		South (0°)
Design: L/ X1/X2/Y	m	1.95/ 1.95/ 0.1/ 0.1
Installation area	m ²	87.8
Nominal capacity	kWp	13.5
Number of modules	unit	45
Solar thermal		
Azimuth		South (0°)
Design: X1/X2/Y	m	2/ 0.1/ 0.1
Installation area	m ²	90
Number of collectors	unit	45



Case 4: Tilt angle: Case 4A = 30° / Case 4B = 20° / Case 4C = 10°
Azimuth: East (90 °) and West (- 90 °)

Azimuth	East (90 °), West (- 90 °)	
Tilt	Case 4A: 30°, Case 4B: 20° Case 4C: 10°	
Photovoltaic	Unit	
Installation area	m ²	82
Nominal capacity	kWp	12.6
Number of modules	unit	42
Solar thermal		
Installation area	m ²	84
Number of collectors	unit	42



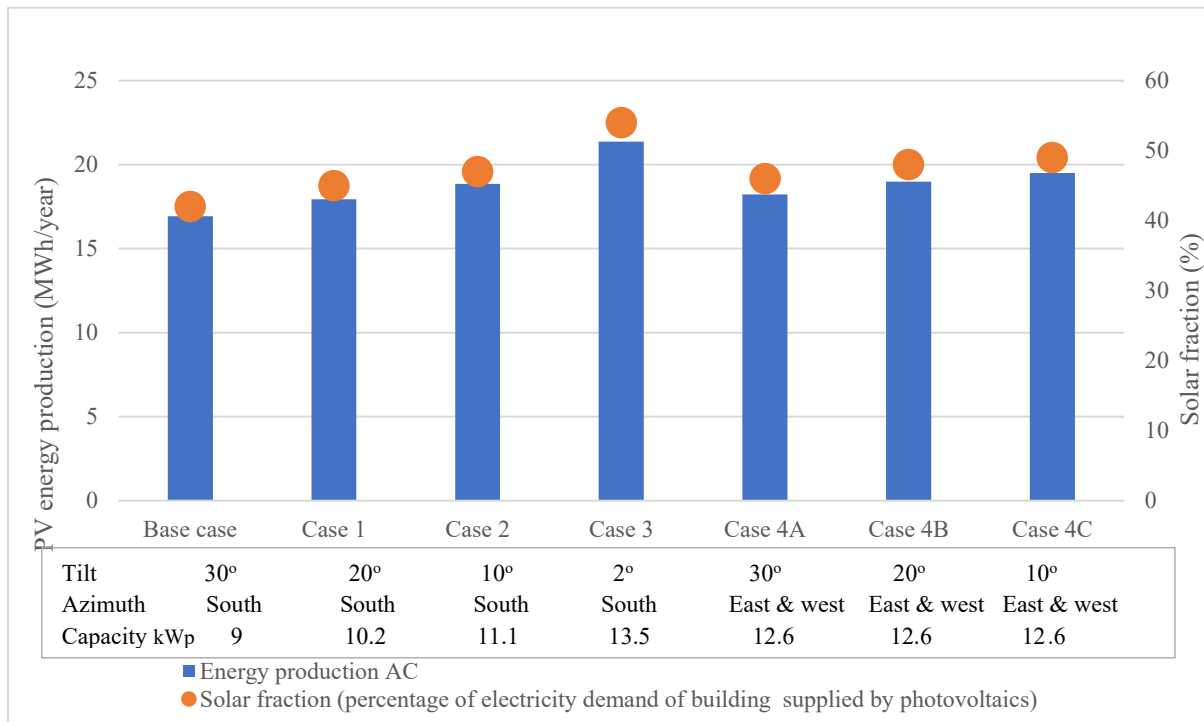


Figure 7-8: Annual energy production and the solar fraction of grid-connected photovoltaic system with different tilt and azimuth angle, and different capacity installed on the top of a residential building in Amman, Jordan. Results obtained from Polysun simulation software.

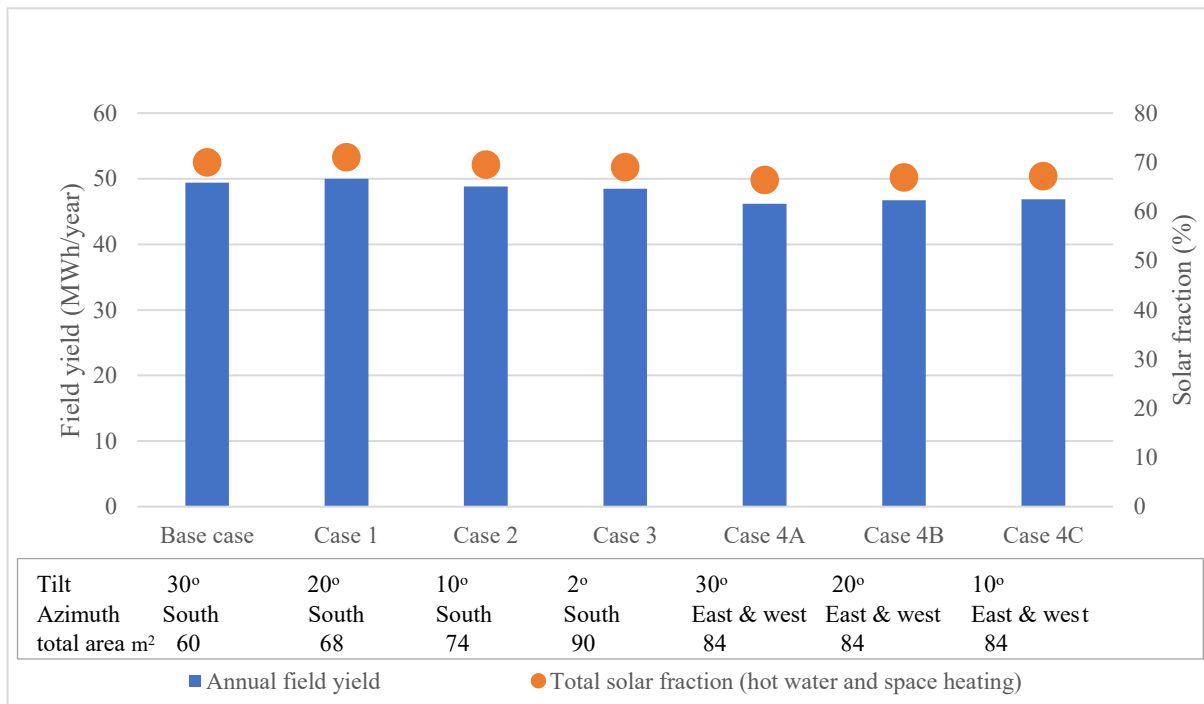


Figure 7-9: Annual field yield and the solar fraction of solar thermal collectors with different tilt angles, azimuth, and installed area on the roof of a residential building in Amman, Jordan. Results obtained from Polysun simulation software.

The selected system configurations are presented in Figure 7-10 and the arrangement for the solar collectors and photovoltaic modules on the roof of the residential buildings is illustrated in Figure 7-11. The centralized solar thermal combi-heating system is selected to supply hot water and heat the space in winter, as illustrated in Figure 7-10 a. The solar thermal collectors installed on the roof with 60 m² total installed area, the tilt angle is 30° and all the collectors are oriented toward the south. The results show that the net energy demand of the system is 22.2 MWh/year (17 kWh/m²/year), corresponding to 24.5 MWh/year (18 kWh/m²/year) primary energy, the total solar fraction is 70% whereas it's only 33% of space heating and 83% of DHW production. The annual field yield of the solar collectors is 49,382 kWh/year (915 kWh/m²/year). Regarding the photovoltaic and cooling system, a centralized compression cooling system is selected, as illustrated in Figure 7-10 b, the photovoltaic system supply electricity to the cooling system, equipment, and lighting. The net electricity demand of the building (including the cooling system, equipment, and lighting) is 16.5 MWh/year (12.2 kWh/m²/year), corresponding to 44.8 MWh/year (33 kWh/m²/year) primary energy. The annual energy production of the photovoltaics is 21.4 MWh/year, and the specific annual yield is 1,583 kWh/kWp (244 kWh/m²), the solar photovoltaic cover 54% of the building electricity need.

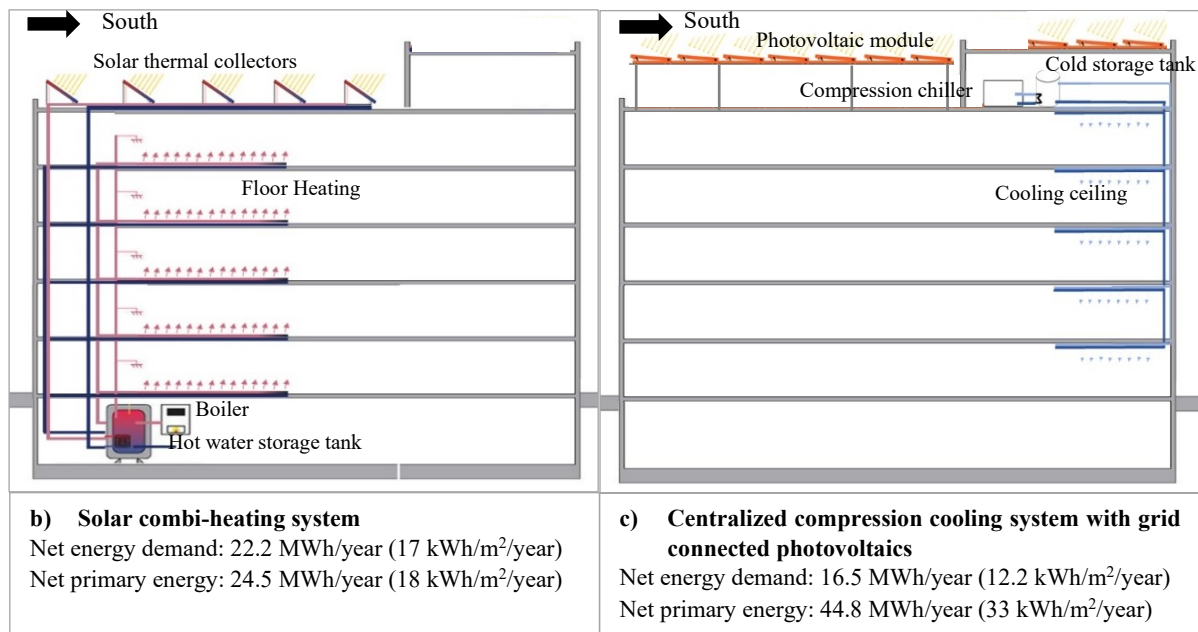


Figure 7-10: Simplified schematic of the selected energy systems for multi-family building in Amman, Jordan a) solar combi heating system b) centralized compression cooling system with grid-connected.

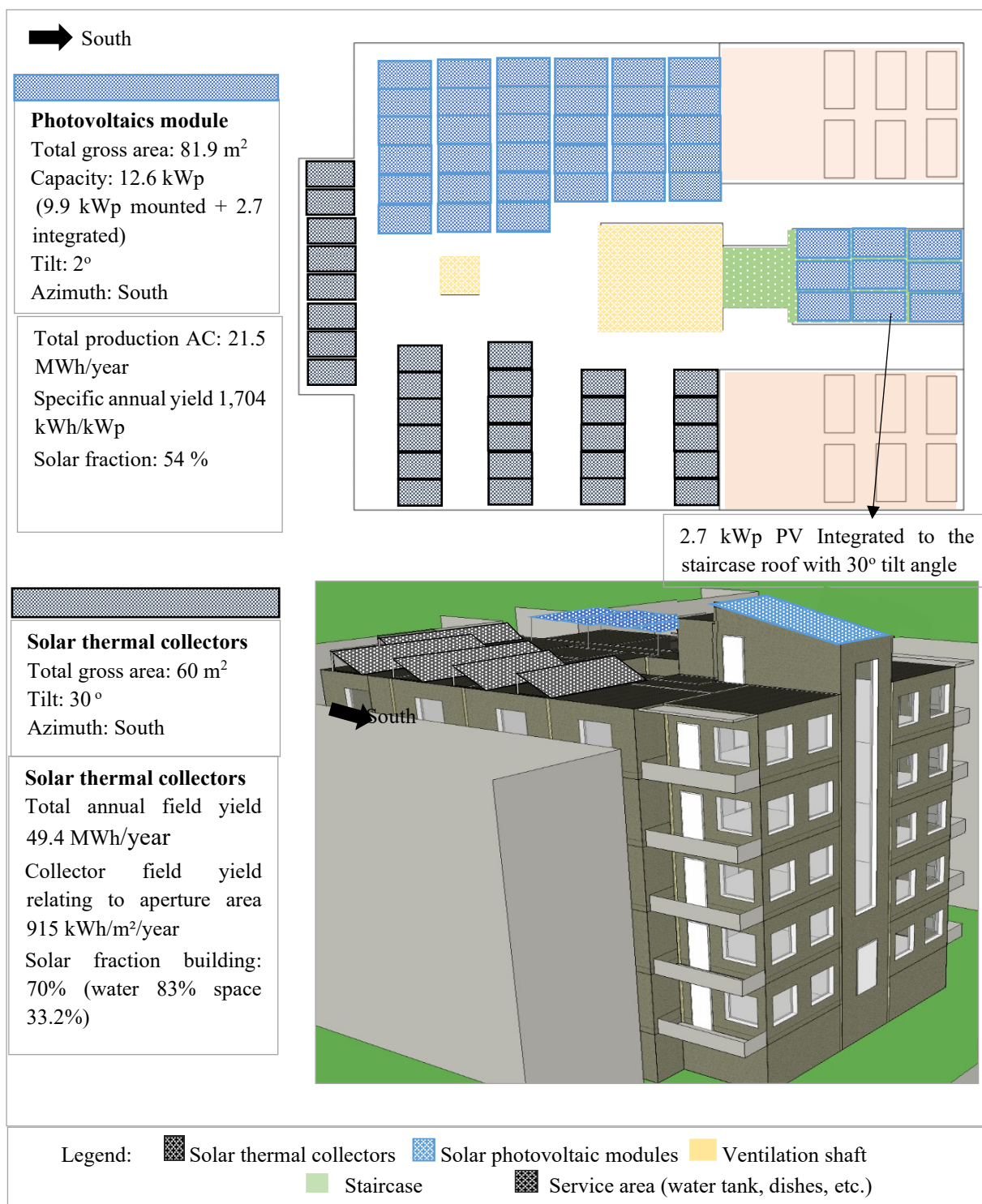


Figure 7-11: The arrangement of the solar collectors, and photovoltaic module on the roof of multi-family building, in Amman, Jordan.

7.4 Façade BIPV application

BIPV or BIST façade application?

In the previous part, the installation of PV and ST technologies on the multi-family building roof is investigated each PV and ST cover half of the available roof area, the photovoltaic system on the roof covered about 21.5 MWh/year (54%) of building demand and around 18 MWh/year of building electricity is imported from the grid. While in the case of solar thermal installation the system can cover 70% of space and water demand (83% water and 33% space heating), and it is also has been noticed that increasing the collector installation area does not have a big advantages of solar fraction due to the summer peak, as the useful solar heat is then only the part that can be directly used or stored. Any additional production is not only useless but increases the overheating risks and should be avoided. Therefore, when the roof occupied with 50% of solar thermal there is no need for more installation areas on the façade. On the other hand, increasing of the photovoltaic installation area lead to increase the amount of covered electricity and if there is overproduction can be sold to the grid and used when it is needed with negligible losses, also the solar photovoltaic can address the domestic hot water and space heating segment, when it coupled with heat pumps. Moreover, as discussed in the literature review (Chapter 3), the PV modules have a better ability to architectural integration than the solar thermal collectors, and the BIPV market will be subject to continuous growth worldwide due to advances in technology, the reduced cost of PV materials, and the increase in incentive policies for renewable energy technologies in some countries, such as Germany, USA, China (Berenschot, 2015; Transparency Market Research, 2015; Global Industry Analysts Inc, 2016; Zhang, Wang and Yang, 2018). In Jordan context (see Chapter 0 for more details), the government of Jordan, set a renewable energy target of 10% of Jordan's energy mix by 2025, this is expected to comprise 15-20% of electricity demand, and more than 70% to be covered by photovoltaic (Jaber, 2016; MEMR, 2017).

Unlike the BIPV global market, the solar thermal market provides a limited variety of products suitable for architectural integration (IEA, 2012; Munari Probst and Roecker, 2013). Moreover, it is facing a challenging time with a continuous shrinking of the annual added collector capacity, which declined from 18% in the period 2010/2011 to 4% in the period 2016/2017. Compared to the year 2016, new installations declined by 4.2% in 2017 (IEA, 2018b).

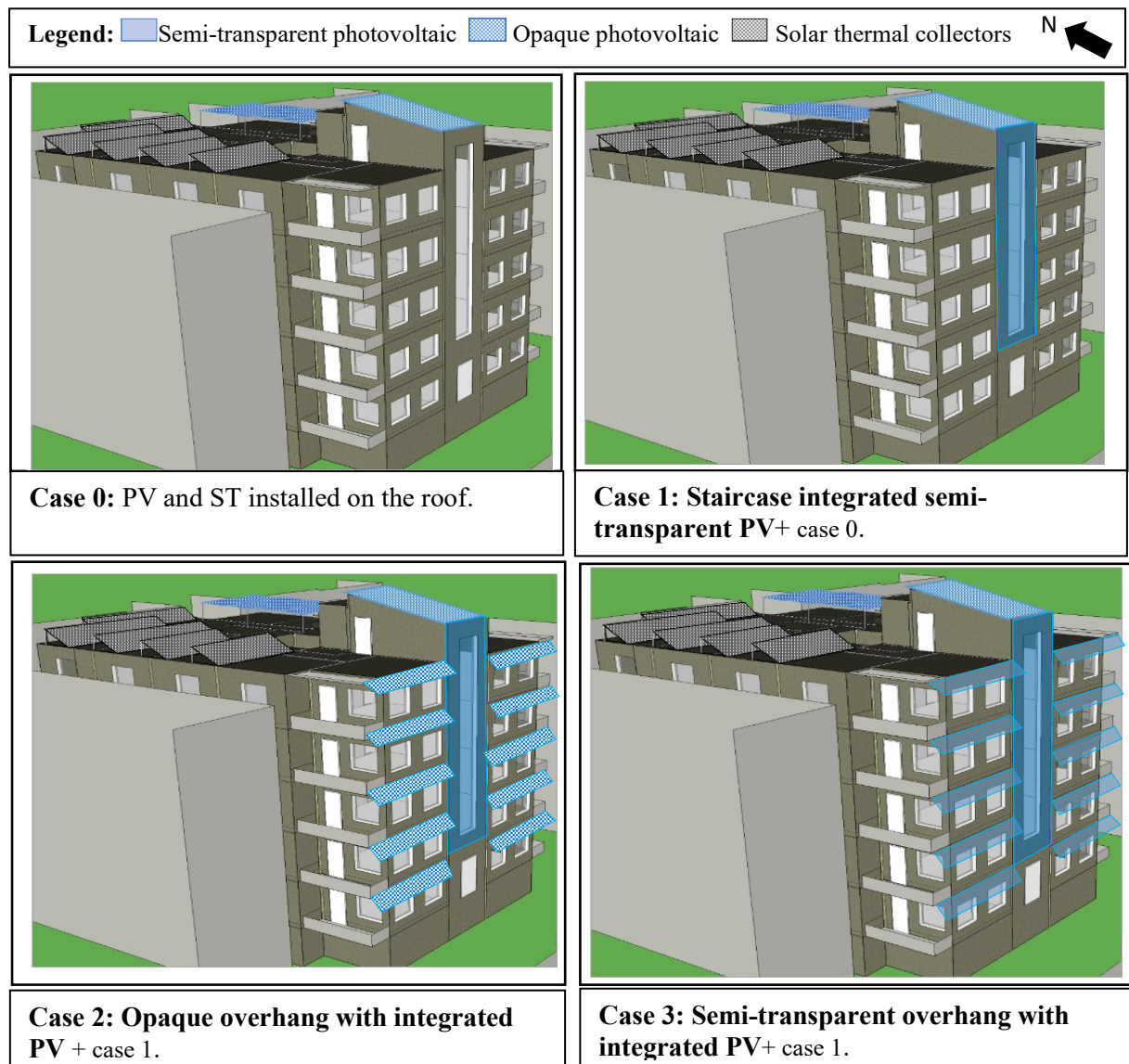
Based on the above discussion, this research is focused on the installation of solar photovoltaic modules to the building façade (in addition to the roof installation), while the solar collectors are only installed on the roof.

Below several design possibilities for PV module installations on the south façade are proposed based on the available façade area, solar radiation, and shading on the façade. In addition to the state of art of the available product for PV integration as discussed in the literature review (Chapter 3). After that, a comparable assessment has been conducted in terms of the energy demand, and energy production of the integrated PV modules. The energy demand for heating, cooling, and lighting in the space have been estimated with simulation software IDA ICE 4.8. The electricity production has been estimated with Polysun 11 simulation software, and IDA ICE 4.8 is also used to estimate the reduction in electrical output due to the shading effect.

For the analysis, invariants are the south orientation of the facades, the geometry, dimensions of the apartment and windows, and the types of the materials used for the PV modules (monocrystalline silicon). The only variables are related to the PV modules in terms of dimensions, tilt angles, and properties to suit the different PV system design.

7.4.1 Defining façade photovoltaic systems

Several designs of photovoltaic systems installed on the south facade are proposed here. An overview of the proposed facade design cases and roof installation case (case 0) are presented in Figure 7-12, case 0 and case 1 are applied to all the rest cases, therefore it is only described once. these cases are explained in detail in the following section.



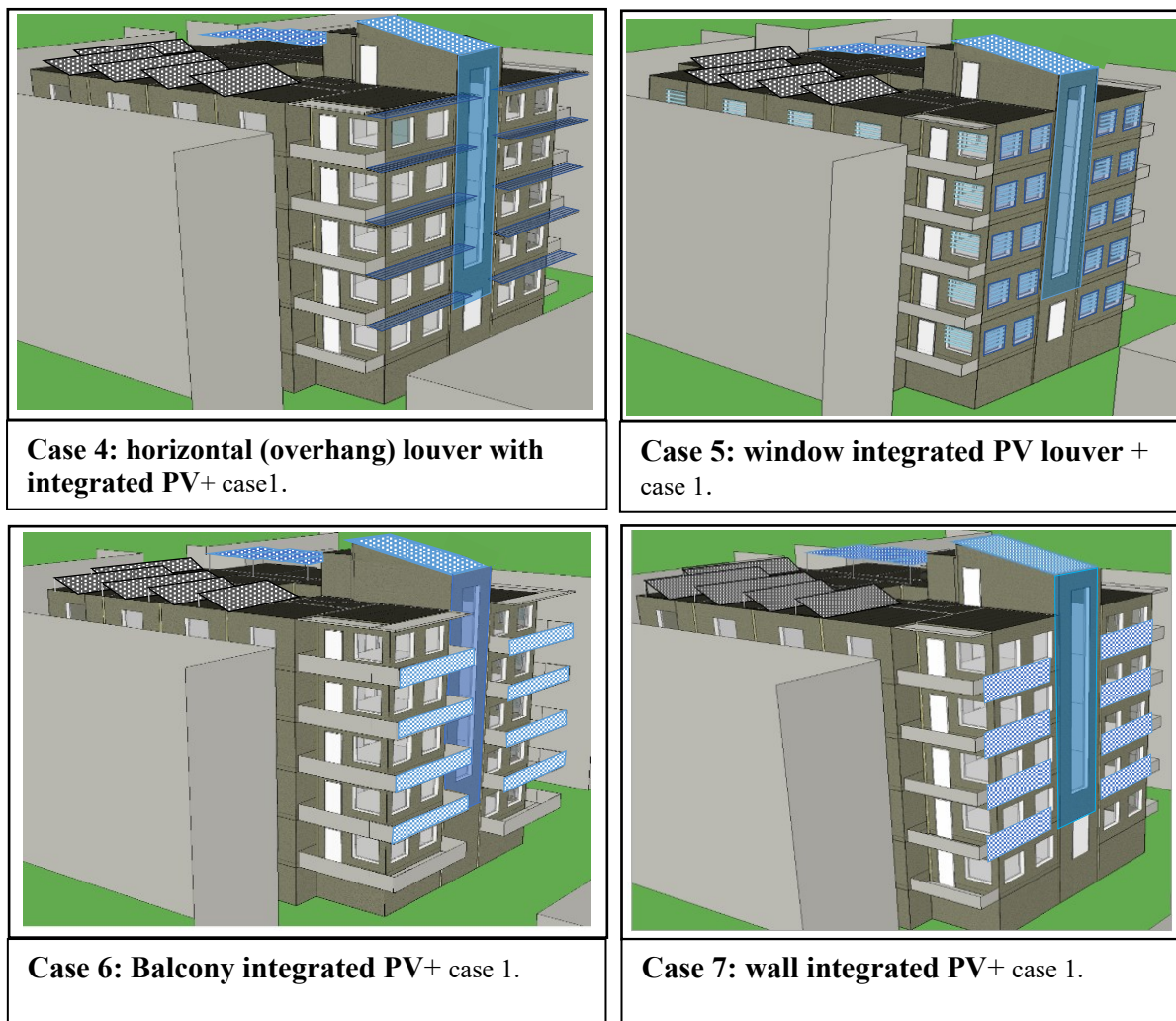


Figure 7-12: Proposed Photovoltaic application on south façade.

The details and examples of each case are described below (more examples are presented in the literature review analysis, Chapter 3:

Case 0: PV and ST installed on the roof

In this case, the PV and ST are installed on the roof of the building, and there is no PV installed into the façade. The total gross area of PV modules is around 82 m² and the total capacity is 12.6 kWp, including 9.9 kWp mounted modules with 2° tilt angle, and 2.7 kWp staircase roof PV integrated with 30° tilt angle. The total photovoltaic production is 21.5 MWh/year, which covers around 54% of the building electricity demand.

Case 1: semi-transparent staircase

In addition to the roof PV installation (case 0), semi-transparent PV modules are integrated into the staircase south wall. Double glass laminated PV modules with mono-crystalline cells covering only a part of the glass area (cell spacing) are integrated into the staircase elevation, the total installed area is around 50 m² the photovoltaic cell covered around 75% of the total PV area. Figure 7-13 illustrate the proposed design and example.

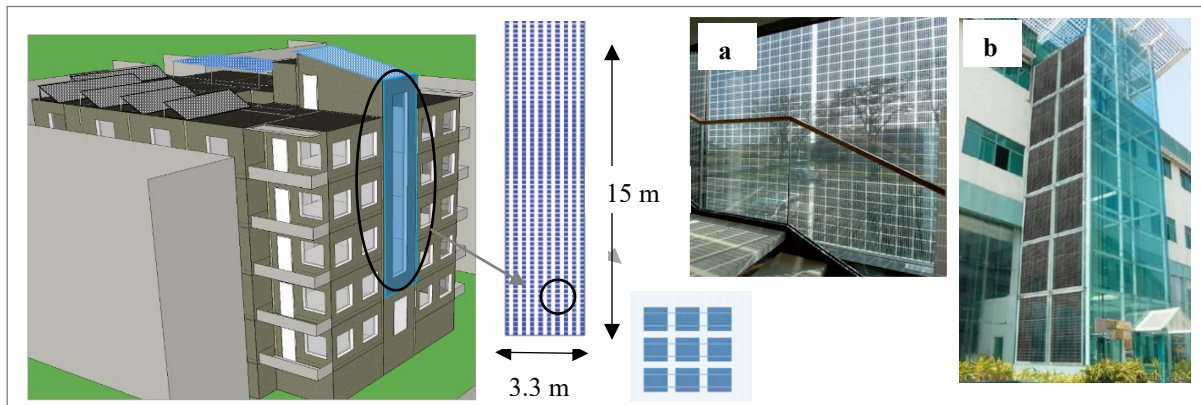


Figure 7-13: Semi-transparent mono-crystalline PV staircase integration design proposal and examples. Source of examples: a) (IEA, 2013; Passera et al., 2018), b) (Alibaba, 2019).

Case 2: Opaque overhang with integrated PV

This shading system is completely covered by PV cells and it is a fixed shading device, it is also designed at the optimal inclination of 30° for maximum electricity production, as illustrated in Figure 7-14 below. The commercially available opaque mono-crystalline modules can be used in this case. Each overhang has 0.70 m depth and 6.50 m length and extended over the window and balcony to cover as much area as possible. The total PV overhang installation area is 45.5 m^2 .

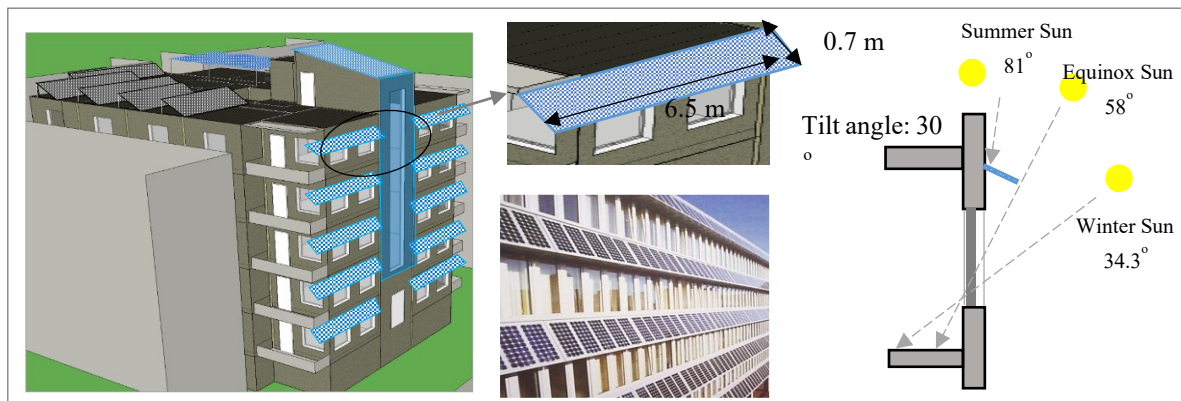


Figure 7-14: Opaque mono-crystalline PV integrated into fixed overhang shading device design proposal and example. Source of example: (IEA, 2013).

As analyzed in Chapter 5, the shading device mainly needed between May and October. Figure 7-15, present the hourly percentage of shading for the suggested shading device design, through using online'' Susdesign'' tool (<http://susdesign.com/tools.php>).

The suggested shading device blocking the sun completely during the hottest months Jun, July and more than 89% in August and allow the sun in the heating months January, February, and December.

	MORNING										AFTERNOON								
	4:00	5:00	6:00	7:00	8:00	9:00	10:00	11:00	12:00	1:00	2:00	3:00	4:00	5:00	6:00	7:00	8:00		
Jan				0%	0%	0%	0%	0%	0%	0%	0%	0%	0%	0%				Jan	
Feb				0%	0%	0%	2%	4%	4%	4%	2%	0%	0%	0%				Feb	
Mar				10%	18%	21%	22%	23%	23%	23%	22%	21%	19%	12%				Mar	
Apr					100%	85%	70%	64%	62%	64%	70%	86%	100%					Apr	
May						100%	100%	100%	100%	100%	100%	100%						May	
Jun						100%	100%	100%	100%	100%	100%	100%						Jun	
Jul						100%	100%	100%	100%	100%	100%	100%						Jul	
Aug					100%	100%	100%	93%	89%	92%	100%	100%	100%					Aug	
Sep				75%	47%	41%	38%	37%	37%	37%	38%	40%	46%	71%				Sep	
Oct				0%	0%	6%	9%	10%	11%	10%	9%	5%	0%	0%				Oct	
Nov				0%	0%	0%	0%	0%	0%	0%	0%	0%	0%	0%				Nov	
Dec					0%	0%	0%	0%	0%	0%	0%	0%	0%					Dec	
	4:00	5:00	6:00	7:00	8:00	9:00	10:00	11:00	12:00	1:00	2:00	3:00	4:00	5:00	6:00	7:00	8:00		
	MORNING										AFTERNOON								

Figure 7-15: Hourly percentage of shading for the suggested shading device design, through using the online'' Susdesign'' tool. Source: (<http://susdesign.com/tools.php>).

Case 3: Semi-transparent PV overhang:

In this case, each integrated PV overhang unit has a 30° slope. Double glass laminated PV modules with mono-crystalline cells are integrated into the shading device, this can allow much more sun and light to penetrate the window, see Figure 7-16.

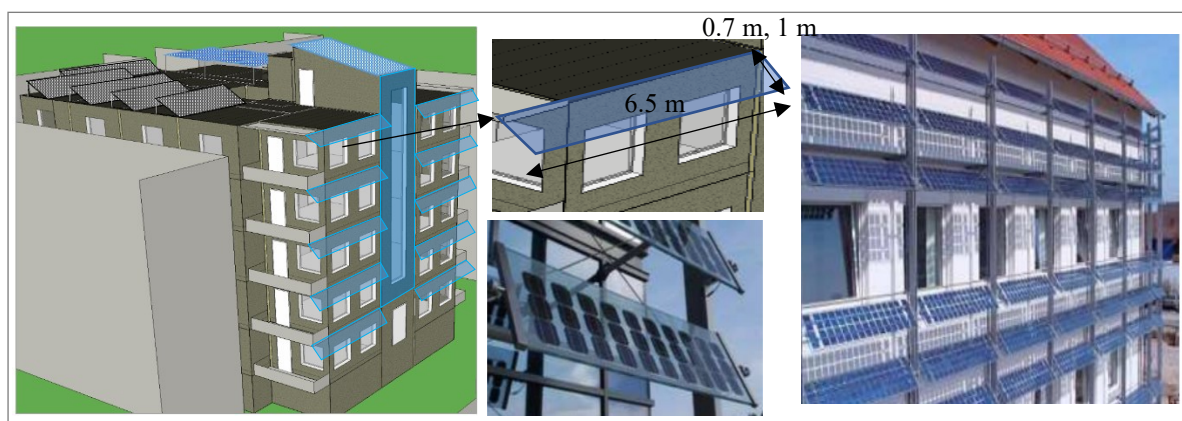


Figure 7-16: Semi-transparent mono-crystalline PV integrated into fixed overhang shading device design proposal and example. Source of example: (IEA, 2013).

As illustrated in Figure 7-17 below, different scenarios are proposed with different PV converge ratio, 75%, 50% and 25%, in addition to 90%, which represent the original glass to glass module selected from Polysun (more details are described in the next step), and also different overhang dimensions (0.7 m, 1 m) depth and 6.50 m length, in order to find the optimal PV ratio and installed area based on net energy performance (heating, cooling, lighting, PV electricity production).

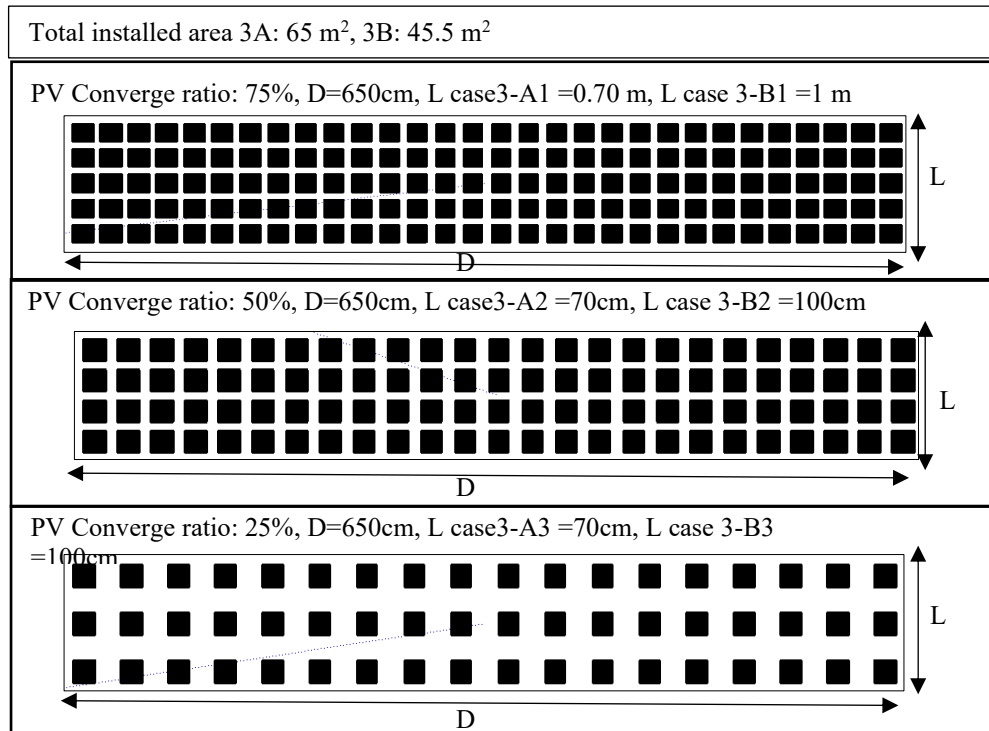


Figure 7-17: Different scenarios of semi- transparent PV overhang with different PV converge ratio, 75%, 50% and 25%, and different dimensions.

Case 4: horizontal PV overhang louvers

The inclination angle of PV slat is 30°, it is the width of 0.23 m and length is 6.5 m the designed width is selected according to the available commercial product in Polysun, more details are described in the next section. The space of 0.36 m is left between the slats to avoid the shading of PV slate on each other and at the same time allow the sun to penetrate through the window in winter and block the sun in summer. The total installed PV louver area is around 60m². Figure 7-18, illustrates the proposed design for this case.

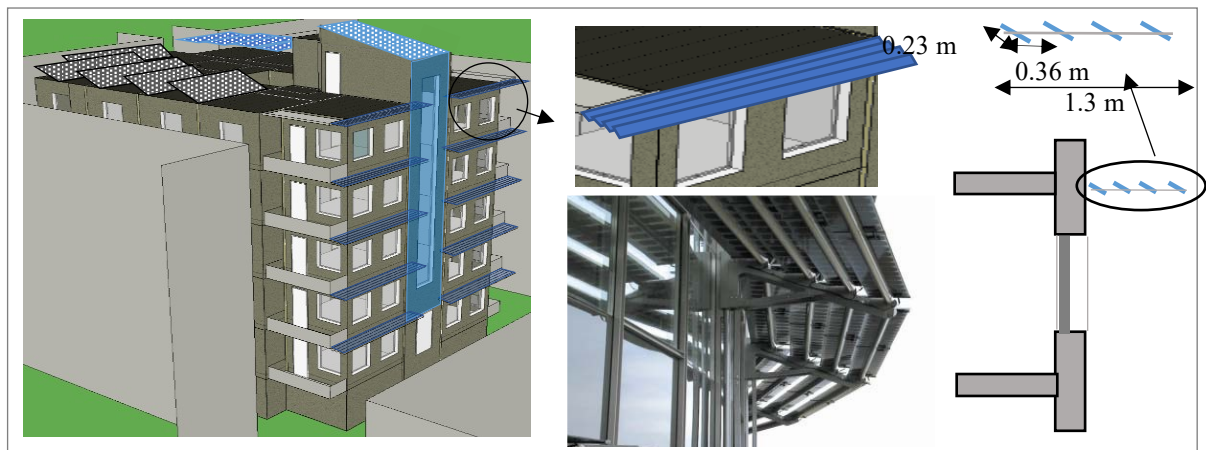


Figure 7-18: PV integrated into fixed louver overhang design proposal and example. Source of example: (IEA, 2013).

Case 5: window integrated PV louver.

The proposed design of this case is presented in Figure 7-19. The inclination angle of each PV slat is 30° , the width is 0.23 m and the length is 1.5 m, the width of the slate is selected to allow the PV integration according to the available commercial product in Polysun.

Regarding the louver control same control strategy used as in base case (details in Chapter 5), the shading device is on between May and October when the sun is available, and they are not activated for the rest of the year, in this case, the PV produces electricity only in the cooling period.

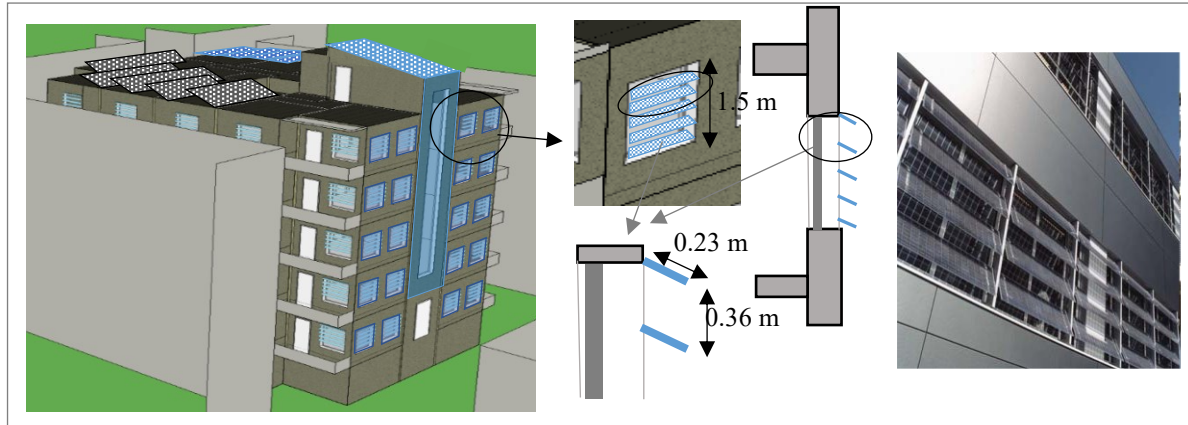


Figure 7-19: PV integrated into window louver design proposal and example. Source of example: (IEA, 2013).

Case 6: Balcony integrated PV.

In this case, the balconies on the west and east façades have been extended to the south façade, see Figure 7-20. Double glass laminated PV modules with mono-crystalline cells are proposed here to be integrated on the south balconies' railings with a 90° tilt angle, the cell coverage ration is 90% represents the commercially available modules as selected from Polysun (details in the next section). The balconies on the ground floor are not integrated with photovoltaic modules in order to avoid the most shaded area on the south façade, moreover, for a safety reason, as the balconies on the ground floor are directly connected to the street level. The total installed area is around 37 m^2 .

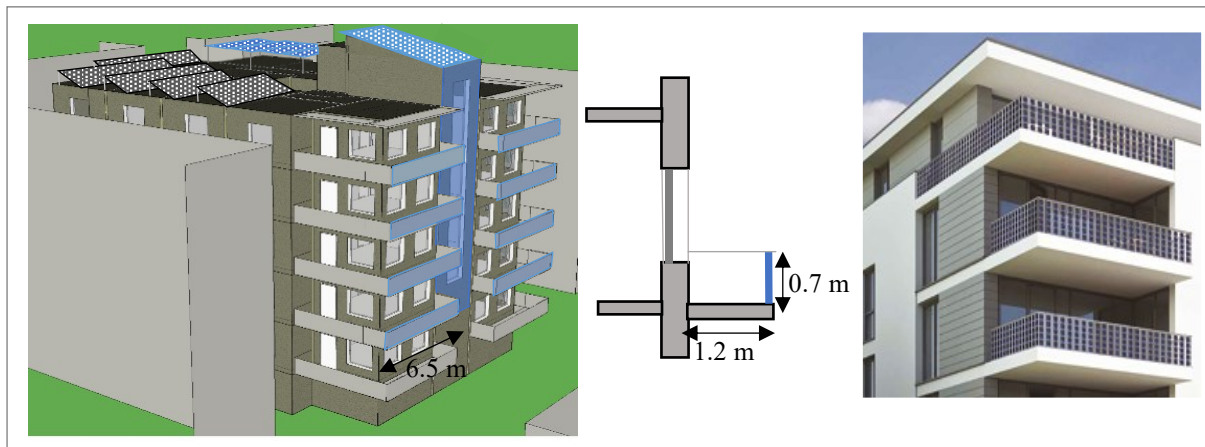


Figure 7-20: PV integrated into the south balcony railings design proposal and example. Source of example: (IEA, 2013)

The PV modules are integrated into the part of the south wall with a tilted of 90°. The proposed design is based on the recent construction trend in the apartment buildings in Jordan (see Figure 7-22). The PV modules are integrated into the insulated wall (4 cm insulation layer) leaving an air gap of 12-15 cm between the modules and the existing wall, which allows good ventilation of the PV modules by natural convection and prevent the heat transmission from the modules to the indoor space. The total installation area is 60 m².

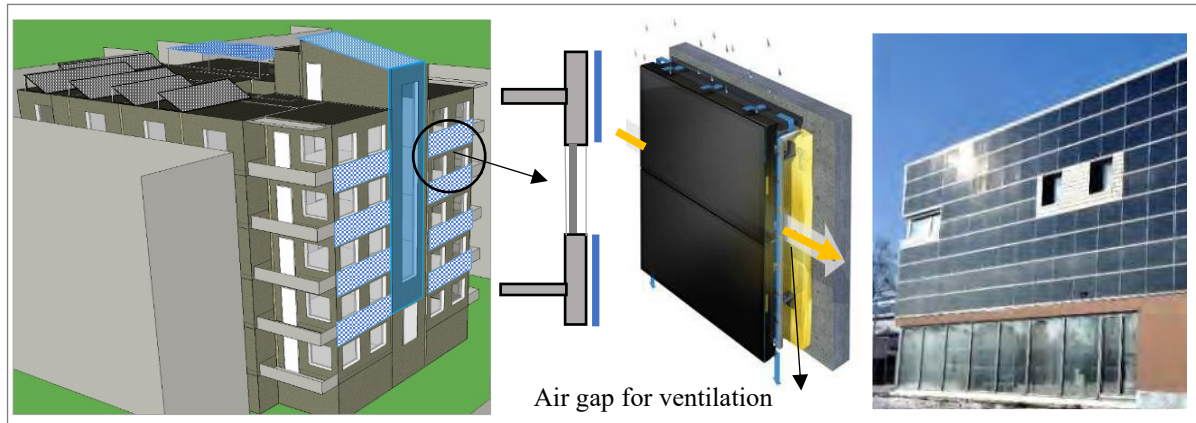


Figure 7-21: Wall integrated PV design proposal and example. Source of example:(IEA, 2013).

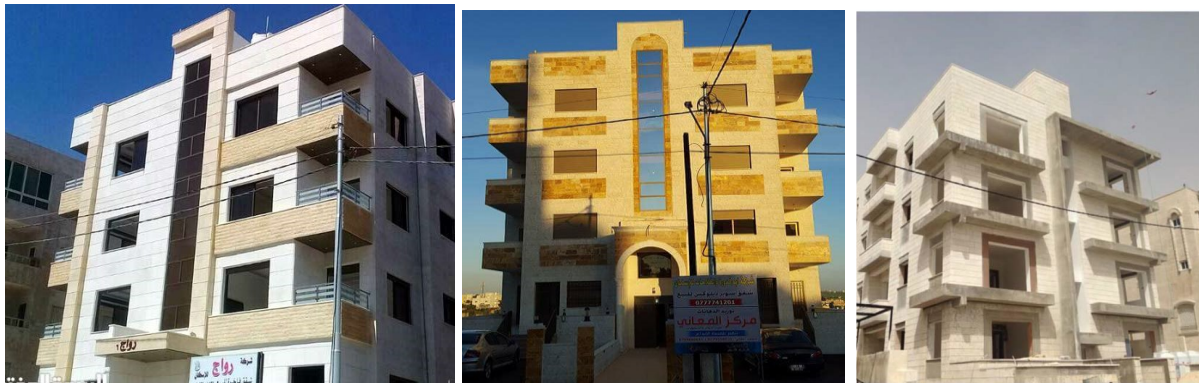


Figure 7-22: Recent construction trend in the multi-family buildings in Jordan. Source: (Attia and Al-Khuraissat, 2016).

7.4.2 Selection of BIPV modules and Polysun input

In this section, PV modules characteristic and assumptions, which have been used for each scenario, are explained, commercially available PV modules are selected from Polysun to match the suggested unique design, in all cases, the PV modules are made of mono-crystalline cells.

In Polysun simulation software, the rear ventilation of the photovoltaic modules in case of a fully integrated photovoltaic is selected to be poor while for the mounted photovoltaic into the facade (shading device and balcony) is medium and as described before the roof-mounted photovoltaic modules the rear ventilation is assumed to be good.

Below is the general description of the selected modules for each case, the general data for each case is taken from Polysun also from the datasheets, which are available on the web under (<https://www.photovoltaikeforum.com/mdb/>). It must be mentioned that case 1 (semi-transparent integrated PV) is also included in all cases from case 2 until case 7, however, it is only described once.

Case1: Staircase integrated semi-transparent PV

In this case, double glass laminated PV modules with mono-crystalline cells covered 75% of the module area (25% transparency) is proposed. However, the available module in the Polysun library has 10% transparency. Therefore, the nominal power and the number of cells in each module are modified to obtain the 25% transparency, while regarding the module efficiency it is assumed the same as the original module. Table 7-2 present the main properties of the modified PV module). For the suggested design 42 modules are needed with a total installed capacity of 5.4 kWp and the rear ventilation is assumed poor. In addition to the roof PV application.

Table 7-2: Semi-transparent PV module specification for case 1: staircase integrated semi-transparent PV.

Module Name	Efficiency (%)	Nominal power (W)	Dimensions (m) Area (m ²)	No. of cells	Dimensions of cells (m)	Appearance
Based on solarwatt 36M facade/style-155	0.14	129	1.520 x 0.710 x 0.010 Area: 1.079	30 cells	0.156 x 0.156	Semi-transparent (25% transparency)

Case 2: Opaque overhang with integrated PV

Table 7-2 below, present the general prosperities for the selected opaque mono-crystalline module from Polysun library. In this case, the total required number of PV modules is 40 modules and the total installed peak capacity is 6 kWp with 42 m² installed area. In addition to the roof PV application and staircase PV integration (case 1).

Table 7-3: Opaque PV module specification for Case 2: Opaque overhang with integrated PV

Name	Efficiency (%)	Nominal power (W)	Dimensions (m) Area (m ²)	No. of cells	Dimensions of cells (m)	Appearance
TEI 150-36M	0.14	150	0.7 x 1.51 x 0.03 1.057	36 cells	0.156 x 0.156	Opaque

Case 3: Semi-transparent PV overhang

In this case, 2 types of PV mono-crystalline modules are selected from the Polysun library to match the dimensions of the different suggested designs. As described before, several scenarios have been proposed with different transparency ratio. As in case 1, the selected modules from the Polysun library have been modified to match the suggested scenarios as presented in Table 7-4. The total installed capacity and area for each scenario are presented in the summary Table 7-7.

Table 7-4: Semi-transparent PV module specification for different scenarios in Case 3.

Name	Efficiency (%)	Nominal power (W)	Dimensions (m) Area (m ²)	No. of cells	Dimensions of cells (m)	Appearance (transparency)
Case3-A: Solarwatt 36M facade/style-155	0.14	155	1.520x 0.710x 0.010 Area: 1.79 m ²	36	0.156x 0.156	Semi-transparent (10%)
Case 3-A1		129		30		25%
Case 3-A2		86		20		50%
Case 3-A3		43		10		75%
Case 3-B: EX-280M (156) transparent	0.14	280	1.956x0.996x 0.045 Area: 1.95 m ²	72	0.156 x 0.156	10%
Case 3-B1		233		60		25%
Case 3-B2		155		40		50%
Case 3-B3		77.6		20		75%

Case 4: horizontal PV overhang louvers

Table 7-5 below, represents the general prosperity for the selected PV module from the Polysun library. 4 slates are needed for each overhang, as there is no PV available in Polysun with the same length, 4 modules are used to design one slate, accordingly, 16 modules needed for each overhang and 160 modules needed for 10 apartments this equal to 4 kWp for all overhangs (0.4 kWp for each overhang).

Table 7-5: PV module specification for Case 4: horizontal PV overhang louvers.

Name	Efficiency (%)	Nominal power (W)	Dimensions (m)	No. of cells	Dimensions of cells (m)	Appearance
Flex025W12V	0.14	25	0.270x 0.626x 0.023	36	0.156x 0.156	opaque

Case 5: window integrated PV louver

The same module used in case 4 is used here, each window consists of 5 slates accordingly 10 modules needed for each window louver and this equal to 0.25 kWp for each window and 5 kWp for all windows.

Case 6: Balcony integrated PV

In this case, the same module used in case 3-A is used here, each balcony consists of 4 PV modules, accordingly, 32 modules are needed for all balconies with the total installed capacity of 4.96 kWp and the total area of 34.5 m².

Case 7: Wall integrated PV

The prosperities of the selected opaque mono-crystalline photovoltaic module from the Polysun library are presented in Table 7-6. For the proposed design 40 modules are needed with a total installed peak capacity of 8.6 kWp and a total area of 59.6 m².

Table 7-6: PV module specification for Case 7: wall integrated PV.

Name	Efficiency (%)	Nominal power (W)	Dimensions (m) Area (m ²)	No. of cells	Dimensions of cells (mm)	Appearance
SAM 54/6-215	0.14	215	0.99x 1.52x 0.03 1.49	36 cells	156x 156	opaque

The main parameters of each proposed design are summarized in Table 7-7 below.

Table 7-7: Main parameters of the suggested PV system design.

	Number of modules	Total installed area (m ²)	Total installed capacity (kWp)	Rear ventilation	Tilt angle	Appearance
Base case: PV and ST installed on the roof						
Mounted	33	64.35	9.9	good	2°	Opaque
Staircase roof integrated PV	9	17.55	2.7	poor	30 °	Opaque
Case 1: staircase integrated semi-transparent PV+ base case.						
Staircase wall integrated PV	40	43.5	5.43	poor	90°	25% transparency
Case 2: Opaque overhang with integrated PV + base case + case 1						
Overhang PV	40	42.4	6	medium	30°	Opaque
Case 3: Semi-transparent overhang with integrated PV+ base case+ case 1						
Case 3-A1	40	42.4	6	medium	30°	10% transparency
Case 3-A2			5.11			25% transparency
Case 3-A3			3.41			50% transparency
Case 3-A4			1.55			75% transparency
Case 3-B1	40	42.4	8.4	medium	30°	10% transparency
Case 3-B2			7			25% transparency
Case 3-B3			4.76			50% transparency
Case 3-B4			2.24			75% transparency
Case4: horizontal (overhang) louver with integrated PV+case1						
horizontal (overhang) louver	40	43.2	6.2	medium	30°	opaque
Case 5: window integrated PV louver + case 1						
window integrated PV louver	200	34	5	medium	30°	opaque
Case 6: Balcony integrated PV + case 1						
Balcony integrated PV	32	34.56	4.96	medium	90°	10% transparency
Case 7: wall integrated PV +case 1						
wall integrated PV	40	59.6	8.6	poor	90°	opaque

7.4.3 Impacts of BIPV on building energy performance

In this part, the overall energy performance of the proposed PV façade systems is investigated, through the consideration of increase/reduction in cooling, heating, daylight demand and production of electricity. IDA ICE 4.8 simulation software is used to estimate the building energy demands for heating, cooling and artificial lighting of each case, and the effect of shading on the PV production. While Polysun 11 simulation software is used to estimate the PV energy production and the heating and cooling system energy demand of each case.

Building energy demand

Among the proposed PV cases, some cases could affect the building energy demand includes integrated the PV as a shading device, as proposed in case 2 (opaque overhang), case 3 (semi-transparent overhang), case 4 (horizontal (overhang) louver, case 5 (window integrated PV louver). While in case 6 (balcony integrated PV), and case 1 (stair façade integrated PV), the PV modules are attached to the building parts which are not directly connected with the indoor apartments' spaces. Regarding the case 7 (wall integrated PV), as mentioned before, it is assumed that the building energy demand is not affected by PV modules, as the wall is well insulated and there is an air gap between the PV modules and the wall.

the base case in this section refers to the improved apartment building in Amman, Jordan based on the analysis in Chapter 5. The building includes 10 apartments with a total heated area of 1,350 m², and in this case, there is no solar system installed. The building is already having a window integrated louver (without PV) as a shading device, the louvers are on during the cooling period from May to October.

The total annual energy demands for the heating, cooling and artificial lighting of the building, under the proposed PV application systems are compared and shown in Figure 7-23. It can be seen that there is an insignificant difference in the building energy demands among all the proposed cases, especially in terms of cooling and lighting demands. Regarding the heating demand, it is ranged between 17.2 MWh/year (12.7 kWh/m²/year) in case 0 to 19.5 MWh/year (14.5 kWh/m²/year) in case 3-B. Accordingly, the heating system fuel demand and the solar fraction are slightly different between the proposed cases, see Figure 7-26.

Figure 7-24 compares the energy demand of semi-transparent overhang PV systems with different transparency and capacity. System 3-B is selected in this study, as there is no significant increase in building energy demand, however, the PV energy production is higher, as the capacity is higher.

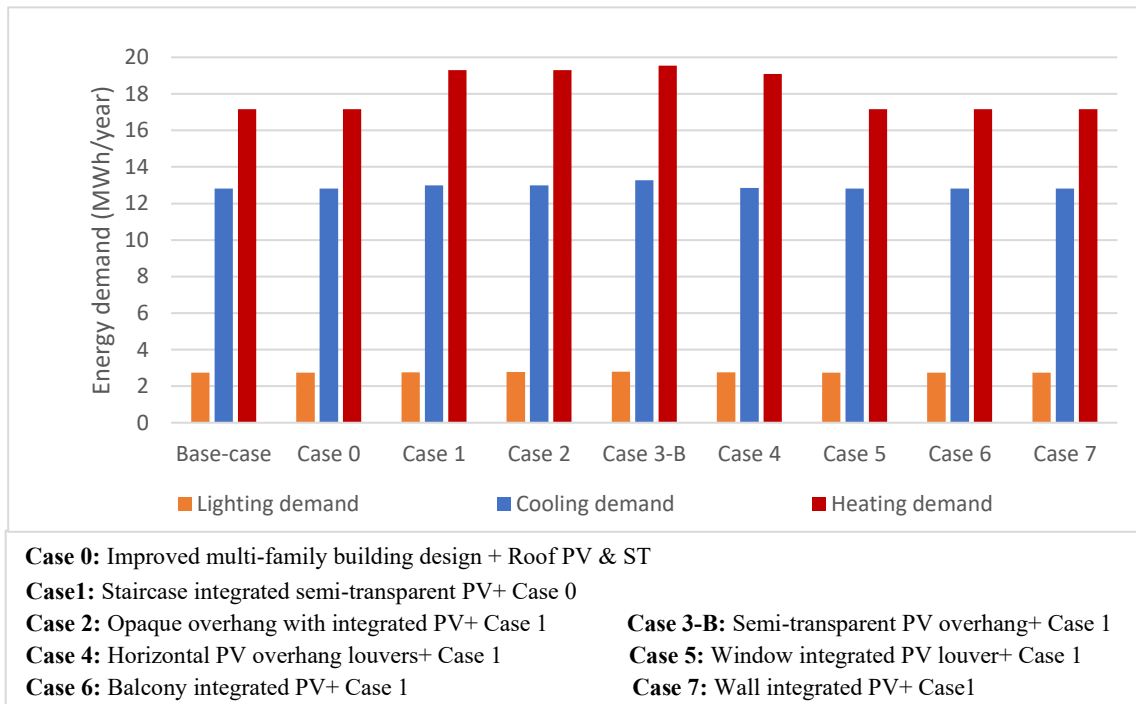


Figure 7-23: Annual energy demand for the improved multi-family building with 1,350 m² heated area in Amman, Jordan under different PV system design cases.

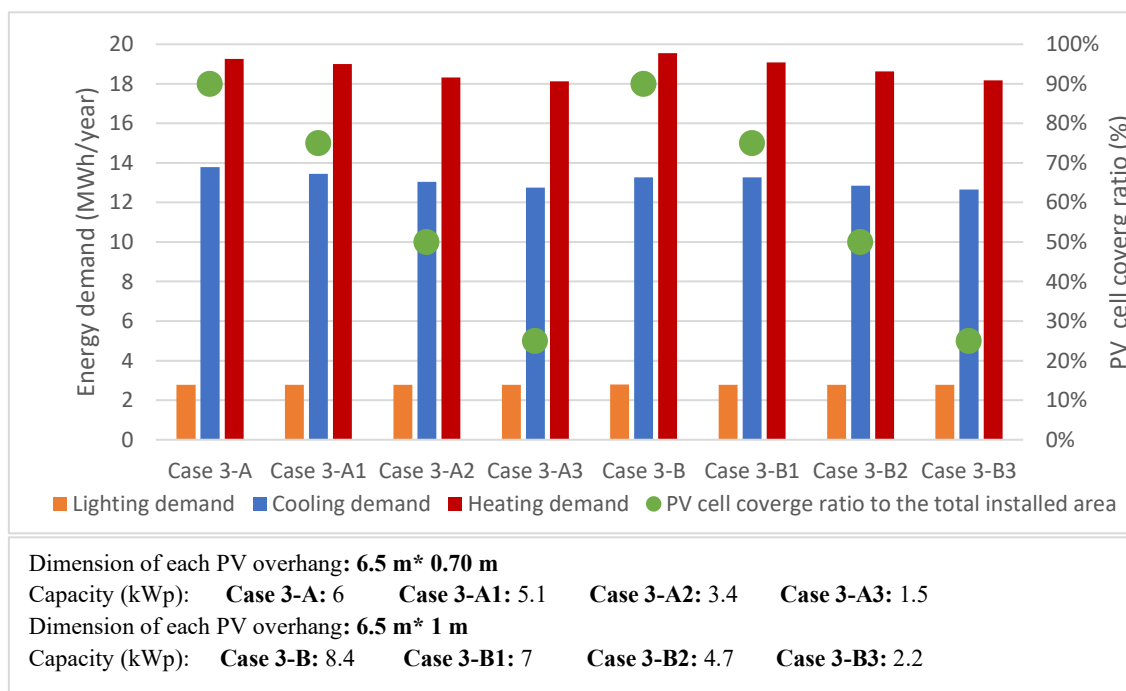


Figure 7-24: Annual energy demand for the improved multi-family building with 1,350 m² heated area in Amman, Jordan under semi-transparent PV overhang with different PV cell coverage ratio and PV overhang dimensions.

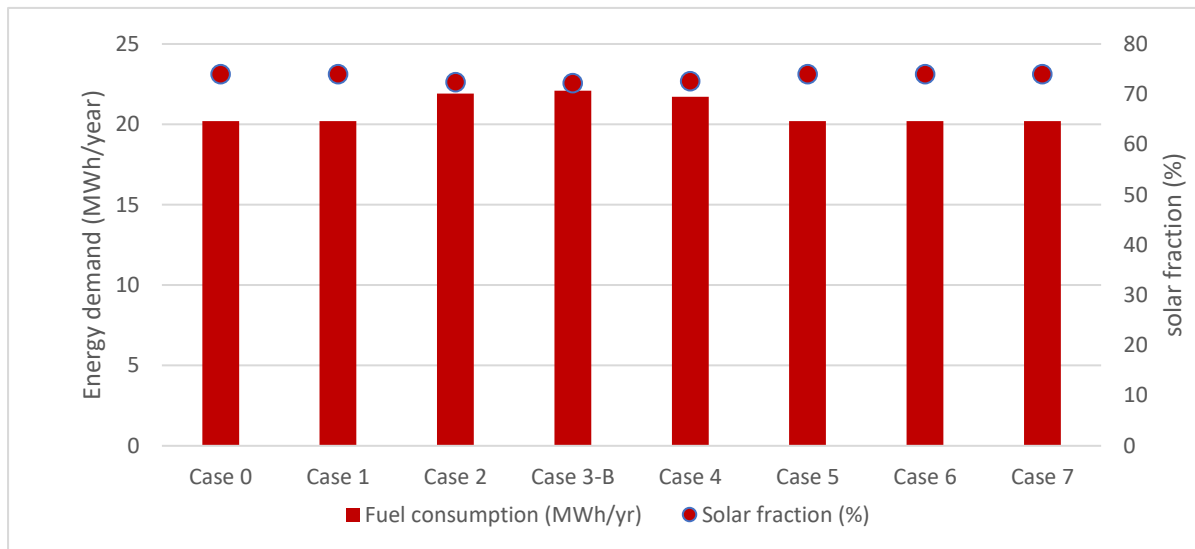
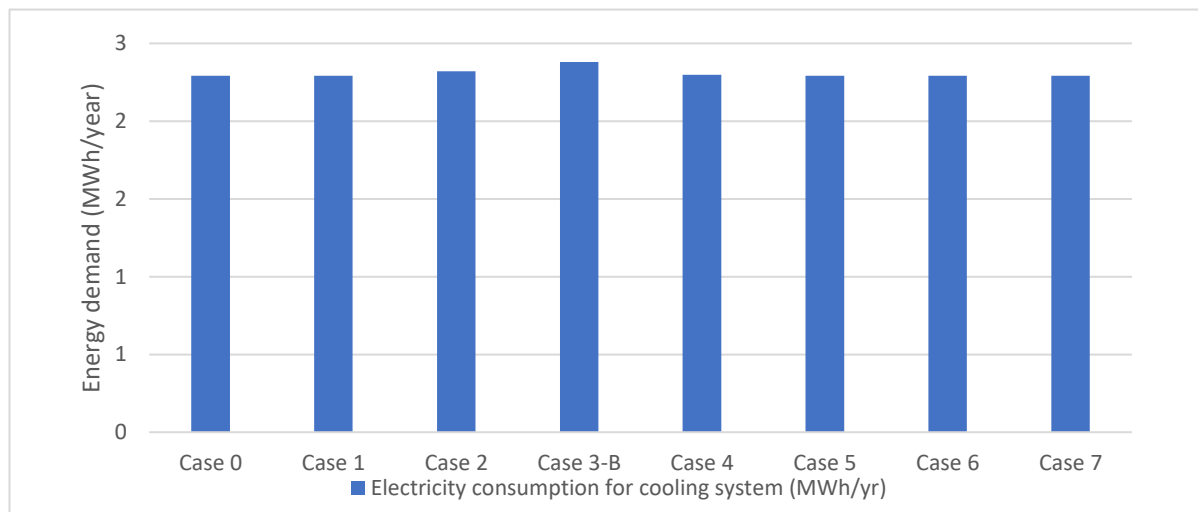


Figure 7-25: Annual solar heating system demand and solar fraction, for the improved multi-family building with 1,350 m² heated area in Amman, Jordan under different PV system design cases.



Case 0: Improved multi-family building design + Roof PV & ST

Case1: Staircase integrated semi-transparent PV+ Case 0

Case 2: Opaque overhang with integrated PV+ Case 1 **Case 3-B:** Semi-transparent PV overhang+ Case 1

Case 4: Horizontal PV overhang louvers+ Case 1 **Case 5:** Window integrated PV louver+ Case 1

Case 6: Balcony integrated PV+ Case 1 **Case 7:** Wall integrated PV+ Case1

Figure 7-26: Annual cooling system demand for the improved multi-family building with 1,350 m² heated area in Amman, Jordan under different PV system design cases.

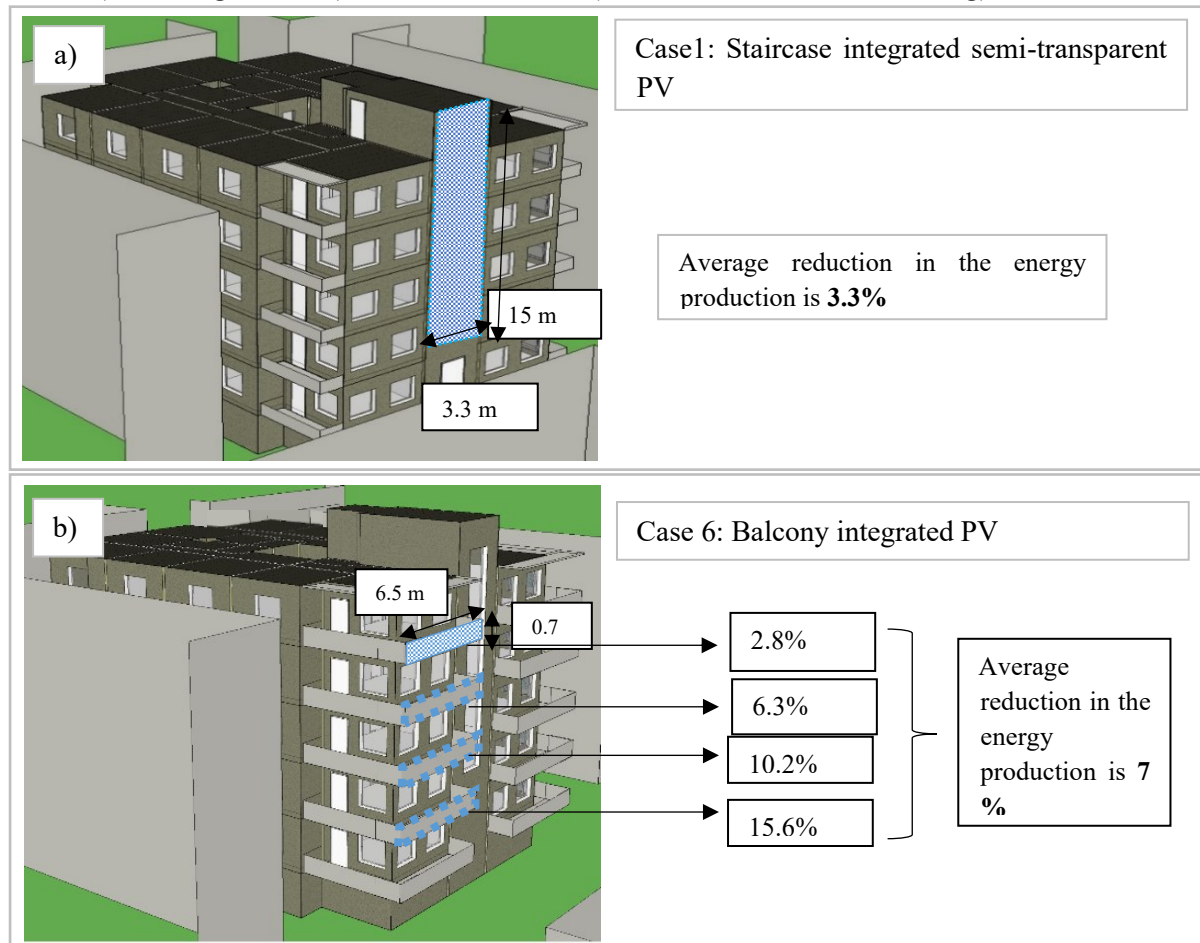
Based on the above discussion, the PV shading systems do not have a significant impact on the building energy demand as the base case building already have window integrated louver shading device and all the PV shading cases are well-designed to block the sun in summer and let it penetrate through the window in winter.

Energy production of PV systems

Polysun 11 simulation software is used to estimate the PV electricity generation. However, Polysun does not consider the reduction of electricity generated by PV due to the shading of the surroundings, therefore IDA ICE 4.8 simulation software is used to estimate the average reduction of the suggested shading photovoltaic system, as described below.

Shading effect

To estimate the effect of the surrounding building on the proposed PV façade production, several simulations have been done in IDA ICE for each case, the production of the PV module at different levels is estimated and compared to the production of the same module without any obstruction. For each case, the module has the same area, dimension, efficiency, and tilt angle. The reduction of the photovoltaic system is estimated as an average reduction of all the levels. As seen in Figure 7-27, generally, it can be said that the effect of the surrounding buildings on the PV electricity production is not significant, as the PV in all cases are installed to the south façade which is facing the main street, and the surrounding buildings are around 20 m² far from the façade. The results showed, that in all cases the upper level has the lowest energy reduction among all the cases as it is unobstructed, and the effect of shading is increased downwards (from the upper-level to lower-level). The reduction of PV energy production in the lower level ranging between 7.9% in case 7 (wall integrated PV) to 27.7% in case 4 (horizontal PV louver overhang).



Case name	Case 5: Window integrated PV louver	Case 2: Opaque PV overhang Case 3-A: semi-transparent PV overhang	Case 3-B: Semi-transparent PV overhang	Case4: Horizontal PV (overhang) louver
X (m)	0.27	0.7	1	1.3
Fourth	0	0.2	0.3	10.3
Third	1.8	8.7	12.8	20.7
Second	4.8	10.6	15.4	22.7
First	6.5	14	18.1	25.3
Ground	11.1	17	21.5	27.7
Average in the energy production	4.8	10.2	13.6	21.4

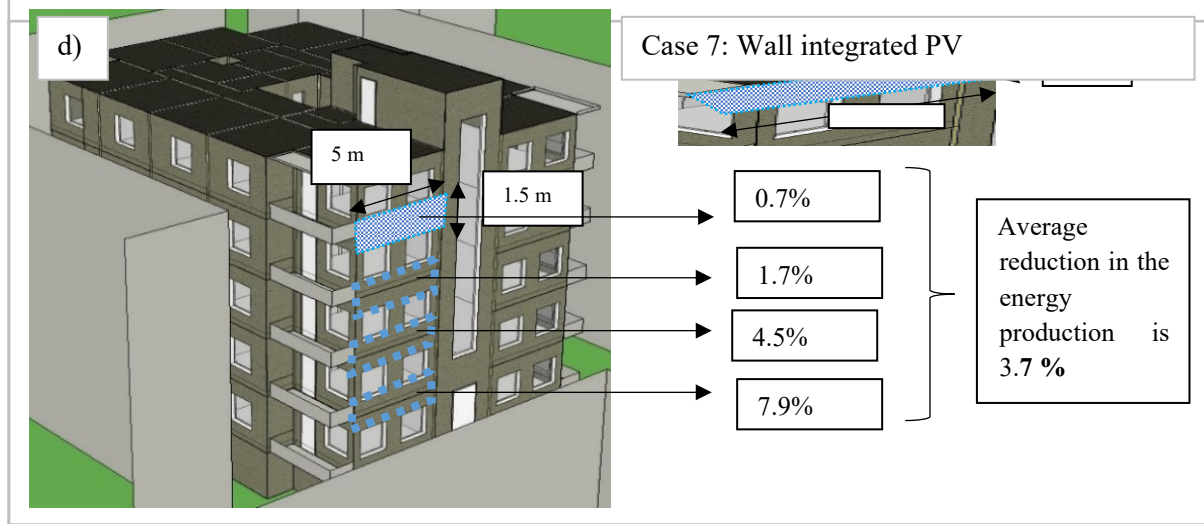


Figure 7-27: The effect of the surrounding building on the electricity reduction of PV façade systems installed on the south façade of multi-family building in typical urban context in Amman, Jordan.

- a) Case1: Staircase integrated semi-transparent PV,
b) Case 6: Balcony integrated PV,
c) Case 5: Window integrated PV louver, Case 2: Opaque PV overhang, Case 3-A: semi-transparent PV overhang, Case 3-B: Semi-transparent PV overhang Case4: Horizontal PV (overhang) louver
d) Case 7: Wall integrated PV

Electricity production of PV systems

The electricity production and the capacity of the proposed PV system design cases are presented in Figure 7-28. The highest electrical output is obtained from the roof PV system (case 0) with 21.5 MWh/year, and it covered around 54% of the total building electricity demand. While, the façade PV systems generate electricity, which is equivalent to 13% to 43% of the total building electricity need. Accordingly, the roof and façade PV systems can cover up to 97% of the building electricity demand as in case 3-B (semi-transparent PV overhang), see Figure 7-29. Moreover, it can be noticed, that the produced electricity per kWp in some of the proposed PV façade system is slightly lower than the roof PV system. As with the roof application (case 0) the produced energy is about 1,700 kWh/kWp, while in the PV façade system cases which the PV modules are 30° tilted the produced electricity is ranging between 1,340 kWh/year in case 4 (horizontal PV overhang louvers) and 1,655 kWh/year in case 5 (window integrated PV louver). For vertically installed PV systems the produced energy is ranging between 970 kWh/kWp in case 7 (wall integrated PV) and 1,000 kWh/kWp in case 6 (balcony integrated PV). The difference in the PV produced electricity per kWp is due to the difference in the tilted angle and the effect of shading from surrounding building on the PV efficiency.

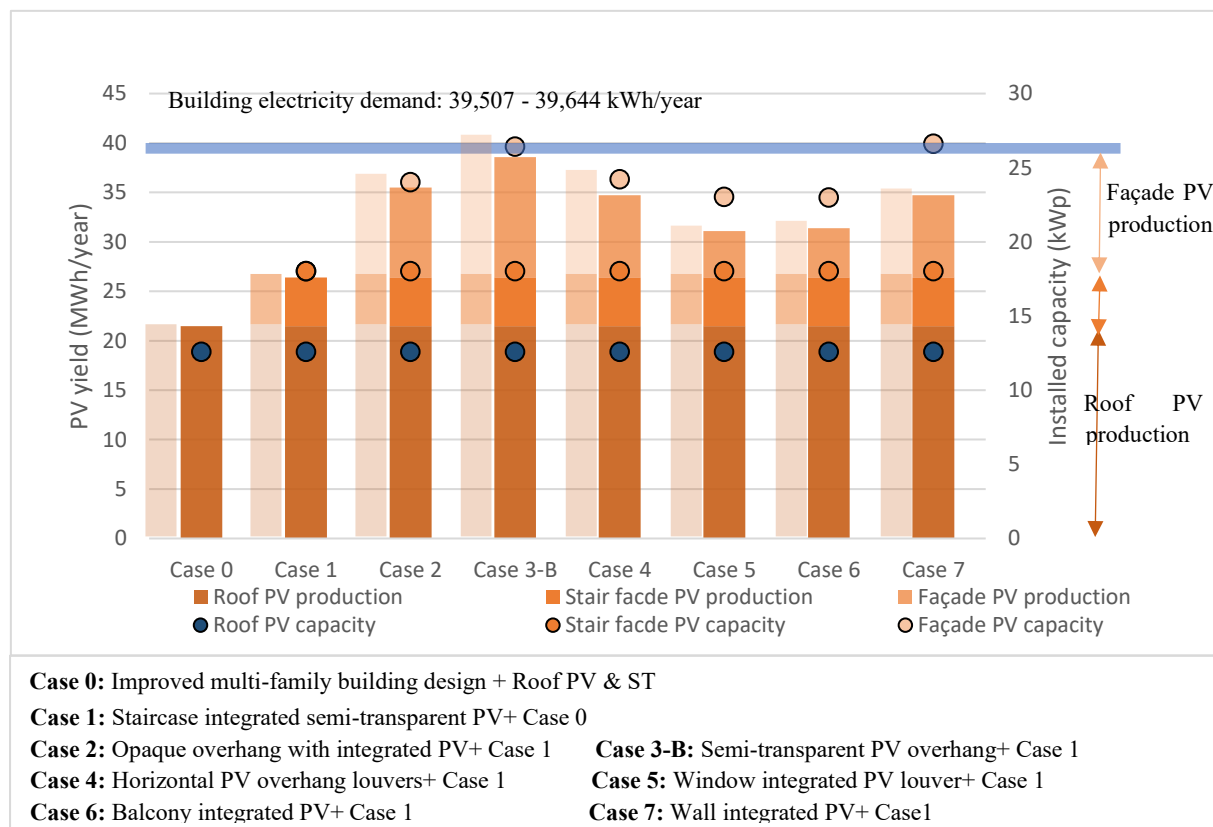


Figure 7-28: Total power capacity and electrical energy production of the proposed PV systems, installed to the improved multi-family building in Amman, Jordan.

Based on the previous results, there is a potential of installing the PV into the façade to cover the building electricity demand, especially in the building with a greater number of floors, and therefore a more façades area and less roof area.

It must be mentioned that in this research, the total electricity benefits of the PV include both the direct consumption and the electricity, which is sold to the grid, considering the grid losses of 2.3% as mentioned in Chapter 0. In all the proposed PV cases, the direct energy consumption is ranging from 11.8 to 13.6 MWh/year, which is equivalent to 30% to 35% of the total building electricity demand.

Overall energy index

As mentioned before, evaluation of the energy performance of the integrated PV should be carried out in terms of the overall energy performance, considering the annual net electricity production of PV and the annual primary energy demand (heating system, cooling system, lighting, and equipment) of the building. Figure 7-29 shows the net PV electricity production and the percentage of net electricity saving for the building for different PV facade design systems, and the PV roof system and compares it to the base case where no PV systems are installed. The effect of PV systems on the building cooling, heating, and lighting demand is also considered. It can be seen that the net electricity demand in the base case is about 39.5 MWh/year (29 kWh/m²/year) and in case of the roof PV, it is decreased to about 18 MWh/year (13.3 kWh/m²/year), while in case of roof and façade PV installation the net electricity demand of the building could be decreased to about 1,1 MWh/year (0.8 kWh/m²/year).

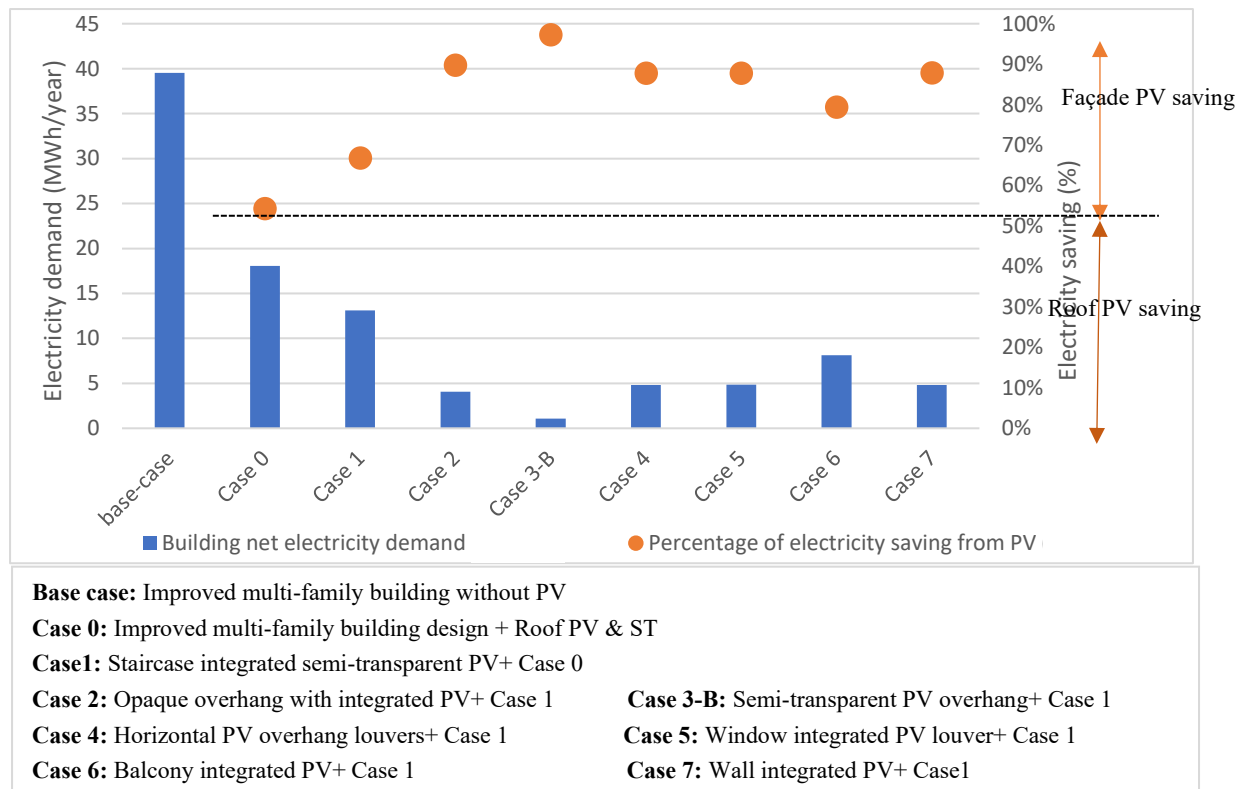


Figure 7-29: Net electricity demand of the multi-family building with 1,350 m² total heated area, in Amman, Jordan, and the electricity-saving percentage of different PV systems in comparison to the base case (no PV installation).

In order to compare the overall energy performance of the different cases with the base case, all the energy demands have been converted into primary energy, the conversion factor of electricity to primary energy is 2.71 and the factor of oil to primary energy is 1.1, as described under the methodology chapter (Chapter 4.5.1), see Table 6-2.

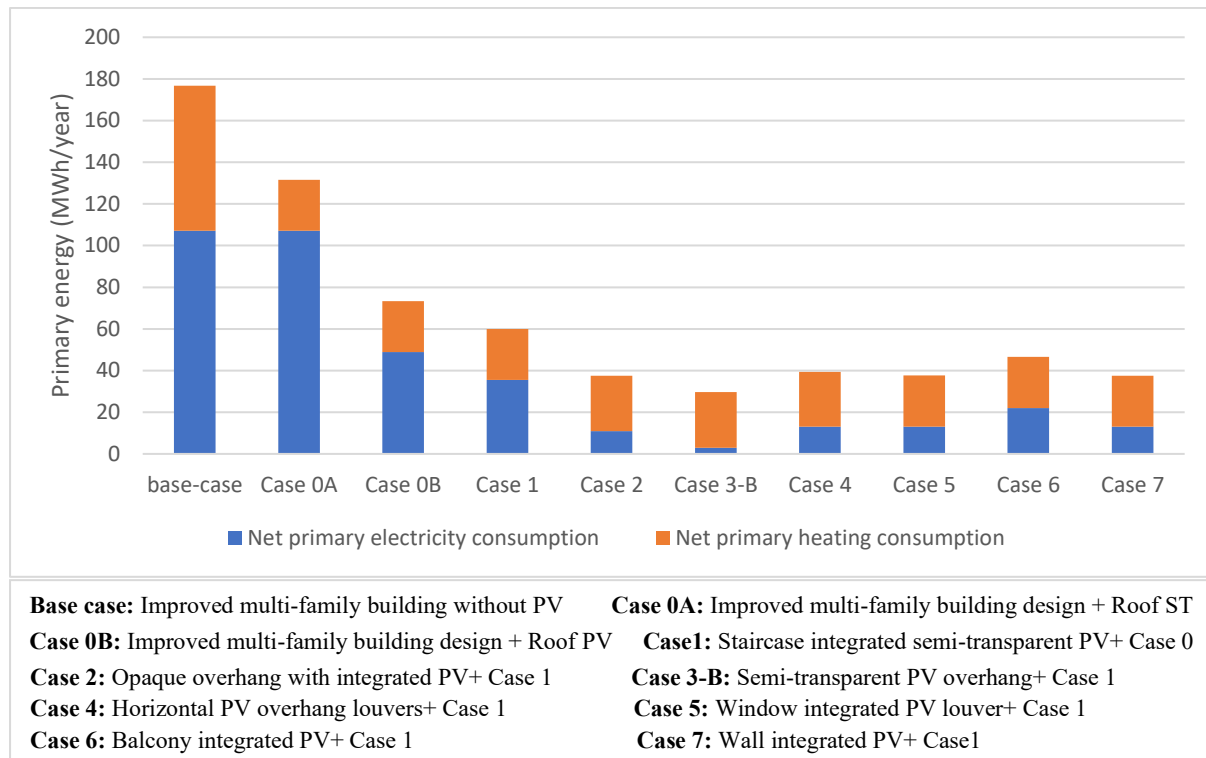


Figure 7-30: Annual primary energy demand of the different solar energy installation cases and compare it to the base case without ST and PV installation, all systems are installed into the improved apartment building with 1,350 m² heated area in Amman, Jordan. Note: the installed area for the solar thermal system is the same in all cases.

7.5 Summary

This chapter started with analyzing the potential building envelope parts, which are suitable for installing the solar technology (ST & PV), by analyzing the solar radiation, shading from the surrounding buildings, and the available building surface area. The results of this part, showed that the highest potential envelop part of installing the solar technologies is the roof as it is unshaded and received the highest solar radiation, followed by the south facade, as the surrounding building is about 20 m far from it, and received the highest solar radiation among all the façades.

After that, as the highest solar architectural suitable building envelop part is the roof, the energy potential of PV and ST installation with different arrangements (tilts angle, direction, space between arrays, etc.) on the roof was investigated and compared to the traditional PV and ST roof arrangement where all the solar modules and collectors are 30° tilted and facing the south. Among the different arrangements, one case was selected based on the energy production potential, where most of the PV modules are mounted on the roof with 2° tilted angle, and part of PV modules are integrated into the staircase roof with 30° tilted angle, the selected system can cover 54% of the building electricity demands. Regarding the ST, all the collectors are mounted on the roof facing the south and 30° tilted, and this system can cover 74% of the building space and water heating. Moreover, it was found that increasing the ST installed capacity, does not improve the solar fraction significantly.

Subsequently, the energy-saving potential of installing the PV into the south façade (in addition to the selected roof PV and ST arrangement) was investigated with different design possibilities, including PV integrated shading device, wall integrated PV, balcony integrated PV, etc. The analysis of this part was done in terms of overall energy performance, including the effect of PV façade application on the building heating, cooling, and artificial lighting demands, and on the PV electricity production considering the effect of shading on the PV production. The results showed that roof PV application can cover 54% of the building electricity demand, and with both façade and roof PV application the covered building electricity demands are between 66% and 97%.

8 Life cycle assessment of photovoltaic applications

8.1 Introduction

This chapter considered the life cycle performance of the previous proposed PV cases, as presented in Chapter 7. The life cycle of the building and the solar thermal system are not included in this research, as it the same in all cases. The analysis is conducted to evaluate the energy, environmental and economic performance of PV systems over its lifetime, which is installed on the roof and façade of the residential apartment building in Amman, Jordan. The performance of PV façade applications not only included electricity generation capabilities, but also the effects on the building energy demand, including electricity demand for cooling, equipment, and artificial lighting, and fuel demand for space and water heating. Energy simulations, previously performed (as discussed in Chapter 7), are adopted to conduct a life cycle assessment to determine the long-term performance in terms of energy and carbon emissions, as well as cost considerations.

The lifetime of the PV modules is assumed to be 25 years. This is also the warranty given by the producers and is also in accordance with the IEA framework for BIPV life cycle assessment and with the latest Ecoinvent database recommendation (Fthenakis and Kim, 2011; Jungbluth et al., 2012; Frischknecht et al., 2016). The inverter life is assumed to be 15 years, therefore, two inverters were required over the 25 year lifetime (Fthenakis and Kim, 2011). Other replacement parts are considered negligible and therefore, disregarded in the calculation. It is also assumed that the electricity production of PV systems reduced by 80% of the initial efficiency at the end of the lifetime (Perez and Fthenakis, 2011).

8.2 Energy life cycle performance

As discussed in the previous chapter, a holistic evaluation of PV facade energy performance should include all its energy-related impacts on a building, including photovoltaic electricity generation, electricity demand for cooling, lighting and equipment, space and water heating system demand. From the simulation results in Chapter 7, the annual simulation results are used to determine the 25 years life cycle energy performance of the PV systems.

The life cycle energy performance results for the studied PV cases are presented in Table 8-1, Figure 8-1 and Figure 8-2. The base case here refers to the improved building without any installed solar system. Avoided CO₂ emissions and primary energy due to the PV system production are calculated based on the output of each system in the entire life cycle. Jordan's national grid electricity mix is considered here, the carbon emissions of Jordan's grid electricity is 0.643 kgCO₂/kWh (Hammad and Ebaid, 2015), and the primary energy factor is 2.71, as described under the methodology Chapter 4.5.1.

Table 8-1, Figure 8-1 and Figure 8-2 show the PV electricity production, net electricity demand and the percentage of net electricity savings over 25 years, for the building for different PV facade design systems, and PV roof system and compares it to the base case where no PV systems are installed. The roof and façade PV systems can cover up to 89% of the building electricity demand over 25 years as in case 3, however, as discussed in Chapter 7, the covered electricity under the same case in the first year is around 97%.

Table 8-1: Annual and life cycle energy performance over 25 years, of the different solar PV installation cases and compare them to the base case without PV installation.

Case name	Life cycle PV electricity production (MWh/25year)	Life cycle net electricity demand ^a (MWh/25year)	Life cycle avoided primary energy (MJ)	Life cycle avoided carbon emissions (kgCO ₂ /MWh)
Base case		988.2		
Case 0	600.4	499.9	1,323,090	313.9
Case 1	807.2	387.5	1,627,140	386
Case 2	617.3	181.6	2,187,587	519
Case 3	876.8	114.3	2,376,106	563.8
Case 4	789.2	199.1	2,138,684	507.4
Case 5	706.9	281.2	1,915,867	454.6
Case 6	713.7	274.4	1,934,228	458.9
Case 7	789.4	198.8	2,139,192	507.6

Base case: Improved multi-family building without PV

Case 0: Improved multi-family building design + Roof PV & ST

Case 1: Staircase integrated semi-transparent PV+ Case 0

Case 2: Opaque overhang with integrated PV+ Case 1

Case 4: Horizontal PV overhang louvers+ Case 1

Case 6: Balcony integrated PV+ Case 1

Case 3: Semi-transparent PV overhang+ Case 1

Case 5: Window integrated PV louver+ Case 1

Case 7: Wall integrated PV+ Case 1

Note ^a Building electricity demand (cooling, lighting, and equipment)- PV production.

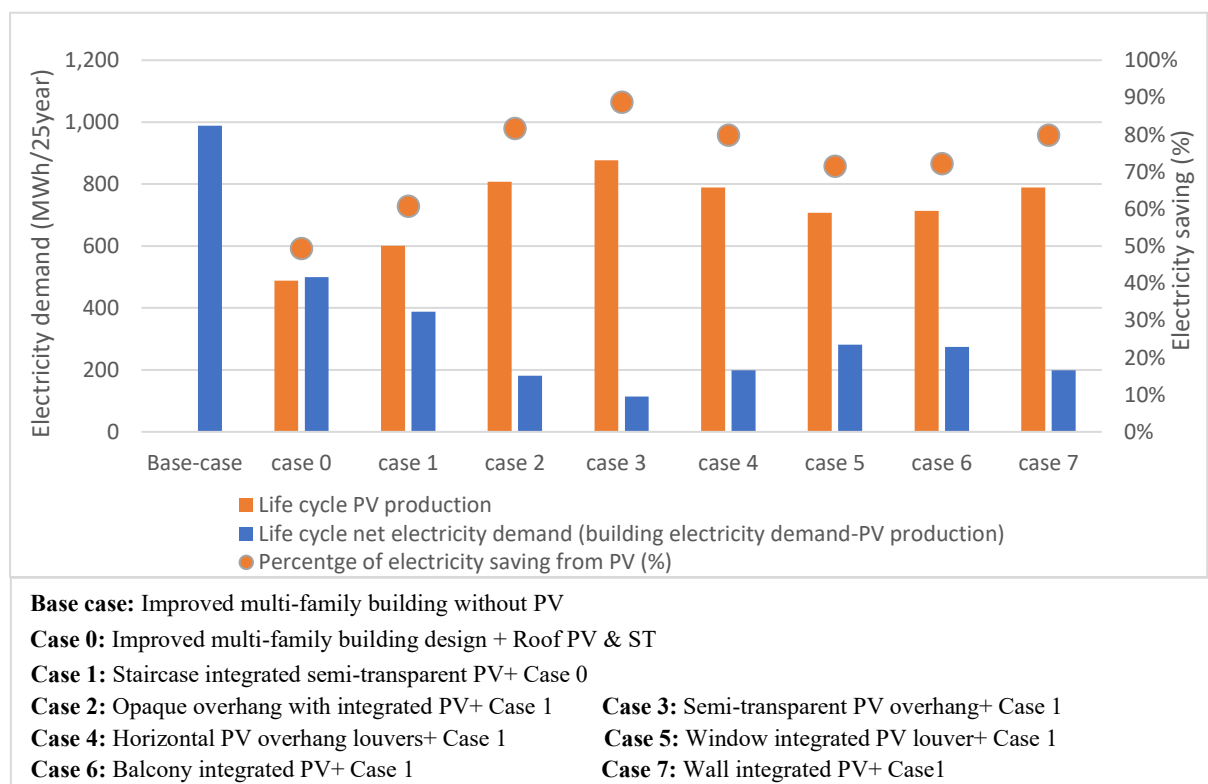


Figure 8-1: Net electricity demand of the multi-family building with 1,350 m² total heated area, in Amman, Jordan, and the electricity-saving percentage of different PV systems in comparison to the base case (no PV installation).

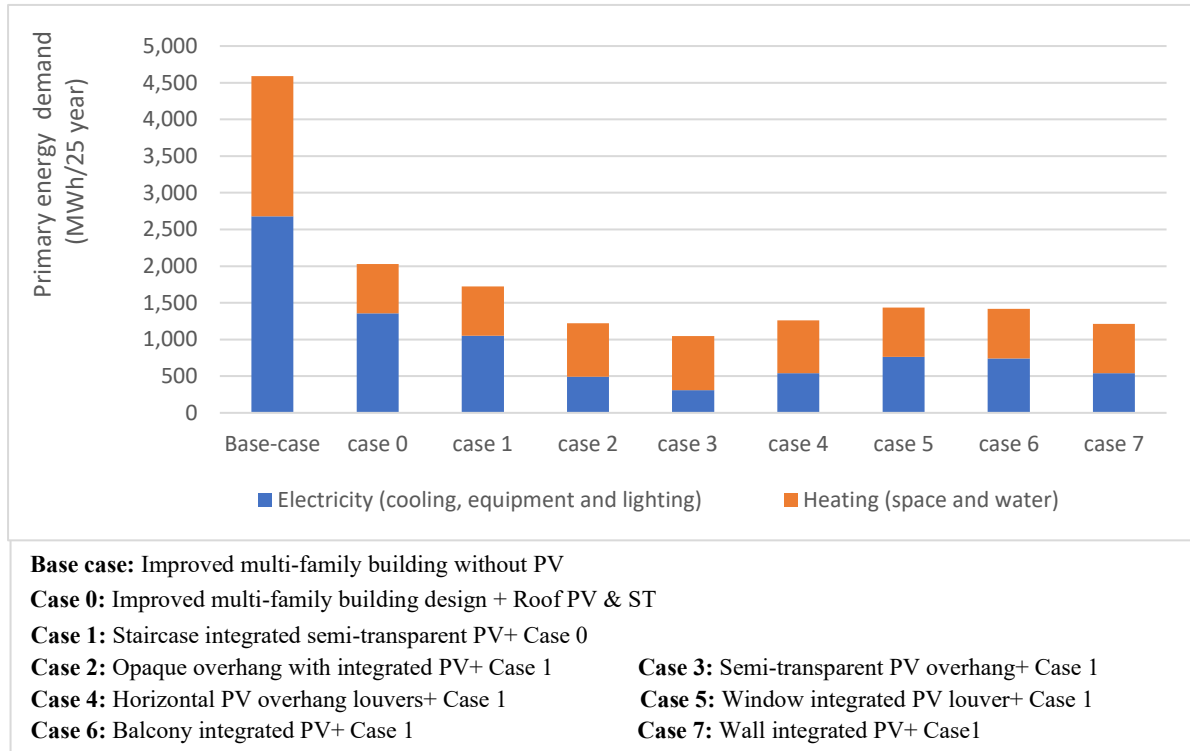


Figure 8-2: Annual primary energy demand of the different solar energy installation cases and compare it to the base case without ST and PV installation, all systems are installed into the improved multi-family building with 1,350 m² heated area in Amman, Jordan. Note: the installed area for the solar thermal system is the same in all cases.

8.3 Environmental life cycle performance

As mentioned in the literature review (Chapter 3.2.5), photovoltaic technology is widely recognized as the cleanest power generating technology, however, some argue that it consumes additional energy during its life cycle, particularly in the manufacturing processes, which may be larger than its energy output in its lifetime (Zhang, Wang and Yang, 2018). Therefore, in order to holistically examine the environmental performance of the photovoltaic system, an LCA which considers the entire life of the proposed PV systems is studied here. Starting with the manufacturing of BIPV components from raw materials, their transport from the country of origin to the site in Jordan, installation on-site, operation and maintenance, and disposal/recycling of waste (Peng, Huang, and Wu, 2011; Lenz *et al.*, 2012). Figure 8-3 shows the diagram of the LCA stages of a PV system. For each process-step direct uses as well as the indirect (grey) demand for energy due to the use of materials consumables necessary for manufacturing and raw materials are considered (Perez and Fthenakis, 2011).

As mentioned before, different manufacturers have different energy requirements for silicon purification and crystallization processes, which increases the difficulty of the research. Finally, there is a fast-technological improvement in the PV industry and cell production, and the energy demands of mono-Si module manufacturing are hard to predict correctly. So, this paper performs the life cycle assessment survey for the mono-Si PV system and discusses the efficiency of energy payback based on the data in the prior literature.

The IEA framework for BIPV LCA assessment is used with the latest Ecoinvent database (version 3.3) (Jungbluth et al., 2012; Frischknecht et al., 2016), along with secondary database from literature to determine the life cycle energy and material requirements of BIPV systems (including modules, BOS and installation), and are modified to represent the actual scenario. The used indicators for evaluating the environmental impacts of PV systems are the cumulative energy demand (CED), greenhouse-gas emissions (GHG), energy payback time (EPBT) and carbon payback time (CPBT), which are very common for the LCA (Frischknecht *et al.*, 2016; P. Wu *et al.*, 2017). As more than 95% of the energy of Si module production is used as electricity the CO₂ emissions due to module production can be estimated rather quickly, using the average value of the emissions caused using electricity from the public electricity grid for the involved country (China). Other effects on the environment, like acidification, eutrophication and abiotic depletion, etc., from mono-Si PV systems not considered in this research.

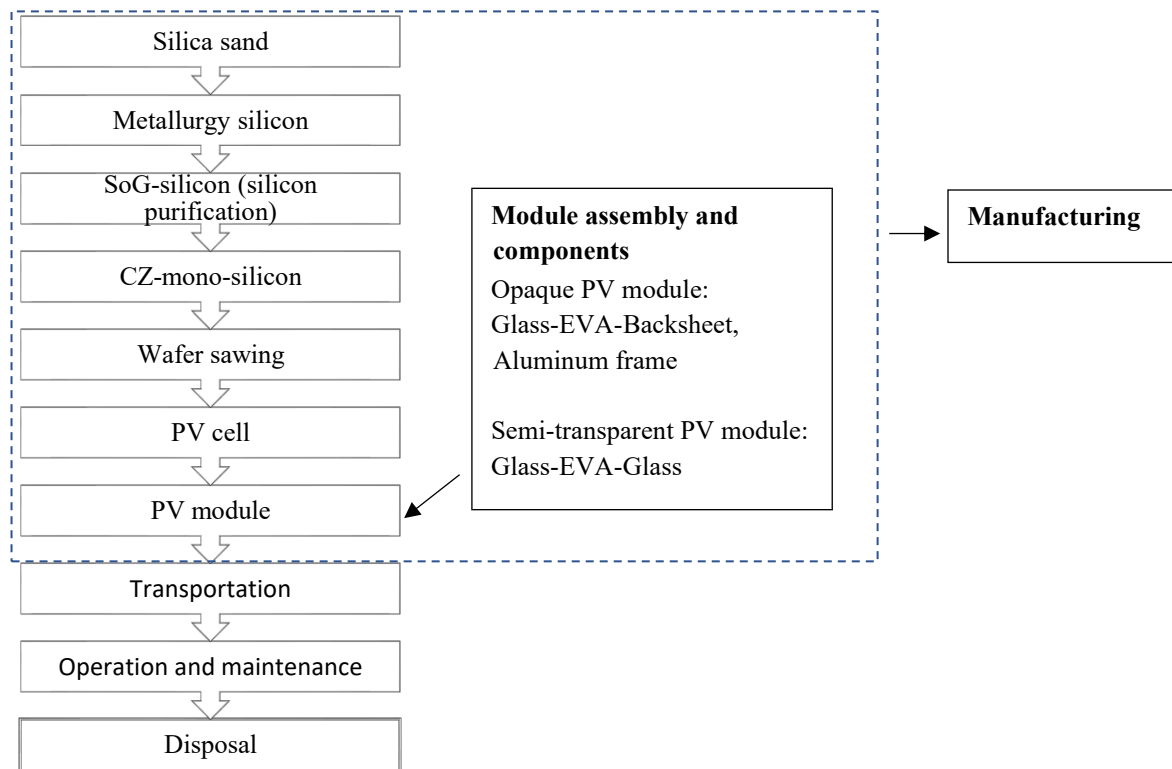


Figure 8-3: The life cycle stages of a mono-Si PV module. Source of data: (Gaidajis and Angelakoglou, 2012; Zhang, Lv and Zhang, 2012).

More details regarding the environmental LCA methodology, performance indicators, etc., have been presented under the methodology chapter (Chapter 4.5.2). The following sections discuss the assumptions used for the life cycle inventory and the estimated embodied energy and carbon emissions for PV systems in different stages.

8.3.1 Manufacturing of PV module

Data source:

The embedded energy in the PV-module (including their materials/processes) is estimated using the Ecoinvent database (Jungbluth et al., 2012) and data presented in (Fthenakis and Kim, 2011; Fu, Liu and Yuan, 2015; Hou et al., 2016). The manufacturing data thus obtained is modified to reflect the country-specific electricity mix used during the manufacturing process based on country of origin. It is assumed that all the PV modules are manufactured in China, as it is one of the world's largest PV producers today (IEA, 2018a).

The production of these PV modules needs considerable energy and since China's primary energy source is coal, therefore the production of PVs indirectly contributes to greenhouse gas (GHG) emissions (Fu, Liu and Yuan, 2015). The GHG emission factor of China's grid electricity is (1.170 kgCO₂/kWh) and the energy conversion factor (11.3 kWh/MJ) (Jungbluth et al., 2012).

As mentioned before, the used PV cell technology in this research is mono-crystalline (mono-Si), due to it is relatively high efficiency and high reliability (based on the discussion in Chapter 3.2.3). Moreover, three types of mono-Si PV module designs are proposed in this research as presented in Chapter 7. Which are: frameless double-glass PV modules (glass/ encapsulant/ cell/ encapsulant/ glass), the conventional PV modules (glass/ encapsulant/ cell/ encapsulant/ back sheet laminate with an aluminum frame) and frameless PV opaque modules (glass/ encapsulant/ cell/ encapsulant/ back sheet). Table 8-2 illustrates the characteristics of the PV modules that are adopted in this part of the research based on a commercially available module (De Wild-Scholten, 2013).

Table 8-2: The characteristics of the PV modules. Source of data: (De Wild-Scholten, 2013).

Parameter	Unit	Opaque module	Semi-transparent module (90% cell coverage ratio)
Module size	m	1.62 x 0.986 x 0.035	1.62 x 0.986 x 0.035
Mass	kg	20	20.2
Frame		Aluminum alloy	
Front glass	mm	3.2 (10.07 kg/m ²)	2 (6.3 kg/m ²)
Back glass	mm	-	2 (6.3 kg/m ²)
Back sheet	mm	330	-
Wafer thickness	mm	200+-20	200+-20
Module efficiency	%	14.2	14.2
Peak capacity per module	kWp	236	236

- **Silicon process and materials**

Table 8-3 summarizes the input and output of materials actually valid for the Chinese PV-industry based on the result of surveys at Chinese PV-factories and is used for conversion purposes during the calculation phase of the life cycle assessment (Fu, Liu and Yuan, 2015).

Table 8-3: Materials input and output for the PV production value chain. The data is representative of the actual state of the art of the Chinese PV industry. The table is used as a mean of conversion for the calculation presented in this chapter.

Material input in m ² module	Output after process
2.5 kg of silica sand	1kg MG-Si
1.3 kg MG-Si	1.0 kg SoG-Si
1.2 kg SoG-Si	1.0 kg CZ-mono (Czochraiski mono-crystalline)
1.2 kg CZ-mono	Wafers 1m ² each (156 mm*156 mm)
1.06 m ² wafer/cell	0.93 m ² cell (38 cell/m ²)

Figure 8-4 presents the process steps and assumptions in the production of the mono-Si PV module. The names within boxes correspond to the products of individual production steps. The direct electricity requirements (or uses) of the steps are also shown, adapted from (Fthenakis and Kim, 2011; Jungbluth et al., 2012; Fu, Liu and Yuan, 2015; Hou et al., 2016)

The LCA calculation is simplified in the sense that only the primary route of silicon manufacturing is considered and no feedbacks from the material uses are considered.

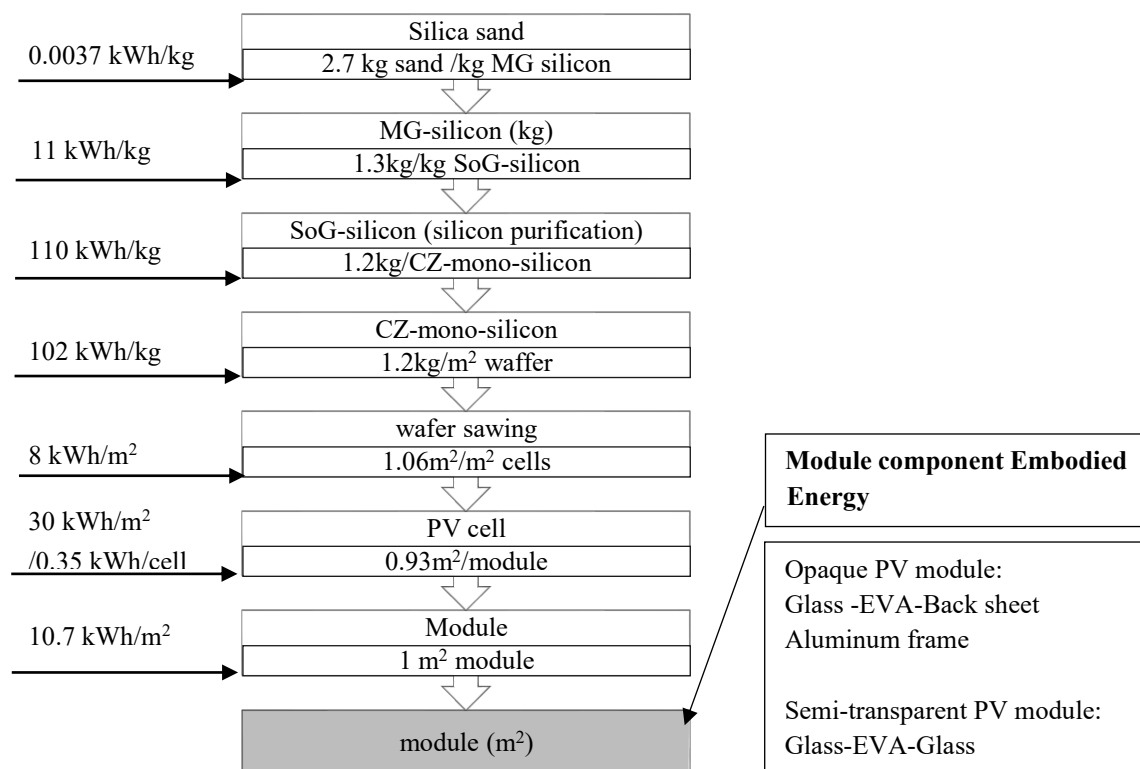


Figure 8-4: Process steps in the production of mono-Si PV module. The horizontal arrows give the electricity requirements for the main steps of the PV production. The vertical arrows represent the exchanges between two consecutive steps. MG=Metallurgical Grade; SG=Solar Grade; CZ=Czochralski Process. Source of data: (Fthenakis and Kim, 2011; Jungbluth et al., 2012; Fu, Liu and Yuan, 2015; Hou et al., 2016).

Based on Table 8-3 and Figure 8-4 the primary embodied energy for silicon process and materials are calculated and presented in Table 8-4, the other module components (frame, glass, etc.) are presented in the next part.

Table 8-4: Primary embodied energy and carbon emission for the silicon process and material required for the 1 m² PV module.

Process of mono-silicon cell manufacturing	Primary embodied energy (MJ/m ²)			Carbon emission (kgCO ₂ /m ²)	Note
Quartz mining energy consumption (Silica sand)	0.11			0.011688	
Metallurgical grade silicon MG-Si	190			16.7	
Solar grade silicon SoG-Si	1,491			168	by a modified Siemens process
Ingot casting Czochralski mono-crystalline silicon (CZ-mono-Silicon)	1,383			143	
Wafer production	93.11			9.6	30% of silicon material loss is considered for wafer production due to the sawing process
Solar cell production	Cell coverage ratio	Number of cells cell/m ²	Embodied energy MJ/m ²		This value is modified for different PV modules according to the PV cell coverage ratio (transparency). Embodied energy for each cell is 3.95MJ/cell
	90%	38	150	14.6	
	75%	31	122	11.9	
Total (silicon process)					
Opaque module	3,309			353	
Semi-transparent module (90% cell coverage ration)	3,309			353	
Semi-transparent module (75% cell coverage ration)	3,280			349	

- **Module assembly and components (other than silicon cells) energy input**

Table 8-5 and Table 8-6 present the energy demand for producing one m² of PV module, including embodied energy and carbon emission in material based on previous research (Hammond and Jones, 2011; Jungbluth *et al.*, 2012; De Wild-Scholten, 2013). Moreover, the average energy demand for assembly of 1 m² of PV module is 3.74 kWh, accordingly, the embodied energy consumption is calculated as 42.26 MJ/m² and the carbon emission is 4.4 kgCO₂/m².

Table 8-5: Primary embodied energy and carbon emission for the opaque PV module component required for 1 m² PV module.

Layer	Material	Weight (kg/m ²)	Embodied energy (MJ/kg)	Primary embodied energy (MJ/m ²)	Carbon (kgCO ₂)	Total carbon (kgCO ₂ /m ²)
Front sheet	low iron glass, tempered	10.07	11.5	115.8	0.86	8.66
Encapsulation	Ethyl Vinyl Acetate (EVA)	0.675	128	86.4	2.3	1.55
Back sheet	Tedlar &Polyester	0.19	64.1	12.2	0.68	0.13
copper ribbons for cell interconnection	Copper	0.1	42	4.2	2.6	0.26
frame	Aluminium	2.13	155	330.15	8.24	17.55
Total Without frame With frame				219 589		10.6 28.1

Table 8-6: Primary embodied energy and carbon emission for semi-transparent PV module component required for 1 m² PV module.

Layer	Material	Weight (kg/m ²)	Embodied energy (MJ/kg)	Embodied primary energy (MJ/m ²)	Carbon (kgCO ₂)	Total carbon (kgCO ₂ /m ²)
Front sheet	low iron glass, tempered	6.3	11.5	72.45	0.86	5.418
Encapsulation	Ethyl Vinyl Acetate (EVA)	0.675	128	86.4	2.3	1.552
Back sheet	low iron glass, tempered	6.3	64.1	72.45	0.68	5.418
copper ribbons for cell interconnection	Copper	0.1	42	4.2	2.6	0.26
Total				235.5		12.648

- **Balance of system components**

It usually includes inverters, cables, support structures, and connectors. However, only the inverter and the support structure are considered in this research as the remaining components (wiring, conduits, connections, etc.) have a low contribution to the embodied energy (Alsema, de Wild-Scholten and Fthenakis, 2006).

Support structures

Two principal options exist when mounting a photovoltaic module on buildings: building-integration or frame-mounting (Jungbluth et al., 2012). A module for frame-mounting means that the laminate needs an aluminum frame, this profile is already accounted for in the previous part. The actual support structures for PV modules required additional aluminum or steel. Table 8-7 presents the amount of kg of steel and aluminum per m² of the PV module and the embodied energy for both mounted structure and integrated structure, which are obtained from the previous research (Jungbluth et al., 2012). Direct energy required for mounting labor is considered insignificant compared to other requirements. However, both direct and indirect embodied energy are considered.

Table 8-7: Embodied energy and carbon emission for the mounting structure and integrated structure per m² of the PV module. Source of data: (Jungbluth et al., 2012).

Type of structure	Mounted façade structure			Integrated façade structure		
Indirect Primary embodied energy	Material	Quantity/m ²	MJ/m ²	Material	Quantity/m ²	MJ/m ²
	Aluminium	2.64	409	Aluminium	3.27	506
	Steel	1.8	36	Steel	0	0
Direct embodied energy		kWh/m ²	MJ/m ²		kWh/m ²	MJ/m ²
	Screws	0.02	0.226	Screws	0.02	0.226
	Aluminium Profile	0.02	0.226	Aluminium Profile	0.02	0.226
Total Embodied Primary Energy	455.7 MJ/m²			516.7 MJ/m²		
Indirect carbon	Material	Carbon kgCO ₂ /kg	Total carbon kgCO ₂ /m ²	Material	Carbon kgCO ₂ /kg	Total carbon kgCO ₂ /m ²
	Aluminium	8.24	21.75	Aluminium	8.24	26.94
	Steel	1.37	2.466	Steel	1.37	0
Direct carbon	0.0468			0.0468		
Total carbon kgCO₂/m²	24.3			27		

Inverters

Limited information exists on the embodied energy of various sizes of inverters. In this research, the energy and material demand data for inverter manufacture are adapted from the Ecoinvent database, the selected inverter database is for the medium-sized system with a nominal capacity of 2.5 kW (Jungbluth et al., 2012). Although the inverter weight per nominal kW generally decreases as the nominal power rating increases, which means that energy demand induced by inverter production becomes less and less important as plant size increases (Jungbluth et al., 2012). Table 8-8 presents the direct and indirect embodied energy demand for inverter production, all the data is downscaled to correspond to an inverter capacity of 1 kW. Regarding the inverter size, it is recommended to use 0.89 kW inverter/kWp modules (Stetz, Braun and Engel, 2011).

Table 8-8: Energy demand for inverter production, including direct and indirect embodied energy and carbon emission. Source of data: (Jungbluth et al., 2012).

Direct embodied energy demand for inverter production					
Material	Quantity, kg	Embodied energy MJ/kg	Primary embodied energy (MJ/ kW)	Carbon kgCO ₂	Total carbon kgCO ₂ /m ²
Steel	9.8	20	208	1.37	13.4
Aluminium	1.4	155	217	8.24	11.53
Copper (transformers, wire-wound)	5.5	42	231	2.6	14.3
Total indirect			656		39.23
Indirect embodied energy demand for inverter production					
	Energy consumption kWh/kWp	Primary embodied energy (MJ/kW)		Total carbon kgCO ₂ /kW	Total carbon kgCO ₂ /m ²
Energy consumption	21.2	241.7		24.8	3.1
Total direct and indirect	897.7	Embodied energy (MJ/ kW)		64.03	42.33

Summary of manufacturing stage embodied the energy and associated carbon emissions

Results of embodied energy and carbon emission analysis of manufacturing the PV system are summarized in Table 8-9. The primary energy required, and the carbon emissions of the silicon process are around 70% of the total values, with 3,309 MJ/m² primary embodied energy, and 353 kgCO₂/m² carbon emissions. The biggest contributor to these values is the conversion of metallurgical-grade silicon to solar-grade silicon, followed by casting and wafer production.

Table 8-9: Summary of the embodied energy and associated carbon emissions during the manufacturing stage, of m² of PV module.

Component	Embodied energy (MJ/ m²)			Carbon (kgCO₂/m²)		
	Opaque PV	Opaque frameless PV	Semi-transparent PV	Opaque PV	Opaque frameless PV	Semi-transparent PV
Silicon process	3,309			353		
PV module component and assembly	631	261	277	32.5	15	17
Inverter	112			42		
Support	455	517	517	24.3	24.3	27
Totals	4,508	4,200	4,187	452	434	435

8.3.2 Transport to site

Since PV modules and inverters are assumed to be imported into Jordan from China, various modes of transport from overseas port to site in Amman, Jordan are included. Data are not available to estimate the land transport distance and mode in the country of origin, therefore this has been omitted. Transoceanic freight is assumed to deliver components from China port to Jordan's port, with onward transport to the site by lorry. With the help of online available shipping distance calculator (Portworld, 2019) and google map, the shipping distance is approximated at 12,386 km, an additional 330 km of lorry freight is added to account for transport within Jordan between the Aqaba ports and Amman, see Table 8-10. The transportation trip is assumed to be one way only. The return of the transportation trucks and ship are assumed to carry other goods and provide other services.

Table 8-10: Port to port distances to transport the PV system from China to the site in Amman, Jordan. Source of distance: <http://www.portworld.com/map/> (Portworld, 2019).

Type of transportation	Loading port	Landing port	Distance (km)
Sea transportation	Shekou, China	Aqaba (Jordan)	12,386 km
Road transportation	Aqaba (Jordan)	Amman	330 km

Sea transportation: according to the previous literature the energy consumption of a container ship traveling at a speed of 44.44 km/hour is 66 tons of marine diesel oil per day (Hickman *et al.*, 1999). For 12,386 km, the length of the journey is estimated at approximately 12 days. The total energy consumption is 792 tons (718,490 kg) of marine diesel oil per the entire shipping journey (Hickman *et al.*, 1999; Raouz, 2017). The energy content of marine diesel oil is 44 kJ/g (M.Felder and W.R, 2005); the total energy consumption during sea shipping for a distance of 12,386 km is 8.78 GWh.

The total freighting capacity of the ship in photovoltaic is approximated using the volume of the solar module and the dimensions of a 20 ft. container (Raouz, 2017), with a loading capacity of 582 modules (150MWp of PV module). The energy consumption of the maritime shipping process is 0,180 MJ/Wp (**28,8 MJ/m²**). The emission factor for a diesel-powered container ship is 0.676 kgCO₂/kWh (Hickman *et al.*, 1999), accordingly, the carbon emissions are **6.2 kgCO₂/m²**.

Road transportation: it is assumed that road transportation is done using lorry, and the used fuel is diesel oil for which the energy density is 32 MJ/liter (Hickman *et al.*, 1999; Medel, 2017). The estimated fuel consumption is 4.5 l/1000 tons.km, see Table 8-11.

Table 8-11: Embodied energy and carbon emission estimation for the transportation of 1 m² of PV module by a lorry in Jordan from Aqaba port to Amman. Source of data: (Hickman et al., 1999; Medel, 2017).

Distance (km)	Consumption of diesel (l/1000 tons.km)	Total amount of diesel (l/1000 tons)	Total amount of diesel (l/module)	Total amount of diesel (l/m ²)	Total primary embodied energy (MJ/m ²)	Total carbon emissions (kgCO ₂ /m ²)
330	4.5	1485 ^a	0.0297 ^b	0.185 ^c	5.92^d	0.58^e

Note:

^a Total amount of diesel consumed by the truck is calculated multiplying the distance (330km) times the consumption rate of 4.5 l/km.

^b Total amount of diesel consumed by the truck per PV module assumed that the weight for each module is 20kg.

^c Total amount of diesel consumed by the truck per m² of the PV module assumed that the area for each module is 1.6 m².

^d Total energy consumed is calculated by multiplying the energy intensity of diesel 32 MJ/l times the total amount of diesel consumed (0.0185 l)

^e Total carbon emission is calculated multiplying the total number of liters of diesel (0.0185 l/m²) times the emission rate of petrol 3.172 kg/l of petrol (Medel, 2017).

8.3.3 On-site installation

The process of constructing a PV system requires energy in the range of 0,15 and 0,31 kWh/kWp (Hou et al., 2016), this includes the energy input required by the integration of controllers, inverters, cables, and the mounting system. The average value of 0,23kWh/Wp (11.4 kWh/m²) is used in this research. Compared to the Jordan electricity mix emissions factor of 0.642 kgCO₂/kWh and cumulative energy demand factor of 9.72 MJ/kWh (Hammad and Ebaid, 2015), the annual carbon emission savings are calculated at **7.3 kgCO₂/m²**, and the embodied primary energy is **110 MJ/m²**.

8.3.4 Operation and maintenance

Once the PV station is constructed the conversion of the solar irradiation to electricity is an emission-free process and no additional energy input required onto the system. Moreover, the PV system requires minimum maintenance, maintenance including cleaning the surface of the modules and checking the system performance periodically, other than that there is no special treatment (Fthenakis and Kim, 2011).

As mentioned before, the lifetime of the modules is assumed to be 25 years. The life of the inverter is assumed to be 15 years, therefore, one replacement with the same inverter is included during the lifetime of the PV system. Other replacement parts are considered negligible, therefore disregarded in the calculation. The energy input due to operation and maintenance is according to literature responsible for 1% of the entire energy input of PV-systems. Accordingly, the estimated required energy of the operation and maintenance process is 415-500 MJ/m² and the estimated carbon emission is 27.5-33 kgCO₂/m².

8.3.5 Decommissioning, disposal, and recycling of waste

The last stage of the PV system life cycle is the decommissioning of the components of the system. This stage includes dismantling solar modules and BOS, transportation to the waste management facility, and/or recycling of the pieces. This stage is not considered in this research as according to the previous research, there is still a lack of reliable scientific or empirical data and established recycling strategies (Lu and Yang, 2010; Fthenakis and Kim, 2011; Hammond and Jones, 2011).

8.3.6 Total life cycle environmental performance

The results of the total energy and carbon analysis of each component of the PV system per m² and the percentage contributions by each component of total embodied energy and to total carbon is provided in Figure 8-5 and Figure 8-6.

It can be seen that for all module design, the photovoltaic manufacturing process and the balance of systems make up the greatest contribution. Most of the energy consumption and carbon emissions (> 64%) arises from silicon purification. This result underlines the importance of energy-oriented process improvements in these areas are critical for further reducing the energy consumption and GHG emissions to produce silicon PV systems in the future.

Moreover, comparing opaque and semi-transparent PV systems, it can also be concluded that frameless double-glass PV module fabrication requires less energy than that of conventional opaque PV modules (~ 5% reduction from a system point of view), largely due to the elimination of the aluminum frame.

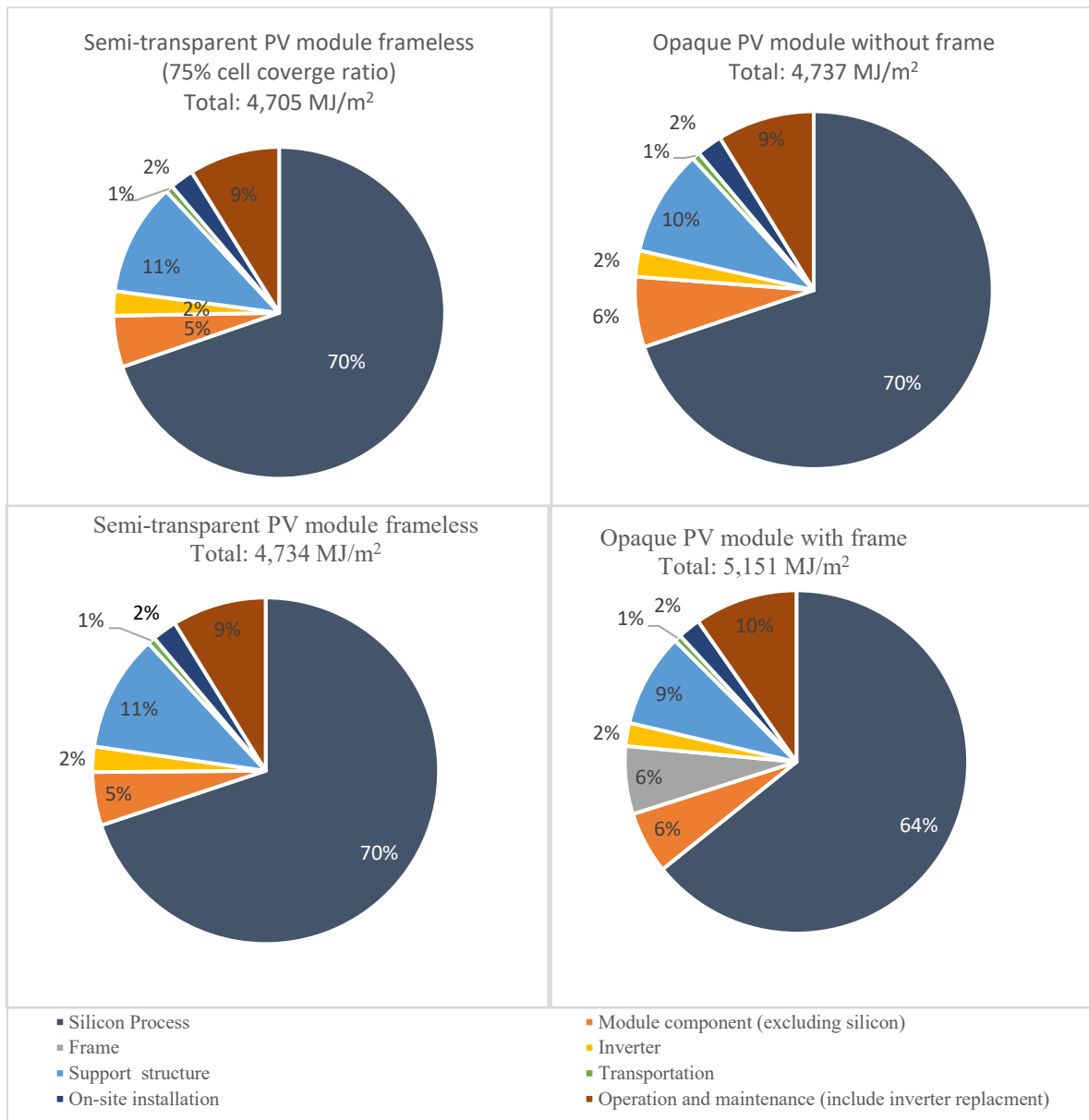


Figure 8-5: Percent contribution to total energy for different stages of the solar PV system.

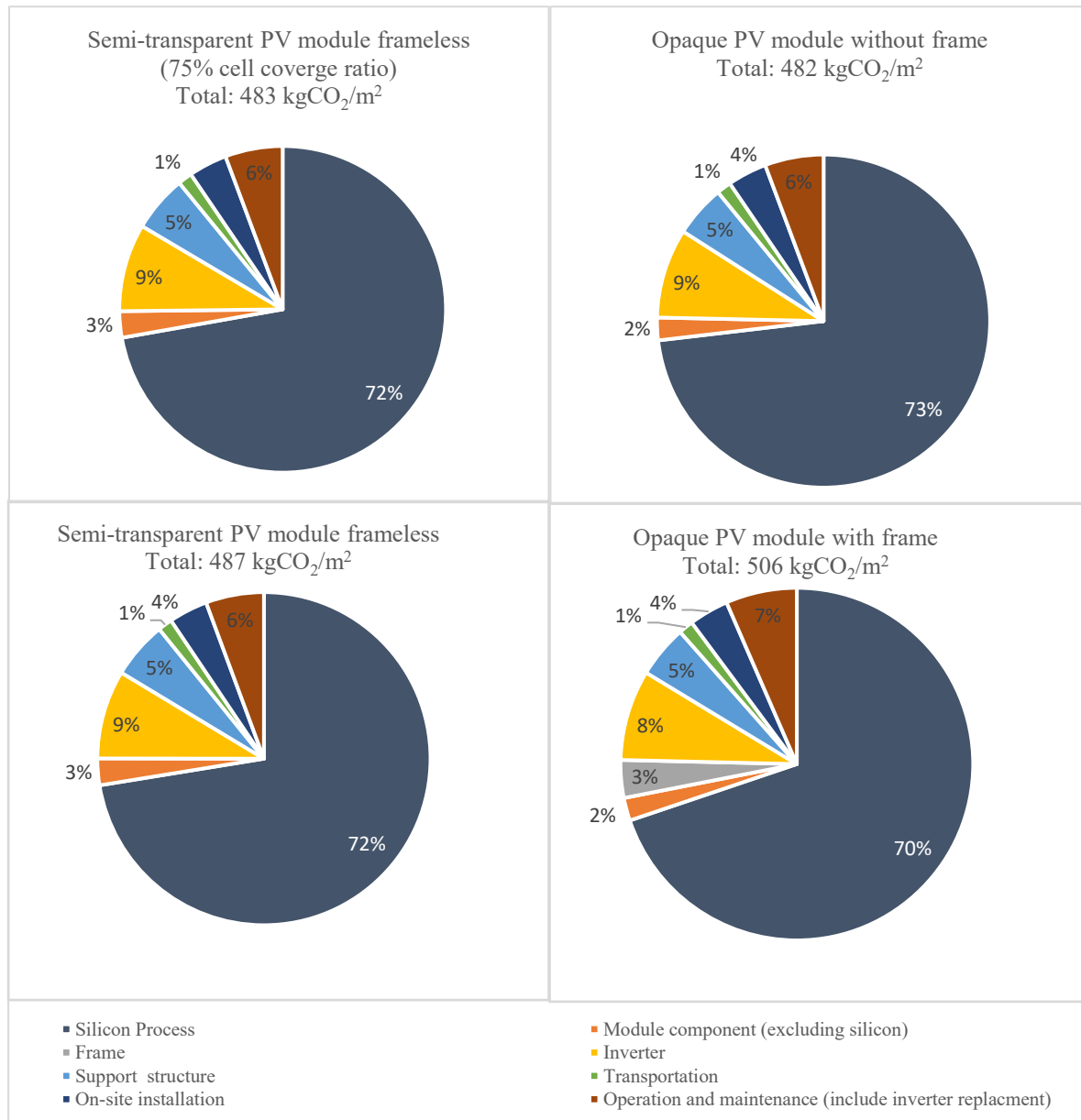

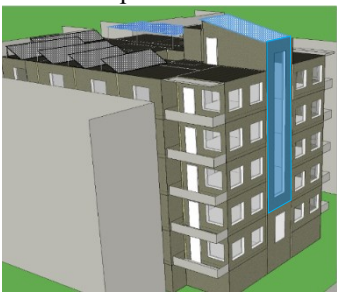
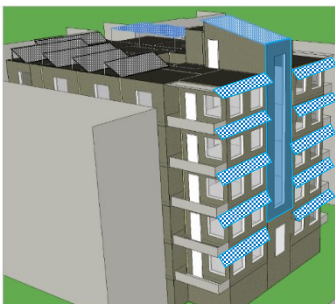

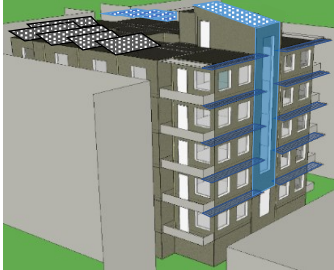
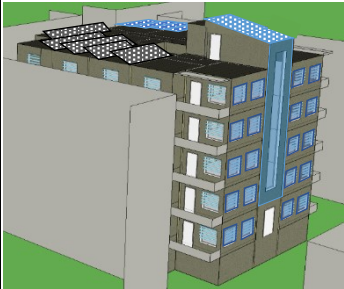
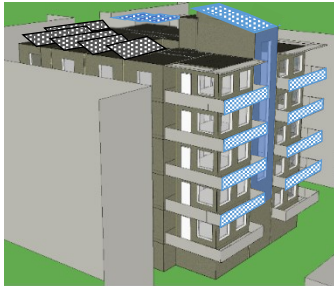
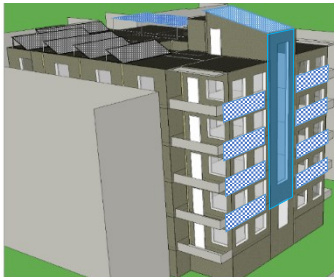


Figure 8-6: Percent contribution to total carbon for different stages of the solar PV system.

Table 8-12 below, illustrates the area, capacity and PV module design of the proposed PV systems, it also shows the total primary embodied the energy and carbon emission for each system. Moreover, the energy payback time and carbon payback time for each system are estimated based on the Equation 4-2 and Equation 4-3, under the methodology (Chapter 4), and based on the illustrated results in Table 8-1 under the energy life cycle performance analysis. The EPBT values range from 1.5 to 3.5 years. Regarding the CPBT it is the shortest in the staircase integrated semi-transparent PV system (case 1) with 3.5 years and the longest in the roof-mounted system with 7.8 years.

Table 8-12: Life cycle energy, carbon emissions, EPBT and CPBT for the proposed PV system over 25 years.

Case	Module design Installed capacity Installed area	Total embodied primary energy (MJ)	Total carbon (kgCO ₂)	EPBT (year)	CPBT (year)
Case 0: Improved apartment building design + Roof PV 	PV module design: Opaque PV module with frame Opaque PV module without frame Installed capacity: 9.9 kWp/ 2.7 kWp Installed area: 64.4 m ² / 17.6 m ²	Total 414,600 Mounted: 331,467 Integrated: 83,134	Total 41,000 Mounted: 325,35 Integrated: 8,470	Total 3.2 Mounted: 2.4 Integrated: 3.5	Total 7.6 Mounted: 7.8 Integrated: 7.5
Case 1: Staircase integrated semi-transparent PV+ Case 0 	PV module design: Semi-transparent PV module (70% cell coverage ratio) Installed capacity: 5.43 kWp Installed area: 43.5 m ²	Total: 619,268 Stair: 204,668 + Case 0	Total: 62024 Stair: 21,019 + Case 0	Total: 2.6 Stair: 1.5 + Case 0	Total: 6.2 Stair: 3.5 + Case 0
Case 2: Opaque overhang with integrated PV+ Case 1 	PV module design: Opaque PV module without frame Installed capacity: 6 kWp Installed area: 42.4 m ²	Total: 820,117 Opaque overhang: 200,849 + Case 1	Total: 82,486 Opaque overhang: 20,462 + Case 1	Total: 2.7 Opaque overhang: 2.8 + Case 1	Total: 6.2 Opaque overhang: 6.5 + Case 1
Case 3: Semi-transparent PV overhang+ Case 1 	PV module design: Semi-transparent PV module (90% cell coverage ratio) Installed capacity: 8.4 kWp Installed area: 60 m ²	Total: 903,309 Semi-transparent overhang: 284,040 + Case 1	Total: 91,262 Semi-transparent overhang: 29,238 + Case 1	Total: 2.6 Semi-transparent overhang: 2.6 + Case 1	Total: 6.2 Semi-transparent overhang: 6 + Case 1

Case 4: Horizontal PV overhang louvers+ Case 1 	PV module design: Opaque PV module without frame Installed capacity: 6.2 kWp Installed area: 43.2 m ²	Total: 823,907 louver-overhang: 204,638 + Case 1	Total: 82,872 louver-overhang: 20,848 + Case 1	Total: 2.6 louver-overhang: 2.5 + Case 1	Total: 6.1 louver-overhang: 5.8 + Case 1
Case 5: Window integrated PV louver+ Case 1 	PV module design: Opaque PV module without frame Installed capacity: 5 kWp Installed area: 34 m ²	Total: 780,326 Window integrated louvers: 161,058 + Case 1	Total: 78,432 Window integrated louvers: 16,408 + Case 1	Total: 2.4 Window integrated louvers: 1.8 + Case 1	Total: 5.7 Window integrated louvers: 4.2 + Case 1
Case 6: Balcony integrated PV+ Case 1 	PV module design: Semi-transparent PV module (90% cell coverage ratio) Installed capacity: 4.96 kWp Installed area: 34.56 m ²	Total: 782,875 Balcony: 163,607 + Case 1	Total: 78,865 Balcony: 163,607 + Case 1	Total: 2.5 Balcony: 1.9 + Case 1	Total: 5.8 Balcony: 4.3 + Case 1
Case 7: Wall integrated PV+ Case1 	PV module design: Opaque PV module without frame Installed capacity: 8.6 kWp Installed area: 59.6 m ²	Total: 901,594 Wall: 282,325 + Case 1	Total: 90,787 Wall: 28,763 + Case 1	Total: 2.3 Wall: 1.8 + Case 1	Total: 5.6 Wall: 4.2 + Case 1

8.4 Economic life cycle performance

In this section, the economic performance of the proposed PV systems is assessed using a life cycle cost (LCCA) assessment method (Reidy et al., 2005; Yang and Zou, 2016). The life cycle cost of PV covers all system life stages including, the initial costs, operation, maintenance, replacement cost, saving in electricity (Knaack et al., 2014; Rodrigues et al., 2016)

The initial cost of the PV systems includes the costs of the module, supply, and fixing of aluminum framing, the balance of system components, inverter and installation (including wiring and other auxiliaries), the purchased estimated costs of the modules are obtained from the previous literature. all the PV systems are a grid-connected system, the battery is not considered in this part of the research, as the analysis of the economic benefits of battery installation has been presented in Chapter 6.5 Operation and maintenance costs include annual periodic expenses for system management, regular maintenance, and site supervision, the maintenance cost includes the inverter replacement costs. Regarding the PV system recycling it is not included in this research, as according to experts, it is not viable because waste volumes generated are too small (Hammad and Ebaid, 2015).

The cost-profit is estimated based on the electricity production and energy saving considering the change in lighting, heating and cooling demand due to the installation of the PV modules into the façade. The current electricity tariff in Jordan is used to estimate the saved electricity costs. For future estimations, the increase in the electricity price has been considered. More details have been presented in the methodology chapter.

8.4.1 Assumptions and values

The fixed data are the electricity prices at their current levels and energy yield of the solar system in Amman, Jordan and the energy demand of the building. Assumptions are made on the cost of PV, financing, and price development for the time beyond, a future increase in electricity price per kWh, etc. Values and assumptions used in the analysis are reported below:

- **Initial cost**

As described in the literature review (Chapter 3.2.4), the cost of the BIPV system can vary in a very wide range, depending on many factors such as the materials and the complexity of the solution, system size, location, BIPV product type, and technical specification, etc. The whole system can be approximately the same as a standard system (when a very simple structure for the installation is designed), up to approximately 10 times as much for devices with complicated installation structures (Baxter et al., 2017; James et al., 2017). BIPV modules may include additional materials (e.g., adhesives and framing and flashing materials) (James et al., 2012), moreover, additional labor costs deriving from specialized architectural design, engineering design, and installation (Greentech Media, 2010). As there is no special database for the BIPV systems, the initial cost of PV systems is estimated based on the previous literature review (Fang, Honghua and Sicheng, 2017; James et al., 2017; Solar, 2017; Passera et al., 2018; PV magazine, 2019; PVinsight, 2019).

An overview of the cost of the different used PV system designs is presented in Table 8-13. Regarding the conventional opaque PV system (with frame), the cost estimated based on China market, as most of the PV modules in Jordan are imported from China (see Chapter 2.6). The price for opaque PV systems with frame is 0.75 €/Wp. Hardware costs (module, inverter, racking, wiring, etc.) account for about 75% of the total costs, whereas soft costs (installation, customer acquisition, profit, permitting, contracting, financing) account for about 25% of the total costs. The modules account for about 70% of the hardware costs (Fang, Honghua and Sicheng, 2017). Regarding the semi-transparent PV module, the cost of the module is higher by 40% than the costs of commercially available PV modules. The other hardware costs are the same, whereas a very sensitive cost item relates to the framing systems (including support structure). For a roof mounting installation, the cost of the framing is about 0.06 €/Wp, whereas, in the case of semi-transparent modules and frameless module, the structure can cost up to 1 €/Wp (Baxter et al., 2017), in this research, the support structure for the semi-transparent and frameless modules assumed to be 0.5 €/Wp. Regarding the cost of the semi-transparent PV module with a 70% cell coverage ratio (30% transparency), it is estimated to be 0.45 €/Wp, as the cell contributes to about 70% of the module cost (Singh et al., 2015).

Table 8-13: Cost breakdown for different PV system design. Estimated cost based on (Fang, Honghua and Sicheng, 2017; James et al., 2017; Solar, 2017; Passera et al., 2018; PV magazine, 2019; PVinsight, 2019).

Hardware			Soft costs		
crystalline silicon module (€/W)	Inverter (€/W)	Other (wiring, monitoring & control equipment ...) (€/W)	installation (Supporting structure+ frame), transport &warehouse (€/W)	Profit (€/W)	Other (permitting, contracting, financing...) (€/W)
Conventional opaque PV system (with frame)					
0.35	0.088	0.1	0.075	0.0625	0.0625
0.54			0.2		
Total: 0.75 €/Wp					
Opaque PV system Without frame					
0.35	0.088	0.1	0.575	0.0625	0.0625
0.54			1.125		
Total: 1.24 €/Wp					
Semi-transparent frameless PV system (90% cell coverage ratio)					
0.55	0.088	0.1	0.575	0.0625	0.0625
0.74			0.7		
Total: 1.44 €/Wp					
Semi-transparent frameless PV system (75% cell coverage ratio)					
0.45	0.088	0.1	0.575	0.0625	0.0625
0.64			0.7		
Total: 1.34 €/Wp					

- **Annual operation and maintenance costs**

According to the previous research, the estimated maintenance cost is between 1- 3% of the initial investment per year (Knaack *et al.*, 2014; Rodrigues *et al.*, 2016; Yang and Zou, 2016). In this research, it is assumed that the O&M costs are 2% of the initial cost per year, in addition to the inverter replacement after 15 years.

- **Jordanian electricity cost**

The Jordanian electricity system pricing is considered as described in Chapter 0, including the cost of buying electricity from the utility grid due to the PV system does not produce enough energy and the savings earned due to selling the PV overproduction electricity to the grid.

As presented in chapter 2, the monthly electricity tariff in Jordan is based on the monthly electricity demand. Regarding selling the electricity to the grid, the current electricity selling tariffs to the grid from photovoltaic is 0.15 €/kWh, however, the cost of using the grid-network is 0.056 €/kWh, resulting in net electricity selling tariffs of 0.094 €/kWh.

8.4.2 Results of economic performance

Based on the previous section, the initial total cost and the contribution percentage of each component to the total cost of different PV system designs is presented in Figure 8-6. As can be seen, the opaque frameless PV system (conventional system) has the lowest capital cost with 1.032 €/W_p. While the semi-transparent PV system with a 90% cell coverage ratio has the highest cost with 1.907 €/W_p, which is around 45% higher than the conventional opaque PV mounting system.

In the conventional opaque PV system (frameless), the PV module has the biggest contribution to the total cost with about 30%, while in frameless PV module designs including opaque PV module without frame, semi-transparent PV module with 90% cell coverage ratio and semi-transparent PV module with 70% cell converge ratio, the biggest contribution to the total cost is the support structure with 35%, 30%, and 32%, respectively.

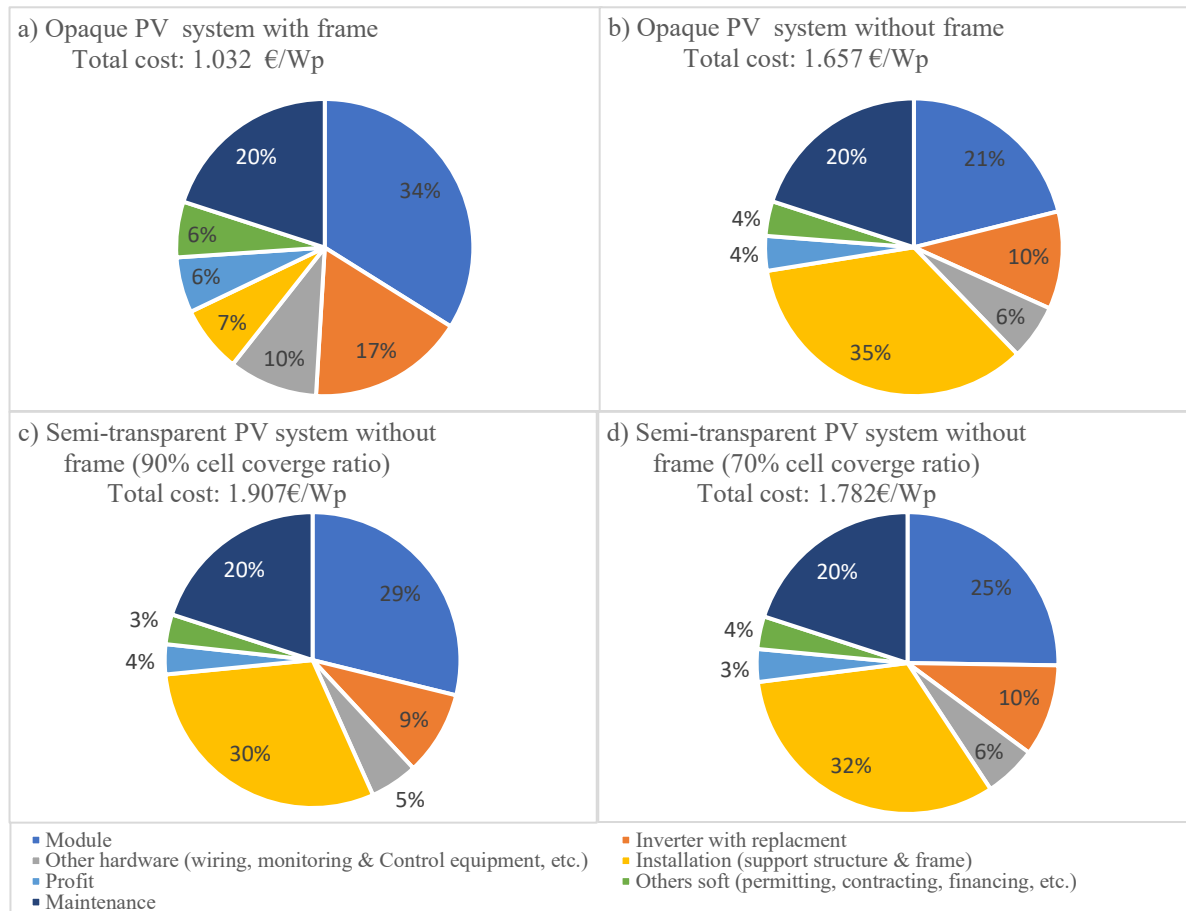
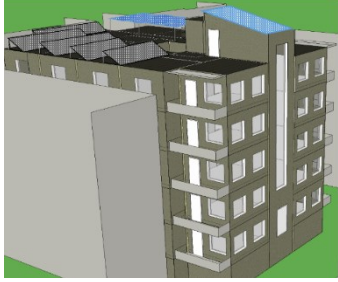
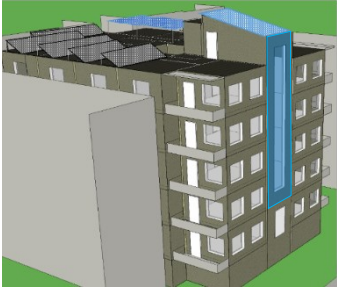
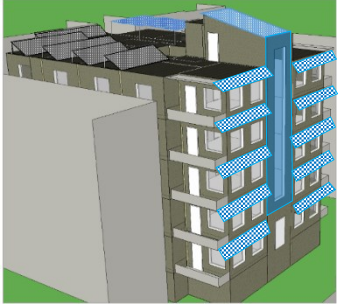



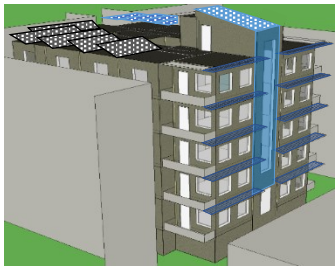
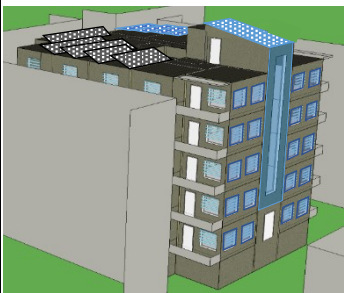
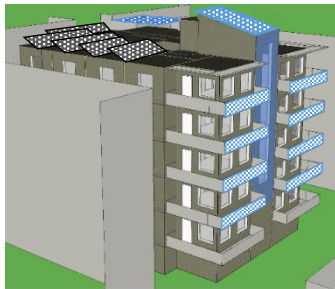
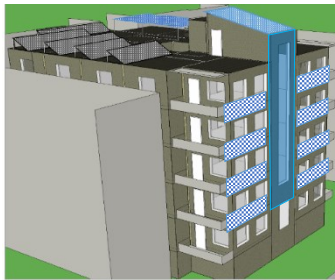
Figure 8-7: Total capital cost and cost breakdown for different PV system design. Estimated cost based on (Fang, Honghua and Sicheng, 2017; James et al., 2017; Solar, 2017; Passera et al., 2018; PV magazine, 2019; PVinsight, 2019)

After estimating the capital cost of PV systems per Wp, the next step is to estimate the total cost of all the proposed PV systems, and then estimate the electricity cost saving based on the PV production, and electricity tariff in Jordan, taking into account the monthly electricity tariff (based on demand). To do this, annual and monthly results of PV generation under different PV cases are obtained from Polysun simulation results, and electricity demands of the building are obtained from IDA ICE simulation results, taking into account the effect of installed PV system into façade on the building energy demand, as presented in Chapter 7. It must be mentioned that the cost of decreasing the façade construction material is not considered.

The total PV systems cost, electricity-saving cost and the payback time (PBT) for all the proposed PV systems are shown in Table 8-14 and Figure 8-8. The PBT is the shortest in the case of roof installation with a total of 6.4 years (mounting and integrating roof PV systems), the roof mounting system is 4.2 years while roof-integrated PV system is 9.6 years. While the longest PBT is 15.7 years for the staircase PV façade system (case 1), as the energy production is the lowest because of the PV modules installed with a 90° tilt angle, and the cost of PV semi-transparent module is relatively high.

Table 8-14: Life cycle PV system cost, cost-saving from electricity and the PBT for the proposed PV system over 25 years.

Case		PV system cost (€/25 year)	Cost-saving from electricity (€/25 year)	PBT (year)
Case 0: Improved apartment building design + Roof PV 	PV module design: Opaque PV module with frame Opaque PV module without frame Installed capacity: 9.9 kWp/ 2.7 kWp Installed area: 64.4 m ² / 17.6 m ²	Total 14,697 Mounted: 10,221 Integrated: 4,475	Total 81,970 Mounted: 65,430 Integrated: 16,540	Total 6.4 Mounted: 5.1 Integrated: 9.6
Case 1: Staircase integrated semi-transparent PV+ Case 0 	PV module design: Semi-transparent PV module (70% cell coverage ratio) + Case 0 Installed capacity: 5.43 kWp + Case 0 Installed area: 43.5 m ² + Case 0	Total: 25,054 Stair: 10,357 + Case 0	Total: 100,800 Stair: 18,830 + Case 0	Total: 8.5 Stair: 15.7 + Case 0
Case 2: Opaque overhang with integrated PV+ Case 1 	PV module design: Opaque PV module without frame+ Case 1 Installed capacity: 6 kWp+ Case 1 Installed area: 42.4 m ² + Case 1	Total: 35,000 Opaque overhang: 9,945 + Case 1	Total: 135,520 Opaque overhang: 34,720 + Case 1	Total: 10 Opaque overhang: 9 + Case 1
Case 3: Semi-transparent PV overhang+ Case 1 	PV module design: Semi-transparent PV module (90% cell coverage ratio) + Case 1 Installed capacity: 8.4 kWp+ Case 1 Installed area: 60 m ² + Case 1	Total: 41,077 Semi-transparent overhang: 16,023 + Case 1	Total: 147,200 Semi-transparent overhang: 46,400 + Case 1	Total: 9.4 Semi-transparent overhang: 11.5 + Case 1

Case 4: Horizontal PV overhang louvers+ Case 1 	PV module design: Opaque PV module without frame+ Case 1 Installed capacity: 6.2 kWp+ Case 1 Installed area: 43.2 m ² + Case 1	Total: 35,330 louver-overhang: 10,276 + Case 1	Total: 132,495 louver-overhang: 31,700 + Case 1	Total: 9.9 louver-overhang: 11.11 + Case 1
Case 5: Window integrated PV louver+ Case 1 	PV module design: Opaque PV module without frame+ Case 1 Installed capacity: 5 kWp+ Case 1 Installed area: 34 m ² + Case 1	Total: 33,342 Window integrated louvers: 8,288 + Case 1	Total: 118,690 Window integrated louvers: 17,890 + Case 1	Total: 9.4 Window integrated louvers: 14.5 + Case 1
Case 6: Balcony integrated PV+ Case 1 	PV module design: Semi-transparent PV module (90% cell coverage ratio) + Case 1 Installed capacity: 4.96 kWp+ Case 1 Installed area: 34.56 m ² + Case 1	Total: 34,515 Balcony: 9,460 + Case 1	Total: 119,830 Balcony: 19,025 + Case 1	Total: 9.2 Balcony: 15.7 + Case 1
Case 7: Wall integrated PV+ Case1 	PV module design: Opaque PV module without frame+ Case 1 Installed capacity: 8.6 kWp+ Case 1 Installed area: 59.6 m ² + Case 1	Total: 39,308 Wall: 14,254 + Case 1	Total: 132,525 Wall: 31,725 + Case 1	Total: 10.1 Wall: 14.9 + Case 1

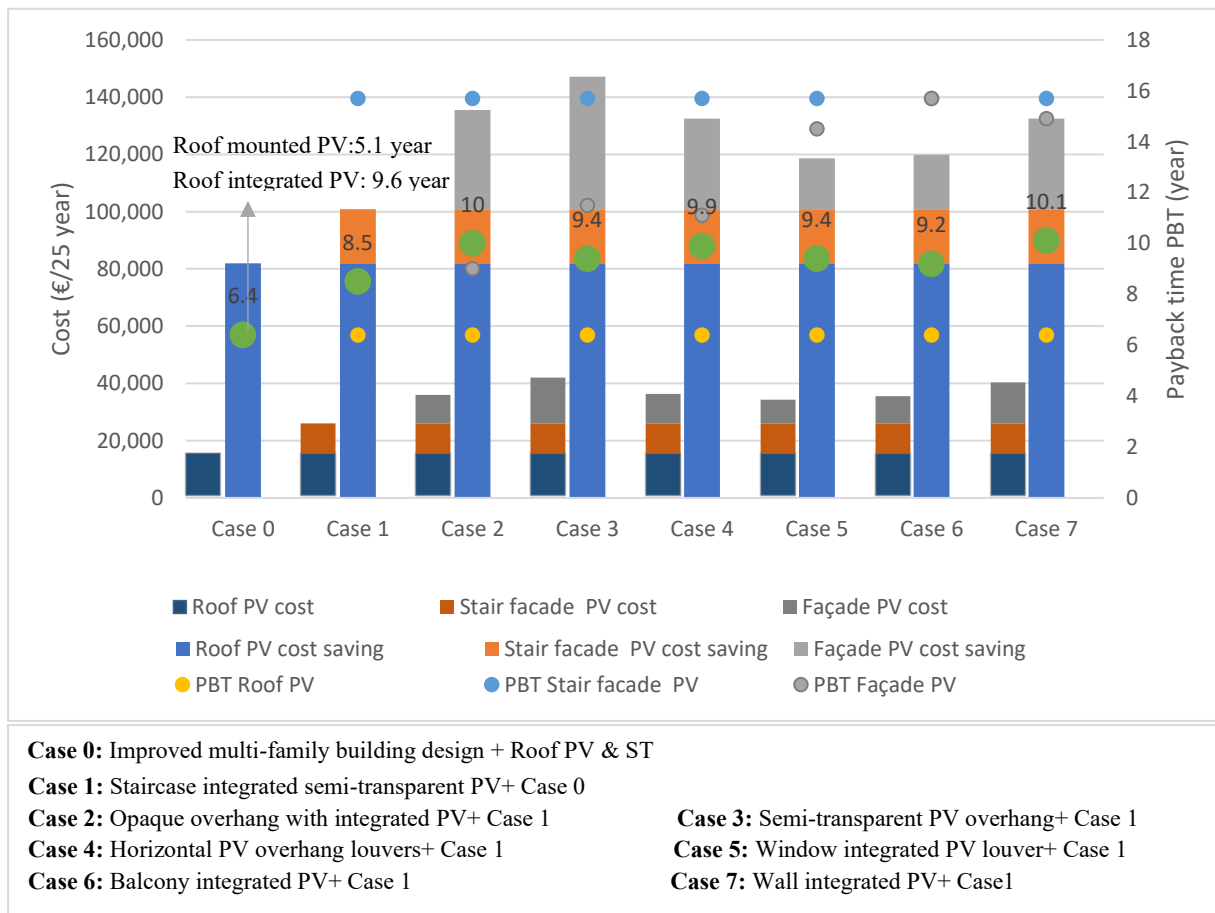


Figure 8-8: Life cycle PV system cost, cost saving from electricity and the PBT for the proposed PV system over 25 years.

Figure 8-9 illustrates the electricity cost of the building over 25 years before installing a PV system (base case) and after installing the PV systems (taking into account the PV system production degradation), it is also illustrating the percentage of cost-saving in comparison to the base case. Installing the PV system can decrease the building electricity cost over 25 years up to 82% (case 3) with roof and façade PV installation the roof contributes to decreasing the cost with 46% while the façade with 36%.

The PV systems also contribute to decreasing the electricity demand from the grid, accordingly, decrease the electricity tariff. In the base case, the electricity tariff in most months is 0.1 €/kWh, while after installing the PV systems the electricity tariff is 0.088 €/kWh in all months. The contribution of PV systems in decreasing the electricity cost can be higher in the case of building with higher electricity demand.

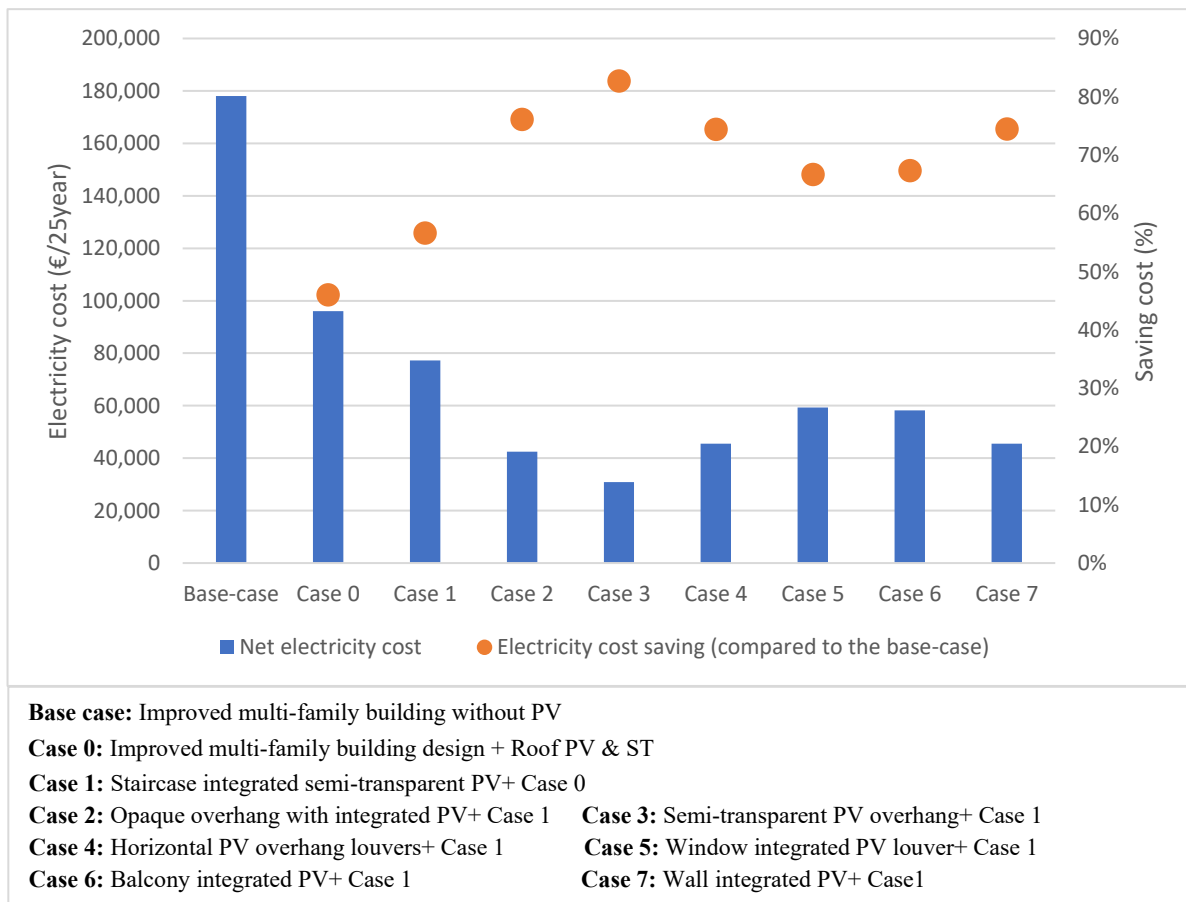


Figure 8-9: Electricity cost of the improved residential multi-family building in Amman, Jordan before installing PV systems (base case), and after installing PV systems, and the percentage of electricity cost in comparison to the base case over 25 years.

8.5 Summary

This chapter considered the life cycle performance of the proposed PV roof and façade systems. The analysis considered the relative environmental and economic performance.

The results indicate the major life cycle stages that require significant primary energy use are the manufacturing of photovoltaic modules followed by the balance of systems. The EPBT is between 1.5- 3.5 years and the CPBT is between 3.4- 7.8 years in all cases. In this research, the PV modules are assumed that imported from China, since most of the energy produced in China comes from coal-fired power plants this leads to large amounts of GHG emissions during the production stage. Therefore, the GHG emissions could be reduced significantly, if China increasing their renewable energy production, or by the production being transferred to a location using renewable energy sources to a higher degree. Moreover, when the production is stationed in China the PV modules must be transported long distances to be installed in Jordan. However, this study indicates that transport, when shipped overseas, is quite an insignificant factor in the perspective of the entire life cycle.

Regarding the life cycle-economic performance, compared with the conventional system design (roof mounting opaque PV system), the frameless double-glass (semi-transparent PV) integrated system cost is significantly higher. The cost of the conventional PV system design can be recovered in about 4 years, while in the integrated systems the cost can be recovered in 5-16 years depends on the module design (opaque frameless, semi-transparent module), tilt angle, and the support structure design (integrated or mounting), etc.

Hence, the frameless double-glass module technology is expected to gain significant market share in the coming years, the costs are also predicted to decrease in the coming year, which could improve the PV system cost viability in the future. Moreover, as all the PV systems are installed to energy improved apartment building in Jordan, and the electricity tariff in Jordan depends on the electricity demand; the greater the demand, the higher the electricity tariff cost. The PV payback time can be reduced significantly in a building with a higher electricity demand or in a country with higher electricity prices.

In this chapter, the effect replacing the construction materials with PV modules, in the case of façade PV integration systems for the embodied energy, carbon emissions and cost is not considered. Which may also have a positive effect in term of cost-saving, avoided embodied the energy and decreasing the GHG emissions.

9 Multi-assessment support matrix

In this chapter, the performance of the PV systems installed into the improved apartment building envelope in Amman, Jordan under different cases has been evaluated using a multi-assessment (criteria) evaluation approach based on the results from previous chapters. As presented in Chapter 4.6, a decision-support matrix is developed in the form of a radar chart to support the architects, building designers, occupants, etc., in their decision to select the suitable PV system application based on the criteria of the user. First, the performance criteria have been chosen and described. Next, the performance of the proposed PV systems has been presented in a graph. Lastly, an example of how the multi-assessment graph may be used is explained.

9.1 Criteria for support matrix

As presented in Chapter 4.1, different criteria have been considered in order to evaluate the performance of the BIPV systems, each of these criteria have been assessed alone in the previous chapters. In order to simplify the decision-making process as much as possible, the key criteria have been presented in a simple graphical matrix, and the exact values derived from the previous parts are hidden in this graph.

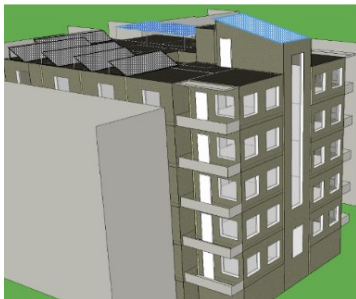

The main indicator within the matrix are:




- Life cycle environmental performance, including carbon emissions payback time (CPBT), and the energy payback time (EPBT). The result of the life cycle environmental performance of the proposed PV systems has been presented in Chapter 8.3.
 - Economic performance includes the capital cost, and the payback time (PBT). For building owners to adopt a certain technology or system, one of the key considerations is the cost. Hence, architects should also take the cost into considerations when adopting BIPV systems. While capital cost is important, the payback time is also essential to determine if it is worth investing in applying photovoltaic systems. Accordingly, both capital costs and payback time are included in the proposed matrix. The detailed analysis has been presented in Chapter 8.4.
- Overall energy performance, due to the multi-functional role that the BIPV systems have, evaluation of energy performance is considered the life cycle PV systems energy production and the primary energy demand (heating system, cooling system, lighting, and equipment) of the building, as mentioned in Chapter 8.2.
- Qualitative performance, the visibility and functionality criteria are also incorporated in the graphical matrix, as described in Chapter 4.5.4. The purpose here is to emphasize the substantial function of BIPV systems. As it not only has the advantage of electricity generation but also can replace current building materials. It is also evaluated by the visibility of the PV technology from the viewpoint of an observer.


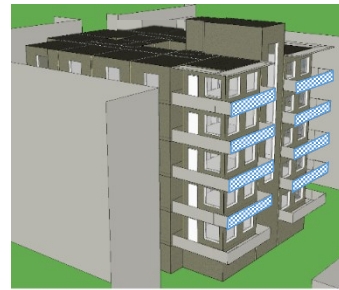

9.2 Development of decision support matrix

The results for the above-mentioned criteria based on the previous chapters are shown in Table 9-1. As this section serves as a guide to the development of the support matrix, all the proposed PV systems data are included to allow comparisons of the relative performance when making the decision to adopt BIPV systems.

Table 9-1: Performance of the proposed solar PV systems including, overall energy performance, Economical performance (PV system initial capital cost and PBT), environmental performance (EPBT and CPBT), qualitative performance (visibility and functionality).

Case	Overall energy performance	Economical performance	Environmental performance	Qualitative performance
Case 0: Improved apartment building design + Roof PV.				
a) Mounted PV system b) Roof integrated PV system				
 PV module design: A: Opaque PV module with frame B: Opaque PV module without frame Installed capacity: A: 9.9 kWp/ B: 2.7 kWp Installed area: A: 64.4 m²/ B: 17.6 m²	Net primary energy demand (MWh) A: 2,654 B: 3,123	Initial capital cost (€) A: 9,910 B: 4,340	EPBT (year) A: 3.5 B: 2.4	Visibility (level) A: 1 B: 2
		PBT (year) A: 5.1 B: 9.6	CPBT (year) A: 7.5 B: 7.8	Functionality (level) A: 1 B: 2
Case 1: Staircase integrated semi-transparent PV				
 PV module design: Semi-transparent PV module (70% cell coverage ratio) Installed capacity: 5.43 kWp Installed area: 43.5 m²	Net primary energy demand (MWh) 3,117	Initial capital cost (€) 10,050	EPBT (year) 1.5	Visibility (level) 4
		PBT (year) 15.7	CPBT (year) 3.5	Functionality (level) 4

Case 2: Opaque overhang with integrated PV				
 <p>PV module design: Opaque PV module without frame Installed capacity: 6 kWp Installed area: 42.4 m²</p>	Net primary energy demand (MWh) 2,980	Initial capital cost (€) 9,646	EPBT (year) 2.8	Visibility (level) 3
		PBT (year) 9	CPBT (year) 6.5	Functionality (level) 3
Case 3: Semi-transparent PV overhang				
 <p>PV module design: Semi-transparent PV module (90% cell coverage ratio) Installed capacity: 8.4 kWp Installed area: 60 m²</p>	Net primary energy demand (MWh) 2,848	Initial capital cost (€) 15,542	EPBT (year) 2.6	Visibility (level) 3
		PBT (year) 11.5	CPBT (year) 6	Functionality (level) 3
Case 4: Horizontal PV overhang louvers				
 <p>PV module design: Opaque PV module without frame Installed capacity: 6.2 kWp Installed area: 43.2 m²</p>	Net primary energy demand (MWh) 3,009	Initial capital cost (€) 9,967	EPBT (year) 2.5	Visibility (level) 3
		PBT (year) 11.11	CPBT (year) 5.8	Functionality (level) 3

Case 5: Window integrated PV louver				
 <p>PV module design: Opaque PV module without frame Installed capacity: 5 kWp Installed area: 34 m²</p>	Net primary energy demand (MWh) 3,129	Initial capital cost (€) 8,039	EPBT (year) 1.8	Visibility (level) 3
		PBT (year) 14.5	CPBT (year) 4.2	Functionality (level) 3
Case 6: Balcony integrated PV				
 <p>PV module design: Semi-transparent PV module (90% cell coverage ratio) Installed capacity: 4.96 kWp Installed area: 34.56 m²</p>	Net primary energy demand (MWh) 3,115	Initial capital cost (€) 9177	EPBT (year) 1.9	Visibility (level) 4
		PBT (year) 15.7	CPBT (year) 4.3	Functionality (level) 3
Case 7: Wall integrated PV				
 <p>PV module design: Opaque PV module without frame Installed capacity:8.6 kWp Installed area:59.6 m²</p>	Net primary energy demand (MWh) 2,958	Initial capital cost (€) 13,826	EPBT (year) 1.8	Visibility (level) 4
		PBT (year) 14.9	CPBT (year) 4.2	Functionality (level) 4

The results presented in Table 9-1 have been normalized as percentage values, as described in Chapter 4.6., then these values have been transferred into the radar chart as shown in Figure 9-1. The higher values (far from the center) indicate better performance for the specific criteria.

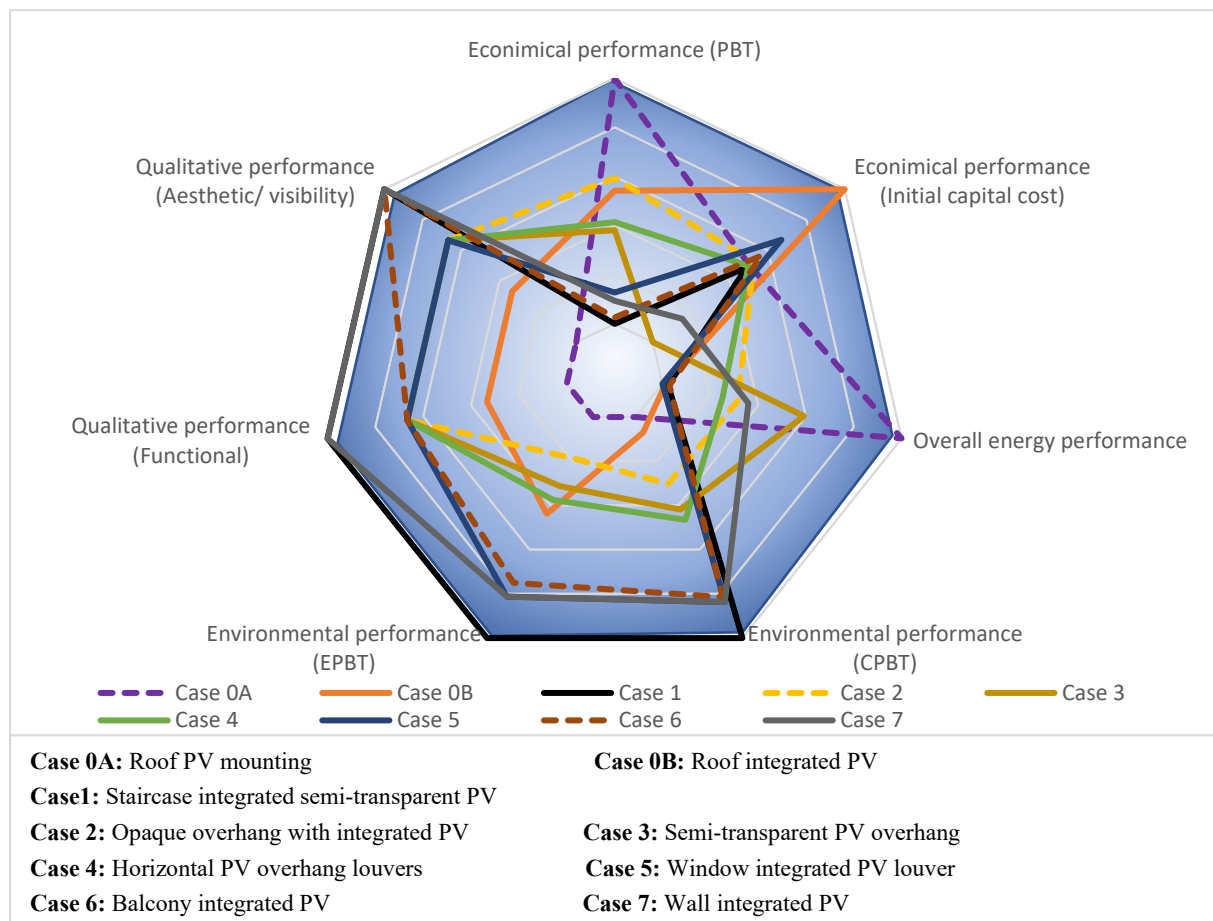


Figure 9-1: Decision support- matrix representing the proposed PV systems.

To simplify the discussion, Figure 9-2 below, illustrates the decision support matrix includes three cases, as can be seen, case 3 is the best in terms of environmental performance, while case 6 has a worst environmental performance, which is observed from the scores for CPBT and EPBT. On the other hand, case 3 has a higher aesthetical performance, while case 0A has a lower aesthetical performance.

In terms of economic performance, case 0A has a higher score regarding the payback time, and case 6 has a higher score regarding the initial cost, followed by case 0A with a small difference. This information allows architects, building designers, clients, etc., to decide on the criteria that they consider as more important. If there are regulations concerning environmental policies, case 0 is likely to be chosen. In the case where the building owner has cost limitations and a short-term view, he might choose case 6, and if he considers also the long-term view case 0A is the best solution. In addition, with the qualitative performance included, the user can also make an informed decision on the effect of the chosen case of the building appearance (visibility).

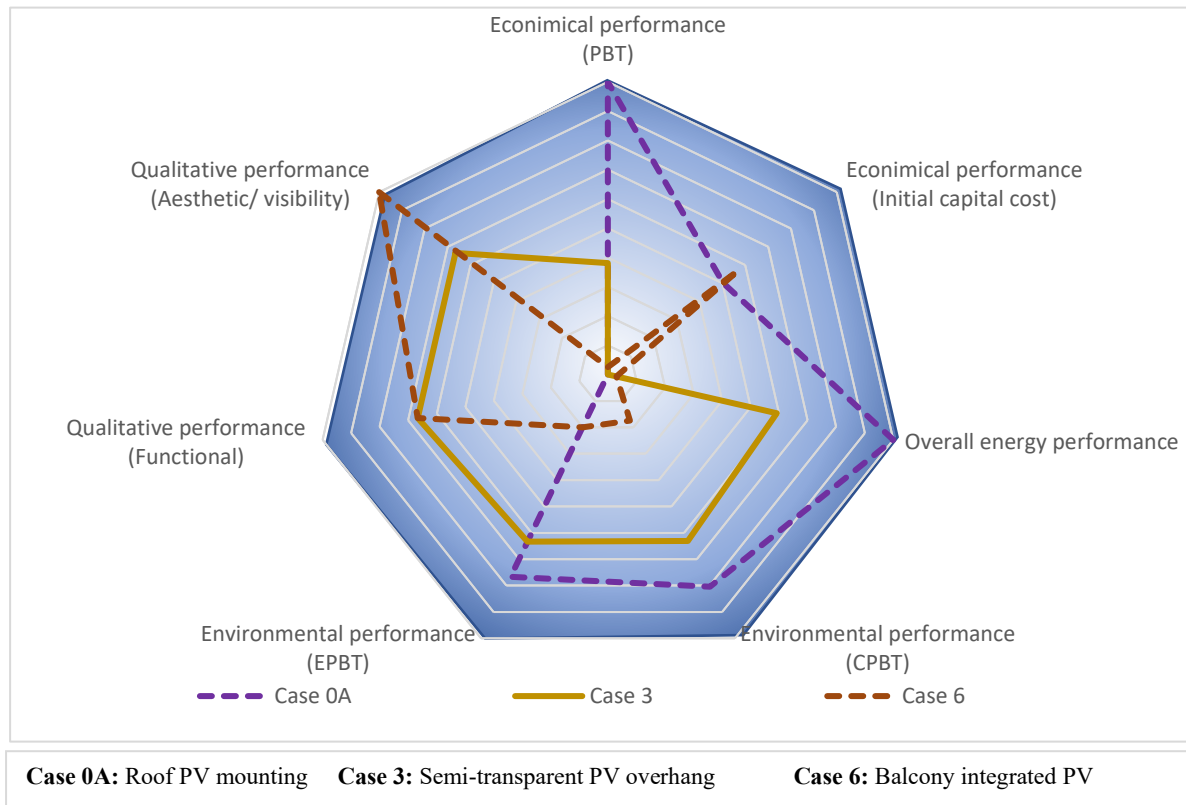


Figure 9-2: Decision support- matrix representing three cases of the proposed PV systems.

9.3 Summary

In this chapter, the performance results for the proposed solar systems applications from the previous chapters, have been presented, including environmental performance, economic performance, overall energy performance, and qualitative performance. After that, all the performance criteria have been presented in the same graphical matrix, and the exact value is hidden in this chart, to simplify the evaluation process. The user can choose a suitable case based on the desired criteria.

10 Research conclusions

In this chapter, the summary of the main steps used in this research and its related conclusions are presented. Also, the research limitations and recommendations for future research are highlighted. The research is focused on the integration of PV and ST systems into the multi-family building, in the Mediterranean area, taking Amman the capital of Jordan as a case study. The typical multi-family buildings in Amman, Jordan was firstly defined under the research context analysis. The studied typical multi-family building in Amman is composed of 5 main floors, 2 apartments on each floor, the total area of each apartment is 150 m² (135 m² heated area). It is assumed that the building is located in a most common typical residential zone in Jordan, which obliges 6 m side offset, and 8 m back offset, and considering one side is facing the main street toward the south, also all the surrounding buildings were assumed that have a maximum allowable height of 15 m. Regarding the PV and ST technologies, the considered technologies were the commercially available mono-crystalline PV modules due to it is relatively high efficiency and high reliability, and flat plate collector which is matching well developed local flat-plate collectors in Jordan.

10.1 Summary and outlook

The key research question of this thesis set out to investigate the potential of integrated PV and ST technologies into the new multi-family buildings in Amman, Jordan, through the multi-assessment approach. Considering different assessment criteria including life cycle energy, environmental, and economic performance, in addition to the visibility (formal) and functional performance criteria. The research question was partially answered, as regarding the ST the system was not integrated into the building envelope and the typical arrangements of the solar thermal on the roof were considered in this research, the reasons for not installation the ST collectors into the façade is described later in this chapter. However, regarding the PV systems, different designs and arrangements for the PV modules were proposed and investigated successfully. Each of the above-mentioned performance criteria was evaluated alone, after that, all the performance criteria results were presented in a decision support matrix, which can be used as a comparison to evaluate and identify the solar system's application of choice, depending on the criteria of the user.

The general conclusion of this research is that BIPV can have a positive contribution in terms of energy as it can cover up to 43% of the building electricity demand, when the PV modules installed into the south façade of the new (low energy) multi-family building in Amman, Jordan but their impact varies according to factors that need to be taken into account before choosing such an energy strategy (façades orientations, shading from the surrounding buildings, etc.). Moreover, it is also proved the environmental feasibility of all the proposed PV systems. In terms of the life cycle cost of the PV façade systems (under the current market price and the electricity tariff in Jordan), it seems that it's not a very economic technology in most cases. However, as the cost of PV is expected to decrease and the efficiency to increase, the cost criteria will be no more issue in the upcoming year. Moreover, removing electricity subsidies will also promote the economic feasibility of the PV systems. The research question was answered by using a mainly quantitative approach, in addition to the qualitative approach.

The quantitative approach is including literature review, numerical simulations analysis, and life cycle assessment, while the qualitative approach was based on the literature review analysis.

Through the literature review the relevant possibilities and the aesthetical solutions the market offers, and the multiple benefits for PV and ST integration were highlighted. Moreover, the knowledge acquired from this part played a significant role in choosing and designing the proposals of PV and ST installation into the multi-story building envelope. For example, it help to decide to install the ST system on the building roof while the PV systems on the building façade, this is because the PV modules have a better ability to architectural integration than the solar thermal collectors, also the BIPV market will be subject to continuous growth worldwide due to advances in technology, the reduced cost of PV materials, and the increase in incentive policies for renewable energy technologies in some countries worldwide.

Regarding the simulation software, different building and energy simulations software was used, mainly IDA ICE 4.8 to simulate and optimize the energy performance of the typical multi-family building in Amman, Jordan through passive and architectural design strategies, and Polysun 11 to find out the optimum design of the energy system in term of energy performance (energy demand of the system, and solar energy fraction), also to investigate the energy-saving potential of PV and ST systems with various designs (tilt angles, azimuth, installed area, etc.). For the IDA ICE building energy simulation, the multi-zone approach was adopted, and the energy demand was calculated on an hourly basis for a period of a whole year. Input data for the modeled building, including building site surroundings, architecture, floor plans, and specifications of walls, roof, and windows are based on the typical multi-family buildings practice in Amman, Jordan, as defined under the research context analysis. Another input data such as lighting, occupants and equipment's internal gains and schedule were defined based on standardized values or assumptions. In Polysun simulations, in order to simulate different solar systems, the available templates in the Polysun library were used and modified to match the proposed systems. Moreover, the energy demands profiles for the new (low energy) multi-family building in Amman, Jordan, were obtained from the detailed energy simulations in IDA ICE.

For the life cycle assessment, the previous literature, guidelines, and the obtained energy simulations results were adopted to determine the long-term performance in terms of energy and carbon emissions, as well as cost considerations, through using spreadsheet calculation. The environmental life cycle assessment considers the entire life of the proposed PV systems starting with the manufacturing of BIPV components from raw materials, their transport from the country of origin (China) to the site in Jordan, installation on-site, operation and maintenance, and disposal/recycling of waste. For each process-step direct uses as well as the indirect (grey) demand for energy due to the use of materials consumables necessary for manufacturing and raw materials was considered. Regarding the life cycle cost assessment of the PV systems, it covers all system life stages including, the initial costs, operation, maintenance, replacement cost, saving in electricity.

The research was conducted in different phases, the main quantitative results from all phases are presented in Figure 10-1 and Figure 10-2. Figure 10-1, show the effect of different design strategies (passive and architectural design, roof PV, roof ST, and different façade PV systems), on the primary energy demand for the studied multi-family building, in Amman, Jordan.

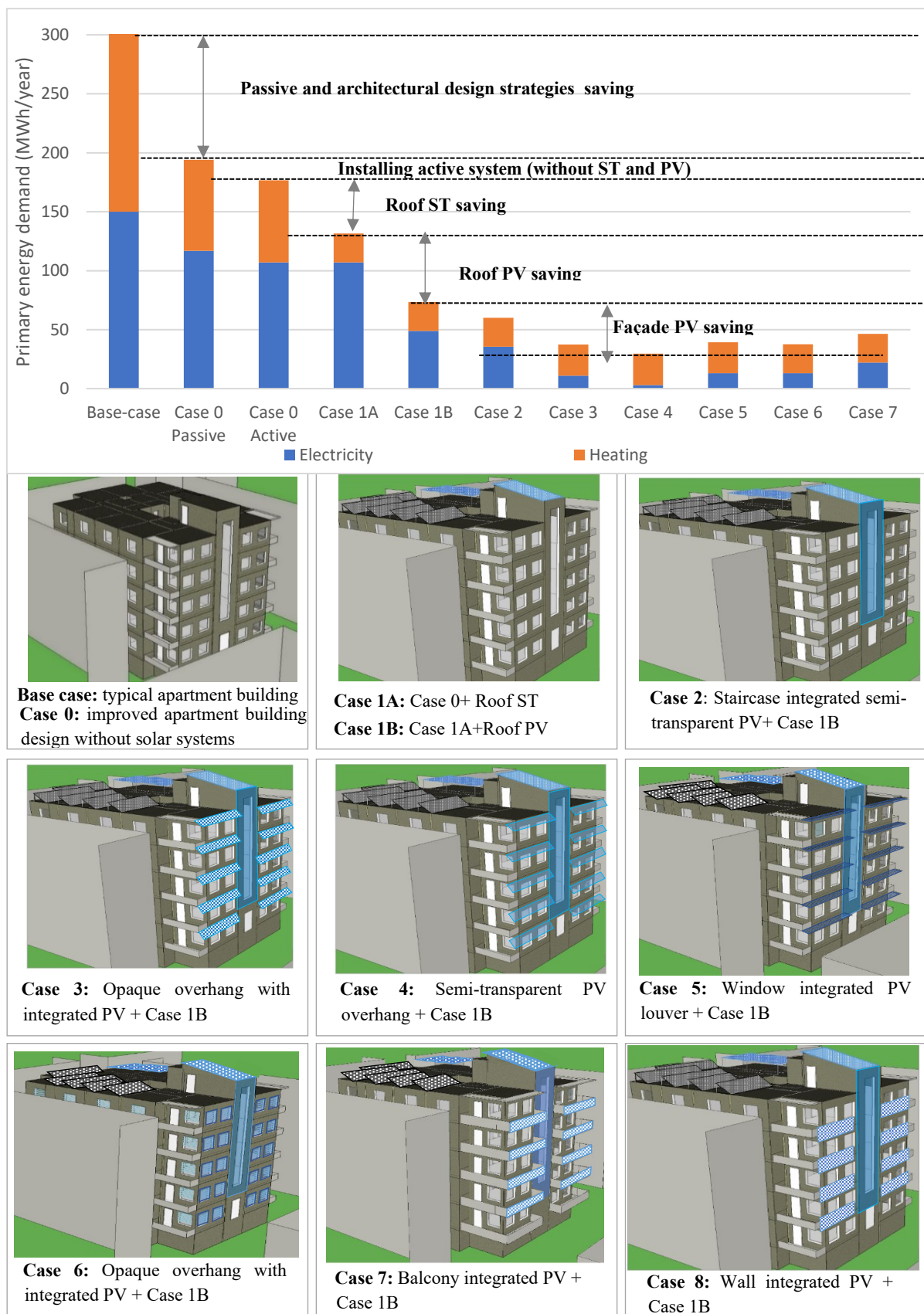


Figure 10-1: Primary energy demand in MWh/year for the multi-family building with 1,350 m² heated area in Amman, Jordan under different design strategies.

Figure 10-2 below, illustrates the energy, carbon, and cost payback time for different PV system designs.

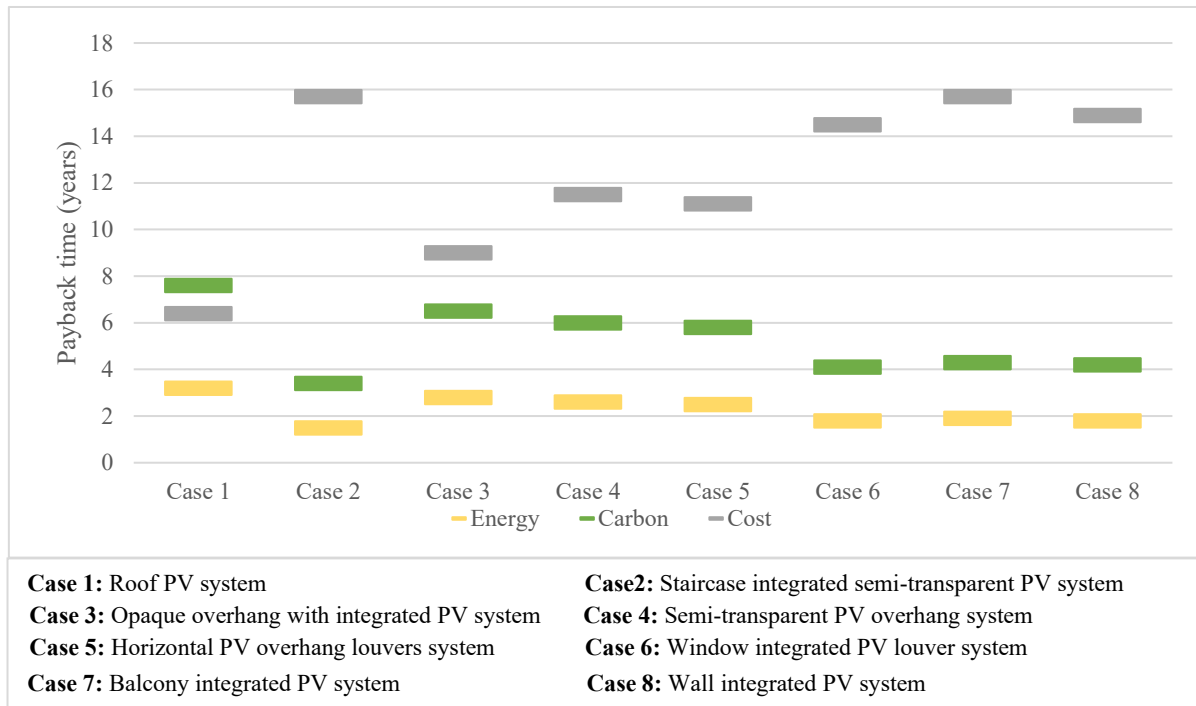


Figure 10-2: Energy, carbon and cost payback time in years for different PV systems designed installed into the multi-family building in Amman, Jordan

Below the summary and conclusions of each step are presented:

Reduce the building energy demands through passive and architectural design strategies

In this step and the next one, the sub research question of: “How can the energy performance of the multi-family building in Amman, Jordan be enhanced by improving the building envelope, passive measures, and energy-efficient systems?”. Firstly, the demand of the multi-family building under the typical practice was investigated by using IDA ICE simulation software, after that several design strategies were proposed, the effect of each strategy on the multi-family building energy demands was investigated alone and then in combination with the other strategies, to find the optimum solution to reduce the energy demand of the typical the multi-family building in Amman, Jordan. The result proved that it’s possible to reduce the annual energy demand of the typical apartment in Amman, Jordan by 53%, 71% and 78% of the annual thermal cooling, thermal heating, and lighting demands, respectively, by introducing passive and architectural design strategies. Around 45% savings of the thermal heating demand were achieved due to adding wall insulation. Regarding the thermal cooling demand about 17%, and 14% were saved due to applying a ventilated blind shading device and used a nighttime ventilation strategy.

Select energy-efficient solar heating and cooling systems

Regarding the solar energy-efficient active systems, the simulation results showed that the centralized solar combi-heating system can save up to 73% of the primary energy demand for heating in comparison to the conventional heating system (decentralized combi-heating system without solar collectors), under the typical arrangement, where the solar thermal collectors and photovoltaic panels are installed on the roof with about 60 m² total installed area, the tilt angle is 30° and all the collectors and panels are oriented toward the south. Regarding the cooling system, a centralized compression cooling system was selected, this system saves about 65% of primary energy for building cooling electricity demand in comparison to using the conventional split air conditioning system. Moreover, the typical installation of the 9 kWp PV system can cover around 42% of the total building electricity demand. An assessment of a battery implementation to this PV system was also carried out, and it was demonstrated as not worth the investment due to the current high price of the battery together with the low electricity tariff for the improved multi-family building in Amman, it was estimated that the cost of the battery will be recovered in 23 years when the battery is installed to the improved multi-family building. However, the battery can be more beneficial in the future, if the battery price reduced and the electricity cost increased, and it could also be more beneficial in a building with higher electricity demand (higher electricity purchase tariff).

Investigate the potential envelop area for the PV and ST technology installation

After reducing the multi-family building energy demand, the potential envelope area for the installation of the solar systems in the typical neighborhood context of Amman, Jordan was investigated. The outcome of this part, answer the research question “Where in the building envelope should the active solar technologies be installed?”, this question was answered by determining the suitable surface areas for the ST and PV installation based on incident solar irradiation on different surfaces, shading analysis and architectural suitable area for integration considering limitations due to the constructions, available surfaces area and use of the available surfaces for other purposes. The incident solar radiation on the building surfaces and the building solar exposure analysis of the location of Amman, Jordan was performed with Autodesk Ecotect analysis 2011 simulation software. Generally, the results of this part indicated that the highest potential envelop part of installing the solar systems is the roof, as most of its area is unshaded and received the highest solar radiation (2,050 kWh/m²/year), followed by the south façade with about 40% (1,300 kWh/m²/year), less received solar radiation and more shaded area, especially in the lower part of the facade. However, it was also noticed that without considering the effect of the surrounding building on the incident solar radiation, east and west facades were not that far behind the south façade in their solar potentials, with 7% (1,210 kWh/m²/year) and 10% (1,170 kWh/m²/year) less received solar radiation for east and west facades, respectively. Which means under different neighborhood context where the east and west not obstructed from the surrounding building, installation for active solar technology on these façades can be beneficial.

Investigate the energy potential of installing the PV modules and ST collectors on the roof

Based on the result from the previous step, the potential of installing the ST collectors and PV modules on the roof with different arrangements (tilts angle, direction, space between arrays, etc.) to cover part of the building energy was firstly investigated and compared to the conventional PV and ST roof arrangement (30° tilt angle, facing south, 60 m² total installed area for each PV modules and ST collectors). It was found that increasing the solar thermal collectors' installed area on the roof didn't increase the solar fraction in comparison to the typical arrangements, the main reason is that the solar fraction is more than 90% during 8 months (from April to November), where only the hot water needed. Accordingly, the typical arrangement of the solar thermal collectors which can cover around 70% of the building water and space heating demand was selected. Regarding the photovoltaic system, the PV modules designed to be mounted above the roof, facing the south and have a 2° tilted angle with the total capacity of 9.9 kWp, in addition to integrate part of the PV modules to the roof of the staircase with 30° tilt angle, and a total capacity of 2.7 kWp, resulting in a total installed PV system capacity of 12.6 kWp on the roof. This design allows using the maximum space of the roof as much as possible, in addition, to use the space under the mounting PV modules for other activities. This PV system can cover about 54% of the building electricity demand.

Investigate the potential of installing the PV modules into the south facade

For the façade application, only the PV application was considered in this research (based on the above-mentioned results, and on the literature review analysis). Different design possibilities for PV module installations on the south façade were proposed based on the available façade area, solar radiation, shading on the façade, and available products in the market. Moreover, an overall energy index was developed considering all the energy factors, including the building primary energy demand taking into account the effect of PV installation into the façade on the building energy demand and the net energy production of the solar PV systems considering the effect of shading on the PV production.

The results showed that although the south façades received lower solar radiation than the roof, their large available area can contribute significantly to the overall solar potential, as the façade can cover between 12% to 43% of the building electricity demand, dependent on the PV systems design and tilt angles (see Figure 10-1). Generally, with both façade and roof PV applications, the covered building electricity demands were estimated to be between 66% and 97%.

Determine the energy, carbon and cost life cycle performance

In order to holistically examine the performance of the photovoltaic system, an LCA which considers the entire life of the proposed PV systems was evaluated. In this step the sub research question of: “What is the energy, environmental and economic performance of a solar system installed in a multi-family residential building in Amman, Jordan over its lifetime?”, was answered. the energy, carbon and cost payback time for all the proposed PV systems have been presented in Figure 10-2.

Regarding the environmental life cycle assessment, it was found that the EPBT (energy payback time) is between 1.5- 3.5 years and the CPBT (carbon payback time) is between 3.4-7.8 years in all cases. These results proved the carbon saving potential of all the proposed PV systems. Moreover, the life cycle energy use at different life stages showed that the photovoltaic manufacturing process makes up the largest contributions for all BI(PV) systems.

In this research, the PV systems were assumed that have been imported from China, where most of its produced energy comes from coal-fired power plants which lead to large amounts of GHG emissions during the production stage. Therefore, the GHG emissions could be reduced significantly, if China increasing their renewable energy production, or by the production being transferred to a location using renewable energy sources to a higher degree.

Regarding the life cycle economic performance, the price of the PV roof mounting system was estimated to be recoverable in about 4 years, whereas the cost of the PV façade systems could be recovered in about 9-16 years depends on the system design (module design (opaque frameless, semi-transparent module), tilt angle, and the support structure design (integrated or mounting), etc.). However, in the future, the cost is expected to decrease, which could improve the PV system cost viability. Moreover, the PV payback time can be reduced significantly in a building with a higher electricity demand or in a country with higher electricity prices. Another aspect that can improve the economic feasibility of the PV systems, is to remove the electricity subsidies, this will increase the electricity price and accordingly decrease the payback time for the photovoltaic systems.

Develop a decision support matrix

This research was finalized with a multi-assessment matrix, including environmental performance (CPBT, EPBT), economic performance (capital cost, PBT), overall energy performance, in addition to the qualitative performance (formal and functional performance), to emphasize the substantial function of BIPV as it not only has the advantage of electricity generation but also can replace current building materials, act as a shading, etc. This step can help to bridge the gap in communication between designers, PV manufacturers, investors, building owners, etc., and to assess them to select a PV system design based on their desired criteria.

Overall conclusions

To sum up, the installation of solar PV modules on building's roof is more beneficial in term energy performance than building's facade, as it received a higher amount of solar radiation, and has more solar exposure, however, the facade significantly higher area can enhance the total solar fraction. Both PV facade and roof application can satisfy up to 66% - 97% of the total electricity demand of 5 floors multi-family improved building in Amman, Jordan, the roof alone can cover around 54% of the building electricity demand. For buildings having the same rooftop surface area, but a bigger number of floors, the available facade area will be far greater than the roof area, thus the PV facades can greatly increase the covered amount of building electricity demand. Moreover, the PV roof application neglects the esthetical aspect of architectural integration, on the other hand, become more interesting in term cost. For facade applications, it seems that it's not a very economical solution at the current point of time, under most of the cases. However, in the case of BAPV (where the PV modules attached to the top of the building), the energy, and cost performance is better than in the case of BIPV (for example wall integrated PV), on the other hand, it has less aesthetical value. The high initial cost of the PV modules could prevent users from integrating or attaching them to their buildings. However, in the future, when the PV modules have higher efficiency and lower prices, and the market is more open toward such applications, the integration of PV into the building will be more widespread and applied.

This research contributes to the knowledge in the solar buildings in the Mediterranean area, using alternative energy sources and making building systems as energy efficient as possible, and optimize the application of BIPV. By proposing the implementation of vertical facades, tall buildings within the urban landscape may also be able to adopt BIPV systems because they are likely to have restricted roof area. In addition, it enhances the ability of the building designer to produce more energy-efficient buildings and promotes building owners to implement PV systems on their building by demonstrating the interest there might be in a BI(PV) systems. Research findings indicate several courses of action and here the government's responsibility should be to provide a comprehensive plan to develop an attitude towards active solar-friendly communities and enhance policies on photovoltaic adoption in buildings, supported by promotion and education to raise public consciousness. Such a market's local entry could generate many work possibilities, it could also enrich the region with an overseas exported renewable energy resource.

10.2 Research limitations and future work

In this part, the limitations of this research are highlighted along with a suggestion for possible further research.

- The research focused on incorporating BIPV into the new multi-family building, further research could focus on the existing multi-family building.
- The BIPV performance was investigated based on multi-family apartment buildings, but it can also be extended to other building types such as educational, industrial or commercial buildings. As buildings with different functions have different designs (height, geometry, material, etc.) and different internal heat loads, energy demands, electricity tariffs, etc.
- The most common urban zone was considered in this research, however, the urban layout's characteristics, such as the widths of the street with different directions, buildings height, setbacks, etc., could greatly affect the solar suitability of the building envelope. Therefore, the effect of different urban environment context layout should be included in future research.
- Mono-crystalline PV cell technology was considered in this research; a different type of PV cell technology might have a different possibility for building integration. Therefore, further research can consider other PV technologies, such as thin-film technology, as it has aesthetic advantages (low thickness, lightweight and high flexibility) that can benefit facades.
- In this research, the effect replacing the construction materials with PV modules, on the embodied energy, carbon emissions and cost were not considered, which may also have a positive effect in terms of cost-saving, avoided the embodied energy and decreasing GHG emissions. Therefore, future research could be considered the entire building life cycle assessment.
- Further research could be the application of BIPV into the real building project to assist practicality in real-life situations. This can be used to highlight the potential benefits and effectiveness of the method so that it can be improved or evaluated accordingly. Moreover, it will allow the validation of the simulation using measurements.
- Finally, interviews and surveys with architects, clients, etc., can be also conducted in order to explore the preferences, perceptions and the recommendations on architectural PV integration, and for a more holistic review of BIPV application.

References

- Abdalla, N. (2013) 'Solar Thermal Energy for Buildings in Jordan', in *National Center for Research & Development (NERC)*. Amman, Jordan.
- Abdelhai, A. (2014) *Solar Water Heating Market Transformation and Strengthening Initiative (GSWH Project)*.
- Aberg, E. *et al.* (2014) 'Up-scaling Solar PV for Self-Consumption in the Jordanian Market'. Jordan: Regional Center for Renewable Energy and Energy Efficiency (RCREEE). Available at: http://www.rcreee.org/sites/default/files/rcreee_up-scaling_solar_pv.pdf.
- Aboushi, A. and Raed, A. (2015) 'Heating Indoor Swimming Pool Using Solar Energy with Evacuated Collectors', in *International Conference on Advances in Environment Research*. Singapore, pp. 90–94.
- Adas, H. (2016) *Installation of solar water heaters*. Jordan: Vocational Training Corporation.
- Al-adwan, I. M. (2013) 'Performance Assessment of the First Residential Grid-Tie PV System in Jordan', 3(4), pp. 7–14.
- Al-Asir, H.S. *et al.* (2009) 'Climate Conscious Architecture and Urban Design in Jordan- Towards energy efficient buildings and improved urban microclimate'. Jordan: Housing Development & Management and the Royal Scientific Society.
- Al-Salaymeh, A. *et al.* (2010) 'Technical and economical assessment of the utilization of photovoltaic systems in residential buildings: The case of Jordan', *Energy Conversion and Management*, 51(8), pp. 1719–1726.
- Alex, P. (2014) 'EE-RE projects with Med North-South involvement, DIDSOLT-project', in *Mediterranean Building Rethinking For Energy Efficiency Improvement (MARIE) 6th Steering Committee*. Malta.
- Ali, A. and Alzaed, A. (2017) 'Residential scale solar driven cooling systems versus conventional air-conditioning in hot arid areas: A comparative study', *Materials Physics and Mechanics*, 32(1), pp. 21–30.
- Alibaba (2019) *BIPV double glass transparent solar pv module for building*. Available at: https://www.alibaba.com/product-detail/BIPV-double-glass-transparent-solar-pv_60437946497.html (Accessed: 5 June 2019).
- Alnsour, J. A. (2016a) 'Affordability of Low Income Housing in Amman, Jordan', *Jordan Journal of Economic Sciences*, 3(1), pp. 65–79.
- Alnsour, J. A. (2016b) 'Managing urban growth in the city of Amman, Jordan', *Cities*. Elsevier B.V., 50, pp. 93–99.
- Alsema, E. A., de Wild-Scholten, M. J. and Fthenakis, V. M. (2006) 'Environmental Impacts of PV Electricity Generation- a Critical Comparison of Energy Supply Options', *The 21st European Photovoltaic Solar Energy Conference, Dresden, Germany*, (September), p. 7.

Alshamaileh, E. (2010) 'Testing of a new solar coating for solar water heating applications', *Solar Energy*. Elsevier Ltd, 84(9), pp. 1637–1643.

Alzoubi, H. and Alshboul, A. (2010) 'Low energy architecture and solar rights: Restructuring urban regulations, view from Jordan', *Renewable Energy*. Elsevier Ltd, 35(2), pp. 333–342.

Amman Municipality (2018) 'Building Regulation and Zoning in Amman City, Ammended regulation of the buildings and zoning in Amman'. Jordan: Amman Municipality.

Antonello, S., Alawneh, F. and Basha, L. (2015) *Fostering solar technology in the Mediterranean area Project - Guidelines*. Italy.

Available at: <http://www.fosterinmed.eu/index.php/project-results>.

Asfour, O. (2018) 'Solar and Shading Potential of Different Configurations of Building-integrated Photovoltaics Used as Shading Devices Considering Hot Climatic Conditions', *Sustainability*, 10(12), p. 4373.

ASHRAE (2004) *ANSI/ASHRAE Standard 55-2004. Thermal Environmental Conditions for Human Occupancy SECTION*. Atlanta: American Society of Heating, Refrigerating and Air-Conditioning Engineers.

ASHRAE (2016) 'ASHRAE Standard 62.2-2016: Ventilation and Acceptable Indoor Air Quality in Residential Buildings'. Atlanta, GA: American Society of Heating, Refrigerating and Air-Conditioning Engineers, Inc.

Attia, S. (2014) 'Strategic Decision Making For Zero Energy Buildings in Jordan', *International Conference on Energy and Indoor Environment for Hot Climates*, pp. 73–81.

Attia, S. and Al-Khuraissat, M. (2016) 'Life cycle Costing for a Near Zero Energy Building in Jordan Initial Study', in *The 5th Architectural Jordanian International Conference*. Amman, Jordan.

Awadallah, T. (2015) 'Role of Street-Level Outdoor Thermal Comfort in Minimizing Urban Heat Island Effect by Using Simulation Program, Envi-Met: Case of Amman, Jordan', *Research Journal of Environmental and Earth Sciences* 7(3):, 7(3), pp. 42–49.

Bakos, G. C., Soursos, M. and Tsagas, N. F. (2003) 'Technoeconomic assessment of a building-integrated PV system for electrical energy saving in residential sector', *Energy and Buildings*, 35(8), pp. 757–762.

Baranda, P. B. and Sartori, I. (2014) *Cost Optimality of Energy Systems in Zero Emission Buildings in Early Design Phase*. NTNU- Norwegian University of science and technology.

Basnet, A. (2012) *Architectural Integration of Photovoltaic and Solar Thermal Collector Systems into buildings*. Norwegian University of Science and Technology.

Bataineh, K. and Alrabee, A. (2018) 'Improving the Energy Efficiency of the Residential Buildings in Jordan', *Buildings*, 8(7), p. 85.

Baxter, R. *et al.* (2017) 'CHAPTER 6 Building-integrated Photovoltaics (BIPV) for Cost-Effective Energy-Efficient Retrofitting', in *Cost-Effective Energy Efficient Building Retrofitting: Materials, Technologies, Optimization and Case Studies*, pp. 169–197.

Beccali, M. *et al.* (2016) 'Building-integrated solar thermal design: assessment of performances of a low cost solar wall in a typical Italian building', *Energy Procedia*. The Author(s), 91, pp. 916–925.

Berenschot (2015) *Roadmap Building-integrated Photovoltaics*.

Bhandari, K. P. *et al.* (2015) 'Energy payback time (EPBT) and energy return on energy invested (EROI) of solar photovoltaic systems: A systematic review and meta-analysis', *Renewable and Sustainable Energy Reviews*. Elsevier, 47, pp. 133–141.

Bizzarri, G., Gillott, M. and Belpoliti, V. (2011) 'The potential of semitransparent photovoltaic devices for architectural integration: The development of device performance and improvement of the indoor environmental quality and comfort through case-study application', *Sustainable Cities and Society*. Elsevier B.V., 1(3), pp. 178–185.

Bonomo, P., Frontini, F. and Chatzipanagi, A. (2015) 'Overview and analysis of current BIPV products: new criteria for supporting the technological transfer in the building sector', *VITRUVIO - International Journal of Architectural Technology and Sustainability*, 1(1), pp. 67–85.

Bonomo, P., Zanetti, I. and Frontini, F. (2016) 'BIPV PRODUCTS OVERVIEW FOR SOLAR BUILDING SKIN', in *33rd European Photovoltaic Solar Energy Conference and Exhibition*, pp. 45–46.

Buker, M. S. and Riffat, S. B. (2015) 'Building-integrated solar thermal collectors – A review', *Renewable and Sustainable Energy Reviews*. Elsevier, 51, pp. 327–346.

Buonomano, A. *et al.* (2015) 'Building façade integrated solar thermal collectors for water heating: simulation model and case studies', in *BIRES 2017 - First International Conference on Building-integrated Renewable Energy Systems*. Dublin, Ireland.

Cannavale, A. *et al.* (2017) 'Improving energy and visual performance in offices using building-integrated perovskite-based solar cells: A case study in Southern Italy', *Applied Energy*, 205(November), pp. 834–846.

Cappel, C. *et al.* (2014) 'Barriers to the market penetration of façade-integrated solar thermal systems', *Energy Procedia*. Elsevier B.V., 48, pp. 1336–1344.

Cappel, C. *et al.* (2015) *AktiFas Fassadenintegrierte Solarthermie: Bestandsaufnahme und Entwicklung zukunftsfähiger Konzepte*.

Carbonell, D., Haller, M. Y. and Frank, E. (2014) 'Potential benefit of combining heat pumps with solar thermal for heating and domestic hot water preparation', *Energy Procedia*. Elsevier B.V., 57, pp. 2656–2665.

CENELEC (2016) 'BIPV Standard EN 50583 - Photovoltaics In Buildings', pp. 1–24.

Cerón, I., Caamaño-Martín, E. and Neila, F. J. (2013) 'State-of-the-art of building-integrated photovoltaic products', *Renewable Energy*. Elsevier Ltd, 58, pp. 127–133.

CIBSE (2006) 'Guide A: Environmental Design'. London: Chartered Institution of Building Services Engineers.

CIBSE (2013) 'Lighting for Communal Residential Buildings - LG9.' Chartered Institution of Building Services Engineers.

Cucchiella, F. *et al.* (2012) 'Renewable energy options for buildings: Performance evaluations of integrated photovoltaic systems', *Energy and Buildings*. Elsevier B.V., 55, pp. 208–217.

Department Of Statistics (2016) *Population and housing census, Department of statistics Jordan*. Jordan.

Dessi, V. (2011) 'Visibility Assessment of the Integration of Technologies from R. E.S. in Sensitive Urban Environments. Proposal for a Simplified Graphical Tool.', in *International Building Performance Simulation Association*, pp. 1–13.

Ekoe A Akata, A. M., Njomo, D. and Agrawal, B. (2017) 'Assessment of Building-integrated Photovoltaic (BIPV) for sustainable energy performance in tropical regions of Cameroon', *Renewable and Sustainable Energy Reviews*. Elsevier Ltd, 80(March 2018), pp. 1138–1152.

ENERGY RATING (2018) *Light bulb buying guide, E3 Equipment Energy Efficiency*. Available at: http://www.energyrating.gov.au/sites/new.energyrating/files/documents/factsheet_light_bulb_buying_guide_1.pdf (Accessed: 15 February 2019).

EQUA (2018) 'Getting Started with IDA Indoor Climate and Energy- Manual version: 4.8', *The Grounded Theory Review: An International Journal*.

EQUA Simulation AB (2010) *Validation of IDA Indoor Climate and Energy 4.0 build 4 with respect to ANSI/ASHRAE Standard 140-2004*. Available at: <http://www.equaonline.com/iceuser/validation/ASHRAE140-2004.pdf>.

Etier, I., Al, A. and Ababne, M. (2010) 'Analysis of Solar Radiation in Jordan', *Jordan Journal of Mechanical and Industrial Engineering*, 4(6), pp. 733–738.

Fang, L., Honghua, X. and Sicheng, W. (2017) *National Survey Report of Photovoltaic Applications in Australia 2017*.

Fasfous, A. *et al.* (2013) 'Potential of utilizing solar cooling in the University of Jordan', *Energy Conversion and Management*. Elsevier Ltd, 65(January), pp. 729–735.

Fattouh, B. (2010) 'Energy Subsidies in the Middle East: Issues & Implications', in *Increasing the Momentum of Fossil-Fuel Subsidy Reform*. Geneva.

Kalogirou, S.A (2015) 'Building-integrated Solar Thermal Systems', in *Proceedings of COST Action*, pp. 1–9.

La Fleur, L., Moshfegh, B. and Rohdin, P. (2017) 'Measured and predicted energy use and indoor climate before and after a major renovation of an apartment building in Sweden', *Energy and Buildings*. Elsevier B.V., 146, pp. 98–110.

Fraunhofer Institute for Solar Energy Systems, I. (2018) *Photovoltaics Report*.

Frischknecht, R. *et al.* (2016) *Methodology Guidelines on Life cycle Assessment of Photovoltaic*

Electricity 3rd edition, International Energy Agency Photovoltaic Power Systems Programme - Task 12. Ursen, Switzerland: IEA PVPS Task 12; International Energy Agency Photovoltaic Power Systems Programme.

Frontini, F. *et al.* (2015) *BIPV Product Overview for Solar Façades and Roofs*. Available at: <https://www.seac.cc/en/publications/>.

Fthenakis, V. M. and Kim, H. C. (2011) 'Photovoltaics: Life cycle analyses', *Solar Energy*. Elsevier Ltd, 85(8), pp. 1609–1628.

Fthenakis, V. M., Kim, H. C. and Alsema, E. A. (2008) 'Emissions from photovoltaic life cycles: Supporting information', *Environmental science & technology*, 42(6), pp. 2168–74.

Fu, Y., Liu, X. and Yuan, Z. (2015) 'Life cycle assessment of multi-crystalline photovoltaic (PV) systems in China', *Journal of Cleaner Production*. Elsevier Ltd, 86(January 2015), pp. 180–190.

Gaidajis, G. and Angelakoglou, K. (2012) 'Environmental performance of renewable energy systems with the application of life cycle assessment: a multi-Si photovoltaic module case study', *Civil Engineering and Environmental Systems*, 29(4), pp. 231–238.

Gan, G. (2009) 'Numerical determination of adequate air gaps for building-integrated photovoltaics', *Solar Energy*. Elsevier Ltd, 83(8), pp. 1253–1273.

Gharras, A. El, Menichetti, E. and Cottret, N. (2014) *Solar Thermal Action Plan for the Mediterranean Countries*.

Global Industry Analysts Inc (2016) *Building-integrated Photovoltaics (BIPV): Technologies and Global Markets*.

Goussous, J. and Al-Refaie, A. (2014) 'Evaluation of a Green Building Design Using LCC and AHP Techniques Jawdat', *Life Science Journal* 2014;11(8s), 11, pp. 29–40.

Goussous, J., Siam, H. and Alzoubi, H. (2014) 'Prospects of green roof technology for energy and thermal benefits in buildings: Case of Jordan', *Sustainable Cities and Society*. Elsevier B.V., 14, pp. 425–440.

Graefenhain, M., Fiedler, F. and Tsanakas, I. (2017) *Energy Yield Simulation Analysis of Bifacial PV Installations in the Nordic Climate, European Solar Engineering School*.

Graillot, A. *et al.* (2014) *The regulatory framework and tariff scheme for grid-connected photovoltaic power plants in Lebanon, Jordan and Palestinian Territories and Recommendations*. Jordan.

Greentech Media (2010) *Building-integrated Photovoltaics: An Emerging Market (Executive Summary)*, GTM-Research.

Grete, A., Prof, H. and Mnal, A. (2001) 'photovoltaics, building integration, PV cell visual characteristics, product development trends', (2).

GTZ (2009) *Solar Thermal Application in Egypt, Jordan, Lebanon, Palestinian Territories, Syria and Tunisia: Technical Aspects, Framework Conditions and Private Sector Needs*. Cairo.

Hafner, M. *et al.* (2012) *Outlook for Electricity and Renewable Energy in Southern and Eastern Mediterranean Countries, Mediterranean prospects.*

Hammad, M. and Ebaid, M. S. Y. (2015) 'Comparative economic viability and environmental impact of PV, diesel and grid systems for large underground water pumping application (55 wells) in Jordan', *Renewables: Wind, Water, and Solar*. Renewables: Wind, Water, and Solar, 2(1), p. 12.

Hammond, G. P. *et al.* (2012) 'Whole systems appraisal of a UK Building-integrated Photovoltaic (BIPV) system: Energy, environmental, and economic evaluations', *Energy Policy*, 40(1), pp. 219–230.

Hammond, P. G. and Jones, C. (2011) 'Inventory of Carbon & Energy (ICE)', *Mechanical Engineering*, 161.

Hanania Energy (2017) *Domestic Hot Water*.

Available at: <http://www.hanania.jo/product.php?id=33> (Accessed: 16 June 2017).

Heinstein, P., Ballif, C. and Perret-Aebi, L. E. (2013) 'Building-integrated photovoltaics (BIPV): Review, potentials, barriers and myths', *Green*, 3(2), pp. 125–156.

Hesaraki, A. and Holmberg, S. (2013) 'Energy performance of low temperature heating systems in five new-built swedish dwellings: A case study using simulations and on-site measurements', *Building and Environment*. Elsevier Ltd, 64, pp. 85–93.

Hestnes, A. G. (1999) 'Building Integration Of Solar Energy Systems', *Solar Energy*, 67, pp. 181–187.

Hickman, J. *et al.* (1999) 'Methodology for Calculating Transport Emissions AND ENERGY CONSUMPTION'. TRANSPORT RESEARCH LABORATORY PROJECT.

Hitchin, R. (2019) 'Primary Energy Factors and the primary energy intensity of delivered energy: An overview of possible calculation conventions', *Building Services Engineering Research and Technology*, 40(2), pp. 198–219.

Hou, G. *et al.* (2016) 'Life cycle assessment of grid-connected photovoltaic power generation from crystalline silicon solar modules in China', *Applied Energy*. Elsevier Ltd, 164, pp. 882–890.

IEA (2001) 'Task 7 of the PV power systems program- Achievements and outlook', *International Energy Agency*.

Available at: http://www.task7.org/Public/17theupvsec/paper_task7_17th_eu_pvsec.pdf.

IEA (2010) *Task 41 - Solar Energy and Architecture- State of the Art of Digital Tools Used by Architects for Solar Design*.

IEA (2012) *IEA SHC Task 41: Building integration of Solar Thermal and Photovoltaics: barriers, needs, strategies*. Available at: <http://task41.iea-shc.org/publications>.

IEA (2013) 'Task-41 Designing Photovoltaic Systems for Architectural Integration'. International Energy Agency, p. 84.

IEA (2016) *Solar Heat Worldwide, Market and Contribution to Energy Supply 2014*, IEA.

- IEA (2017a) *Energy Access Outlook 2017: From poverty to prosperity*, International Energy Agency.
- IEA (2017b) 'IEA PVPS- Task 15: Enabling Framework for the Acceleration of BIPV'. International Energy Agency.
- IEA (2018a) *Snapshot of Global Photovoltaic Markets*.
- IEA (2018b) *Solar Heat Worldwide-Global Market Development and Trends in 2017-Detailed Market Figures 2016*.
- IEA (2019a) *Jordan energy balance*, International Energy Agency. Available at: <https://www.iea.org/sankey/#?c=Jordan&s=Balance> (Accessed: 22 July 2019).
- IEA (2019b) 'Statistics & Data', International Energy Agency P. Available at: <https://www.iea.org/statistics/?country=JORDAN&year=2016&category=Key indicators&indicator=TPESbySource&mode=chart&categoryBrowse=false&dataTable=BALANCES&showDataTable=false> (Accessed: 10 January 2016).
- IEA SHC Task 51 (2016) *Innovative Solar Products for Building Integration -Website startet by Task 41 in 2013*. Available at: <https://solarintegrationsolutions.org/index.php?page=solarthermal> (Accessed: 6 December 2018).
- Isa Zanetti *et al.* (2017) *building-integrated Photovoltaics: Product overview for solar building skins*. Available at: [http://www.bipv.ch/images/Report 2017_SUPSI_SEAC_BIPV.pdf](http://www.bipv.ch/images/Report%202017_SUPSI_SEAC_BIPV.pdf).
- Jaber, J. (2016) 'Renewable Energy Policies Case Study For Jordan', in *7TH INTERNATIONAL FORUM ON ENERGY FOR SUSTAINABLE DEVELOPMENT*.
- Jaber, J. and Probert, S. (2002) 'Purchased-energy consumptions in Jordan's commercial and public-service sector', *Applied Energy*, 71(1), pp. 31–34.
- Jaber, S. (2012) *Solar Water Heater in Jordan*. Jordan: NERC, Jordan National Energy Research Center.
- Jaber, S. and Ajib, S. (2011a) 'Evaporative cooling as an efficient system in Mediterranean region', *Applied Thermal Engineering*. Elsevier Ltd, 31(14–15), pp. 2590–2596.
- Jaber, S. and Ajib, S. (2011b) 'Thermal and economic windows design for different climate zones', *Energy and Buildings*. Elsevier B.V., 43(11), pp. 3208–3215.
- Jaber, S. and Hawa, A. A. (2016) 'Optimal design of PV system in passive residential building in Mediterranean climate', *Jordan Journal of Mechanical and Industrial Engineering*, 10(1), pp. 39–49.
- Jäger, J. *et al.* (2012) *Stone and Architecture: In the Mountainous Regions of Jordan and Syria*. Available at: http://books.google.co.uk/books/about/Stone_and_Architecture.html?id=_oASkgEACAAJ&pgis=1.
- James, T. *et al.* (2012) 'Building-integrated Photovoltaics (BIPV) in the Residential Sector: An Analysis of Installed Rooftop System Prices', *Technical Report NREL/TP-6A20-53103*, (November), p. 50.

James, T. *et al.* (2017) *Building-integrated Photovoltaics (BIPV) in the Residential Sector: An Analysis of Installed Rooftop System Prices*, NREL/national laboratory of the U.S. Department of Energy, Office of Energy Efficiency & Renewable Energy.

Jelle, B. P. (2016) 'Building-integrated photovoltaics: A concise description of the current state of the art and possible research pathways', *Energies*, 9(1), pp. 1–30.

Jelle, B. P., Breivik, C. and Drolsum Røkenes, H. (2012) 'Building-integrated photovoltaic products: A state-of-the-art review and future research opportunities', *Solar Energy Materials and Solar Cells*. Elsevier, 100(7465), pp. 69–96.

Jfranews (2013) '' *Economists: Require housing to install solar heaters hasty decision* ''. Available at: <http://www.jfranews.com.jo/post.php?id=66509> (Accessed: 25 February 2019).

Jordanian Department of Statistics (2015) *General Population and Housing Census 2015 Main Results*. Jordan.

Jungbluth, N. *et al.* (2012) 'Life cycle Inventories of Photovoltaics'. Swiss Federal Office of Energy SFOE, p. 238.

Kaan, H. and Reijenga, T. (2004) 'Photovoltaics in an architectural context', *Progress in Photovoltaics: Research and Applications*, 12(6), pp. 395–408.

Karlsson, F., Rohdin, P. and Persson, M. L. (2007) 'Measured and predicted energy demand of a low energy building: Important aspects when using building energy simulation', *Building Services Engineering Research and Technology*, 28(3), pp. 223–235.

Kawkabuna (2013) *Water heating systems*. Available at: <http://www.kawkabuna.com/Content/Content.aspx?c=Waterheatingsystems> (Accessed: 25 February. 2019).

Kayali, H. and Dr. Halil Alibaba, A. P. (2017) 'Comparison of Different Solar Thermal Energy Collectors and Their Integration Possibilities in Architecture', *Sustainability in Environment*, 2(1), p. 36.

Kiki, P. *et al.* (2008) *Integration of Solar Technologies into Buildings in Mediterranean Communities Electronic guide CRES*. Pikermi.

Knaack, J. M. *et al.* (2014) *Enabling PV in the MENA Region, The Emerging PV Market in Jordan*. Germany: Deutsche Gesellschaft für Internationale Zusammenarbeit (GIZ) GmbH.

Koo, C. *et al.* (2017) 'Development of the smart photovoltaic system blind and its impact on net-zero energy solar buildings using technical-economic-political analyses', *Energy*. Elsevier Ltd, 124(February), pp. 382–396.

Kosic, T. (2015) 'Economic aspect of solar thermal collectors' integration into facade of multifamily housing', in *Proceedings of COST Action TU1205 Symposium*.

Kuhn, T. E. (2017) 'State of the art of advanced solar control devices for buildings', *Solar Energy*. Pergamon, 154, pp. 112–133.

- Lai, C.-M. and Hokoi, S. (2015) 'Solar façades: A review', *Building and Environment*. Elsevier Ltd, 91, pp. 152–165.
- Lamnatou, C. *et al.* (2014) 'Life cycle analysis of a building-integrated solar thermal collector, based on embodied energy and embodied carbon methodologies', *Energy and Buildings*. Elsevier B.V., 84, pp. 378–387.
- Lamnatou, C. (2015) 'Evaluation of the environmental profile of a building-integrated solar thermal collector, based on multiple life cycle impact assessment methodologies', in *Proceedings of COST TU1205 Symposium*.
- Lamnatou, Chr *et al.* (2015) 'Modelling and simulation of Building-integrated solar thermal systems: Behaviour of the coupled building/system configuration', *Renewable and Sustainable Energy Reviews*. Elsevier, 48, pp. 178–191.
- Lamnatou, Chrysovalantou *et al.* (2015) 'Review and perspectives on Life cycle Analysis of solar technologies with emphasis on building-integrated solar thermal systems', *Renewable Energy*. Elsevier Ltd, 75, pp. 833–846.
- Lamnatou, C. *et al.* (2018) 'Cumulative energy demand and global warming potential of a building-integrated solar thermal system with/without phase change material', *Journal of Environmental Management*. Elsevier Ltd, 212, pp. 301–310.
- Lenz, K. *et al.* (2012) 'LCA of energy generating components for facade integration in existing high-rise buildings', *International Journal of Sustainable Building Technology and Urban Development*, 3(3), pp. 168–176.
- Leone, G. and Beccali, M. (2016) 'Use of finite element models for estimating thermal performance of façade-integrated solar thermal collectors', 171, pp. 392–394.
- Li, D. H. W. *et al.* (2012) 'A study of grid-connected photovoltaic (PV) system in Hong Kong', *Applied Energy*. Elsevier, 90(1), pp. 122–127.
- Li, L., Qu, M. and Peng, S. (2016) 'Performance evaluation of building-integrated solar thermal shading system: Building energy consumption and daylight provision', *Energy and Buildings*, 113, pp. 189–201.
- Li, L., Qu, M. and Peng, S. (2017) 'Performance evaluation of building-integrated solar thermal shading system: Active solar energy usage', *Renewable Energy*, 109, pp. 576–585.
- Liu, L. *et al.* (2014) 'Comprehensive investigation on energy retrofits in eleven multi-family buildings in Sweden', *Energy and Buildings*. Elsevier B.V., 84, pp. 704–715.
- Liu, L., Rohdin, P. and Moshfegh, B. (2015) 'Evaluating indoor environment of a retrofitted multi-family building with improved energy performance in Sweden', *Energy and Buildings*. Elsevier B.V., 102, pp. 32–44.
- Lu, L. and Law, K. M. (2013) 'Overall energy performance of semi-transparent single-glazed photovoltaic (PV) window for a typical office in Hong Kong', *Renewable Energy*. Elsevier Ltd, 49, pp. 250–254.

Lu, L. and Yang, H. X. (2010) 'Environmental payback time analysis of a roof-mounted building-integrated photovoltaic (BIPV) system in Hong Kong', *Applied Energy*, 87(12), pp. 3625–3631.

M.Felder, R. and W.R, R. (2005) *Elementary Principles of Chemical Processes.PDF*. 3rd_Editio. USA: John Wiley and Sons.

Maaytah, M., Nsour, F. and Heffner, G. (2015) *Impacts evaluation jreeef - jordan river foundation impacts evaluation jreeef - jordan river foundation solar hot water heater program*. Jordan.

Mahmoud, M. (2013) *Renewable Electricity in the Arab Region: the Prospects of Trading?*

Mandalaki, M. *et al.* (2012) 'Assessment of fixed shading devices with integrated PV for efficient energy use', *Solar Energy*. Elsevier Ltd, 86(9), pp. 2561–2575.

Mandalaki, M., Tsoutsos, T. and Papamanolis, N. (2014) 'Integrated PV in shading systems for Mediterranean countries: Balance between energy production and visual comfort', *Energy and Buildings*. Elsevier B.V., 77, pp. 445–456.

Maps Jordan (2019) *Jordan world map (Western Asia - Asia)*. Available at: <http://maps-jordan.com/> (Accessed: 14 January 2019).

Martin-Chivelet, N. *et al.* (2018) 'Building retrofit with photovoltaics: Construction and performance of a BIPV ventilated façade', *Energies*, 11(7).

Maturi, L. and Adami, J. (2018) *Building in Trentino Alto Photovoltaic (BIPV) Integrated Adige*. Switzerland: Springer International Publishing AG.

Maurer, C., Cappel, C. and Kuhn, T. E. (2017) 'Progress in building-integrated solar thermal systems', *Solar Energy*. The Authors, 154, pp. 158–186.

Medel, F. J. (2017) *Life cycle Energy and CO2 Analysis of a Student Residential Building in Ningbo*.

MEMR (1997) *Energy annual report*. Jordan.

MEMR (2003) *Energy annual report*. Jordan.

MEMR (2011) *Energy annuual report*. Jordan.

MEMR (2013) *Survey of Energy Consumption in Residential Buildings in Jordan*. Jordan.

MEMR (2017) *Energy Annual Report*. Jordan.

MEMR (2018) *Energy 2018 - Facts & Figures*. Jordan.

Mertin, S. *et al.* (2014) 'Reactively sputtered coatings on architectural glazing for coloured active solar thermal façades', *Energy and Buildings*. Elsevier, 68, pp. 764–770.

Meza, E. (2015) 'PV magazine photovoltaic market and technology', *Philadelphia signs 50 MW agreement*. Available at: http://www.pv-magazine.com/news/details/beitrag/egypt--philadelphia-signs-50-mw-agreement-_100018667/#axzz4PJxXgYNz.

- Milić, V., Ekelöw, K. and Moshfegh, B. (2018) 'On the performance of LCC optimization software OPERA-MILP by comparison with building energy simulation software IDA ICE', *Building and Environment*. Elsevier Ltd, 128, pp. 305–319.
- Molin, A., Rohdin, P. and Moshfegh, B. (2011) 'Investigation of energy performance of newly built low-energy buildings in Sweden', *Energy and Buildings*. Elsevier B.V., 43(10), pp. 2822–2831.
- Montoro, D. F. F., Vanbuggenhout, P. and Ciesielska, J. (2011) 'Building-integrated Photovoltaics: An overview of the existing products and their fields of application'.
- Motasem, S. (2011) 'Sustainable Energy Mix and Policy Framework for Jordan'. Friedrich-Erbert-Stiftung Royal Scientific Society, p. 140.
- Moreno, A. *et al.* (2017) 'Building Integration of Solar Thermal Systems', in *Proceedings of COST Action TU1205 Symposium*, pp. 1–9.
- Munari Probst, M. C. and Roecker, C. (2012) 'Criteria for architectural integration of active solar systems IEA Task 41, Subtask A', *Energy Procedia*, 30(March 2015), pp. 1195–1204.
- Munari Probst, M. C. and Roecker, C. (2013) *Report T.41.A.3/1 Designing solar thermal systems for Architecture integration -criteria and guidelines*.
- Munari Probst, M. C. and Roecker, C. (2019) 'Criteria and policies to master the visual impact of solar systems in urban environments: The LESO-QSV method', *Solar Energy*. Elsevier, 184(February 2019), pp. 672–687.
- Munari Probst, M. and Roecker, C. (2007) 'Towards an improved architectural quality of building-integrated solar thermal systems (BIST)', *Solar Energy*, 81(9), pp. 1104–1116.
- Nadel, S. (2002) 'Appliance and Equipment Efficiency Standards', *Annual Review of Energy and the Environment*, 27(1), pp. 159–192.
- NEPCO (2016) *National Electric Power Company, annual report*. Jordan.
- NEPCO (2017) *National Electric Power Company, annual report*. Jordan.
- Ng, P. K. and Mithraratne, N. (2014) 'Lifetime performance of semi-transparent building-integrated photovoltaic (BIPV) glazing systems in the tropics', *Renewable and Sustainable Energy Reviews*. Elsevier, 31, pp. 736–745.
- Ng, P. K., Mithraratne, N. and Kua, H. W. (2013) 'Energy analysis of semi-transparent BIPV in Singapore buildings', *Energy and Buildings*. Elsevier B.V., 66, pp. 274–281.
- O'Hegarty, R., Kinnane, O. and McCormack, S. J. (2016) 'Review and analysis of solar thermal facades', *Solar Energy*. Elsevier Ltd, 135 (October), pp. 408–422
- OME (2012) *SOLAR THERMAL IN THE MEDITERRANEAN REGION: MARKET ASSESSMENT REPORT*.

Osseweijer, F. J. W. *et al.* (2017) ‘A Review of the Dutch Ecosystem for Building-integrated Photovoltaics’, *Energy Procedia*. Elsevier B.V., 111(September 2016), pp. 974–981.

Palmero-Marrero, A. I. and Oliveira, A. C. (2006) ‘Evaluation of a solar thermal system using building louvre shading devices’, *Solar Energy*, 80(5), pp. 545–554.

Passera, A. *et al.* (2018) ‘BIPV Facades : Market Potential of Retrofit Application in the European Building Stock’, (May).

PASSERA, A. (2017) *Developing a tool to assess the business concept of solar thermal façades*. POLITECNICO DI MILANO.

Peng, C., Huang, Y. and Wu, Z. (2011) ‘Building-integrated photovoltaics (BIPV) in architectural design in China’, *Energy and Buildings*. Elsevier B.V., 43(12), pp. 3592–3598.

Peng, J. *et al.* (2015) ‘Comparative study of the thermal and power performances of a semi-transparent photovoltaic façade under different ventilation modes’, *Applied Energy*. Elsevier Ltd, 138, pp. 572–583.

Peng, J. *et al.* (2016) ‘Numerical investigation of the energy saving potential of a semi-transparent photovoltaic double-skin facade in a cool-summer Mediterranean climate’, *Applied Energy*. Elsevier Ltd, 165, pp. 345–356.

Perez, M. J. R. *et al.* (2012) *Façade-integrated photovoltaics: A life cycle and performance assessment case study, 40th ASES National Solar Conference 2011, SOLAR 2011*.

Perez, M. J. R. and Fthenakis, V. (2011) ‘A lifecycle assessment of façade BIPV in New York’, in *37th IEEE Photovoltaic Specialists Conference*. Seattle, WA, USA, pp. 003271–003276.

Persson, T. *et al.* (2016) *SINTEF Energy Research Efficient Energy usage TR A7570-Unrestricted Software for modelling and simulation of ground source heating and cooling systems WP2 INTERACT and Building construction ** NTNU, Department of Geology and Mineral Resources Engineering*.

Philadelphia Solar (2018) *Official Web Page for Philadelphia Solar Manufactures of high quality solar panels*. Available at: http://www.philadelphia-solar.eu/philadelphia_solar_about.html (Accessed: 1 November 2016).

Pittaluga, M. (2013) *Fostering Solar Technology in the Mediterranean Area, FOSTERinMED*.

Portworld (2019) *No Title*. Available at: <http://www.portworld.com/map> (Accessed: 1 July 2019).

Potter, R. B. *et al.* (2009) ‘“Ever-growing Amman”, Jordan: Urban expansion, social polarisation and contemporary urban planning issues’, *Habitat International*. Elsevier Ltd, 33(1), pp. 81–92.

Prieto, A. *et al.* (2017) ‘Solar coolfacades: Framework for the integration of solar cooling technologies in the building envelope’, *Energy*. Elsevier Ltd, 137, pp. 353–368.

Probst, M. C. M. and Roecker, C. (2011) *Architectural Integration and Design of Solar Thermal Systems*. Oxford, UK: Routledge Taylor and Francis Group.

Probst, R. (2017) 'A Guide to Renewable Energy in Egypt and Jordan: Current Situation and Future Potentials'. Amman, Jordan: Friedrich-Ebert-Stiftung Jordan & Iraq (FES).

PV magazine (2019) 'Module Price Index December- 2018: Zero planning security'. Available at: <https://www.pv-magazine.com/features/investors/module-price-index/>.

PVinsight (2019) *Fourth Quarter and Fiscal Year 2018 Results*. Available at: <http://pvinsights.com/> (Accessed: 2 March 2019).

Qawasmeh, B. R. *et al.* (2017) 'Energy Rating for Residential Buildings in Amman', *Int. J. of Thermal & Environmental Engineering*, 14(2), pp. 109–118.

R2CITIES Project (2014) " *Renovation of Residential urban spaces : Towards nearly zero energy CITIES* ". Available at: <http://r2cities.eu/>.

Rahman, M. M., Haur, L. K. and Rahman, H. Y. (2012) 'Building-integrated Photovoltaic (BIPV) in Malaysia: An Economic Feasibility Study', 45, pp. 7683–7688. Available at: http://www.elixirpublishers.com/articles/1350369798_45 (2012) 7683-7688.pdf.

Raouz, K. (2017) *Environmental Impact Assessment of a Photovoltaic Power Station in Stockholm* Khalid Raouz. KTH Industrial Engineering and Management.

Raugei, M. *et al.* (2017) 'Energy {Return} on {Energy} {Invested} ({ERoEI}) for photovoltaic solar systems in regions of moderate insolation: {A} comprehensive response', *Energy Policy*. Elsevier, 102(June 2016), pp. 377–384.

Reidy, R. *et al.* (2005) *GUIDELINES FOR October 2005*.

Ritzen, M. J. *et al.* (2017) 'Environmental impact comparison of a ventilated and a non-ventilated building-integrated photovoltaic rooftop design in the Netherlands: Electricity output, energy payback time, and land claim', *Solar Energy*, 155, pp. 304–313.

Rodrigues, S. *et al.* (2016) 'Economic feasibility analysis of small scale PV systems in different countries', *Solar Energy*, 131(June), pp. 81–95.

RSS (2007) 'Climatic design of buildings and urban areas ; advanced training programme'. Sweden: Royal Scientific Society, Jordan and Lund University.

Ruysevelt, P. (2014) *IEA design tools activities for photovoltaics in buildings*, *National Solar Architecture Research Unit*.

Ryan, E. M. and Sanquist, T. F. (2012) 'Validation of building energy modeling tools under idealized and realistic conditions', *Energy and Buildings*. Elsevier B.V., 47, pp. 375–382.

Sakhrieh, a. and Al-Ghandoor, A. (2013) 'Experimental investigation of the performance of five types of solar collectors', *Energy Conversion and Management*, 65, pp. 715–720.

Salem, T. and Kinab, E. (2015) 'Analysis of Building-integrated Photovoltaic Systems: A Case Study of Commercial Buildings under Mediterranean Climate', *Procedia Engineering*. Elsevier B.V., 118, pp. 538–545.

- Shariah, A. *et al.* (1998) 'Effects of absorptance of external surfaces on heating and cooling loads of residential buildings in Jordan', *Energy Conversion and Management*, 39(3–4), pp. 273–284.
- Shariah, A., Al-Akhras, M. A. and Al-Omari, I. A. (2002) 'Optimizing the tilt angle of solar collectors', *Renewable Energy*, 26(4), pp. 587–598.
- Shariah, A., Tashtoush, B. and Rousan, A. (2002) 'Cooling and heating loads in residential buildings in Jordan', *Energy and Buildings*, 26(2), pp. 137–143.
- El Shenawy, E. T., Hegazy, A. H. and Abdellatef, M. (2017) 'Design and optimization of stand-alone PV system for Egyptian rural communities', *International Journal of Applied Engineering Research*, 12(20), pp. 10433–10446.
- Shukla, A. K., Sudhakar, K. and Baredar, P. (2016) *A comprehensive review on design of building-integrated photovoltaic system*, *Energy and Buildings*. Elsevier B.V.
- Siebert, M. (2011) *Advantages and opportunities of the use of solar energy to produce hot water :Assessment of the state of the art and feasibility in Syria and Jordan*. Germany.
- Simonetti, M. *et al.* (2017) 'In-field monitoring and numerical parametric analysis of a small size adsorption solar cooling plant in Italy', *Renewable Energy and Power Quality Journal*, pp. 997–1001.
- Singh, J. P. *et al.* (2015) 'Comparison of Glass/Glass and Glass/Backsheet PV Modules Using Bifacial Silicon Solar Cells', *IEEE Journal of Photovoltaics*, 5(3), pp. 783–791.
- Solar, O. (2017) 'Opaque photovoltaic glazing solutions based on crystalline silicon with hidden busbars and L interconnections Project report', (April 2017).
- Stetz, T., Braun, M. and Engel, B. (2011) 'Cost optimal sizing of photovoltaic inverters-Influence of new grid codes and cost reductions', in *29th European Photovoltaic Solar Energy Conference*. Germany.
- Tabakovic, M. *et al.* (2017) 'Status and Outlook for Building-integrated Photovoltaics (BIPV) in Relation to Educational needs in the BIPV Sector', *Energy Procedia*. Elsevier B.V., 111(September 2016), pp. 993–999.
- Taher, A. Al *et al.* (2011) *Potential Analysis for a New Generation of Solar Thermal Systems in the Southern Mediterranean Countries*, *SOLATERM Project Report*. Germany.
- Tian, H. *et al.* (2018) 'Study on the energy saving potential for semi-transparent PV window in Southwest China', *Energies*, 11(11).
- Tina, G. M. *et al.* (2013) 'Photovoltaic glazing: Analysis of thermal behavior and indoor comfort', *Energy Procedia*. Elsevier B.V., 42, pp. 367–376.
- Tominaga, M. (2009) *Opportunities for thin-film photovoltaics in Building-integrated Photovoltaics (BIPV) with a focus on Australia*. Murdoch University.
Available at: http://researchrepository.murdoch.edu.au/id/eprint/2081/1/Tominaga_2009.pdf.

Tous, Y. El (2013) 'Feasibility of Residential Grid Connected PV System under the Jordanian Net Metering Renewable Energy Law', 3(7), pp. 34–40.

Transparency Market Research (2015) *Building-integrated Photovoltaics Market: Global Industry Analysis, Size, Share, Growth, Trends and Forecast, 2013–2019*. Albany, NY, USA.

Tripathy, M. and Sadhu, P. K. (2015) 'Building-integrated Photovoltaic Market trend and its Applications', *TELKOMNIKA Indonesian Journal of Electrical Engineering*, 14(2), pp. 185–190.

Tsagas, I. (2015) 'Pv magazine photovoltaic market and technology', *Jordan's Science and Technology University tenders 5 MW of PV*.

Available at: http://www.pv-magazine.com/archive/articles/beitrag/jordans-science-and-technology-university-tenders-5-mw-of-pv_100018846/#axzz4PJxXgYNz.

Twidell, J. and Weir, T. (2015) *Renewable energy resources, Desalination and Water Resources (DESWARE), Renewable Energy Systems and Desalination, Vol. 1*.

USAID (2014) 'JORDAN ENERGY SECTOR CAPACITY BUILDING ACTIVITY QUARTERLY PERFORMANCE REPORT'. Jordan: United States Agency for International Development.

Vadiee, A., Doodoo, A. and Gustavsson, L. (2018) 'A Comparison Between Four Dynamic Energy Modeling Tools for Simulation of Space Heating Demand of Buildings', in *Cold Climate HVAC 2018*, pp. 701–711.

Vartianinen, E. (2018) 'Battery Storage Costs and Impact on PV Competitiveness'. Fortum Growth. Vela solaris (2018) 'Polysun simulation software user manual', *Vela Solaris AG*. Switzerland.

De Wild-Scholten, M. J. (2013) 'Energy payback time and carbon footprint of commercial photovoltaic systems', *Solar Energy Materials and Solar Cells*. Elsevier, 119, pp. 296–305.

Witzig, A. *et al.* (2017) 'Teaching Renewable Energy Systems by Use of Simulation Software: Experience At Universities of Applied Sciences, in In-Service Training, and from International Know-How Transfer', in *Eurosun 2016*, pp. 1–10.

Witzig, A., Foradini, F. and Probst, M. (2009) 'Simulation tool for architects- optimization of active and passive solar use', in *international conference CISBAT*. Switzerland., pp. 2–3.

World bank group (2019) *Global horizontal irradiation, Global solar atlas*. Available at: <https://globalsolaratlas.info/downloads/world> (Accessed: 1 September 2019).

Wu, P. *et al.* (2017) 'Review on Life cycle Assessment of Energy Payback of Solar Photovoltaic Systems and a Case Study', *Energy Procedia*. The Author(s), 105, pp. 68–74.

Wu, Y. W. *et al.* (2017) 'LCA-Based Economic Benefit Analysis for Building-integrated Photovoltaic (BIPV) Façades: A Case Study in Taiwan', *International Journal of Green Energy*, 15(1).

Xu, S. *et al.* (2014) 'Optimal PV cell coverage ratio for semi-transparent photovoltaics on office building façades in central China', *Energy and Buildings*. Elsevier B.V., 77, pp. 130–138.

- Yang, R. J. and Zou, P. X. W. (2016) 'Building-integrated photovoltaics (BIPV): Costs, benefits, risks, barriers and improvement strategy', *International Journal of Construction Management*, 16(1), pp. 39–53.
- Younis, A. (2017) 'Towards Resilient Low-Middle Income Apartments in Amman, Jordan : a Thermal Performance Investigation of Heating load', in *CIBSE ASHRAE Technical Symposium*. Loughborough, UK.
- Yudha, H. M. (2018) 'Life cycle Analysis for the Feasibility of Photovoltaic System Application in Indonesia Life cycle Analysis for the Feasibility of Photovoltaic System Application in Indonesia', *IOP Conference Series: Earth and Environmental Science*.
- Zawaydeh, S. (2015) 'Renewable Energy and Energy Efficiency Legal Framework in Jordan Presented by', in *Renewable Energy and Energy Efficiency*. Amman, Jordan: Jordan Environmental Society.
- Zawaydeh, S. (2015) 'Economical, Environmental and Social Advantages of Net Zero Energy Buildings', in *Energy Economy & Energy Management Forum for MENA & Fourth Renewable Energy National Dialogue*. Amman, Jordan.
- Zawaydeh, S. (2016) 'Developing Solar Roofs in Buildings generates Profit and makes Cities More Resilient', in *Third International Engineering Conference Environmental Design and Innovation*. Jordan.
- Zerohomebill (2019) *SOLAR BATTERY STORAGE SYSTEM COST AND ADVANTAGES*. Available at: <https://zerohomebills.com/solar-battery-storage-system-cost-and-advantages/> (Accessed: 21 April 2019).
- Zhang, J., Lv, F. and Zhang, L. (2012) 'Discussion on Environment Impact Assessment in the Lifecycle of PV Systems', *Energy Procedia*, 16, pp. 234–239.
- Zhang, T., Wang, M. and Yang, H. (2018) 'A Review of the Energy Performance and Life cycle Assessment of Building-integrated Photovoltaic (BIPV) Systems', *Energies*, 11(11), p. 3157.
- Zhang, X., Shen, J., Lu, Y., *et al.* (2015) 'Active Solar Thermal Facades (ASTFs): From concept, application to research questions', *Renewable and Sustainable Energy Reviews*. Elsevier, 50, pp. 32–63.
- Zhang, X., Shen, J., Campus, N., *et al.* (2015) 'Building-integrated Solar Thermal (BIST) Technologies and Their Fundamentals of Renewable Energy and Applications', *Journal of Fundamentals of Renewable Energy and Applications*, (November), pp. 0–21.

List of Acronyms

a-Si	Amorphous silicon
BAPV	Building attached photovoltaic
BOS	Balance of systems
BIPV	Building-integrated photovoltaic
BIST	Building-integrated solar thermal
CAGR	Compounded annual growth rate
CdTe	Cadium telluride
CED	Cumulative energy demand
COP	Coefficient of performance
CPBT	Carbon payback time
c-Si	Crystalline silicon
DHW	Domestic hot water
EE	Embodied energy
EC	Embodied carbon
EPBT	Energy payback time
EROEI	Energy return on energy investment
GHG	Greenhouse gas emissions
GHI	Global horizontal irradiance
LCA	Life cycle assessment
LCCA	Life cycle cost analysis
Mono-Si	Mono-crystalline silicon
OEP	Overall energy performance
poly-Si	Polycrystalline silicon
PV	Photovoltaic
PBT	Payback time
ROI	Return on investment
STC	Standard test conditions
TFSC	Thin-film solar cell

List of Figures

Figure 1-1: Global horizontal Irradiance (GHI), world, Mediterranean area, and Jordan Maps..	2
Figure 1-2: Primary energy consumption mix for the southern and eastern Mediterranean countries in 2011.	3
Figure 1-3: Climate overview for the Mediterranean cities around the Red sea.....	6
Figure 1-4: Research thesis structure.	9
Figure 2-1: Jordan location, map..	10
Figure 2-2: Jordan population growth from 1950-2015.....	11
Figure 2-3: Climate regions in Jordan..	11
Figure 2-4: Annual global horizontal irradiance in Jordan..	12
Figure 2-5: Mean minimum, maximum and average temperatures in Amman..	13
Figure 2-6: Mean minimum, maximum and average relative humidity and average precipitation in Amman..	14
Figure 2-7: Wind velocity range in m/s in Amman..	14
Figure 2-8: Monthly average diurnal solar radiation in Amman.	15
Figure 2-9: Daily solar radiation profile for Amman for each month.....	15
Figure 2-10: Sun path diagram for Amman, and sun altitude at 12:00 pm in different season in Amman...	16
Figure 2-11: Energy consumption and population trends in Jordan from 1992 to 2018 and energy demand forecast from 2019 to 2025	17
Figure 2-12: Primary energy consumption mix in Jordan from 1990 to 2015 and the government plan for 2020, 2025.	18
Figure 2-13: Primary energy consumption by sector in Jordan from 1990 to 2017..	18
Figure 2-14: Electricity consumption in Jordan by sector between 1990-2017 and the total expected electricity consumption in 2020,2025.....	19
Figure 2-15: Installation of solar thermal collectors in multi-family residential building roof in Jordan.....	26
Figure 2-16: Application of photovoltaic in a residential building in Jordan..	27
Figure 2-17: Lack of experience in installation of solar energy system in Jordan.....	28
Figure 2-18 : Solar energy system installed without consideration to safety and easy maintenance in Jordan.....	28
Figure 2-19: Multi-family residential building roof used for many purposes.....	29
Figure 2-20: A typical floor plan for multi-family residential buildings in Jordan..	31
Figure 2-21: A view for a multi-family building in Jordan.	31
Figure 2-22: Regulations of plot size, building percentage, and setbacks for housing sectors.....	33
Figure 2-23: a) Land divisions according to residential land use for type C. b) Residential multi-family blocks under zone sector C..	34
Figure 3-1: BIPV system classifications.	38
Figure 3-2: Example of roof-integrated PV..	40
Figure 3-3: Example of facade-integrated PV..	41
Figure 3-4: Examples of BIPV tile products.....	42

Figure 3-5: Examples of BIPV foil products..	42
Figure 3-6: Example of BIPV modules.....	43
Figure 3-7: Examples of solar glazing.....	44
Figure 3-8: Example of BIPV accessory.....	44
Figure 3-9: Global solar thermal capacity in operation and annual energy yields 2000-2017.....	51
Figure 3-10: World distribution of the total installed capacity in operation by collector type in 2016.	52
Figure 3-11: BIST system classification.....	53
Figure 3-12: Evacuated tube collectors' structure and the possibility to orient the absorbers.....	55
Figure 3-13: a) Integration of a glazed flat plate collector as part of the multilayer roofing system, b): Roof integration of unglazed flat plate collectors used as roof covering. c): Evacuated tubes collectors used as glazed roof sun shading.	56
Figure 3-14: Two typical solutions of façade building-integrated flat plate collectors.	57
Figure 3-15: Example of façade integrated evacuated collectors' system.	57
Figure 3-16: Example of a façade integrated flat plate collector's system	58
Figure 3-17: Design variants 1– 4 (a - d) cross-sections.....	59
Figure 4-1: The main steps adopted in this research to reduce the energy demand of typical multi-family building in Amman, Jordan.....	67
Figure 4-2: The main steps used for energy supply systems selection for improved multi-family building in Amman, Jordan.....	68
Figure 4-3: The main steps followed to evaluate the performance of different proposed solar systems cases, in multi-family building in Amman, Jordan.	69
Figure 4-4: Life cycle assessment stages adopted in this research for the PV systems.	71
Figure 4-5: The proposed decision-making matrix, with two examples.....	74
Figure 5-1: 3D view of the base case building within the typical urban context in Amman, Jordan.....	77
Figure 5-2: Site plan and the assumed surrounding building modeled in IDA ICE 4.8.	78
Figure 5-3: 3D view of the base case building and surrounding buildings modeled in IDA ICE 4.8.....	78
Figure 5-4: Typical floor plan for the simulated multi-family building in Amman, Jordan	79
Figure 5-5: Apartment occupancy schedules: a) weekdays, b) weekends.	80
Figure 5-6: Bedrooms lighting schedules: (a) master bedroom, (b) children's bedrooms.....	83
Figure 5-7: Window opening control macro in IDA-ICE used in simulations..	84
Figure 5-8: Annual energy demand for different apartments of the base case model representing a typical residential apartment building in Amman, Jordan..	86
Figure 5-9: Floor plan and 3d view of the simulated apartment building.....	86
Figure 5-10: Annual energy balance (sensible only) result during the heating period for the base case simulated apartments in multi-family building in Amman, Jordan. The heated area of each apartme.....	87
Figure 5-11: Annual energy balance result during the cooling period for the base case simulated apartments in residential building in Amman, Jordan.....	87
Figure 5-12: Monthly energy demands of the top floor apartment 1, in the base case typical apartment building in Amman, Jordan.....	88
Figure 5-13: Monthly energy balance (sensible only) results for the base case top floor apartment 1 in residential building in Amman, Jordan.....	89

Figure 5-14: Monthly envelop transmission results for the base case top floor apartment 1 in residential building in Amman, Jordan.....	89
Figure 5-15: Break-down of transmission losses in the heating period and transmission gains through the building envelope elements for the base case top floor apartment 1.	90
Figure 5-16: Proposed cases of windows recess depth with respect to the façade.	91
Figure 5-17: Proposed shading device types.....	92
Figure 5-18: The effect of thermal insulation thickness applied to the wall on heating and cooling energy demand for the top-floor apartment 1, and the energy-saving percentage in comparison with the base case model.	93
Figure 5-19: The effect of thermal insulation thickness applied to the roof of the top floor apartment on heating and cooling energy demands, and the energy-saving percentage in comparison with the base case model..	94
Figure 5-20: The effect of installing double clear glazing windows with U-values of 2.86 W/m ² K, on different orientations on the heating, cooling, and lighting energy demands, and the energy-saving percentage in comparison with the base case model.....	95
Figure 5-21: The effect of installing low-emission double glazing windows with U-values of 1.59 W/m ² K double glazing windows on different orientations on the heating, cooling, and lighting energy demands, and the energy-saving percentage in comparison with the base case model.....	95
Figure 5-22: The effect of window recess depth with respect to the facade (at the outer edge, on the center line, at the inner edge) on the heating, cooling and lighting energy demands, and the energy saving percentage in comparison with the base case model.....	96
Figure 5-23: The effect of overhang with a different projection on the south elevation on the heating, cooling, and lighting energy demands, and the energy-saving percentage in comparison with the base case model.	97
Figure 5-24: The effect of side-fines with different projections on the east elevation on the heating, cooling, and lighting energy demands, and the energy-saving percentage in comparison with the base case model..	97
Figure 5-25: The effect of ventilation blinds on the south elevation on the heating, cooling and lighting energy demands, and the energy-saving percentage in comparison with the base case model.....	98
Figure 5-26: the effect of ventilation blinds on the east elevation on the heating, cooling and lighting energy demands, and the energy-saving percentage in comparison with the base case model. ²	99
Figure 5-27: the effect of night ventilation from May to October on the heating, cooling and lighting energy demands, and the energy saving percentage in comparison with the base case model.....	100
Figure 5-28: The effect of installed energy-efficient light LED bulbs on the energy demands and the energy-saving percentage in comparison with the base case model..	100
Figure 5-29: Annual energy demands for different energy-saving strategies in comparison with the base case apartment in Amman, Jordan, and the energy-saving percentage in comparison with the base case model.	101
Figure 5-30: Energy demand of the improved apartment building in comparison to the base case apartment building, in Amman, Jordan.....	102
Figure 5-31: Annual energy demand for different apartments of the improved apartment building in Amman, Jordan.....	103
Figure 6-1: Simplified schematic of the proposed solar space and water heating systems and conventional heating system for multi-family building in Amman, Jordan.	105
Figure 6-2: Simplified schematic of the proposed solar cooling system configurations and the conventional cooling for multi-family building in Amman, Jordan.....	106

Figure 6-3: Hourly heating and cooling energy demand for an improved apartment building in Amman, Jordan.....	108
Figure 6-4: Daily hot water demand profile (300 l/day) in percentage for each family in the residential building in Amman, Jordan, used in Polysun simulation software.....	109
Figure 6-5: Proposed arrangement for the solar collectors, and photovoltaic module on the roof of residential building, in Amman, Jordan.....	110
Figure 6-6: Model layout of the conventional heating system in Jordan (system 0).	111
Figure 6-7: Model layout of (a) System 1: thermosiphon solar hot water system (b) System 1: conventional heating system.....	112
Figure 6-8: Model layout of the decentralized solar combi-heating system (system 2).	113
Figure 6-9: Model layout of the centralized solar combi-heating system (system 3).	114
Figure 6-10: Conventional split air condition system in Jordan.	116
Figure 6-11: Grid-connected photovoltaic system powered conventional cooling system (system 1) and building electricity demand.....	116
Figure 6-12: Grid-connected photovoltaic system powered centralized compression cooling system (system 2) and building electricity demand.	118
Figure 6-13: The annual primary energy demand for different heating systems (water + space heating), and the primary energy saving in comparison to the system 0.	120
Figure 6-14: The monthly heating demand (water + space heating), and the monthly solar thermal energy yield, solar fraction of the centralized solar combi-heating system (system 3)	121
Figure 6-15: Monthly primary energy saved by solar thermal energy and primary energy demand of the centralized solar combi-heating system.	122
Figure 6-16: The monthly electricity demand and the monthly solar photovoltaic energy yield, solar fraction of the photovoltaic system with centralized compression chiller system 2	124
Figure 6-17: Monthly primary energy saved by solar photovoltaic energy and net primary energy demand of the multi-family building in Amman, Jordan.	124
Figure 6-18: Hourly PV production and electricity consumption profiles in 11th of July of multi-family building in Amman, Jordan with 9 kW photovoltaics system and 1,350 m ² heated area.	126
Figure 6-19: Hourly PV production and electricity consumption profiles in 11th of July of multi-family building in Amman, Jordan with 9 kW photovoltaics system.	126
Figure 6-20: The relation between battery capacity and not stored energy (energy to the grid) of 9 kWh photovoltaic system with 5,745 kWh overproduction	128
Figure 6-21: Simplified schematic of the selected energy systems for multi-family building in Amman, Jordan a) solar combi heating system b) centralized compression cooling system with grid-connected. ..	132
Figure 7-1: Influence of tilt and orientation on the percent of total solar radiation received annually in Amman, Jordan.....	135
Figure 7-2: Monthly solar radiation available on the horizontal surface, and on 30°, 60° and 90° south exposed a tilted surface in Amman, Jordan	136
Figure 7-3: Accumulative incident solar radiation through all the year, and average daily incident radiation through heating and cooling periods, on studied multi-family building envelope.....	137
Figure 7-4: Hourly incident solar radiation received by the roof and south façade of the studied multi-family building in Amman, Jordan.	138
Figure 7-5: Hourly solar exposure analysis in percentage (%) received by the roof and south façade of the studied multi-family building in Amman, Jordan.	139

Figure 7-6: Shadow analysis on the studied apartment building in the typical urban context in Amman, Jordan during the different times for three days of the year: winter solstice (21st December), spring equinox (21st March) and summer solstice (21st June).....	140
Figure 7-7: Available surfaces area for solar technology installations.	141
Figure 7-8: Annual energy production and the solar fraction of grid-connected photovoltaic system with different tilt and azimuth angle, and different capacity installed on the top of a residential building in Amman, Jordan.....	145
Figure 7-9: Annual field yield and the solar fraction of solar thermal collectors with different tilt angles, azimuth, and installed area on the roof of a residential building in Amman, Jordan.....	145
Figure 7-10: Simplified schematic of the selected energy systems for multi-family building in Amman, Jordan a) solar combi heating system b) centralized compression cooling system with grid-connected. ..	146
Figure 7-11: The arrangement of the solar collectors, and photovoltaic module on the roof of multi-family building, in Amman, Jordan.....	147
Figure 7-12: Proposed Photovoltaic application on south façade.....	150
Figure 7-13: Semi-transparent mono-crystalline PV staircase integration design proposal and examples.	151
Figure 7-14: Opaque mono-crystalline PV integrated into fixed overhang shading device design proposal and example.....	151
Figure 7-15: Hourly percentage of shading for the suggested shading device design.....	152
Figure 7-16: Semi-transparent mono-crystalline PV integrated into fixed overhang shading device design proposal and example.....	152
Figure 7-17: Different scenarios of semi-transparent PV overhang with different PV converge ratio, 75%, 50% and 25%, and different dimensions.	153
Figure 7-18: PV integrated into fixed louver overhang design proposal and example.....	153
Figure 7-19: PV integrated into window louver design proposal and example.....	154
Figure 7-20: PV integrated into the south balcony railings design proposal and example.....	154
Figure 7-21: Wall integrated PV design proposal and example.....	155
Figure 7-22: Recent construction trend in the multi-family buildings in Jordan.....	155
Figure 7-23: Annual energy demand in kWh for the improved multi-family building in Amman, Jordan under different PV system design cases.....	160
Figure 7-24: Annual energy demand for the improved multi-family building in Amman, Jordan under semi-transparent PV overhang with different PV cell coverage ratio and PV overhang dimensions.....	160
Figure 7-25: Annual solar heating system demand and solar fraction, for the improved multi-family building in Amman, Jordan under different PV system design cases.....	161
Figure 7-26: Annual cooling system demand for the improved multi-family building in Amman, Jordan under different PV system design cases.....	161
Figure 7-27: The effect of the surrounding building on the electricity reduction of PV façade systems installed on the south façade of multi-family building in typical urban context in Amman, Jordan.....	163
Figure 7-28: Total power capacity and electrical energy production of the proposed PV systems, installed to the improved multi-family building in Amman, Jordan.....	164
Figure 7-29: Net electricity demand of the multi-family building in Amman, Jordan, and the electricity-saving percentage of different PV systems in comparison to the base case (no PV installation).	165
Figure 7-30: Annual primary energy demand of the different solar energy installation cases and compare it to the base case without ST and PV installation, all systems are installed into the improved apartment building in Amman, Jordan.....	166

Figure 8-1: Net electricity demand of the multi-family building in Amman, Jordan, and the electricity-saving percentage of different PV systems in comparison to the base case (no PV installation).	169
Figure 8-2: Annual primary energy demand of the different solar energy installation cases and compare it to the base case without ST and PV installation, all systems are installed into the improved multi-family building in Amman, Jordan.....	170
Figure 8-3: The life cycle stages of a mono-Si PV module.	171
Figure 8-4: Process steps in the production of mono-Si PV module.	173
Figure 8-5: Percent contribution to total energy for different stages of the solar PV system.	181
Figure 8-6: Percent contribution to total carbon for different stages of the solar PV system.	182
Figure 8-7: Total capital cost and cost breakdown (in percentage) for different PV system design.....	188
Figure 8-8: Life cycle PV system cost, cost saving from electricity and the PBT for the proposed PV system over 25 years.....	191
Figure 8-9: Electricity cost of the improved residential multi-family building in Amman. Jordan before installing PV systems (base case), and after installing PV systems, and the percentage of electricity cost in comparison to the base case over 25 years.	Error! Bookmark not defined.
Figure 9-1: Decision support- matrix representing the proposed PV systems.	198
Figure 9-2: Decision support- matrix representing three cases of the proposed PV systems.	199
Figure 10-1: Primary energy demand in MWh/year for the multi-family building in Amman, Jordan under different design strategies.	202
Figure 10-2: Energy, carbon and cost payback time in years for different PV systems designed installed into the multi-family building in Amman, Jordan	203

Appendixes

Appendix A

Input parameters and component overview for the simulation of the installed solar heating system in Jordan.

Component		Characteristic		
Location of the system				
Latitude:	31.95			
Longitude:	35.94			
Elevation:	779 m			
Meteorological data-overview				
Weather data source		Imported from Metronome 7 (the same used in IDA ICE 4.8)		
Average outdoor temperature (°C)		18		
Global irradiation, the annual sum (kWh/m²)		2,049		
Diffuse irradiation, the annual sum (kWh/m²)		579		
Hot water demand				
Daily demand (l/day)	300 for each apartment			
Temperature setting (C°)	Temperature: 50			
Annual energy demand (kWh)	4,072			
Building				
Heating setpoint temperature (C°)	20			
Heating energy demand excluding DHW (kWh)	16,159 for all apartments			
Solar thermal collector				
	System 0	System 1	System2	System 3
Solar thermal collector model		Flat-plate, good quality		
Number of collectors		2 for each apartment	3 for each apartment	30 for all apartments
Total gross Area (each collector) (m²)		1.8		
Total aperture area (each collector) (m²)		1.8		
Total absorber area (each collector) (m²)		2		
Tilt angle (hor.=0°, vert.=90°)		30°		
Orientation		South (0°)		
Hot water storage tank				
	System 0	System 1	System2	System 3
Decentralized or centralized	Decentralized	Decentralized	Decentralized	Centralized
Volume (l)	300	Space heating: 200 Hot water: 300 thermosiphon tank	300	3000

Boiler				
	System 0	System 1	System 2	System 3
Decentralized or centralized	Decentralized	Decentralized	Decentralized	Centralized
Energy source	Oil	Space heating: Oil Hot water: Continues flow electric heater	Oil	Oil
Maximum power (kW)	5 for top floor apartments 4 for other apartments	Space heating: 4 Hot water: 4	4 for top floor apartments 3 for other apartments	20
Maximum efficiency (%)	85	85	85	85
Heating element				
	System 0	System 1	System2	System 3
	Radiator	Radiator	Radiator	Floor heating
Number of the heating element	Automatic number			
Nominal inlet temperature (C ^o)	60	60	60	40
Nominal inlet temperature (C ^o)	50	40	40	35

Appendix B

Input parameters and component overview for the studied photovoltaics and cooling systems in Jordan.

Component	Characteristic
Location of the system	
Latitude:	31.95
Longitude:	35.94
Elevation:	779 m
Meteorological data-overview	
Weather data source	Imported from Metronome 7 (the same used in IDA ICE 4.8)
Average outdoor temperature (C ^o)	18
Global irradiation, the annual sum (kWh/m ²)	2,049
Diffuse irradiation, the annual sum (kWh/m ²)	579
Building	
Heating setpoint temperature	27 C ^o
Cooling energy demand	12,807 kWh/year for all apartments
Electric consumers	Equipment and lighting: 37,298 kWh/year
Solar photovoltaic module	
	System 0 System 1 System2
Modules name	“PS-M 2H-300”
Manufacturer	“Philadelphia solar” (local company in Jordan)
Module type	Mono-crystalline
Nominal power STC	300 W

Efficiency		0.154	
Number of modules		3 for each apartment	30 for all apartments
Total nominal power DC (kW)		0.9 for each apartment	9
Total gross area (m²)		1.95 (each module), 58.5 (all module)	
Tilt angle (hor.=0°, vert.=90°)		30°	
Orientation		South (0°)	
Inverter (by using the wizard)			
Number of inverters		1	
A number of strings		5	
Modules per string		6	
Total nominal power AC		10KVA	
Other related input (defined in the PV field)			
Soiling (%)		2 (default value)	
Degradation (%)		0.2(default value)	
The standard deduction for piping losses, module mismatch (%)		4 + 4	
Rear ventilation		Good (assumed for all solar photovoltaic mounted on the roof of the building-without integration)	
Wind fraction (%)		80 (for all roof installation)	
Coldwater storage tank			
	System 0	System 1	System2
Decentralized or centralized			Centralized
Volume (l)			1,000
Chiller (heat pump)			
Decentralized or centralized	Decentralized air split-unit	Decentralized air split-unit	Centralized compression chiller
Energy source	Electricity	Electricity	Electricity
Maximum power (kW)	3 for each apartment	4 for each apartment	15
Maximum COP	2.5-3	2.5- 3	4.36

Appendix C

Life cycle electricity cost analysis for the 9 kWp grid-connected photovoltaic system without a battery installed in a residential building with 1,350 m² heated area in Amman, Jordan.

Grid-connected system without battery							
Input in the excel sheet							
Note and assumptions	The PV production and to the grid decreased /from the grid increased by:	Grid network transmission losses	Annual increase in electricity cost sold to the grid	Electricity cost to the grid - Cost benefits of selling PV electricity 15 Cent/ kWh - Cost of network connection is 5.6 Cent/ kWh Assumed constant		The annual increase in electricity cost	Net electricity cost= cost of electricity from the grid- the cost of sold electricity to the grid
	0.75	2.3%	0%	9.40 Cent/ kWh		5%	
Year	Electricity to the grid (kWh/ year)	Electricity to the grid - network transmission losses (kWh/ year)	Cost benefits of energy sold to the grid (€)	Electricity from the grid (kWh/ year)	Electricity cost from the grid (Cent/kWh)	Electricity cost from the grid (€/year)	Net electricity cost (€/year)
1	3,672	3,672	345.2	34,240	8.80	3,013 €	2,668 €
2	3,644	3,644	342.6	34,496	9.2	3,188 €	2,845 €
3	3,617	3,617	340.0	34,755	9.7	3,372 €	3,032 €
4	3,590	3,590	337.5	35,016	10.2	3,567 €	3,230 €
5	3,563	3,563	334.9	35,278	10.7	3,774 €	3,439 €
6	3,536	3,536	332.4	35,543	11.2	3,992 €	3,660 €
7	3,510	3,510	329.9	35,810	11.8	4,223 €	3,893 €
8	3,484	3,484	327.4	36,078	12.4	4,467 €	4,140 €
9	3,457	3,457	325.0	36,349	13.0	4,726 €	4,401 €
10	3,431	3,431	322.6	36,621	13.7	4,999 €	4,677 €
11	3,406	3,406	320.1	36,896	14.3	5,289 €	4,969 €
12	3,380	3,380	317.7	37,173	15.1	5,595 €	5,277 €
13	3,355	3,355	315.4	37,451	15.8	5,919 €	5,603 €
14	3,330	3,330	313.0	37,732	16.6	6,261 €	5,948 €
15	3,305	3,305	310.6	38,015	17.4	6,624 €	6,313 €
16	3,280	3,280	308.3	38,301	18.3	7,007 €	6,699 €
17	3,255	3,255	306.0	38,588	19.2	7,413 €	7,107 €
18	3,231	3,231	303.7	38,877	20.2	7,842 €	7,538 €
19	3,207	3,207	301.4	39,169	21.2	8,295 €	7,994 €
20	3,183	3,183	299.2	39,463	22.2	8,775 €	8,476 €
21	3,159	3,159	296.9	39,758	23.3	9,283 €	8,986 €
22	3,135	3,135	294.7	40,057	24.5	9,821 €	9,526 €
23	3,112	3,112	292.5	40,357	25.7	10,389 €	10,096 €
24	3,088	3,088	290.3	40,660	27.0	10,990 €	10,700 €
25	3,065	3,065	288.1	40,965	28.4	11,626 €	11,338 €
life cycle total			7895 €		34,240	160,450 €	152,554 €

life cycle electricity cost analysis for the 9 kWh grid-connected photovoltaic system with battery installed in a residential building with 1,350 m² heated area in Amman, Jordan.

Grid-connected system with battery							
		Input in the excel sheet					
	The PV production and to the grid decreased /from the grid increased by:	Grid network transmission losses	Annual Increase in electricity cost sold to the grid	Annual increase in electricity Cost from the grid	Electricity cost to the grid - Cost benefits of selling PV electricity 15 Cent/ kWh - Cost of network connection is 5.6 Cent/ kWh	Net electricity cost= cost of electricity from the grid- the cost of sold electricity to the grid	
Note	0.75	2.3%	0%	5%	9.4 Cent/ kWh		
Battery efficiency degradation have been not considered							
Year	Electricity to the grid (kWh/ year)	Electricity to the grid - network transmission losses (kWh/year)	Cost benefits of energy sold to the grid (€)	Electricity from the grid (kWh/year)	Electricity cost from the grid (Cent/ kWh)	Electricity cost from the grid (€/ year)	Net electricity cost (€/year)
1	172	168	16	31,651	8.80	2,785	2,769
2	171	167	16	31,888	9.2	2,918	2,903
3	169	165	16	32,127	9.5	3,058	3,042
4	168	164	15	32,368	9.9	3,204	3,189
5	167	163	15	32,611	10.3	3,357	3,342
6	166	162	15	32,855	10.7	3,518	3,503
7	164	161	15	33,102	11.1	3,686	3,671
8	163	159	15	33,350	11.6	3,862	3,847
9	162	158	15	33,600	12.0	4,047	4,032
10	161	157	15	33,852	12.5	4,240	4,225
11	160	156	15	34,106	13.0	4,443	4,428
12	158	155	15	34,362	13.5	4,655	4,641
13	157	153	14	34,620	14.1	4,878	4,863
14	156	152	14	34,879	14.7	5,111	5,096
15	155	151	14	35,141	15.2	5,355	5,341
16	154	150	14	35,404	15.8	5,611	5,597
17	152	149	14	35,670	16.5	5,879	5,865
18	151	148	14	35,938	17.1	6,160	6,146
19	150	147	14	36,207	17.8	6,455	6,441
20	149	146	14	36,479	18.5	6,763	6,750
21	148	145	14	36,752	19.3	7,087	7,073
22	147	143	13	37,028	20.1	7,425	7,412
23	146	142	13	37,306	20.9	7,780	7,767
24	145	141	13	37,585	21.7	8,152	8,139
25	144	140	13	37,867	22.6	8,542	8,529
life cycle total			361			128,972	128,661